International Agreement Report

TRAC–PF1/MOD1 Calculations of LOFT Experiment LP–02–6

Prepared by
P. Coddington, C. Gill

Winfrith Technology Centre
United Kingdom Atomic Energy Authority
Winfrith, Dorchester
Dorset, England DT 28 DH

Office of Nuclear Regulatory Research
U.S. Nuclear Regulatory Commission
Washington, DC 20555

April 1992

Published by
U.S. Nuclear Regulatory Commission

International Agreement Report

TRAC–PF1/MOD1 Calculations of LOFT Experiment LP–02–6

Prepared by
P. Coddington, C. Gill

Winfrith Technology Centre
United Kingdom Atomic Energy Authority
Winfrith, Dorchester
Dorset, England DT 28 DH

Office of Nuclear Regulatory Research
U.S. Nuclear Regulatory Commission
Washington, DC 20555

April 1992

NOTICE

This report is based on work performed under the sponsorship of the United Kingdom Atomic Energy Authori . The information in this report has been provided to the USNRC under the terms of the International Code Assessment and Application Program (ICAP) between the United States and the United Kingdom (Administrative Agreement - WH 36047 between the United States Nuclear Regulatory Commission and the United Kingdom Atomic Energy Authority Relating to Collaboration in the Field of Modelling of Loss of Coolant Accidents, February 1985). The United Kingdom has consented to the publication of this report as a USNRC document in order to allow the widest possible circulation among the reactor safety community. Neither the United States Government nor the United Kingdom or any agency thereof, or any of their employees, makes any warranty, expressed or implied, or assumes any legal liability of responsibility for any third party's use, or the results of such use, or any information, apparatus, product or process disclosed in this report, or represents that its use by such third party would not infringe privately owned rights.

TRAC-PF1/MOD1 CALCULATIONS OF LOFT EXPERIMENT LP-02-6

P CODDINGTON
C GILL

SUMMARY

The report describes four TRAC-PF1/MOD1 calculations modelling
the OECD-LOFT experiment LP-02-6. This was a 200% double-ended
cold leg break experiment performed at nearly full power (47 MW)
and with a loop mass flow of 248 kg/s. In the experiment the
pumps were tripped and then allowed to coast down naturally after
the start of the transient. Two of the calculations compared the
results of two versions of the code (12.2 and 13.0), one
incorporated a reduced gap between the fuel and the cladding to
reduce the initial fuel stored energy, and the other had the TRAC
interface sharpener model switched off.

Following the opening of the quick acting blowdown relief valves
to initiate the transient there is a net flow out of the vessel
until about 2 seconds, at which time the broken loop cold leg
flow out of the vessel drops below the flow into the vessel from
the intact loop cold leg, being driven by the pumps' inertia.
This net flow into the vessel, enhanced by flashing of subcooled
liquid in the downcomer and lower plenum, causes a bottom-up flow
of liquid and quenches about 2/3 of the core. Additionally a
top-down partial quench, extending to about the 30 inch
elevation, is observed at about 15 seconds. This corresponds to
fluid running back into the upper plenum and down into the core
as the fluid in the pressurizer and steam generator begins to
flow back along the intact loop hot leg.

The nature of the observed quenching is not entirely clear; it
may be genuine fuel pin quenching or simply localised quenching
of the thermocouples.

At 17.5 seconds, the primary system pressure reaches 42 bars, at
which point the Emergency Core Cooling System trips.
Measurements suggest oscillatory flow immediately upstream of the
accumulator injection point in the intact loop cold leg. Except
for two slugs of liquid, totalling about 200-250 kg, compared to
a total accumulator flow of about 1,690 kg, no continuous
bypassing of the downcomer by the accumulator fluid occurs.
Most of it finds its way to the lower plenum. As the water level
here rises, it begins to quench the bottom of the core at about
37 seconds and the quench moves progressively upwards. The final
quench of the uppermost elevations is coincident with the entry
of accumulator nitrogen into the intact loop cold leg and the
consequent rise in the primary system pressure.

SUMMARY (Continued)

All four TRAC calculations predict similar hydraulic behaviour to
each other. The bottom-up liquid flow at 4 seconds extends to
the top of the core, as opposed to just 2/3 of the way up as in
the experiment. The TRAC modelling does not predict either the
bottom-up or the top-down quench at 15 seconds and following the
subsequent fuel rod dryout the calculated temperatures are too
high, particularly at the top and bottom of the fuel rods. The
reduced fuel-gap calculations (ZEROGAP and ISHARP) are
considerably better in this respect due to their lower stored
energy The calculations predict no bypass of ECCS fluid in line
with the experiment and all predict oscillatory core inlet flow.
There were differences, however, in the behaviour of fluid in the
intact loop cold leg, for in some of the calculations the
production of liquid slugs was predicted, in others it was not.
These differences are believed to be due to the sensitivity of
the TRAC condensation model rather than any specific changes to
the models.

All the calculations predict a surge of fluid into the core on
the entry of nitrogen into the intact loop cold leg. However,
the higher rod temperatures in the calculations mean that the
final quench is delayed longer than in the experiment.

The main differences between the calculations are therefore
restricted to the thermal behaviour of the fuel rods due for
example to the different dispersed flow heat transfer used in
versions 12.2 and 13.0 and the reduced fuel stored energy in the
ZEROGAP and ISHARP calculations.

CONTENTS

FIGURES

FIGURES (Continued)

FIGURES (Continued)

FIGURES (Continued)

TABLES

1   INTRODUCTION

This report provides a description of the results of four
TRAC-PF1/MOD1 calculations of the OECD-LOFT experiment LP-02-6.
This experiment was the third of the high power LOFT large break
experiments (L2-3 and L2-5 being the previous two experiments)
and although it was performed at the beginning of the OECD-LOFT
project, the boundary conditions for the experiment were
specified by the USNRC. The primary boundary conditions that
distinguish this experiment from the previous experiments L2-3
and L2-5 were the increased power, ie 47 MW and the fact that the
primary coolant pumps were tripped but not decoupled from their
flywheel systems at the start of the transient. This resulted in
a positive (bottom-up) core flow during the blowdown period, ie
at about 5 secs, but the magnitude of this flow was less than
that observed in the earlier experiment L2-3 where the pumps
where kept running, such that the fuel rod external thermocouples
quenched immediately only in the bottom 2/3 rds of the central
fuel assembly. The remainder of the core (ie the top 1/3 rd)
quenched subsequently during the top-down flow period after about
12 secs.

A description of the LP-02-6 experiment can be found in the Quick
Look Report, Ref 1.

2   TRAC INPUT MODEL AND NODALISATION

Diagrams showing the LOFT facility and instrument locations are
given in Figs 1 and 2 while noding diagrams of the TRAC
representation of the LOFT facility are shown in Figs 3, 4, 5 and
6 for all the calculations presented in this report, all of which
used the same nodal representation. The noding scheme and input
model is based upon the original TRAC-PD2 model which was
modified for TRAC-PF1/MOD1 at LANL for the analysis of L2-3 and
at AEEW for the analysis of LP-LB-1 (Ref 2). However subsequent
to the analysis of LP-LB-1 the input deck was modified (Ref 3) to
improve the modelling in the areas of:-

   (i) Primary coolant loop and vessel flow resistance.

  (ii) Renodalisation of the ECCS injection line (Ref 4).

 (iii) Revision of the fluid volumes and flow areas within the
       reactor vessel.

  (iv) Inclusion of core bypass paths in the reactor vessel (lower
       plenum and core to upper plenum and downcomer to upper
       plenum).

   (v) Revision of the vessel metal-work heat structures (Ref 5).

  (vi) A revision and inclusion of ambient heat losses.

All of the above are likely to have an influence on the
calculated results when compared to those calculated for
experiment LP-LB-1 and in fact some of the revisions, eg (i),

(ii) and (v) were a result of recognised inadequacies of that analysis (see Refs 2 and 3).
The results of the renoualisation of the ECCS line can be seen in Fig 3, and the inclusion of the lower plenum and core to upper plenum bypass in Fig 6i. Also shown in Figs 3 and 4 is the location of the experimental measurement rakes in the intact and broken loop hot and cold legs.

3   TRAC CALCULATIONS

As stated above, this report contains the results of four TRAC-PF1/MOD1 calculations, these were performed sequentially and the results of the calculations are presented in three groups each containing a pair of calculations together with the experimental data where appropriate. This report therefore provides both the results of a limited sensitivity study together with a comparison of the TRAC calculat   with the experimental data.

The four TRAC calculations, identified by their differences, are as follows:-

(1)   A calculation using the 'Standard' Winfrith version of TRAC-PF1/MOD1, Version 12.2 (ie code version UK refer e X26). This calculation used the "as manufactured" fuel-clad gap of 100 ▸on, on the figures this calculation is labelled "JON'S" and is the subject of a separate report (Ref 6).

(2)   The above calculation was repeated using the Winfrith version of TRAC-PF1/MOD1 Version 13.0 (ie code version UK Reference B03). This calculation is labelled "ORIGINAL" on the figures.

(3)   Calculation (2) was repeated but with the "fuel-clad" gap reduced to zero to reduce the steady state fuel stored energy and hence the peak cladding temperatures during blowdown. This calculation is labelled "ZERO-GAP" on the figures.

(4)   Finally calculation (3) was repeated but with the TRAC-PF1/MOD1 core interface sharpener logic removed. The core interface sharpener logic is a facility for overwriting the axial mass flux in the core calculated from the constitutive relations with an externally imposed model to produce a "sharp" core liquid level. The interface sharpener restricts the axial flow of liquid in the core by limiting the core cell exit void fraction to be greater than 90% irrespective of that calculated by the constitutive relations. The operation of the interface sharpener has been seen to produce unphysical behaviour during blowdown when applied to reactor calculations and to produce too sharp a liquid vapour interface during reflood (Ref 7). Its use is therefore not currently recommended. This calculation is labelled "ISHARP" in the figures.

A review of the four calculations is given in Table 1.

4   INITIAL CONDITIONS

The initial conditions for experiment LP-02-6 and the calculated
transients are given in Table 2. The data for the experiment was
taken from the Experiment Quick Look Report (Ref 1) and the
Experiment Specification Document (Ref 8). The data for the TRAC
calculations was taken from the "ZERO-GAP" calculation which was
the calculation used as the submission to the OECD-LOFT LP-02-6
experiment comparison exercise (Ref 9). There are no significant
differences between the initial conditions of the four
calculations and in fact transient calculations 3 and 4 used the
same steady-state calculation.

One major difference between this series of calculations and all
previous TRAC calculations, ie PD2 L2-3 and L2-5 (Ref 10) and
PF1/MOD1 LP-LB-1 (Ref 2) and LP-02-6 (Ref 11) calculations is the
improvement in the bypass modelling. As we see from Table 2, for
example, the total calculated bypass of ~ 10% is divided into a
lower plenum to upper plenum bypass of 2.6%, a downcomer to upper
plenum bypass of 2.26% with the remainder, 5.25%, flowing through
the Reflood Assist Bypass Valves (RABV). Previously only the
flow through the RABVs was represented.

The power was increased in experiment LP-02-6 from the 36 MW used
in L2-3 and L2-5, to 47 MW, an increase of ~ 1.3. However the
flow rate was only increased by ~ 25% from 200 kg/sec to 250
kg/sec, producing therefore a slightly increased temperature rise
across the core. The contrasts with experiment LP-LB-1 where the
loop flow rate was increased to ~ 300 kg/sec for a small (49
compared to 47 MW) increase in core power, producing a
significantly smaller core ΔT.

The relative magnitude of loop flow and core power is likely to
influence the vessel hydraulic behaviour during blowdown, as is
the bypass representation for the calculated transients.

The total accumulator liquid available in experiment LP-02-6 was
~ 1.69 m^3 which is lower than that for experiments L2-5 (1.96 m^3)
and L2-3 (2.166 m^3), but higher than that of experiment LP-LB-1
(1.18 m^3) (Ref 12). These numbers should be compared with the
vessel volumes of 0.60 m^3 for the lower plenum, 1.017 m^3 for the
downcomer (this number was significantly increased from that of
0.672 m^3 used in previous TRAC analyses of LOFT) and 0.272 m^3 for
the core.

As will be seen from Table 2 the accumulator gas volume used in
the calculation is significantly smaller than the experimental
value (0.642 m^3 compared to 0.95 m^3). This difference was
introduced into the input deck to compensate for the fact that
the TRAC code places a lower limit on the Nitrogen gas
temperature of 273 k (0°C) ie the freezing point of water, and
that the gas temperature will fall well below this value during
the emptying of the accumulators.

Apart from the above accumulator gas volume difference, Table 2 shows that the TRAC calculated initial conditions for the primary circuit are within the uncertainty levels of the corresponding measured quantities. There is however a small difference in the pressuriser volumes used in the calculations (liquid 0.555, steam $0.376 \, m^3$) compared to those for the experiment (liquid 0.607, steam $0.39 \, m^3$).

5 ANALYSIS OF LP-02-6 TRANSIENT

5(i) Sequence of Events

The sequence of the significant events for LOFT experiment LP-02-6 are listed in Table 3, where the times of occurrence are compared with the times predicted by the "ZERO-GAP" TRAC calculation. This is the same calculation as that for which the initial conditions were presented in Table 2.

Experiment LP-02-6 was initiated (0.0 secs) by the opening of the quick-opening blowdown valves in the broken loops. The reactor was scrammed on low hot leg pressure at 0.1 secs and the pumps were tripped at 0.8 secs. (The pumps were not immediately decoupled from their flywheels as in experiment L2-5, but allowed to coast down naturally). The pumps coasted down until 16.5 secs when their rotational speed fell below the trip point and they were decoupled from their flywheels. Following the opening of the blowdown valves the system pressure falls rapidly to the saturation pressure of the hot leg fluid and voids form in the upper plenum, core and hot leg. The flow into the core quickly reverses as a result of the large subcooled critical flow out of the broken loop cold leg. The core therefore rapidly voids such that the fuel rods begin to dryout in the centre of the core at about 0.9 secs. The fuel rod cladding temperatures (recorded by the thermocouples located on the outside of the cladding) rise as the energy stored within the UO_2 is equalised radially across the whole of the fuel rod. The fuel rod cladding temperatures continue to rise until approximately 5 secs when a positive flow through the core was re-established. This flow through the core at about 5 secs, occurs as the flow into the vessel downcomer from the intact loop, which remains almost constant as a result of the high pump inertia and single-phase nature of the cold leg fluid, exceeds the falling flow out of the vessel downcomer through the broken loop cold leg. The broken loop cold leg flow falls as the system pressure falls from hot leg saturation pressure to the cold leg saturation pressure. The flow through the core at 5 secs is enhanced by the flashing of the cold leg fluid in the vessel lower plenum and downcomer and the intact loop cold leg. The positive flow through the core cools the core and produces a rapid quench of the cladding (external) thermocouples in the lower ~ 2/3 rds of the central fuel assembly. After the system pressure falls below the cold leg saturation pressure the flow of liquid into the downcomer decreases as the intact loop cold leg voids, so that this flow quickly falls below that out of the broken loop cold leg, and the core once again empties. After ~ 10 secs therefore the fuel rods in the core begin to heat up again. A partial top-down quench is initiated at about 15 secs

AEEW - M 2464   4

and lasts until ~ 18.5 secs as liquid flowing out of the
pressuriser and along the hot leg into the upper plenum flows
down into the core.

The system pressure falls below the accumulator trip point at
~ 17.5 secs and the ECCS liquid begins to flow into the primary
circuit, the HPIS and LPIS began at 21.8 and 34.8 secs
respectively. The flow out of the broken loop continues to fall
as the primary system pressure falls with no obvious direct
bypass of liquid (ie subcooled liquid in the broken loop cold
leg), except for one slug of liquid between 30 and 32.5 secs.

The lower plenum was estimated to have filled at 30.7 secs
(Ref 1) which is the time that the lowest core thermocouple (ie
at a 2 inch elevation) is observed to quench. This is well in
advance of the time that the accumulator empties. The
accumulator tank for example empties at about 48 secs, while an
additional ~ 7 secs is required to clear the ECCS line, so that
the ECCS accumulator liquid flow into the intact loop cold leg is
not complete until about 55 secs. Following this the effect of
the accumulator nitrogen flow into the primary circuit is seen as
part of the slug of subcooled liquid, resident in the intact loop
cold leg, is swept out of the broken loop cold leg.

Following the cooling of the fuel rods during the blowdown
period, once the cladding thermocouples dry out they heat up
rapidly in the centre of the core to a temperature of about
800 K, which is close to the corresponding fuel temperature. The
cladding temperatures then increase slowly as a result of the
fuel decay heat until the bottom of the core begins to quench at
about 31 secs as outlined above. Following this, liquid flows
into the bottom of the core and begins to cool the lower parts of
the fuel rods while the fuel rod quench progresses intermittently
up the bottom part of the core reaching the 21 inch elevation at
about 48 secs. Above the peak power elevation ie at a height of
greater than about 30 inches, the fuel rods do not begin to cool
until about 42 secs at which time the cladding temperatures range
from ~ 750 K at 31 inches to ~ 500 K at 62 inches. The quench
time of the fuel rods at these elevations corresponds to the end
of the accumulator liquid flow, with for example times of 54.5
secs at 31 inches, 56 secs at 43.8 inches and 49 inches and 54.5
secs again at 62 inches. (The end of the accumulator liquid flow
into the primary circuit is estimated to occur at about 55 secs -
see above). It is postulated therefore that the flow of
accumulator nitrogen into the intact loop cold leg initates the
flow of a slug of liquid into the core as well as one out of the
broken loop cold leg as described above. The mechanism that
leads to this is described in Ref 13 for example. The flow of
liquid into the core at the time is able to quench the upper
parts of the fuel rods as the majority of the cladding is at a
temperature below the minimum film boiling point of ~ 650 K. The
quench of the core therefore was complete by 56 secs and occurs
as a direct result of the flow of a slug of liquid into the
bottom of the core driven by the system pressurisation as the
flow into the primary circuit from the accumulator changes from
water to nitrogen.

5(ii)   TRAC Calculations

In the following three Sections of the report we present the
results of the four TRAC calculations of experiment LP-02-6
described in Section 3 and Table 1. The results of the four
calculations are presented in the following three groups of
Figures together with the experimental measurements where
appropriate.

GROUP 1, Figure 7 to 77

Calculations (see Section 3 and Table 1)

- "JON'S", "ORIGINAL"

and the experimental data.

GROUP 2, Figures 78 to 148

Calculations: "ORIGINAL", "ZERO-GAP"

and the experimental data.

GROUP 3, Figures 149 to 219

Calculations: "ZERO-GAP", "ISHARP"

and the experimental data.

The results from each of the above groups is described in turn in
the following Sections. In the first Section a detailed
description of the experimental measurements together with a
comparison with the general results of the TRAC calculations is
provided in addition to comments on the differences between the
two calculations. The subsequent Sections just review the
differences between the calculations and how these influence the
main elements of the calculated transient.

5(iii)   "JONS" and "ORIGINAL" Calculations

LOOP BEHAVIOUR

These two calculations of the LOFT large break transient
experiment LP-02-6 are identical in the sense that they used
exactly the same input deck. The difference between the two
calculations being that the "JON'S" calculation was performed
using code version X26 (UK version of LANL code version 12.2) and
the "ORIGINAL" calculation was performed using code version B03
(UK version of LANL code version 13.0). There are obviously
likely to be many differences between the two code versions - in
spite of the fact that the code from version 12.1 was formally a
frozen code, however it is thought that none of these changes,
except for one, are likely to have a significant influence on the
behaviour of a large break calculated transient. We consider

that this observation is confirmed by the results presented in Figures 7 to 77. The one area in which there is a known difference between the two code versions that is likely to influence large break calculations are the changes made the post-dryout heat transfer. This accounts for the difference in the calculated cladding temperatures which occur primarily during the reflood period. In code version X26 the "error" in the Forslund-Rohsenow dispersed flow heat transfer coefficient (ie the use of the liquid thermal conductivity instead of the vapour conductivity) had been corrected by the UK. In version B03 the Forslund-Rohsenow relation had been changed by LANL in such away as to correct the "error" in the value of the thermal conductivity used but to also increase the numerical coefficient in order to preserve the resultant value of the heat transfer coefficient. This revised value of the Forslund-Rohsenow dispersed flow heat transfer coefficient introduced by LANL in version 13.0 was kept in the equivalent UK version B03. The result of this change can be seen as a more rapid cooling of the cladding temperatures during reflood with the revised form of the heat transfer term in the "ORIGINAL" ie B03 calculation.

The first observation from the results of these two calculations is that their behaviour particularly that reflected by the global parameters is very similar especially during the blowdown period (ie 0.0 to 20.0 secs), where the results of the two calculations are almost indistinguishable. The calculated and experimental pressure decay, shown for example in Fig 7 for the broken loop cold leg and Fig 30 for the intact loop hot leg shows a very good comparison between the two calculations and the experiment, and a significant improvement over that calculated for LOFT experiment LP-LB-1 (Ref 2). For experiment LP-LB-1 the TRAC calculation underestimated the primary system pressure after approximately 13 secs. The improvement in the calculation for LP-02-6 is ascribed to the revised vessel metal heat structures contained within the LP-02-6 input deck as these produce a significant increase in the heat released from the vessel metal-work to the fluid (see Fig 51). There is a small difference in the calculated system pressure between about 26 and 33 secs, with the "JON'S" calculation providing a better comparison with the experimental data. It is thought that this difference is possibly due to different condensation rates in the intact loop cold leg and Fig 20 for example shows that during the approximate same time period in the "JON'S" calculation a liquid slug forms upstream of the ECCS injection point whereas one is not formed in the "ORIGINAL" calculation. Previous experience of large break TRAC calculations has shown that the details of the intact loop cold leg behaviour during the accumulator flow period is both difficult to predict and very sensitive to the details of the loop and ECCS flows. This of course is always likely to be the situation when large changes in condensation rates are involved.

The broken loop cold leg density and mass flow shown in Figs 8 and 9 show that although the density is well calculated during the blowdown period the calculated mass flow is overestimated both during the subcooled period and during the saturated flow period when the calculations are approximately 20 kg/sec higher

than the experimental value. This is a consistent feature of all
of the calculated transients, but is different to that of the
LP-LB-1 comparison (Ref 2), however that probably just reflects
the difference in the calculated primary system pressures for
LP-LB-1 and LP-02-6 (see above). The calculated mass flow during
the saturated blowdown period is high in spite of the fact that
a critical flow multiplier of 0.84 is used, a value of 1.0 is
used during the subcooled blowdown. (These numbers were
inherited from LANL and have not been the subject of a study in
the UK, however it would not be possible to justify a number of
less than 0.84 for the saturated flow period). As observed in
Section 5(i), neither of the calculated transients shows any
direct ECCS bypass, until the accumulator empties at about 53
secs, whereas the experiment shows the flow of two distinct slugs
of subcooled water through the broken loop cold leg (Figs 8, 9,
10) the first betwen 29 and 33 secs and the second between 49.5
and 51.5 secs. Both the calculations and the experiment show the
flow of a slug of subcooled liquid coincident with nitrogen
entering the intact loop cold leg from the accumulator, however,
the calculated flow is much more extensive than that observed in
the experiment.

Rather surprisingly both of the calculations show some reverse
flow at the measurement location in the broken loop cold leg,
during the bypass phase of the transient. The "JON'S"
calculation shows some reverse flow at ~ 43 secs while the
"ORIGINAL" calculation shows reverse flow at ~ 42.5 secs and
46.5 secs, whereas none is observed in the experiment. Given the
good agreement between the calculated and experimental primary
system pressure during this period it is possible that the
reverse flow results from an error in the break pressure used in
the calculation to simulate the presure in the blowdown
suppression tank.

The calculated and experimental intact loop cold leg behaviour is
shown in Figs 20 to 26, the first point to note is the different
pump behaviour as shown in Fig 25. The "ORIGINAL" calculation
used the INEL specified pump inertia and so produces a long coast
down such that the pump is not calculated to decouple from its
flywheel system (ie at a velocity of 75 rads/sec) until after
70 secs, this is consistent with other calculations of the pump
behaviour, see for example Ref 11, Fig 79. The experimental
curve shows a much faster initial rundown of the pump such that
the pump decouples from its flywheel at ~ 16.5 secs, because of
the subsequent reduced inertia the pump velocity increases during
the bypass phase of the transient as a result of the ECCS related
condensation induced pressure drop across the intact loop. The
main feature of the pump velocity curve for the "JON'S"
calculation is that the pumps were tripped to decouple from their
flywheels at the experimental time of 16.5 secs. In spite of the
different pump behaviour seen in the two calculations there is
almost no observable difference in the intact loop cold leg flow,
see for example Fig 21 which shows the cold leg mass flow.

The intact loop cold leg calculated and experimental fluid
densities show very good agreement up to ~ 12.5 secs, both

showing for example the start of the voiding in the cold leg at
~ 6 secs. Between 12.5 and 20 secs the calculated densities are
slightly higher than the average experimental value, but well
within the range of the experimental error. The calculated
velocity and hence mass flow are however lower than the
experimental values (by about 25 kg/sec in the case of the mass
flow) during the first 6 secs when the flow is single-phase
liquid. Following this the experimental fluid velocity and
therefore mass flow falls rather more abruptly than the
calculated values.
Following the initiation of the flow of liquid from the
accumulators into the intact loop cold leg at ~ 17.5 secs, the
formation of oscillating slugs of subcooled liquid immediately
upstream of the ECCS injection point are observed starting at
about 21 secs. The oscillatory nature of the liquid slugs can be
seen in the measurements of fluid density, mass flow, fluid
velocity and temperature. These observations are consistent with
the behaviour of all of the other LOFT large break experiments,
although as was mentioned in the analysis of experiment LP-LB-1
(Ref 2) a detailed analysis of the individual density and
momentum flux measurements (not shown here) shows that the fluid
flow is unlikely to be one of a simple 1-D slug moving back and
forth along the cold leg pipe. The calculated behaviour is not
one of an oscillatory slug although the calculated fluid
densities, Fig 20, show that in the case of the "JON'S"
calculation there is some intermittent slug flow upstream of the
ECCS injection point but almost none in the case of the
"ORIGINAL" calculation. It is not possible currently to offer an
explanantion for the different behaviours. Both calculations
produce a stable liquid slug downstream of ECCS injection
location.

The broken and intact loop hot leg comparisons are shown in
Figs 14 to 19 and 26 to 32 respectively. The differences in the
behaviour of the two calculations in both the broken loop and
intact loop hot legs is almost negligable. However both
calculations underestimate the broken loop hot leg fluid density
and mass flow after the first few seconds, although the errors on
both measurements are quite large.

The flow in the intact loop hot leg remains in a positive
direction for approximately the first 9 secs as a result of the
pressure drop provided by the slow rundown of the pumps. (This
is in contrast to a positive flow period of approximately
4.5 secs for experiment LP-LB-1 where the pumps were decoupled
from their flywheels at the start of the transient). After
9 secs the flow reverses and two peaks in the mass flow are
observed, the first at ~ 12 secs occurs as liquid flows out of
the pressuriser and back along the hot leg to the upper plenum
and the second at ~ 16.5 secs when liquid from the upside of the
steam generator tubes flows back along the hot leg. In both of
these instances Fig 27 shows that the magnitude of the reverse
flow peaks is much greater in the calculation than in the
experiment. During the initial (0 to 9 secs) positive flow
period an increase in flow is observed, ie at about 6.5 secs in
the experiment but not in the calculations this attributed

(Ref 1) to be a consequence of the bottom-up flow through the core at this time. However no significant hot leg flow is calculated even when the core interface sharpner is turned off - see Section 5(v). As the hot leg side of the reactor drains the hot leg mass flow falls, and the flow becomes positive again at about 30 secs. However in the experiment a surge in the hot leg flow is seen at about 26.5 secs, and several peaks in the flow are observed between 42 and 51 secs. These later ones presumably occur as a result of liquid carry over from the core as the lower part of the core quenches during the period. An increase in the hot leg flow is seen at ~ 54 secs in both the experiment and the calculations coincident with the surge of liquid into the core following the initial injection of accumulator nitrogen into the intact loop cold leg.

The depressurisation and water level of the pressuriser is shown in Figs 31 and 32, the calculated depressurisation rate is slightly faster than the experimental value as a result of the underestimation of the initial pressuriser liquid level.

The accumulator level and pressure is shown in Figs 33 and 34, the agreement between the calculations and the experimental values is now very good following the renodalisation of the ECCS line (Ref 3). However no explanation can be found for the discrepancy between the calculated and measured accumulator pressure during the period when nitrogen flows from the tank.

VESSEL HYDRAULIC AND THERMAL BEHAVIOUR

The vessel hydraulic and thermal behaviour is shown in Figs 35 to 52, while the fuel rod cladding temperatures are shown in Figs 53 to 77. The global vessel behaviour, ie vessel mass, lower plenum liquid volume fraction etc is shown in Figs 43 to 48, for the two calculations, there is of course no direct experimental equivalent data. The results from the two calculations are virtually identical during the first 20 secs, while after this there is a slight delay in the filling of the vessel in the "JON'S" calculation as the ECCS liquid accumulates as a slug in the intact loop cold leg extending upstream of the injection point.

The calculated behaviour of the vessel during blowdown shows that the core, lower plenum and downcomer void during the first 3 to 4 secs as subcooled liquid flows out of the broken loop cold leg. The core rapidly empties while the lower plenum and downcomer liquid volume fractions fall to about 0.7. As the flow of subcooled liquid out of the broken loop cold leg falls it is exceeded by the flow of liquid into the vessel from the intact loop cold leg so that the liquid volume fractions of the lower plenum and downcomer increase. These then fall again after about 6 secs when the flow of liquid into the vessel decreases as the fluid in the intact loop cold leg flashes. The increase in the flow of liquid into the vessel produces a flow of liquid into the bottom of the core beginning at about 4 secs. The flow through the core is enhanced by the flashing of the liquid in the lower plenum and downcomer at about 6 secs and then falls to zero again

between about 9 and 10 secs as the lower plenum and downcomer void. (See Fig 35). In addition to the above flow of liquid into the bottom of the core a flow of liquid from the upper plenum down through the core is observed to occur between about 16 and 22 secs. This is shown as a reverse flow in the core outlet mass flow, Fig 44.

As stated above, the calculations show that, following the initiation of the accumulator flow at about 17 secs, the accumulator liquid flows into and down the vessel downcomer to fill the vessel lower plenum, and there is no observed direct bypass of the accumulator liquid out of the broken loop cold leg. Although of course fluid continues to flow out of the broken loop cold leg this fluid is saturated and is provided by the flashing of the liquid in the lower plenum as the pressure falls. The flow of accumulator liquid into the lower plenum produces an increase in the liquid volume fraction beginning at about 25 secs. Almost immediately some small quantity of liquid enters the bottom of the core and its influence can be seen on the cladding temperature (thermocouples) located at the bottom of the core. Initially all the accumulator liquid flows down the downcomer into the lower plenum so that the liquid volume fraction rises to ~ 0.75 at about 33 secs. Following this the liquid flow into the core increases and some liquid begins to accumulate in the downcomer. At about 40 secs in both calculations the lower plenum is liquid full and the core liquid volume fraction is ~ 0.2. (Note this is still some ~ 15 secs before the end of accumulator injection). After 40 secs when the lower plenum is full the accumulator liquid continues to flow into the downcomer which therefore rapidly fills, with the downcomer in the version 13.0 (ie "ORIGINAL") calculation filling somewhat faster than in the version 12.2 (ie "JON'S") calculation. The downcomer continues to fill in the calculation well above the level of the nozzles as a consequence of the fact that the primary system pressure falls below the boundary pressure used to model that in the blowdown suppression tank. The downcomer begins to empty at about 52 to 53 secs which is coincident with the end of the accumulator liquid flow as the primary system pressure once more exceeds that at the break. Following this there is a rapid increase in the liquid content of the core.

As stated above there is no detectable difference in the vessel behaviour between the two calculations during the blowdown period, and although there are some differences in detail between the two calculations following the initiation of the accumulator liquid the global behaviour is the same. The differences in behaviour almost certainly arise from the extreme sensitivity of the 1-D condensation model which as we have seen produces an upstream liquid plug in one instance but not in the other, rather than a specific difference between the two code versions.

As has been stated in relation to the analysis of other LOFT large break experiments (see Ref 2), the level and interpretation of the LOFT vessel instrumentation is both limited and difficult. However the lower plenum velocity and mommentum flux measurements (Figs 36 and 42) do confirm the bottom up flow of liquid observed

during blowdown, ie between about 4.0 and 9 secs. Also it is possible to estimate that the peak velocity and mass flux of the flow was ≈ 1 m/sec and between 500 and 1000 kg/m² sec respectively. The downcomer fluid temperature measurements, located on the broken loop side, also confirm the broken loop cold leg measurements in that there was only a small amount of direct subcooled liquid bypass. Fig 38 for example shows liquid subcooling only, between 31 and 32 secs and between 50 and 53 secs, prior to the end of the accumulator liquid injection.

CORE THERMAL RESPONSE

Central Bundle

The fuel rod cladding temperatures for the "JON'S" and "ORIGINAL" calculations together with the experiment are shown if Figs 53 to 63 for the central fuel assembly (ie LOFT assembly 5) and in Figs 64 to 67 for the instrumented peripheral fuel bundles (ie LOFT fuel assemblies 2, 4 and 6). In addition Table 4 shows the axial location of the calculational fine mesh together with the relative power density at the coarse mesh boundaries.

Two features of the calculated temperature transients are immediately obvious, (1) is the fact that during blowdown (and therefore for the remainder of the transient) the calculated peak clad temperatures are more than 100K too high and (2) the fact that the "ORIGINAL" calculation (version 13.0) cools faster than the "JON'S" calculation (version 12.2).

The peak clad temperature of a fuel rod during the initial blowdown period of a large break transient is determined primarily by the transfer of heat from the centre of the fuel to the cladding as the cladding to fluid heat transfer falls following dryout and as the heat generated within the core falls to the decay heat level. This means that the peak cladding temperature is particularly sensitive to the fuel rod pre-transient (steady state) stored energy, ie fuel rod centre temperature. The only unknown parameter of any significance in the calculation of t... steady state fuel stored energy is the fuel to cladding heat transfer, ie the fuel-clad gap conductance. In the TRAC code this is determined from the input value of the fuel-clad gap width, and in both of these calculations this was set to the "as manufactured" value of ~ 100 μons. Because of the obvious error in the resultant peak clad temperatures particularly at the bottom of the fuel rods, the influence of changing the fuel clad gap to fully closed, ie no gap, is evaluated as part of this sensitivity study (see Section 5.iv). Calculations of the initial cladding temperature response over the whole core is made more difficult because of the limitations of the TRAC fuel pin model, for example there is only a single fuel pin representation for the whole of the core and for this pin only a single set of radial dimensions can be input. So that changes in the pin dimensions both axially and between pins cannot be modelled. Also changes in the fuel clad gap width and the fuel and clad dimensions generally, due to mechanical

effects, cannot be modelled, only changes due to thermal effects are considered.

From Figs 53 and 54 we see that the fuel rod cladding temperatures during blowdown of the two calculations are identical and although there are some small differences in the cladding temperatures during the refill period the largest and most consistent difference is the fact that during reflood the "ORIGINAL" calculation (version 13.0) cools faster than the "JON'S" calculation (version 12.2). The major identifiable difference between the two code versions as was reviewed in Section 3, is that the dispersed flow (ie void fraction ≯ 0.5) heat transfer coefficients in the UK version of 13.0 were significantly higher than those in the UK version of 12.2. (For the reasons mentioned in Section 3 the LANL version of both codes would have given the higher of the two heat transfer coefficients). The higher heat transfer for the "ORIGINAL", ie v13.0 calculation would of course produce the observed earlier cooling of the cladding for identical core fluid conditions. Although as we see from Fig 48 for example, there are some small differences in the core liquid mass during reflood, but these on their own are not enough to be responsible for the different cladding behaviour.

The experimental cladding temperatures in LOFT are those recorded by thermocouples attached to the surface of the cladding. This has lead to intense speculation both to whether they truly reflect the temperature of the cladding particularly during the very rapid quench periods and to whether the thermocouples themselves induce additional cooling that would not be present on uninstrumented fuel rods. Both of these questions have been subject to separate effects experimental investigations at both high and low pressures (Ref 14 and 15) and a review of this information is currently taking place at AEEW (Ref 16).

The general response of the calculated and experimental cladding temperatures during the transient just reflects the vessel hydraulic behaviour described above. The cladding temperatures rise rapidly after about 1 sec as the fuel rods in the central assembly begin to dry out, increasing to over 1000K after about 3 secs in the experiment at the peak power location. The calculated peak temperatures are higher by up to 100K, because of the too large a value of the steady state stored energy, as explained above. After approximately 5 secs the surge of liquid into the bottom of the core produces a rapid cool down (quench) of the experimentally observed temperatures at all elevations up to and including the 39 inch level, but not at elevations above this. In the calculation the cladding is cooled by more than 200K at the 24 and 27 inch elevations, but of course this is not sufficient to produce a quench. More significant is that in the calculation the cooling extends all the way to the top of the fuel assembly so that at the 62 inch elevation for example, where the temperatures are low because of the lower power, a quench occurs in the calculation but not in the experiment.

Following the rapid cool down (quench) of the thermocouple-cladding in the experiment, dryout occurs again at the centre of the core after about 11 secs, and the temperature across the the fuel rod is once again re-equalised as the observed temperatures rise rapidly to about 800K. This behaviour is confirmed by the limited fuel rod centre line temperature measurements which show the centre of the fuel at the 27 inch elevation (Fig 63) to cool slowly to ~ 800K at about 15 secs. In the calculated transients following the blowdown cooling of the fuel rods the cladding temperatures rise to ~ 1000K, ie some 200K higher than the experimental values.

At the higher elevations in the central fuel assembly for the experiment the influence of the top down flow of liquid from the upper plenum is seen as the fuel rods quench from the top downwards between about 15 and 19 seconds. Although a small downflow of liquid is observed in the calculations (Fig 44) between 16 and 22 secs. This does not appear to have a major influence on the cladding temperatures except at the highest (62 inch) elevation (Fig 62).

Following the blowdown cooling and the re-equalisation of the fuel rod temperatures, ie after ~ 15 secs, the cladding temperatures rise slowly as the core is steam cooled and the vessel fills with water from the accumulator. This continues until the first sign of reflood cooling occurs at about 30 secs which is well before the accumulator empty time of ~ 54 secs. The temperature rise turns over at about the same time in both the experiment and the calculations (particularly the "ORIGINAL" v13.0 calculation) especially towards the bottom of the core, ie below ~ 21 inches. Above this, ie up to 31 inch level the cooling effect of the core flows is seen in the experiment, but not in the calculation until ~ 40 secs, when as Fig 48 shows there is an increase in the flow of water into the core. Above the 31 inch elevation both the experiment and calculations show a cooling of the fuel rods after 40 secs. The cooling of the cladding particularly in the experiment is distinctly oscillatory in nature, indicating an oscillating flow at the core inlet, this is likely to arise both as a result of increases in the core pressure as steam is produced and as a reduction in the pressure in the intact loop cold leg as steam condenses on the subcooled accumulator liquid.

The fuel rod cladding in the central fuel assembly continues to cool and subsequently quenche, such that, except at the very bottom of the core, the quench takes place coherently over significant lengths of the core. The following for example shows the quench times at the various elevations in the central assembly, and we see that

Elevation	Quench Time
2"	31 secs
11"	46.7 secs
21"	46.7 secs
24"	54.2 secs
27"	54.2 secs
31"	55.8 secs
43.8"	55.8 secs
49"	55.8 secs
62"	54.6 secs

the core quenches at the 11 and 21 inch elevation at ~ 47 secs while the remainder of the core, ie 24 to 62 inches quenches between 54 and 56 secs. The final core quench (ie between 54 and 56 secs) occurs at the same time as the termination of the accumulator liquid flow and the initiation of the accumulator nitrogen flow, and as is explained in Refs 13 and 17 and above this produces a surge of liquid both out of the broken loop cold leg and into the core. The coherency of the final quenches indicate that for this experiment, and for LOFT in general, the quench process is dictated by the fluid conditions, rather than thermal conditions within the fuel rod. In this sense it is different from the propagating quench fronts observed in slow forced reflood experiments. The experimental quench temperature in this experiment are by and large determined by the fuel rod temperatures at the time of the "end of accumulator" inflow of liquid into the core, but are typically less than 700K even at the peak power elevation. As explained above the relation of the observed quench temperatures in LOFT to a minimum in the boiling "Tmin" has been the subject of several separate effects studies, some of which (Ref 15) have shown that at reflood pressures (typically ~ 3 bars) the presence of the external thermocouples can promote quenches at temperatures higher that "Tmin". The fuel centre line temperatures (Fig 63) show that in line with the separate effects studies (Ref 15) that the quench of the external thermocouples quickly promotes cooling radially across the fuel.

In the calculations the surge of liquid into the core at ~ 54 secs (Fig 48) which results from the termination in the accumulator liquid flow, produces an increase in the cooling of the cladding; but because the temperatures are typically 200K too high at this time and no account of the influence of the external thermocouples on the quench process is allowed for, the final calculated quench is delayed by some 40 to 50 secs.

Peripheral Bundles

The fuel rod cladding temperatures for the three LOFT peripheral instrumented bundles 2, 4 and 6 are shown in Figs 64 to 77. Fuel assembly 4 is located between the intact loop hot leg and the broken loop cold leg, fuel assembly 2, between the broken loop cold leg and the broken loop hot leg and fuel assembly 6 between the broken loop hot leg and the intact loop cold leg, this arrangement is shown in Fig 6ii. All of the instrumented rods except one, 4G08-21 (Fig 70), are located on the side of the

peripheral bundles adjacent to the central bundle, whereas rod 4G08 is located towards the middle of assembly 4.

The thermal behaviour of the peripheral bundles, particularly that of 2 and 6, for the most part just mirrors the behaviour of the central bundle, except that the temperatures are lower as the result of the lower power level. The fuel rods dryout as the core voids during blowdown, reaching a peak temperature of ~ 900K at the peak power elevation in all 3 bundles. The bottom-up core liquid flow produces a rapid cooldown (quench) of all of the instrumented rods, even at the highest elevation of 49 inches, between 6 and 8 secs. In bundle 6 the fuel rods dryout again after about 12 secs rising rapidly to a temperature of ~ 650K to 700K then more slowly to a peak reflood temperature of ~ 750K (Fig 75, rod 6H12-026). In bundle 2 the fuel rods dryout at about 12 secs, but are then "quenched" again at all but the bottom elevation from the top-downwards between 14.5 and 18 secs. These rods then dryout between 18 and 21 secs rising to a peak temperature of ~ 700K (rod 2614-011, Fig 64). In fuel assembly 4, Figs 69 to 72, we see that following the blowdown "quenching" the fuel rods do not immediately dryout again, so that the resultant reflood peak temperatures are significantly lower, ie less than 600K. From the instrumented rod located in the middle of assembly 4 (ie rod 4G08, Fig 70), we see that at this location the fuel rods do not dryout during the blowdown period. The lowest elevation on assembly 4 dryout at about 18 secs in line with the fuel rods in assembly 2, while the higher elevations do not dryout until about 29 to 30 secs.

Cooling of the rods during reflood begins at about 29 to 30 secs at the 11 inch elevation (Figs 64, 73) in bundles 2 and 6 and this is consistent with the temperature measurements for the central bundle (see previous Section). Following this the thermocouples show an oscillatory behaviour similar to that observed in the cetral bundle, and again provide a confirmation of the likely oscillatory flow conditions at the core inlet. The cladding temperatures for bundles 2 and 6, during this reflood period lie between ~ 600K (2H13-049, Fig 68) and 750K (6H15-026, Fig 75) and these therefore are the temperatures from which the fuel rods quench. The quench times for assemblies 2 and 6 are given below; these as with the quench of the central fuel assembly show that the quench (of the thermocouples) is determined by the fluid conditions rather than the thermal behaviour of the fuel rods. For example the quenches occur coherently and are most likely coincident with the flow of liquid into the bottom of the core. In addition the final quench at the top of the peripheral fuel rod bundles occurs at ~ 55 secs, which again is in line with the data from the central fuel assembly, and

Height	ASSEMBLY 2	ASSEMBLY 6
11 inch	46.7 secs	40.8 secs
21 inch	43.3 secs	-
26 inch	-	47 secs
30 inch	40 secs	49 secs
39 inch	54.6 secs	54.6 secs
45 inch	-	54.6 secs
49 inch	52.5 secs	-

results from the surge of liquid into the core following the change of fluid flow, from the accumulator into the intact loop cold leg from that of water to nitrogen.

The calculated cladding temperatures for the peripheral bundles just reflect the general behaviour of those for the central bundle, ie (1) the blowdown peaks are too high because of the "high" initial fuel stored energy and (2) the "ORIGINAL" (ie v13.0) calculation cools quicker during reflood than the "JON'S" (v12.2) calculation. In addition to these, the first of the above leads to an overestimation of the cladding temperatures for bundle 6 during reflood of between 100 and 200K (eg Figs 74 to 77). Finally in bundles 2 and particularly 4 where in addition to the experimental bottom-up blowdown quench the fuel rods are subsequently quenched from the top downwards, the calculated temperatures which do not show this asymmetric top-down cooling are some 300K too high.

5(iv)   "ORIGINAL" and "ZERO-GAP" Calculations

The "ZERO-GAP" calculation was the second in the series of TRAC sensitivities performed as part of the comparison with LOFT experiment LP-02-6. This calculation was performed because of the obvious overestimation of the steady-state fuel stored energy calculated in the first two calculations when the "as manufactured" fuel clad gap was used. In the "ZERO-GAP" calculation the fuel clad gap was set to zero, while in all other ways the calculation was identical to the "ORIGINAL" calculation (ie it used code version B03, the UK version of LANL code version 13.0). As would be expected the major effect of the above change is to the calculated core cladding temperatures, however it might be anticipated that this change could influence the heat transferred to the fluid and hence the hydraulic behaviour.

The improvement in the calculated cladding temperatures during blowdown for the "ZERO-GAP" calculation can be easily seen in Figs 124 etc for the central fuel bundle, and Figs 136 etc for the peripheral bundles. However one consequence of reducing the fuel clad gap over the whole length of the fuel rod, as is required by the TRAC simplified fuel rod model, is that the peak temperature during blowdown at the top of the core is now underestimated. This can be seen particularly in the central fuel bundle at all elevations above about 40 inches.

Note   Comparisons of the TRAC calculations with the experimental results for the peripheral bundles is made difficult in

some instances because of an error in the TRAC (v13.0) heat
transfer logic that artificially quenches some rods during
the blowdown period (Ref 18), see for example Fig 146.

An improved fit to the overall blowdwn temperatures could
obviously be made by adjusting the fuel clad gap along the length
of the fuel rods, ie a closed up gap at the bottom and a
partially open one at the top. However for this to be more than
just a "fitting" exercise additional information ought to be
available either from fuel PIE or a fuels code.

In the centre of the core, eg Figs 127, 128, where the "ZERO-GAP"
blowdown peak temperatures are now well-represented, the
calculated temperatures fall to ~ 800K as a result of the bottom-
up core cooling, and subsequently rise to about 850K as the
cooling diminishes and the temperatures across the fuel rod
equalise out. In the experiment the recorded temperatures on the
external thermocouples cool down rapidly to the saturation
temperature as a consequence of the bottom-up liquid flow, but
then rise to ~ 800K as the cooling diminishes and the
temperatures across the rod re-equalise. The average rod
temperature therefore after the blowdown cooling is only some 50K
higher in the "ZERO-GAP" calculation than in the experiment.
This shows therefore that at this elevation the net heat transfer
from the cladding to the coolant is only marginally smaller in
the case of TRAC compared to the experiment. The difference in
the net cooldown of the fuel rod could therefore be well-
accommodated within the uncertainty of the inlet fluid
conditions, without requiring major changes to the TRAC heat
transfer package. The above observations also apply in general
to the lower core elevations, although the difference between the
TRAC "ZERO-GAP" and experiment clad temperatures after the end of
the blowdown cooling are in some instances somewhat higher.

In the upper part of the central fuel bundle and generally across
the peripheral bundles, differences between the calculated and
experimental fluid conditions make comparisons more difficult.
At the 43.8 inch elevation (Fig 131) for example, we see that

(1)   The calculated cladding temperature shows dryout well in
       advance of the experiment.

(2)   As mentioned above the "ZERO-GAP" calculated peak clad
       temperature is lower than the measured value (assumed to be
       due to a partially open gap towards the top of the core).

(3)   In the experiment the bottom-up liquid flow is limited so
       that the temperature of thermocouple does not fall to
       saturation, whereas in the calculation more extensive
       cooling is observed, and finally;

(4)   The rod thermocouple cools to saturation at ~ 19 secs due
       to the top-down flow of liquid from the upper plenum and
       this is not predicted in either calculation except at the
       highest elevation (ie at 62 inches, see Fig 133).

As stated above differences 1, 3 and 4 arise because of
inaccuracies in the calculated core blowdown fluid conditions and
the sensitivity of the thermal response to them, and for this
reason it is not easy to see how to improve the accuracy of the
calculation. However it does go to show that an accurate
calculation of the core blowdown hydraulics is a pre-requisit to
the calculation of the core blowdown cooling.

As a full review of the loop and vessel behaviour is contained in
the previous Section we only comment here on the observed
differences between the two calculations and their relation to
the experimental data. As might be expected there are only minor
differences in both the loop and vessel hydraulic conditions
between the "ORIGINAL" and "ZERO-GAP" calculations. In line with
the comments in the previous Section we see that neither
calculation produces any direct bypass of subcooled ECCS liquid,
whereas the experiment shows subcooled bypass at ~ 31 secs,
estimated to be between 80 and 130 kg. The calculated broken
loop mass flow (Fig 80) also shows that there is no reverse flow,
ie flow from the BST to the reactor vessel in the "ZERO-GAP"
calculation, as there is in the "ORIGINAL" calculation between
~ 42 and 48 secs. This results from the fact that the system
pressure is fractionally higher in the "ZERO-GAP" calculation due
to the increased heat transfer from the core fuel rods to the
coolant.

The calculated intact loop cold leg behaviour during refill, as
explained in the previous Section, is very sensitive to the
details of the calculated transient particularly through the
condensation model and this can then feed back and influence the
vessel refill and early core reflood behaviour. Figs 91 and 92
which show the intact loop cold leg density and mass flow,
upstream of the ECCS injection point, show that there is a
difference in the behaviour of the two calculations during the
refill (accumulator flow) period, with the "ZERO-GAP" calculation
producing some rapid liquid slugs after ~ 38 secs. This movement
and accumulation of the ECCS liquid in the intact loop cold leg,
through the behaviour of the condensation model, then modifies
the subsequent core reflood. An additional consequence of the
different intact loop cold leg behaviour is that the pump in the
"ZERO-GAP" calculation runs down slightly quicker after
~ 45 secs, (Fig 96).

One interesting feature of both the calculation and the
experiment observed in the intact loop cold leg is that following
the exhaustion of the nitrogen from the accumulators, the liquid
begins to accumulate, producing an increase in the intact loop
cold leg density, (Fig 91), at about 85 secs.

Finally the other observable difference between the two
calculations, is that following the end of the accumulator liquid
flow, the pressure drop from the reactor vessel to the BST
produced by the flow of nitrogen steam and water is smaller in
the "ZERO-GAP" calculation than in the "ORIGINAL" calculation.
So that after 55 secs the system pressure (see Fig 114 for
example) is lower in the "ZERO-GAP" calculation. Fig 114 however

also shows that it is now closer to the experimental value. The
difference in this pressure rise results from the different mass
flow and densities calculated along the broken loop cold leg
(Figs 80 and 79) after 55 secs, and these differences result from
the way liquid has accumulated in the intact and broken loop cold
legs and along the top of the downcomer prior to this time.

5(v)   "ZERO-GAP" and "ISHARP" Calculations

The fourth TRAC-PF1/MOD1 calculation ("ISHARP") of experiment
LP-02-6 performed was a repeat of the previous "ZERO-GAP"
calculation (code version UK B03, LANL 13.0) except that the core
interface sharpener logic was bypassed. The reason for carrying
out this calculation was to examine the effect of bypassing this
logic in an integral calculation. Previous analysis of separate
effects reflood experiments (Ref 7) had recommended bypassing
this logic as the best way of modelling the core void fraction
above the quench front and previous plant studies had also shown
that the interface sharpener logic could produce unphysical
liquid holdup in the core during blowdown. As the differences
between the "ZERO-GAP" and "ISHARP" calculations relate to the
core hydraulics, one would expect to see differences primarily in
the core flows and from these differences in the fuel rod
cladding temperatures, and possibly via the heat input to the
fluid from the fuel rods, differences in the loop behaviour.

The results from the two calculations together with the
experimental data, where appropriate are shown in Figs 149 to
219. The most striking feature of the comparison taken as a
whole is that the difference between the two calculations is
relatively small. The resultant cladding temperatures for
example (Figs 195 to 219) are very similar, this just amplifies
the fact that for large break transients performed in LOFT
(primarily because of the size and location of the core) the
cooling of the fuel rods during both blowdown and reflood is
dictated by the system hydraulics in the loops and the vessel
downcomer.

It should be noted, that as for the previous calculations
performed with code verison 13.0, the "ISHARP" calculated
cladding temperatures are subject to the error in the heat
transfer logic (Ref 18) described in the previous Section. (See
for example Figs 195, 206, 207, 212, 213 and 217).

The core inlet and outlet flows together with the core liquid
mass (Figs 185, 186 and 189), show for the ISHARP calculation, as
would be expected, that during blowdown more of the liquid
flowing into the bottom of the core flow out of the top and so
less accumulates in the core. After the flow into the core
during blowdown, liquid re-enters the core just after 30 secs in
both calculations, as the lower plenum fills. After ~ 40 secs
the core flow oscillations for the "ISHARP" calculation increase
in magnitude with the liquid fraction (Fig 190) oscillating
between ~ 0.2 and zero, this is also reflected in the behaviour
of the downcomer and lower plenum volume fractions (Figs 189 and
188), so that the average quantity of liquid in the core after

40 secs is slightly less for the "ISHARP" calculation. Following the end of the accumulator liquid flow at ~ 54 secs the surge of liquid into the core occurs in both calculations, only the absence of the interface sharpener logic in the "ISHARP" calculation allows more of the liquid to flow out of the top of the core and so the mass of liquid retained in the core is slightly less. Also the subsequent oscillations in the core liquid content that result from the fuel rods quenching are greater in magnitude for the "ISHARP" calculation.

As stated above, the above differences in the core hydraulics produce only small changes to the cladding temperatures. At the peak power elevation of the central fuel assembly, Figs 197 to 200, we see that during blowdown the "ISHARP" transient cools somewhat quicker following the bottom-up flow of liquid as liquid flows through the core rather than being retained at the bottom. However the period of cooling is slightly shorter so that the net heat loss from the fuel rod to the coolant is about the same. So that following the blowdown cooling the calculated cladding temperatures in the centre of the core rise to about the same value, ie ~ 50K higher than those in the experiment. If anything the "ISHARP" calculated blowdown temperature transient is in close agreement with the experimental data.

At these elevations (ie 20 to 30 inches) reflood cooling in the calculations begins just prior to 40 secs and although the cladding temperatures level off they do not fall (in the "ISHARP" calculation) until after the "post accumulator" flow of liquid into the core at ~ 54 secs. This just reflects the slightly lower average core liquid content in the "ISHARP" calculation during this period. However following 54 secs the cooling is such that both calculations have near identical quench times.

At the bottom of the central fuel assembly (Figs 195 and 196) the initial dryout of the "ISHARP" calculated fuel rod is delayed, due in part to the heat transfer error described above, so that the resultant cladding temperatures during blowdown are lower than both the "ZERO-GAP" calculation and the experiment. Towards the top of the core (Figs 201 to 204) the overcooling and resultant quenching of the fuel rods due to the bottom-up flow of liquid is even more exaggerated for the "ISHARP" calculation (see Fig 203) and although some influence of the top-down flow of liquid is seen this is not enough to extend the area of quenching below that resulting from the bottom-up liquid flow.

A comparison between the two calculated cladding temperature transients for the peripheral fuel bundles is made almost impossible because of the error in the heat transfer logic described above and in Ref 18. The spurious cooling produced by this error which is restricted to high void fractions is more prevalent in the "ISHARP" calculation than in the other 13.0 calculations because of the changed core hydraulic conditions.

The changes in the loop flows produced by the change in the core hydraulic modelling are very small. As a result of the slightly

lower quantity of heat transferred from the core to the coolant during the early part of reflood the system pressure falls just below that used to represent the BST, so that liquid flows back along the broken loop cold leg at ~ 48 secs. As a consequence of the increased flow out of the top of the core during blowdown for the "ISHARP" calculation one might expect to see a change in the intact and broken loop hot leg flows, and although a small increase in the broken loop hot leg flow is seen (Fig 158) at ~ 9.5 secs the change is very small.

As might be expected there are some changes to the intact loop cold leg behaviour during reflood (Figs 162, 163) but again these are small and the flow of liquid up-stream of the ECCS injection point is limited to a short period of between ~ 38 to 48 secs for both the "ISHARP" and "ZERO-GAP" calculations. These cold leg flow oscillations occur either in part or whole as a consequence of the pressure induced oscillations in the core flow rather than being induced by changes in the cold leg condensation. This contrasts with the experimentally observed intact loop cold leg flow oscillations which extend for most of the accumulator flow period, ie from ~ 21 to 54.5 secs, and must arise at least initially from the condensation of the intact loop steam flow by the subcooled ECCS liquid.

6 SUMMARY AND CONCLUSIONS

This report compares the results of four TRAC-PF1/MOD1 calculations with the experimental data for the LOFT large break experiment LP-02-6. The four calculations compare changes to; code version, ie versions 12.2 and 13.0, fuel pin modelling, ie "as manufactured" and zero steady state fuel clad gap and to core hydraulic modelling, ie with and without the core interface sharpener logic.

The features that distinguish the LOFT LP-02-6 experiment from the previous 200% double-ended cold leg break experiments L2-3 and L2-5 and the subsequent experiment LP-LB-1 were the fact that it was performed at near full power (ie 47 MW) with a relatively low loop flow (248 kg/sec) and therefore a high core ΔT and the fact that the pumps were tripped and allowed to coast down naturally at the start of the transient. This contrasts with L2-3 where the pumps were kept running and L2-5 and LP-LB-1 where the pumps were decoupled from their flywheels at the start of the transient.

The transient was initiated at time zero by the opening of the quick acting blowdown relief valves, and the upper plenum and core rapidly void as subcooled liquid flows out of the broken loop cold leg. As the core voids the reactor power falls and the fuel rods dry out. The cladding temperatures rise as the stored energy in the fuel equalises out across the fuel pin. The subsequent behaviour of the fuel rods during blowdown in LP-02-6 is dictated by the core hydraulics as for the other LOFT large break experiments. The balance of liquid flow into the vessel downcomer is such that after ~ 4 secs there is a net inflow as the broken loop cold leg flow falls, as the system pressure falls

to the 'cold leg' saturation pressure, and the inertia of the pumps produce a flow of liquid along the intact loop cold leg close to the steady state value. The net inflow into the vessel produces a small bottom-up core flow which is enhanced by the flashing of the cold liquid in lower plenum and downcomer. The core flow primarily cools the lower 2/3 rds of the fuel rods - to the extent that the recorded temperatures on the external thermocouples fall to saturation. However in addition to the bottom-up flow there is a significant downflow at about 15 secs, as liquid flowing back along the intact loop hot leg from the pressuriser and the up (hot) side of the steam generator tubes accumulates in the upper plenum. This downflow is sufficient to cool the external thermocouples to saturation at all elevations from the top of the core down to about 30 inches. Therefore the whole of the core is subjected to blowdown cooling either from the bottom-up flow or the top-down flow and the central region from ~ 30 to 40 inches experiences both. This "double" cooling is unique to experiment LP-02-6 and reduces significantly the core stored energy.

There has been considerable speculation as to whether the observed LOFT fuel rod behaviour is indicative of what is happening on the unistrumented fuel rods, and this is currently the subject of a separate investigation. However an indication of the heat removed from the instrumented fuel rods can be obtained from the thermocouple temperatures flowing the blowdown cooling, when the fuel rod temperatures are once again re-equalised. At the peak power elevations, ie between about 24 and 30 inches the cladding temperature rises to ~ 800K.

The primary system pressure falls to the accumulator trip point of 42 bars (600 psi) at about 17.5 secs and accumulator liquid begins to flow into the intact loop cold leg. In line with all the other LOFT large break experiments the measurement rake immediately upstream of the ECCS injection location indicates an oscillatory flow of subcooled liquid along the intact loop cold leg starting at about 21 secs. This flow continues until the flow of accumulator liquid into the intact loop cold leg terminates at ~ 54 secs. The accumulator liquid flows into and down the downcomer filling the lower plenum. The broken loop cold leg measurements supported by the downcomer measurements located on the broken loop side show that there is no continuous bypass of subcooled liquid. However a slug of subcooled liquid is observed to flow along the broken loop cold leg between ~ 29 and 32 secs, the total mass of this slug is estimated to be very roughly about 100 kg; compared to the total accumulator volume of 1.69 m³, ie ~ 1,690 kg. An additional slug of subcooled liquid flows along the broken loop cold leg at ~ 50 secs, again with a total mass of roughly 100 to 150 kg. Because of the small scale of the LOFT facility and therefore the relatively high metal-work heat flux the primary system pressure never falls below that in the BST. So that in addition to the flow of the two slugs of subcooled liquid along the broken loop cold leg there is a flow of two-phase saturated fluid as the liquid in the lower plenum continues to flash and steam and entrained liquid flow from the vessel to the BST.

The lower plenum fills rapidly with ECCS liquid so that the
bottom of the core begins to cool again at ~ 31 secs. Following
this time cooling is observed progressively up the core with a
turnover, in the cladding temperature rise above 30 inches
occurring at about 40 secs. The most noticeable effect observed
by the cladding thermocouples once reflood cooling starts is that
they behave in an oscillatory manner. This is attributed to an
oscillatory core flow which is likely to occur as a result of a
combination of core-steam generation oscillations and intact loop
cold leg condensation induced oscillations. Just as the core
inlet hydraulics determines the fuel rod cooling it also
determines the fuel rod quench. Except at the very bottom of the
core a significant degree of coherency is seen in the fuel rod
quench, for example in the central fuel assembly the 11 inch and
21 inch thermocouples and some of the 15 inch thermocouples all
quench at ~ 46.7 secs, and above 24 inches the final quench
occurs between 54 and 56 secs. The final quench coincides with
the termination of the accumulator liquid flow, and results from
a surge of liquid into the core as the reduction in condensation
and the presence of the accumulator nitrogen causes the intact
loop cold leg pressure to rise. The rise in the intact loop cold
leg pressure also causes some of the ECCS liquid located in the
intact loop cold leg and at the top of the downcomer to flow out
of the broken loop cold leg to the BST. Because of the blowdown
cooling of the core the maximum cladding temperature at ~ 54 secs
when the surge of liquid into the core occurs is only ~ 700K, so
that the whole of the core in experiment LP-02-6 is cooled and
quenched by the liquid from the accumulator.

The results from the four TRAC-PF1/MOD1 calculations bear a large
degree of similarity particulary in their hydraulic behaviour.
They all therefore, in the main, produce the same global
transient and suffer from the same modelling deficiencies. Those
sensitivities performed for a specific reason, eg reducing the
steady state fuel clad gap obviously produced the desired result
of lower cladding temperatures.

In spite of the fact that the calculated transients overestimate
the observed subcooled flow in the broken loop cold leg, flow
into the core after ~ 4 secs extends to the top of the core and
quenches the 62 inch elevation whereas in the experiment the
"quench" only reaches the 45 inch level. However whereas in the
experiment the subsequent top-down liquid flow "quenches" the top
of the core particulary in the peripheral fuel bundles no such
cooling is observed in the calculations. Therefore particularly
towards the top and the bottom of the core the calculated fuel
rod temperatures after blowdown are higher than the experimental
values. In the centre of the core however (ie ~ 24 to 27 inches)
for the "ZERO-GAP" calculations the calculated cladding
temperatures are only about 50K too high showing that the net
heat loss from the fuel rod for the calculations is only slightly
lower than in the experiment.

In all four calculations there is no direct bypass of the ECCS
subcooled liquid so that, as in the experiment, the lower plenum
fills up rapidly with some liquid first entering the bottom of

the core at ~ 28 secs. The subsequent core inlet flow is oscillatory as a result of steam production in the core, and the fuel rods begin to cool at ~ 32 secs at 11 inches and at ~ 39 secs at 21 inches.

One region where there is a difference in the behaviour of the four calculations is in the intact loop cold leg during the accumulator liquid flow period. In some cases liquid slugs form upstream of the ECCS injection point and in other cases not. These differences are attributed to the sensitivity of the TRAC condensation model to small changes in the steam and liquid flows rather than to any specific modelling changes between the four calculations. In none of the calculations however was the calculated flow similar to the experimental observations, and because no bypass was calculated the differences in the calculated intact loop cold leg behaviour only had a very minor effect on the vessel refill and subsequent core reflood.

In all of the calculations a surge of liquid into the core occurs as a result of the pressurisation of the intact loop cold leg as the flow from the accumulator changes from subcooled water to nitrogen. This liquid surge effectively fills the small LOFT core and so the fuel rods cool. The final quench is delayed because the cladding temperatures are at least 80 to 100K higher than the equivalent experimental values and no modelling of the influence of the external thermocouples on the quench process is included in the calculations.

One may conclude therefore that although small variations were observed in the hydraulic behaviour of the four calculations, because no changes were made to the following sensitive areas the general behaviour of all the calculations was the same; ie the nature of a LOFT transient is determined by:

- the blowdown cooling, in which the calculations show too much bottom-up flow and not enought top-down.

- ECCS bypass, none is calculated and only small slugs of direct bypass are observed in the experiment.

- the slug of liquid forced into the core following the termination of the accumulator liquid flow, which is sufficient to cool/quench the whole of the "short" LOFT core.

The thermal response of the core to the above hydraulics is of course different for the different calculations, with those calculations with the reduced fuel stored energy (ie zero fuel clad gap) producing results closest to the experiment. However the very limited fuel pin model available in TRAC restricts the modelling ability to better simulate the observed thermocouple behaviour.

7   ACKNOWLEDGEMENTS

LOFT from that used in the previous analysis of experiment
LP-LB-1 and who performed the first of the calculations analysed
in the report.

8 REFERENCES

(1)   J P Adams, K G Condie, D I Blatt. Quick-Look Report on
       OECD LOFT Experiment LP-02-6. OECD LOFT-T-3404,
       October 1983.

(2)   P Coddington. Analysis of LOFT Experiment LP-LB-1 Using
       the TRAC-PF1/MOD1 Code. UKAEA Internal Publication.

(3)   J Birchley. Modifications to the TRAC-PF1/MOD1 Input
       Models for LOFT. UKAEA Internal Publication, March 1986.

(4)   M Blackmore, J Birchley. Modelling of LOFT ECC Injection
       Line for TRAC-PF1/MOD1. UKAEA Internal Publication, May
       1986.

(5)   J Birchley. Heat Structures for the 3-D Vessel
       Representation of LOFT with TRAC-PF1/MOD1. UKAEA Internal
       Publication.

(6)   J Birchley, P Coddington. Post Experimental Analysis of
       OECD-LOFT Experiment LP-02-6 with TRAC-PF1/MOD1. To be
       published.

(7)   R O'Mahoney. A Study of the Reflood Characteristics of
       TRAC-PF1/MOD1. AEEW - M 2305, April 1986.

(8)   E M Feldman. OECD LOFT Project Experiment Specification
       Document, Cold Leg Break Experiment LP-02-6.
       OECD LOFT-T-3402, July 1983.

(9)   Private Communication. Letter: P Coddington to
       Salih Guntay, EIR Switzerland, July 1987.

(10)   TRAC-PD2 Independent Assessment.
       NUREG/CR-3866, LA-10166-MS, December 1984. Pages 234 to
       291.

(11)   T D Knight. TRAC Analysis of LOFT LP-02-6. LA-UR-85-3723,
       October 1985.

(12)   A B Wahba. Emergency Core Coolant Systems and Their
       Effectiveness in Large Break LOCA.
       Paper presented to the OECD-LOFT Specialist Meeting on
       Large Break LOCA, 24-27 March 1987, Grindelwald,
       Switzerland.

(13)   P Coddington. Comments on the Accumulator Nitrogen
       Injection Phase of a Large Cold Leg Break PWR
       Loss-of-Coolant Accident. UKAEA Internal Publication,
       August 1986.

(14)   S N Aksan. Evaluation of Analytical Capability to Predict
       Cladding Quench. EGG-LOFT-5555, August 1982.

and

R C Gottula. Effects of Cladding Surface Thermocouples and
Electrical Heater Rod Design on Quench Behaviour.
NUREG/CR-2691, February 1984.

(15) S Yanar, S Guntay. Effect of External Thermocouples on
Quench Temperatures Evidence From NEPTUN Reflooding
Experiments. Paper presented at the OECD-LOFT Specialist
Meeting on Large Break LOCA, Grindelwald, Switzerland.
24-27 March 1987.

G Class et al. Measurement of Cladding Temperatures with
Loss-of-Fluid-Test Thermocouples in the COSIMA Blowdown
Test Facility. Nuclear Technology, Vol 69 (April 1985)
p 72.

and

G L Shires et al. An Experimental Study of the Effect of
External Thermocouples on Rewetting During Reflood.
AEEW - R 1357.

(16) R O'Mahoney, C Gill, P Coddington. Status of the high and
Low Pressure Quenching Studies at AEEW, Spetember 1987.
UKAEA Internal Publication.

(17) P Coddington. The Effect of Accumulator Nitrogen on the
Reflood of a PWR Core During a Large Break LOCA.
Paper presented to the IAEA Specialist Meeting on Fuel
Behaviour Under Accident Conditions and Acceptance
Creiteria, 30 September-4 October 1985, Warsaw, Poland.

(18) Private Communication. Letters: P Coddington to R Jenks,
LANL, USA. 29 January 1987, and 7 and 24 April 1987.

TABLE 1

TRAC CALCULATIONS

NO	LABEL	CODE VERSION		FUEL CLAD GAP WIDTH	INTERFACE SHARPENER LOGIC
		LANL	UK		
1	"JONS"	12.2	X26	100 μon	Yes
2	"ORIGINAL"	13.0	B03	100 μon	Yes
3	"ZERO-GAP"	13.0	B03	0.0	Yes
4	"ISHARP"	13.0	B03	0.0	No

AEEW - M 2464

TABLE 2

INITIAL CONDITIONS FOR EXPERIMENT LP-02-6

Parameter	TRAC Calculated Value	Experimental Value
Primary Coolant System		
Temperature across core (K)	34.5	33.1±1.4
Hot leg pressure (MPa)	15.04	15.09±0.08
Cold leg temperature (K)	556.7	555.9±1.1
Mass flow rate (Kg/s)	248.1	248.7±2.6
Primary coolant pump injection (both pumps) (ℓ/s)	0.0	0.092±0.003
Core bypass pipe flow (Kg/s)	6.5	
Hot leg nozzles bypass flow (Kg/s)	5.6	Not measured directly
Reflood assist valve flow rate (Kg/s)	13.1	
Total core bypass flow (Kg/s)	25.2	
Reactor Vessel		
Power level	47.0	46.0±1.2
Maximum line heat generation rate (KW/ft)	15.07 (Av rods) 16.20 (Peak rods)	14.9±1.1
Steam generator secondary side		
Pressure (MPa)	5.62	-
Steam generator feedwater flow rate (Kg/s)	2.53	-
Pressuriser		
Liquid volume (m³)	0.555	0.607±0.02
Steam volume (m³)	0.376	0.39±0.02

AEEW - M 2464

TABLE 2 (Continued)

Water temperature (K)	615.4	615.6±5.8
Pressure (MPa)	15.03	15.3±0.11
Liquid level (m)	1.26	1.04±0.04

Broken Loop

Cold leg temperature (K)	556.7	553±6
Hot leg temperature (K)	556.1	560±6
Reflood assist valve leak flow rate (Kg/s)	13.1	-

Suppression Tank

Pressure (gas space) (KPa)	15.04	

Emergency Core Cooling System

Accumulator liquid level (m)	1.05	-
Accumulator liquid volume (m^3)	1.315 (tank)	1.2360
	0.36 (line)	0.4559
Accumulator gas volume (m^3)	0.642	0.9506
Accumulator pressure (MPa)	4.11	4.11±0.06
Accumulator liquid temperature (K)	302.0	302±6.1
High pressure injection flow rate (ℓ/s)	1.50	1.04±0.04
High pressure injection liquid temperature (K)	302.1	305±7
Low pressure injection flow Rate (ℓ)	3.5	-
Low pressure injection liquid temperature (K)	302.9	305±7

AEEW - M 2464

31

TABLE 3

CHRONOLOGY OF EVENTS FOR EXPERIMENT LP-C2-6

Event	TRAC Calculated Value	Experimental Value
Blowdown valves opened	0.0	0
End of sub-cooled blowdown	0.05	0.05±0.05
Reactor scrammed	-	0.1±0.01
Primary coolant pumps tripped	0.8	0.8±0.01
Cladding temperatures initially deviated from saturation	0.32	0.9±0.01
End of sub-cooled break flow	4.9	4.0±0.5
Maximum cladding temperature (1061 K @ 24 in) reached (blowdown)	4.6	4.9±0.2
Bottom-up core rewet initiated	4.2	5.2±0.2
Bottom-up core rewet complete	13.1	9.1±0.2
Partial core top-down quench initiated		14.8±0.02
Pressuriser emptied	13.6	15.5±0.5
Primary coolant pumps disconnected from flywheels	-	16.5±0.01
Accumulator injection initiated	16.6	17.5±0.5
Partial core top-down quench complete		18.6±0.2
High pressure injection initiated	22.0	21.8±0.01
Lower plenum refill complete (from void)	26.5 to 48.2	
Lower plenum refill complete (thermocouple)	28.7	30.7±0.2
Low pressure injection initiated	35.1	34.8±0.01

TABLE 3 (Continued)

Maximum cladding temperature (929.7 K @ 24 in) reached (reflood)	40.5	41 ± 0.2
Accumulator empty	48.0	
Accumulator injection complete	53.0	57 ± 5[a]
Core quench complete	91.1	56 ± 0.2

[a] Ref 1 calculates the accumulator injection complete time by extrapolating from the time the accumulator is empty to the time the connecting piping is empty assuming a constant mass flow

TABLE 4

CORE AXIAL FINE MESH ELEVATIONS AND RELATIVE POWER DENSITY

Fine Mesh	Height Metres	Inches	Power Density
* 1	0.0	0.0	0.59415
2	0.07625	3.0	
3	0.1525	6.0	
4	0.22875	9.0	
* 5	0.305	12.0	1.35550
6	0.362	14.25	
7	0.419	16.50	
8	0.476	18.75	
* 9	0.533	21.00	1.54060
10	0.59025	23.25	
11	0.6475	25.50	
12	0.70475	27.75	
* 13	0.762	30.00	1.47230
14	0.87625	34.5	
15	0.9905	39.0	
16	1.10475	43.5	
* 17	1.219	48.0	0.78851
18	1.33325	52.5	
19	1.4475	57.0	
20	1.56175	61.5	
* 21	1.676	66.0	0.029708

* Fluid dynamic cell boundaries

AEEW - M 2464

34
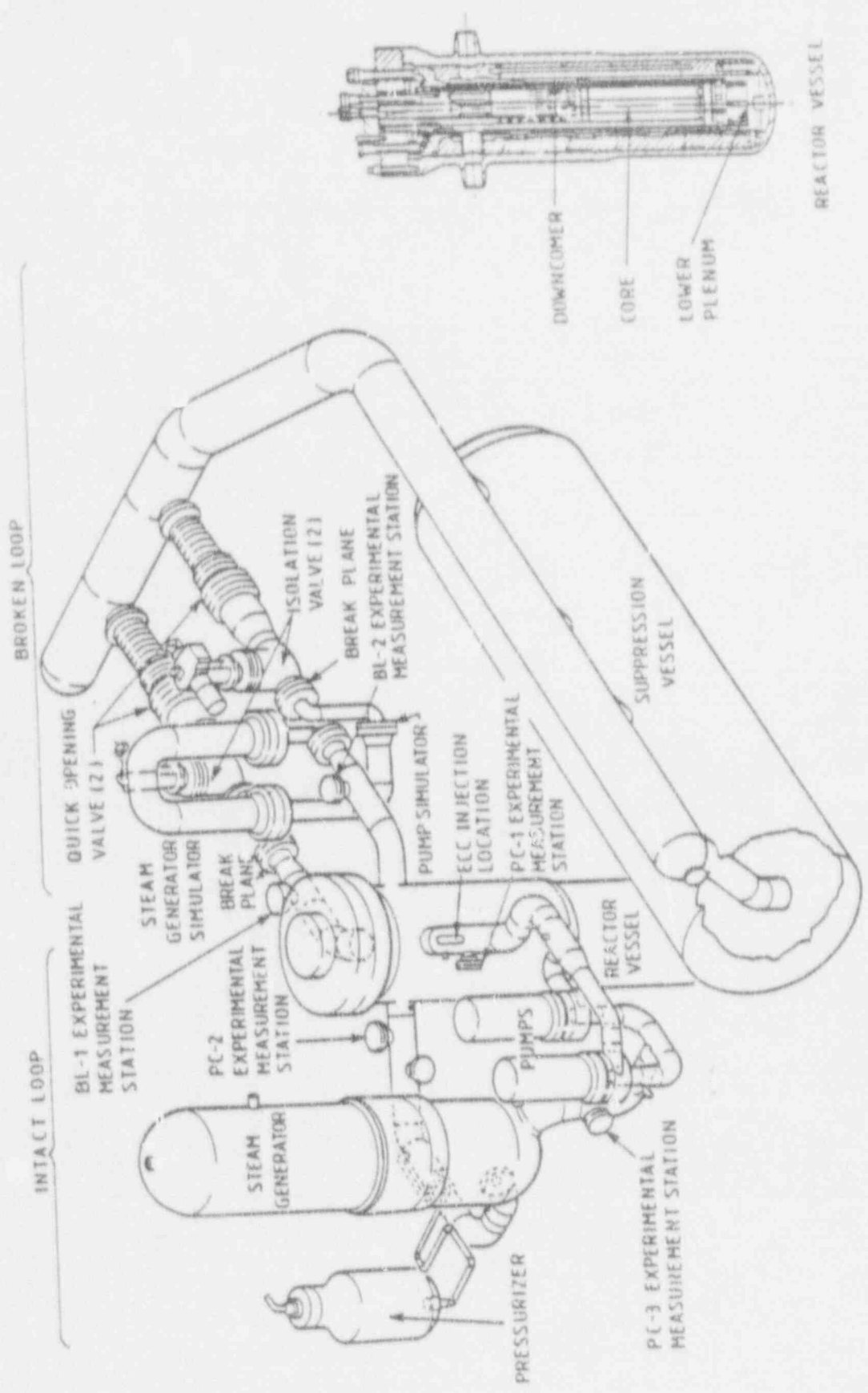
FIG.1. MAJOR COMPONENTS OF LOFT SYSTEM

FIG. 2. LOFT PIPING SCHEMATIC WITH INSTRUMENTATION

FIG. 3. INTACT LOOP NODALISATION

COMPONENT NUMBERS

JUNCTION NUMBERS

REFLOOD ASSIST
BYPASS VALVE

STEAM
GENERATOR
SIMULATOR

BROKEN LOOP
HOT LEG

BL-2

PUMP
SIMULATOR

BREAK
PLANE

BREAK

BROKEN LOOP
COLD LEG

BL-1

BREAK

BREAK
PLANE
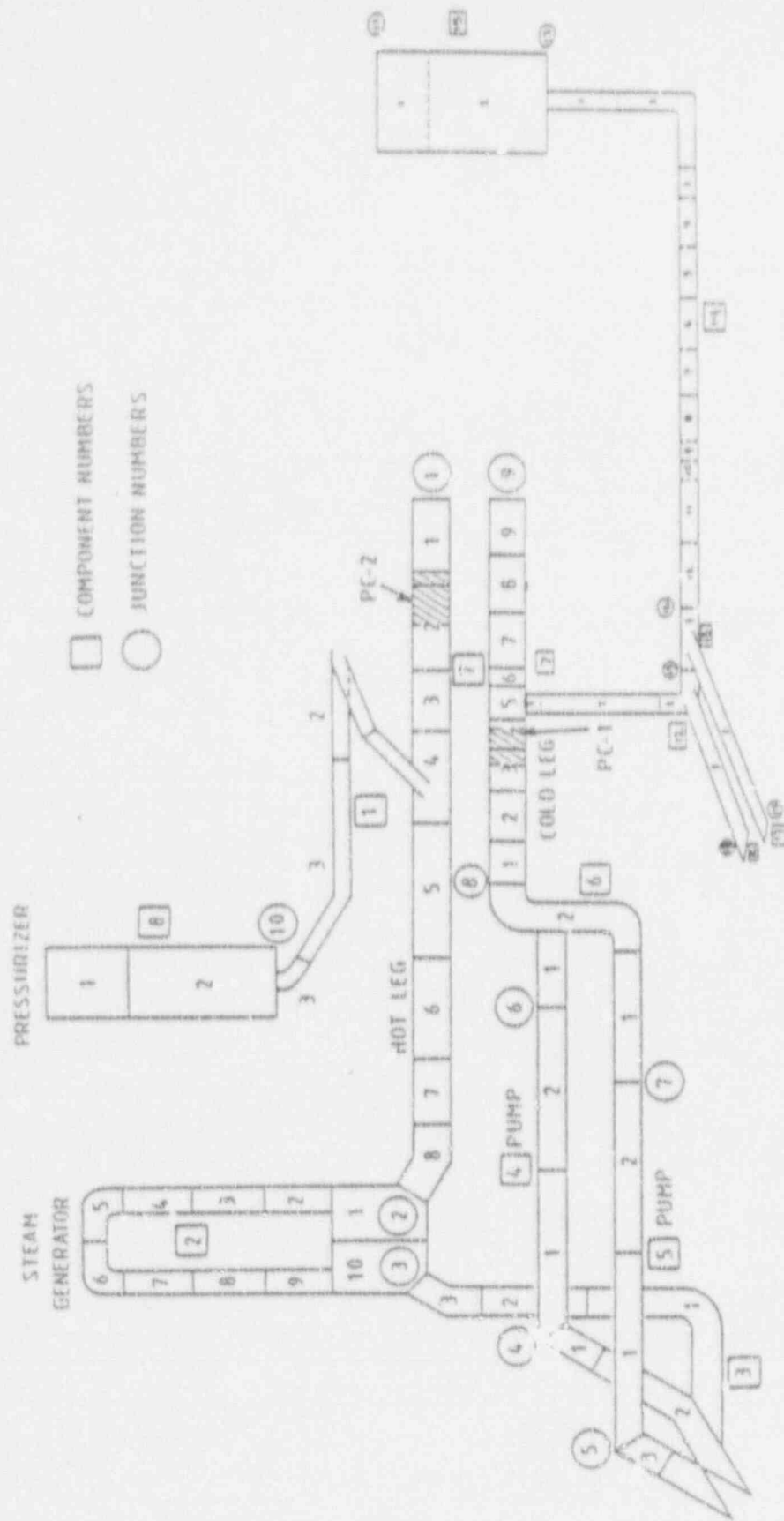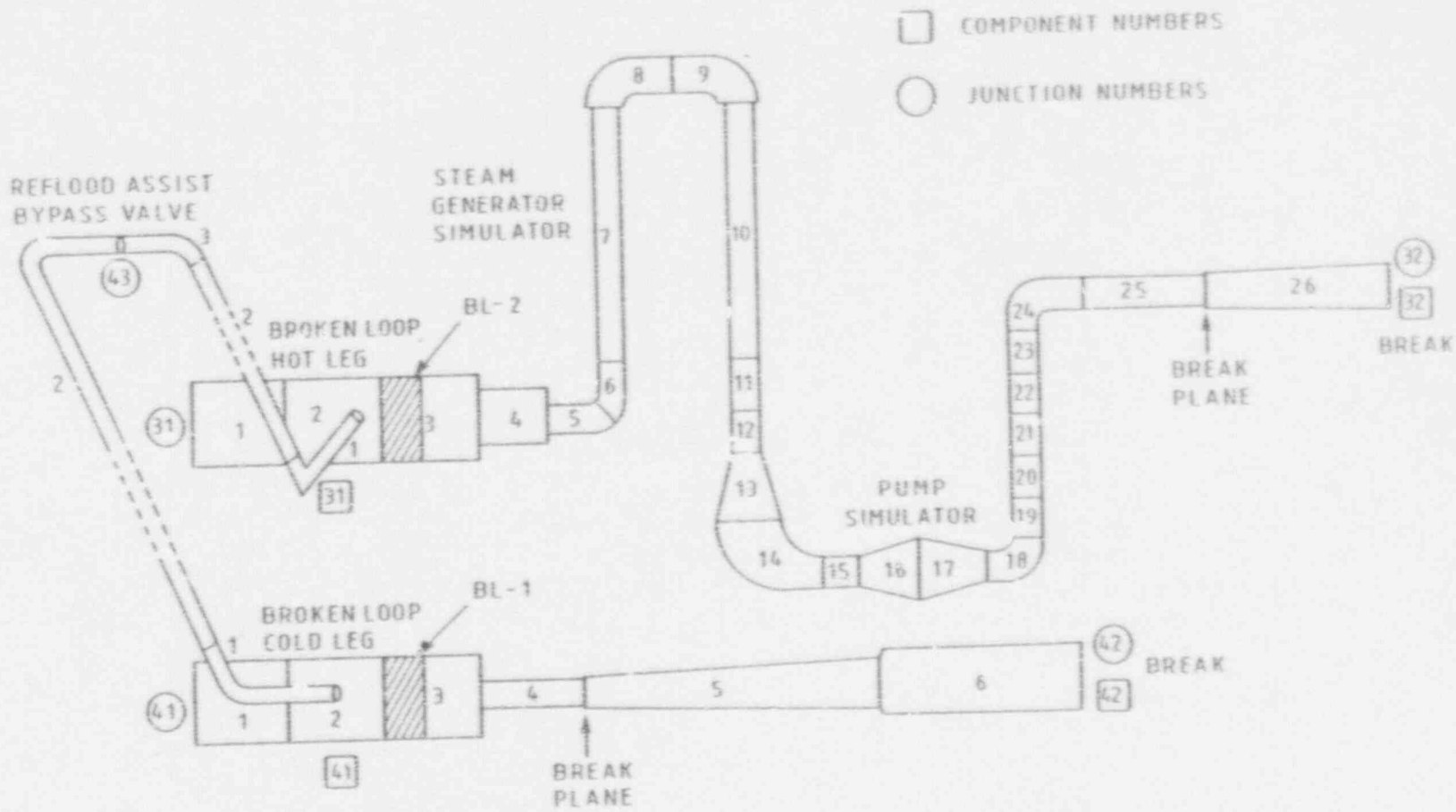
FIG. 4. BROKEN LOOP NODALIZATION
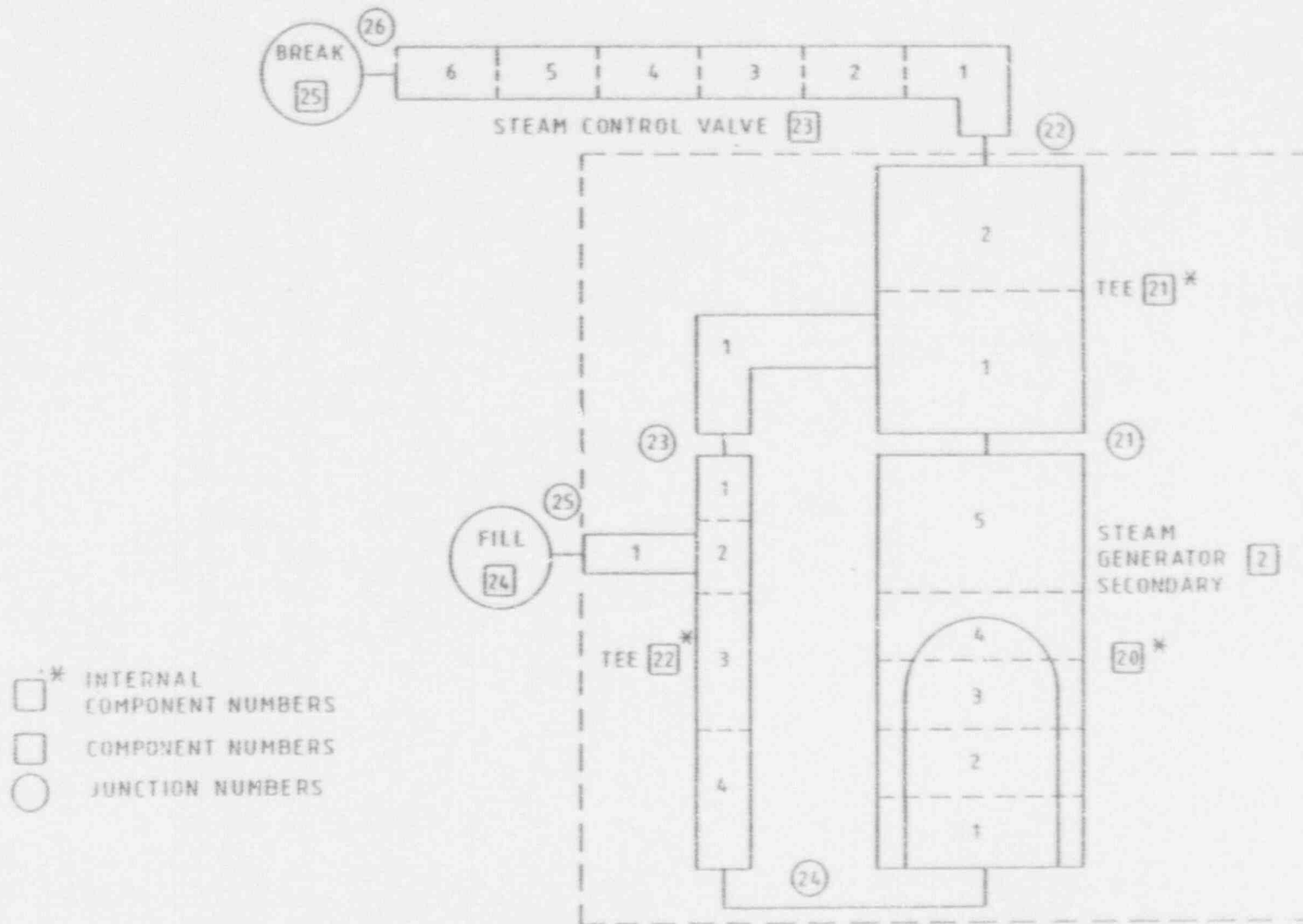
FIG. 5. STEAM GENERATOR SECONDARY NODALIZATION

The top of level 3, third radial ring, is linked for each of the four azimuthal sectors to the bottom of level 11 (rings 2 and 3) by four TEE components. The horizontal side arms of the TEEs are connected to the outer surface (ring 3) of level 8.

The arrangement is such that Bypass TEE Components 101 and 103 are connected to $r = 3$, $\theta = 1$ (3) at levels 3 and 11, while Bypass TEE Components 102 and 104 are connected to $r = 3$, $\theta = 2$ (4) at level 3 and $r = 2$, $\theta = 2$, (4) at level 11. (This is to allow for the Upper Plenum Hot Leg connections in radial ring 3 azimuthal sectors 2, 4 at level 11).
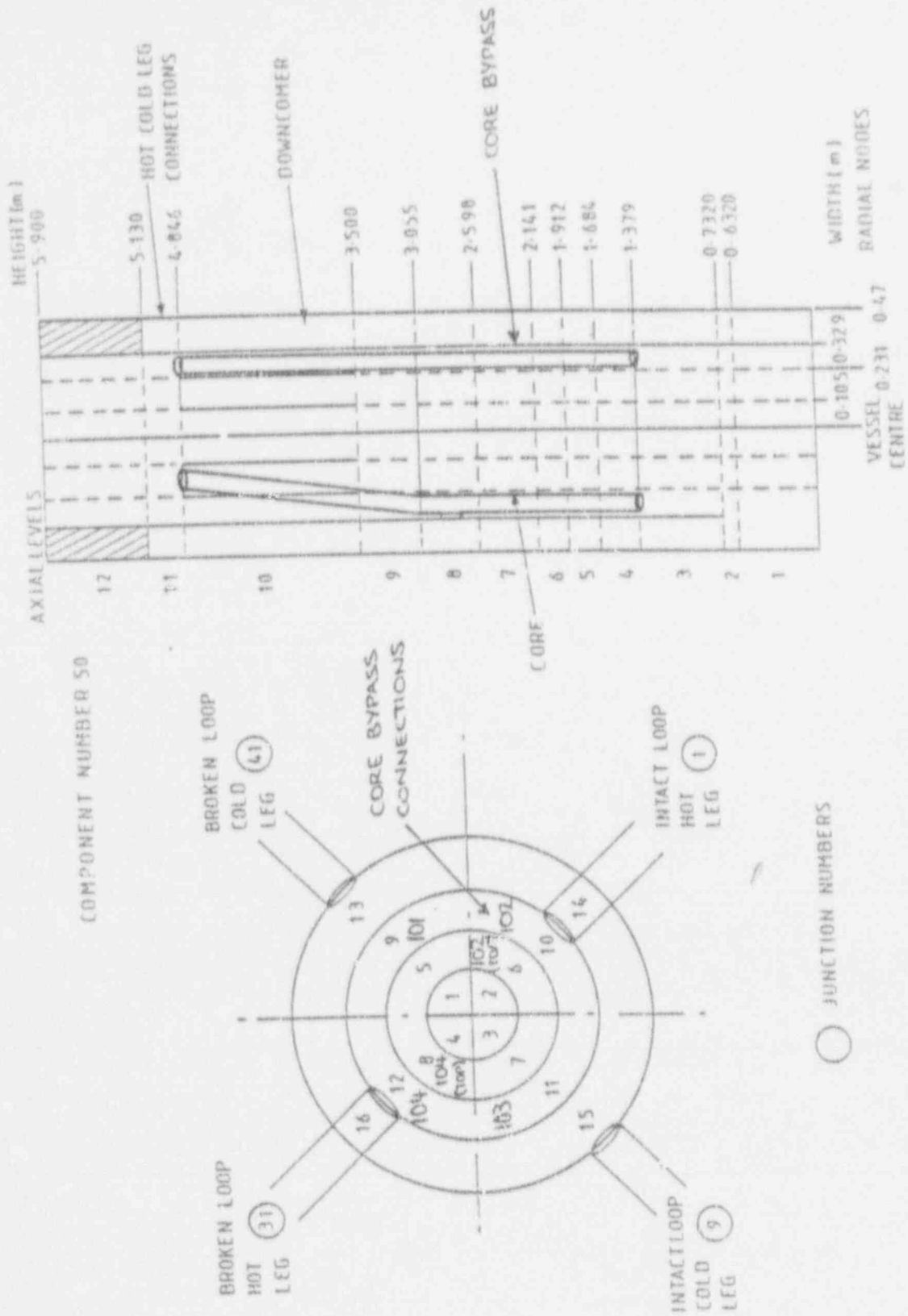
FIG. 61 REACTOR VESSEL NODALISATION
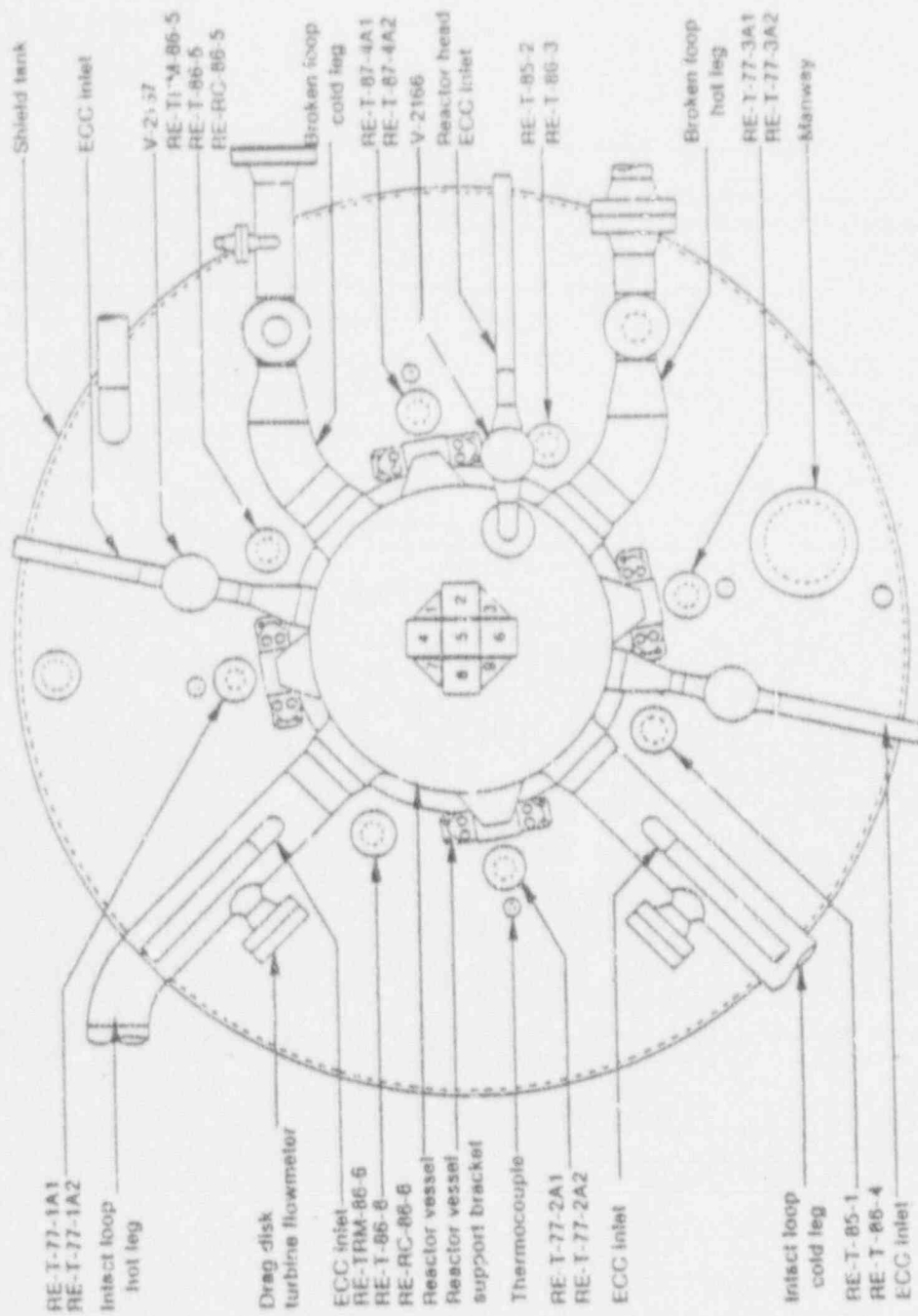
Figure 6.11 Reactor Vessel Instrument Locations

Labels (upper/right side, reading around the diagram):
- Shield tank
- ECC inlet
- V-2157
- RE-T-4-86-5
- RE-T-86-5
- RE-RC-86-5
- Broken loop cold leg
- RE-T-87-4A1
- RE-T-87-4A2
- V-2166
- Reactor head
- ECC inlet
- RE-T-85-2
- RE-T-86-3
- Broken loop hot leg
- RE-T-77-3A1
- RE-T-77-3A2
- Manway

Labels (lower/left side):
- RE-T-77-1A1
- RE-T-77-1A2
- Intact loop hot leg
- Drag disk turbine flowmeter
- ECC inlet
- RE-TRAA-86-6
- RE-T-86-8
- RE-RC-86-6
- Reactor vessel
- Reactor vessel support bracket
- Thermocouple
- RE-T-77-2A1
- RE-T-77-2A2
- ECC inlet
- Intact loop cold leg
- RE-T-85-1
- RE-T-86-4
- ECC inlet

PRESSURE   ,PE-BL-001
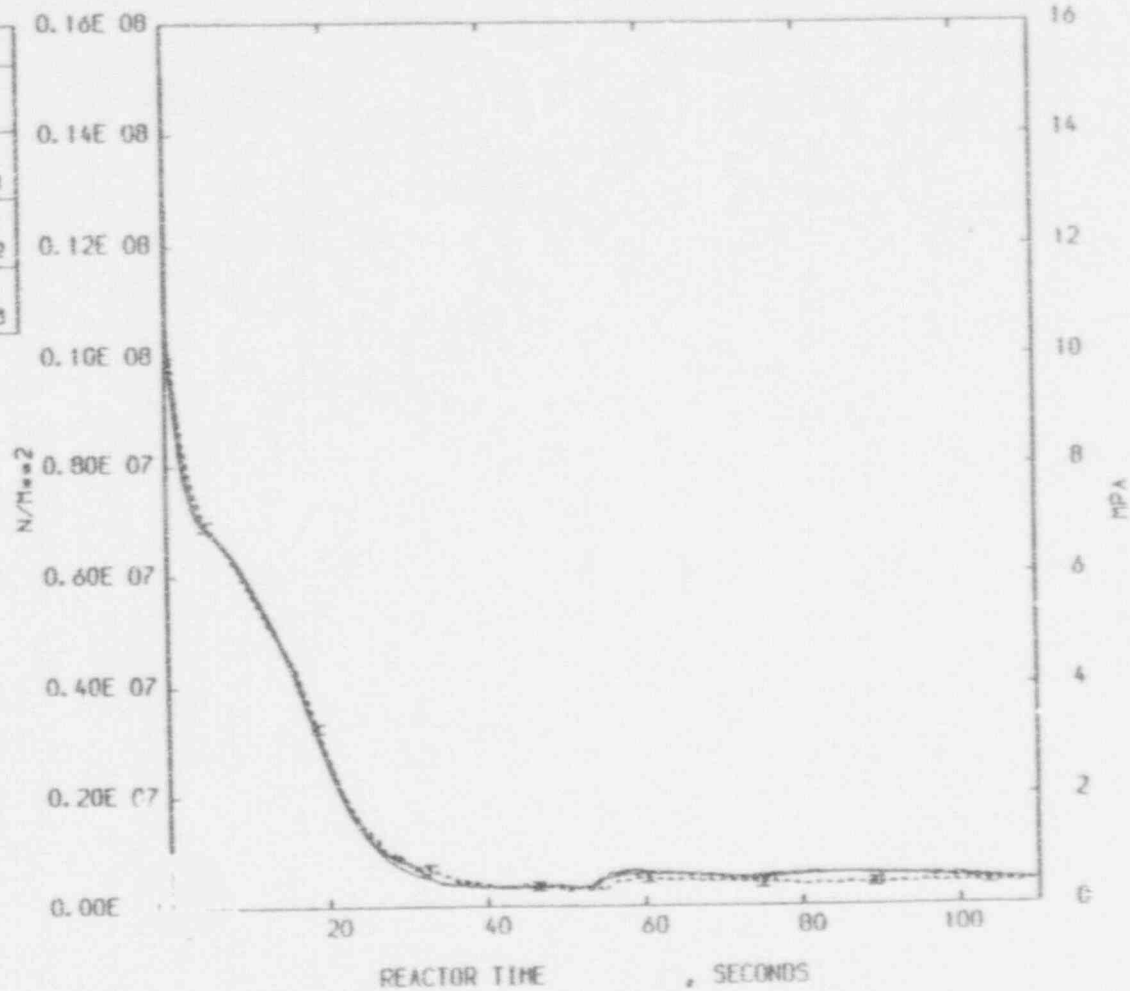
FIGURE 7   INF 1 JON'S, INF 2 ORIG, INF 3 EXP
BROKEN LOOP COLD LEG - EXPERIMENTAL LOCATION BL-1

THE FOLLOWING ARE PLOTTED AGAINST REACTOR TIME

MIXTURE DENSITY ,DE-BL-001A

SYM BOL	NAME	UNITS
	MIXTURE DENSITY	,KG/M**3
	LOC= 41/ 0/ 3 MXTR-DENM INF=1	
	MIXTURE DENSITY	,KG/M**3
	LOC= 41/ 0/ 3 MXTR-DENM INF=2	
	DE-BL-001A	,MG/M**3
	LOC= 7/ 0/ 0 MXTR-DENM INF=3	

KEY

MG/M**3

KG/M**5

REACTOR TIME , SECONDS

FIGURE 8 INF 1 JON'S, INF 2 ORIG, INF 3 EXP
BROKEN LOOP COLD LEG - EXPERIMENTAL LOCATION BL-1

AEEW - M 2464

44

AEEW - M 2464

45

KEY

SYM BOL	NAME	UNITS
——	MASS FLOW RATE	,KG/SEC
	LOC= 41/ 0/ 3 MNEM=FLOW INF=1	
——	MASS FLOW RATE	,KG/SEC
	LOC= 41/ 0/ 3 MNEM=FLOW INF=2	
----	FR-BL-105	,KG/SEC
	LOC= 32/ 0/ 0 MNEM=FLOW INF=3	
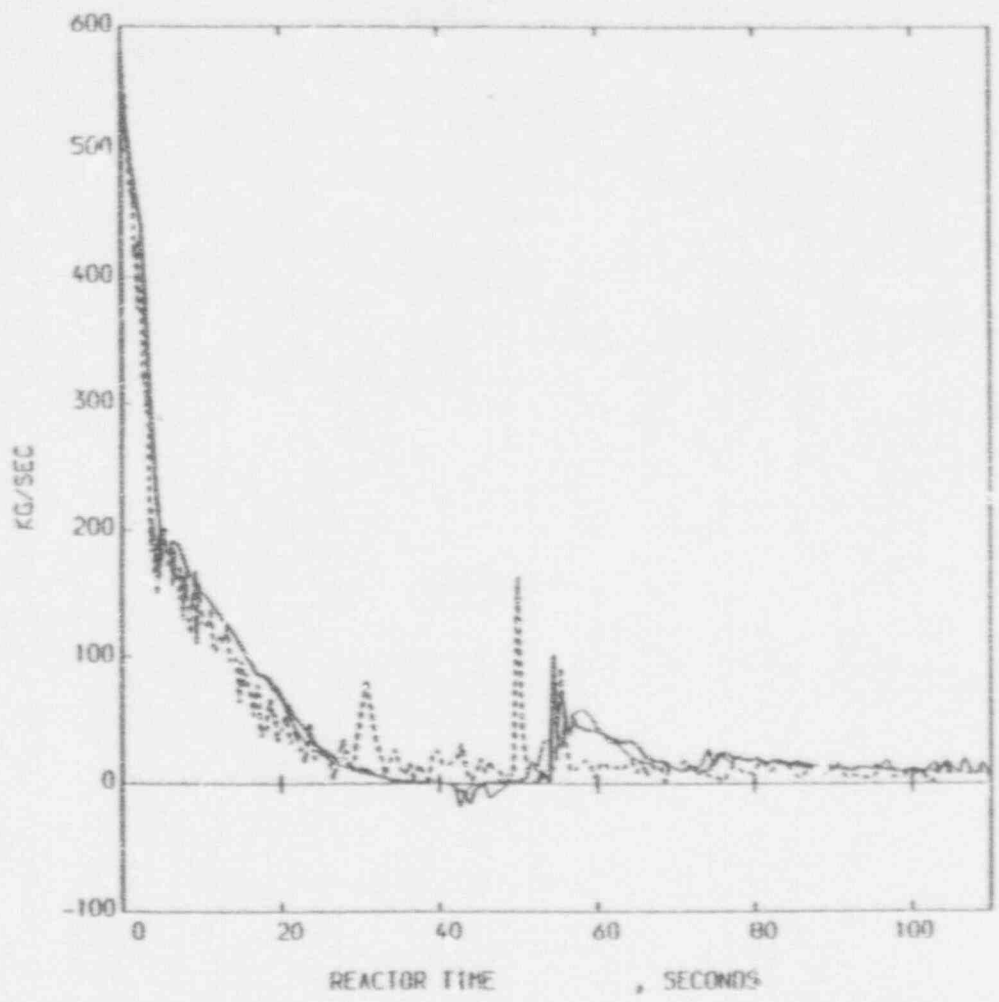
FIGURE 9   INF 1 JON'S, INF 2 ORIG, INF 3 EXP
BROKEN LOOP COLD LEG – EXPERIMENTAL LOCATION BL-1

THE FOLLOWING ARE PLOTTED AGAINST REACTOR TIME

LIQUID TEMPERATURE ,TE-BL-001A

560

540

520

500

480

460

440

420

400

380

DEG. K

0   20   40   60   80   100

REACTOR TIME   , SECONDS

FIGURE 10   INF 1 JOIN'S, INF 2 ORIG, INF 3 EXP

BROKEN LOOP COLD LEG — EXPERIMENTAL LOCATION BL-1

KEY		
SYM BOL	NAME	UNITS
——	LIQUID TEMPERATURE ,DEG.K LOC= 4/ 0/ 3 MACH=TEMP INF=1	
——	LIQUID TEMPERATURE ,DEG.K LOC= 4/ 0/ 3 MACH=TEMP INF=2	
----	TE-BL-001A ,DEG.K LOC= 17/ 0/ 0 MACH=TEMP INF=3	

Winfrith
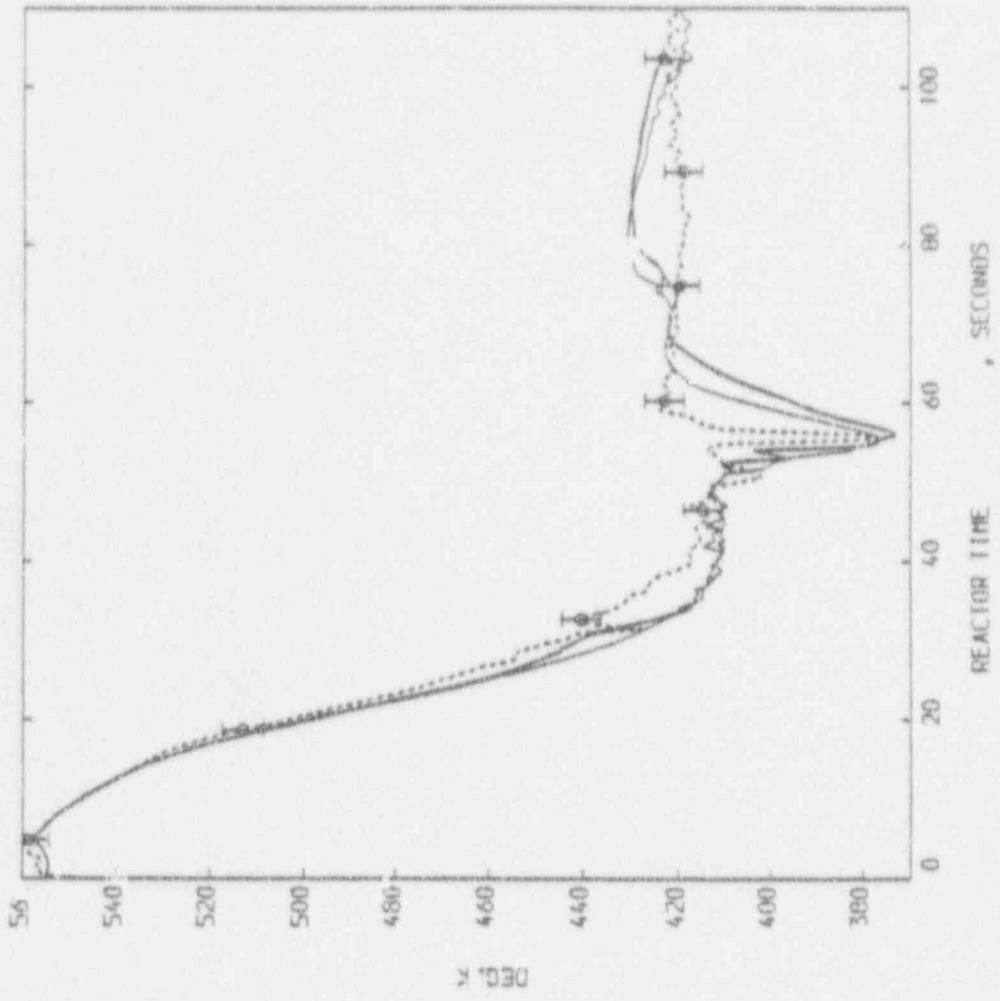
THE FOLLOWING ARE PLOTTED AGAINST REACTOR TIME

VAPOR TEMPERATURE ,TE-BL-001C

	KEY	
SYM BOL	NAME	UNITS
	VAPOR TEMPERATURE ,DEG.K	
	LOC= 41/ 0/ 3 MREH-TEMV INF-1	
	VAPOR TEMPERATURE ,DEG.K	
	LOC= 41/ 0/ 3 MREH-TEMV INF-2	
	TE-BL-001C ,DEG.K	
	LOC= 173/ 0/ 0 MREH-TMCL INF-3	

DEG, K

REACTOR TIME , SECONDS

FIGURE 11 INF 1 JON'S, INF 2 ORIG, INF 3 EXP
BROKEN LOOP COLD LEG - EXPERIMENTAL LOCATION BL-1

FIGURE 12 INF 1 JON'S, INF 2 ORIG, INF 3 EXP
BROKEN LOOP COLD LEG - EXPERIMENTAL LOCATION BL-4

FIGURE 13 INF 1 JUN'S, INF 2 ORIG, INF 3 EXP
BROKEN LOOP COLD LEG - EXPERIMENTAL LOCATION BL-8

THE FOLLOWING ARE PLOTTED AGAINST REACTOR TIME

PRESSURE ,PE-BL-002

MPA

16

14

12

10

8

6

4

2

0

REACTOR TIME , SECONDS

0.16E 08

0.14E 08

0.12E 08

0.10E 08

0.80E 07

0.60E 07

0.40E 07

0.20E 07

0.00E 00

N/M**2

KEY

SYM BOL	NAME	UNITS
——	PRESSURE	,N/M**2
	LOC= 31/ 0/ 3 MNEM=PRES INF=1	
——	PRESSURE	,N/M**2
	LOC= 31/ 0/ 3 MNEM=PRES INF=2	
----	PE-BL-002	,MPA
	LOC= 116/ 0/ 0 MNEM=PRES INF=3	

FIGURE 14 INF 1 JON'S, INF 2 ORIG, INF 3 EXP
BROKEN LOOP HOT LEG - EXPERIMENTAL LOCATION BL-2

AEEW - M 2464

50

THE FOLLOWING ARE PLOTTED AGAINST REACTOR TIME

MIXTURE DENSITY ,DE-BL-002A
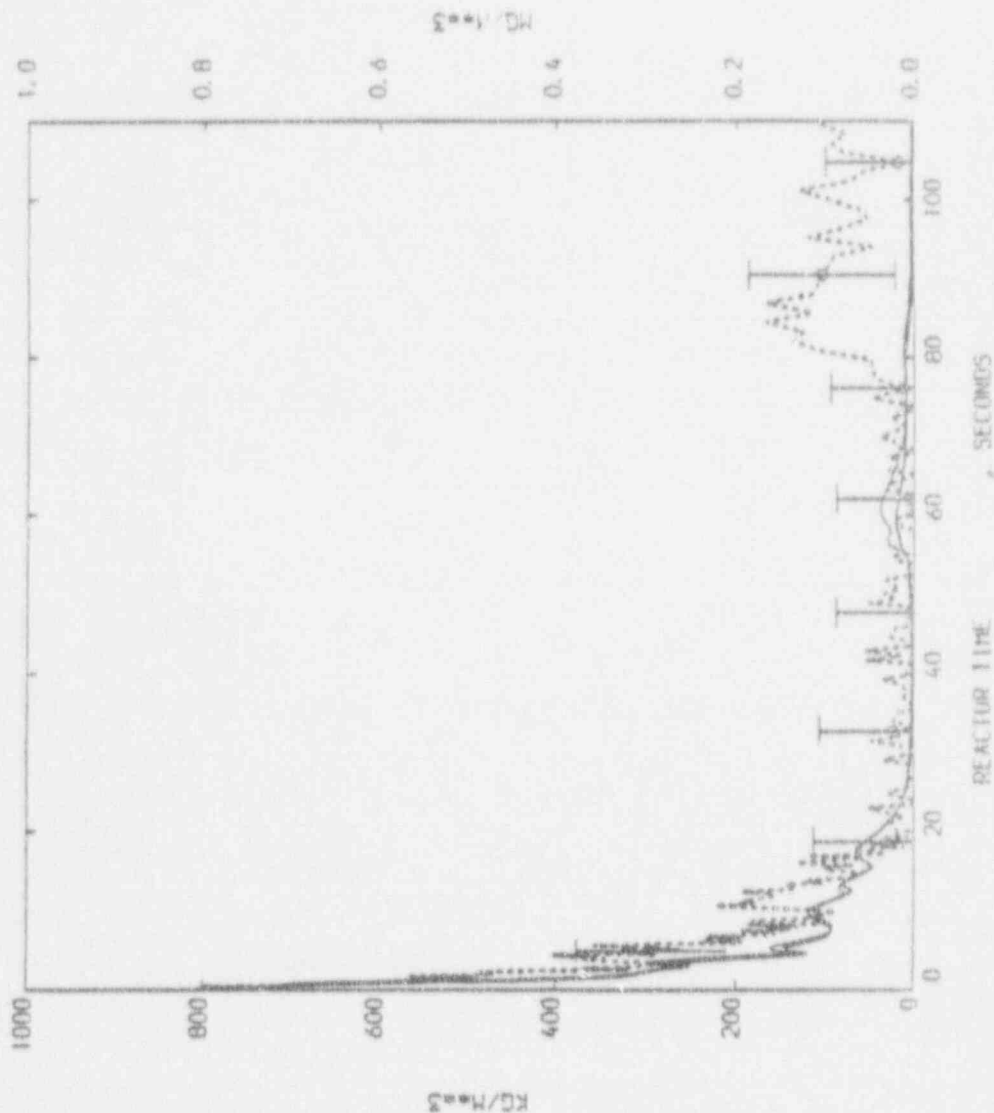
Winfrith

KEY

SYM BOL	NAME	UNITS
	MIXTURE DENSITY ,KG/M**3 LOC= 31/ 0/ 3 MNEM=DENM INF=1	
	MIXTURE DENSITY ,KG/M**3 LOC= 31/ 0/ 3 MNEM=DENM INF=2	
	DE-BL-002A ,MG/M**3 LOC= 9/ 0/ 0 MNEM=DENM INF=3	

FIGURE 15 INF 1 JON'S, INF 2 URIG, INF 3 EXP

BROKEN LOOP HOT LEG - EXPERIMENTAL LOCATION BL-2

THE FOLLOWING APE PLOTTED AGAINST REACTOR TIME

MASS FLOW RATE   ,FR-BL-205

APEW : M 2464

52

KEY		
SYM BOL	NAME	UNITS
——	MASS FLOW RATE	,KG/SEC
	LOC= 31/ 0/ 3 MNEM=FLOW INF=1	
—	MASS FLOW RATE	,KG/SEC
	LOC= 31/ 0/ 3 MNEM=FLOW INF=2	
----	FR-BL-205	,KG/SEC
	LOC= 33/ 0/ 0 MNEM=FLOW INF=3	

KG/SEC

REACTOR TIME   , SECONDS
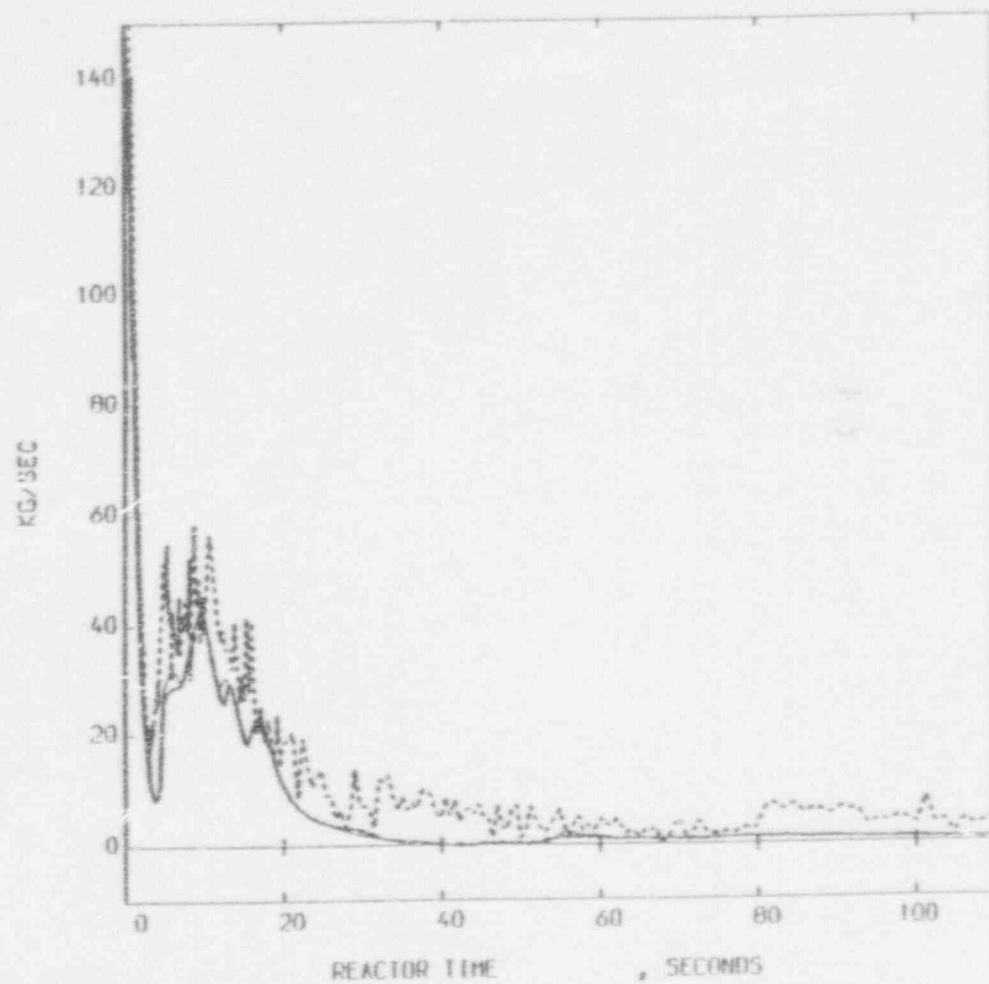
FIGURE 16   INF 1 JON'S, INF 2 ORIG, INF 3 EXP
BROKEN LOOP HOT LEG - EXPERIMENTAL LOCATION BL-2

THE FOLLOWING ARE PLOTTED AGAINST REACTOR TIME

LIQUID TEMPERATURE , TE-BL-002B

Winfrith

KEY		
SYM BOL	NAME	UNITS
——	LIQUID TEMPERATURE , DEG. K	
LOC= 31/ 0/ 3 MNEM=TEML ENF=1		
——	LIQUID TEMPERATURE , DEG. K	
LOC= 31/ 0/ 3 MNEM=TEML ENF=2		
----	TE-BL-002B , DEG. K	
LOC= 174/ 0/ 0 MNEM=THCL ENF=3		

DEG. K

REACTOR TIME , SECONDS

FIGURE 17   INF 1 JCV'S, INF 2 ORIG, INF 3 EXP

BROKEN LOOP HOT LEG - EXPERIMENTAL LOCATION BL-2

THE FOLLOWING ARE PLOTTED AGAINST REACTOR TIME

VAPOR TEMPERATURE , TE-BL-002B , TE-BL-002C

DEG. K

REACTOR TIME , SECONDS

KEY

SYM BOL	NAME	UNITS
	VAPOR TEMPERATURE , DEG K	
	LOC= 31/ 0/ 3 MAEA-TEMV INF=1	
	VAPOR TEMPERATURE , DEG K	
	LOC= 31/ 0/ 3 MAEA-TEMV INF=2	
	TE-BL-002B , DEG K	
	LOC= 174/ 0/ 0 MAEA-TMCL INF=3	
	TE-BL-002C , DEG K	
	LOC= 175/ 0/ 0 MAEA-TMCL INF=3	

FIGURE '8 INF 1 JRN'S, INF 2 ORIG, INF 3 EXP.
BROKEN LOOP HOT LEG - EXPERIMENTAL LOCATION BL-2

AEEW - M 2464

54

THE FOLLOWING ARE PLOTTED AGAINST REACTOR TIME

PRESSURE   ,PE-BL-003

FIGURE 19 INF 1 JON'S, INF 2 ORIG, INF 3 EXP
BROKEN LOOP HOT LEG - EXPERIMENTAL LOCATION BL-3

MPA

16
14
12
10
8
6
4
2
0

REACTOR TIME   , SECONDS

N/M**2

0.16E 08
0.14E 08
0.12E 08
0.10E 08
0.80E 07
0.60E 07
0.40E 07
0.20E 07
0.00E 00

KEY:

SYMBOL	NAME	UNITS
——	PRESSURE LOC= 31/ 0/ 17 MNEM=PRES INF=1	,N/M**2
——	PRESSURE LOC= 31/ 0/ 17 MNEM=PRES INF=2	,N/M**2
----	PE-BL-003 LOC= 115/ 0/ 0 MNEM=PRES INF=3	,MPA

AEEW - M 2464

55

FIGURE 20 INF 1 JON'S, INF 2 ORIG, INF 3 EXP
INTACT LOOP COLD LEG - EXPERIMENTAL LOCATION PC-1

THE FOLLOWING ARE PLOTTED AGAINST REACTOR TIME

MASS FLOW RATE   ,FR-PC-100

FIGURE 21 INF 1 JOHN'S, INF 2 ORIG, INF 3 EXP
INTACT LOOP COLD LEG - EXPERIMENTAL LOCATION PC-1

KEY		
SYM BOL	NAME	UNITS
——	MASS FLOW RATE	,KG/SEC
	LOC= 7/ 0/ 4 MNEM=FLOW INF=1	
——	MASS FLOW RATE	,KG/SEC
	LOC= 7/ 0/ 4 MNEM=FLOW INF=2	
····	FR-PC-100	,KG/SEC
	LOC= 34/ 0/ 0 MNEM=FLOW INF=3	

AEEW - M 2464

57

THE FOLLOWING ARE PLOTTED AGAINST REACTOR TIME

LIQUID VELOCITY ,FF-PC-G29A

FIGURE 22 INF 1 JOHN'S, INF 2 ORIG, INF 3 EXP
INTACT LOOP COLD LEG - EXPERIMENTAL LOCATION PC-1

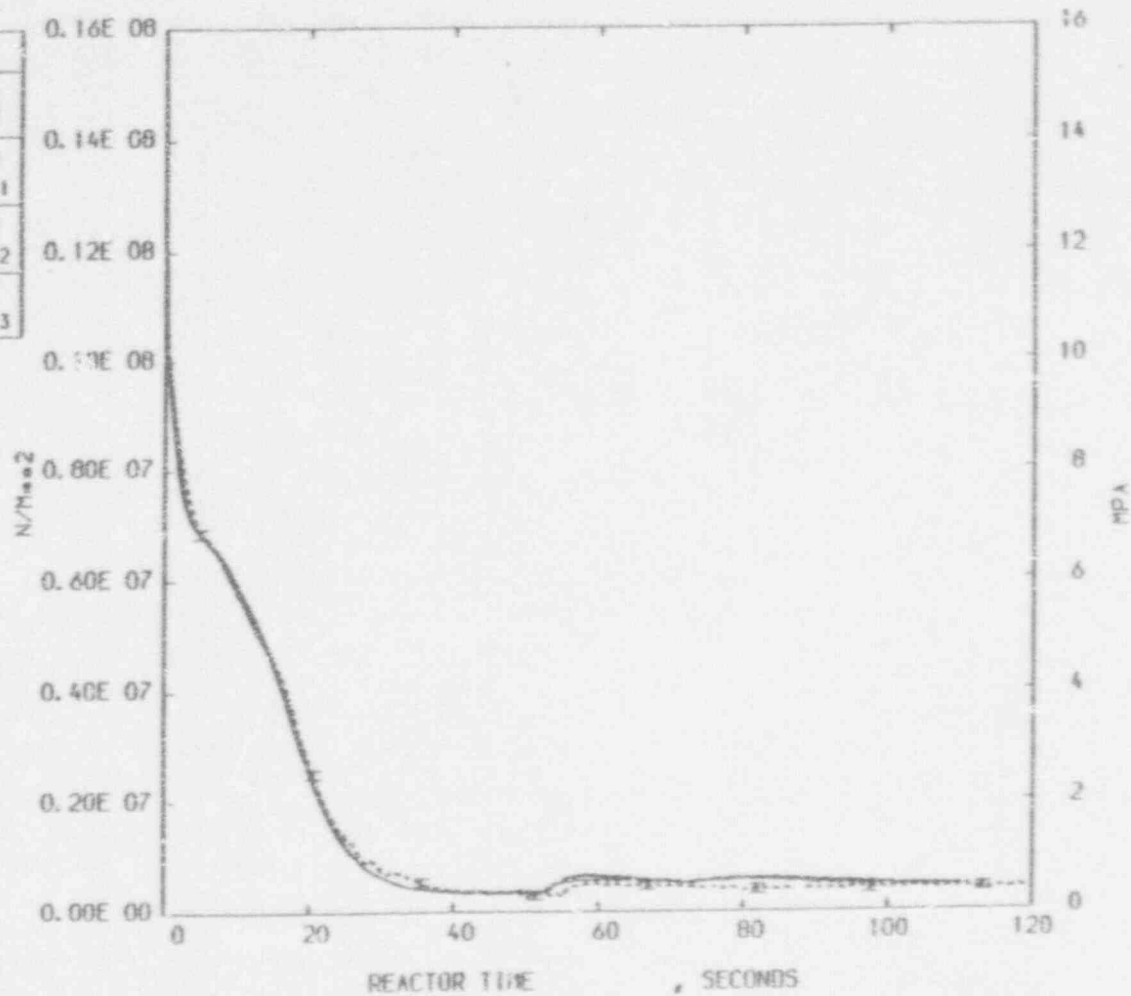| KEY		
SYMBOL	NAME	UNITS
——	LIQUID VELOCITY	,M/SEC
	LOK= 7/ 0/ 4 MMEMI=VLIQ INF=1	
———	LIQUID VELOCITY	,M/SEC
	LOK= 7/ 0/ 4 MMEMI=VLIQ INF=2	
----	FF-PC-002A	,M/SEC
	LOK= 20/ 0/ 0 MMEMI=FE INF=3	

FIGURE 23 INF 1 JON'S, INF 2 ORIG, INF 3 EXP
INTACT LOOP COLD LEG - EXPERIMENTAL LOCATION PC-1

THE FOLLOWING ARE PLOTTED AGAINST REACTOR TIME

VAPOR TEMPERATURE ,TE-PC-091C

FIGURE 24 INF 1 MON'S, INF 2 ORIG, INF 3 EXP
INTACT LOOP COLD LEG - EXPERIMENTAL LOCATION PC-1

	KEY	
SYM BOL	NAME	UNITS
	VAPOR TEMPERATURE ,DEG.K LOC= 7/ 0/ 4 MNEM=TEMV INF=1	
	VAPOR TEMPERATURE ,DEG.K LOC= 7/ 0/ 4 MNEM=TEMV INF=2	
	TE-PC-091C ,DEG.K LOC= 178/ 0/ 0 MNEM=TMCL INF=3	

THE FOLLOWING ARE PLOTTED AGAINST REACTOR TIME

PUMP SPEED   , FUNCTION

FIGURE 25   INF 1 JON'S, INF 2 ORIG, INF 3 EXP
PUMP SPEED

RAD/SEC

REACTOR TIME   , SECONDS

KEY		
SYMBOL	NAME	UNITS
	PUMP SPEED	, RAD/SEC
	LOC= 4/ 0/ 1 MECH-SPEED INF=1	
	PUMP SPEED	, RAD/SEC
	LOC= 4/ 0/ 1 MECH-SPEED INF=2	
	FUNCTION	,
	FUNCTION	,

AEEW - M 2464

61

THE FOLLOWING ARE PLOTTED AGAINST REACTOR TIME

MIXTURE DENSITY ,DE-PC-002A ,DE-PC-002C
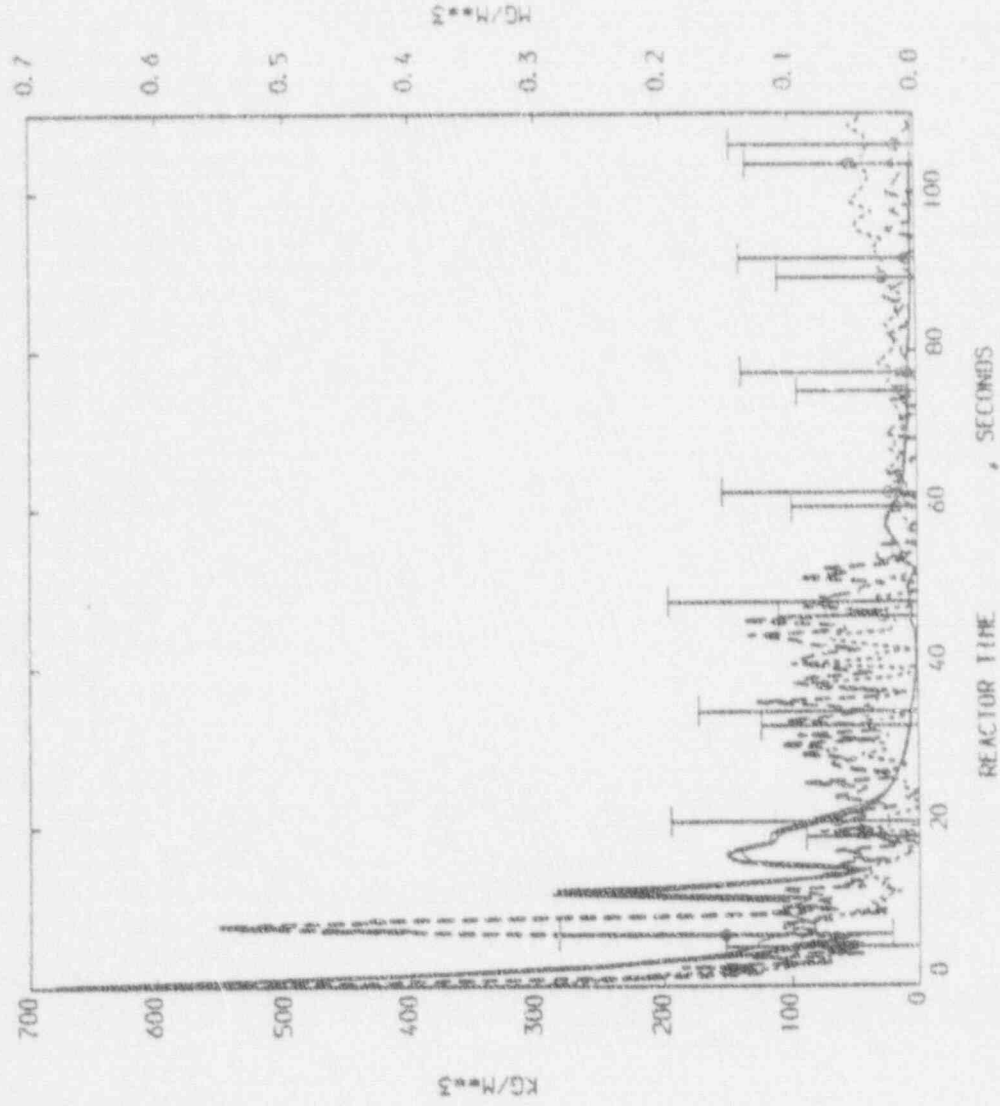
MG/M**3

REACTOR TIME , SECONDS

KG/M**3

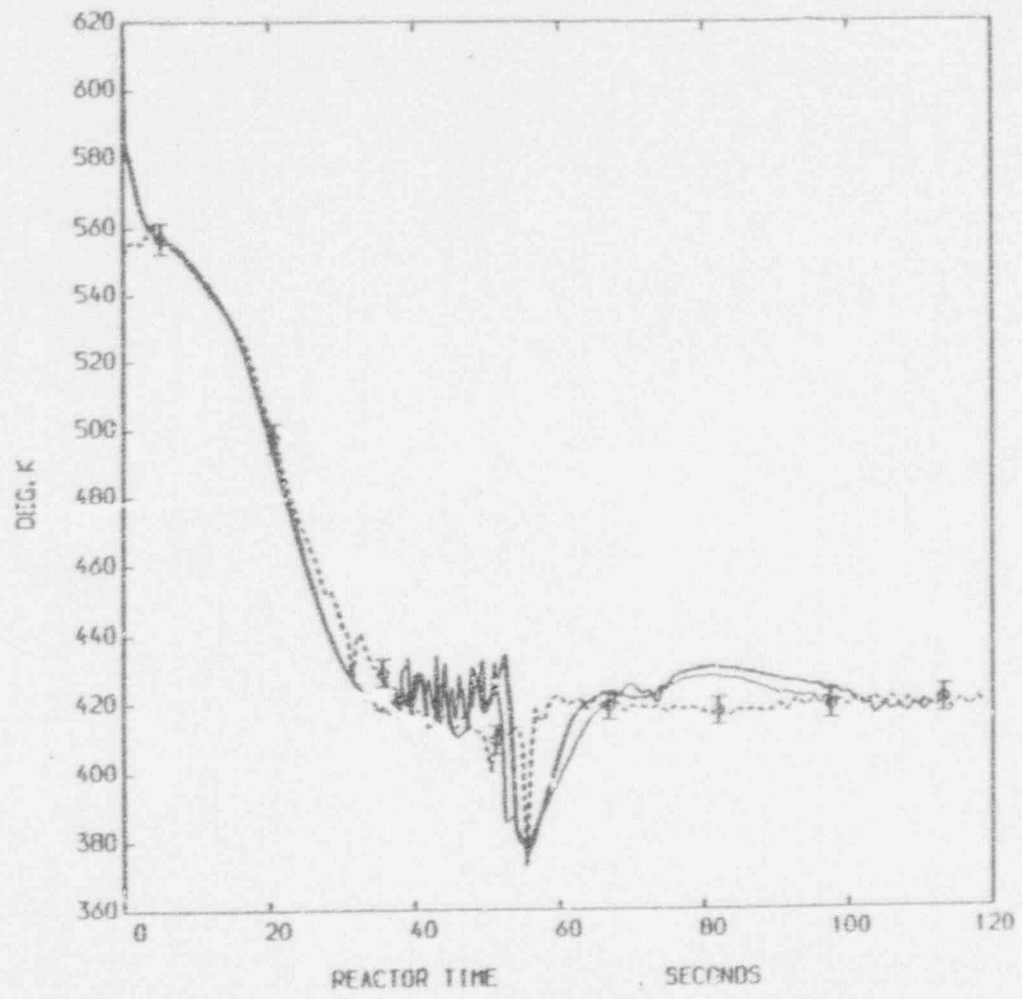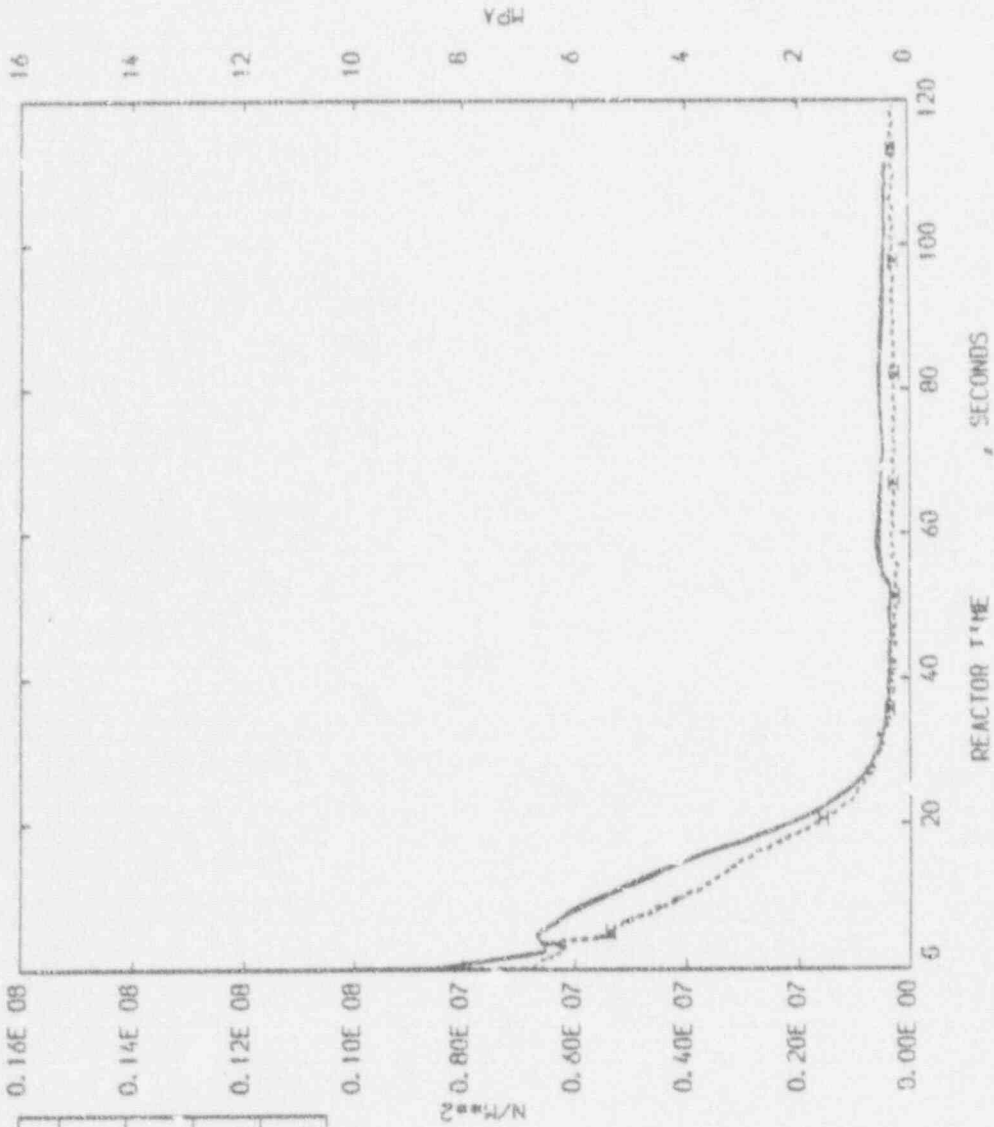|	KEY	
SYM BOL	NAME	UNITS
	MIXTURE DENSITY	,KG/M**3
	LOC= 1/ 0/ 2 MNEM-DENM INF=1	
	MIXTURE DENSITY	,KG/M**3
	LOC= 1/ 0/ 2 MNEM-DENM INF=2	
	DE-PC-002A	,MG/M**3
	LOC= 16/ 0/ 0 MNEM-DENM INF=3	
	DE-PC-002C	,MG/M**3
	LOC= 17/ 0/ 0 MNEM-DENM INF=3	

FIGURE 26 INF 1 JON'S, INF 2 ORIG, INF 3 EXP
INTACT LOOP HOT LEG - EXPERIMENTAL LOCATION PC-2

AEEW - M 2464

62

THE FOLLOWING ARE PLOTTED AGAINST REACTOR TIME

MASS FLOW RATE ,FR-PC-201 ,FR-PC-205

KEY		
SYM BOL	NAME	UNITS
——	MASS FLOW RATE	,KG/SEC
	LOC= 1/ 0/ 2 MNEM=FLOV INF=1	
——	MASS FLOW RATE	,KG/SEC
	LOC= 1/ 0/ 2 MNEM=FLOV INF=2	
····	FR-PC-201	,KG/SEC
	LOC= 37/ 0/ 0 MNEM=FLOV INF=3	
— —	FR-PC-205	,KG/SEC
	LOC= 38/ 0/ 0 MNEM=FLOV INF=3	
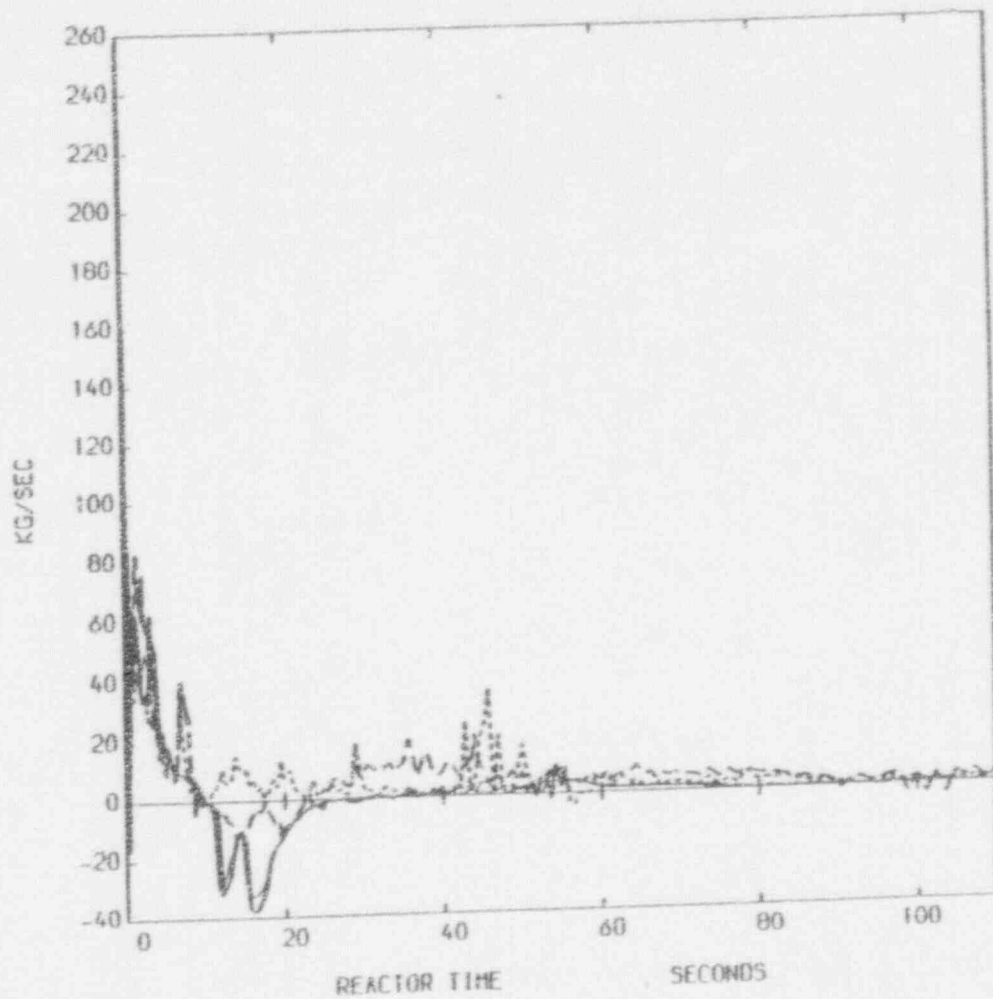
FIGURE 27   INF 1 JON'S, INF 2 ORIG, INF 3 EXP
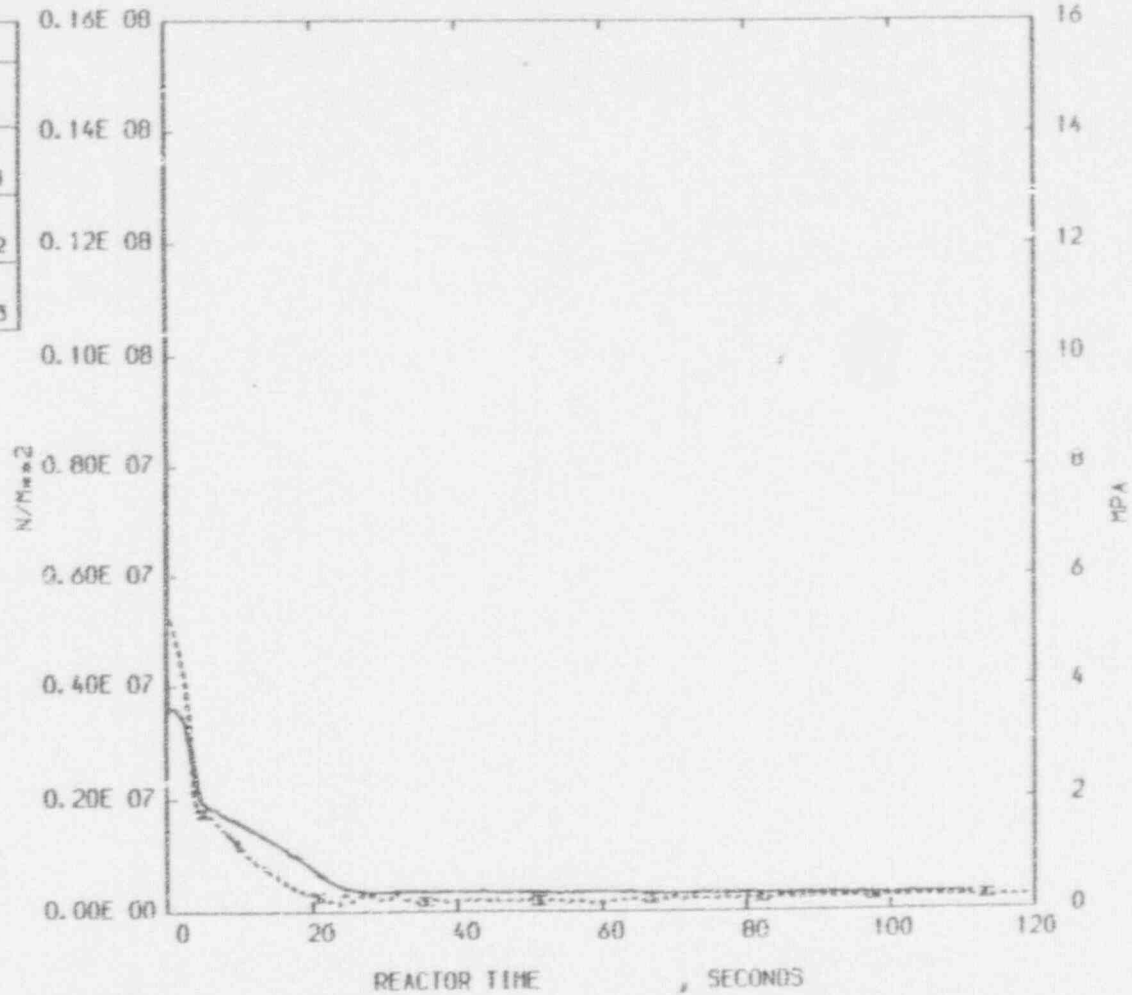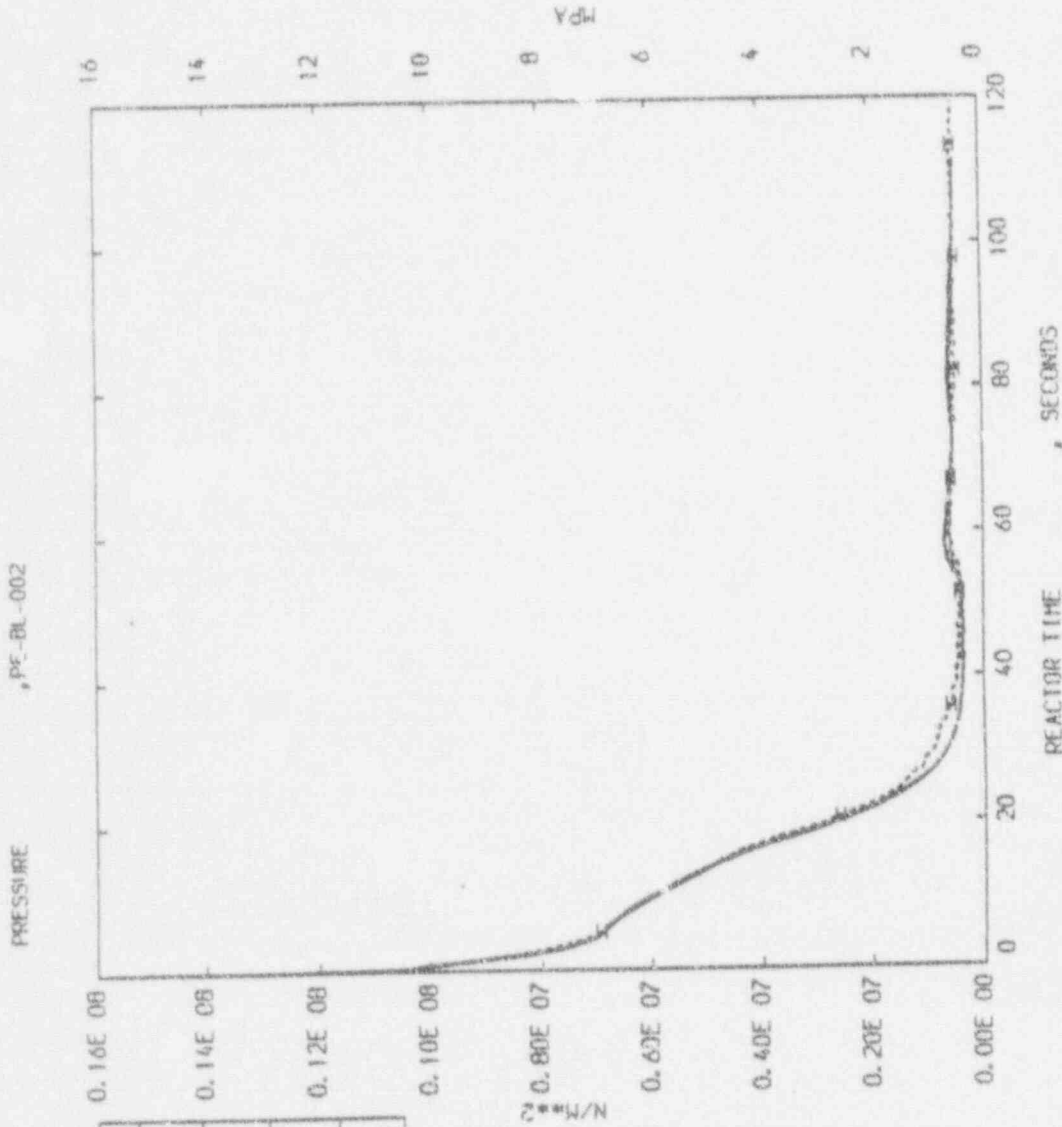INTACT LOOP HOT LEG - EXPERIMENTAL LOCATION PC-2

AEEW - M 2464

63
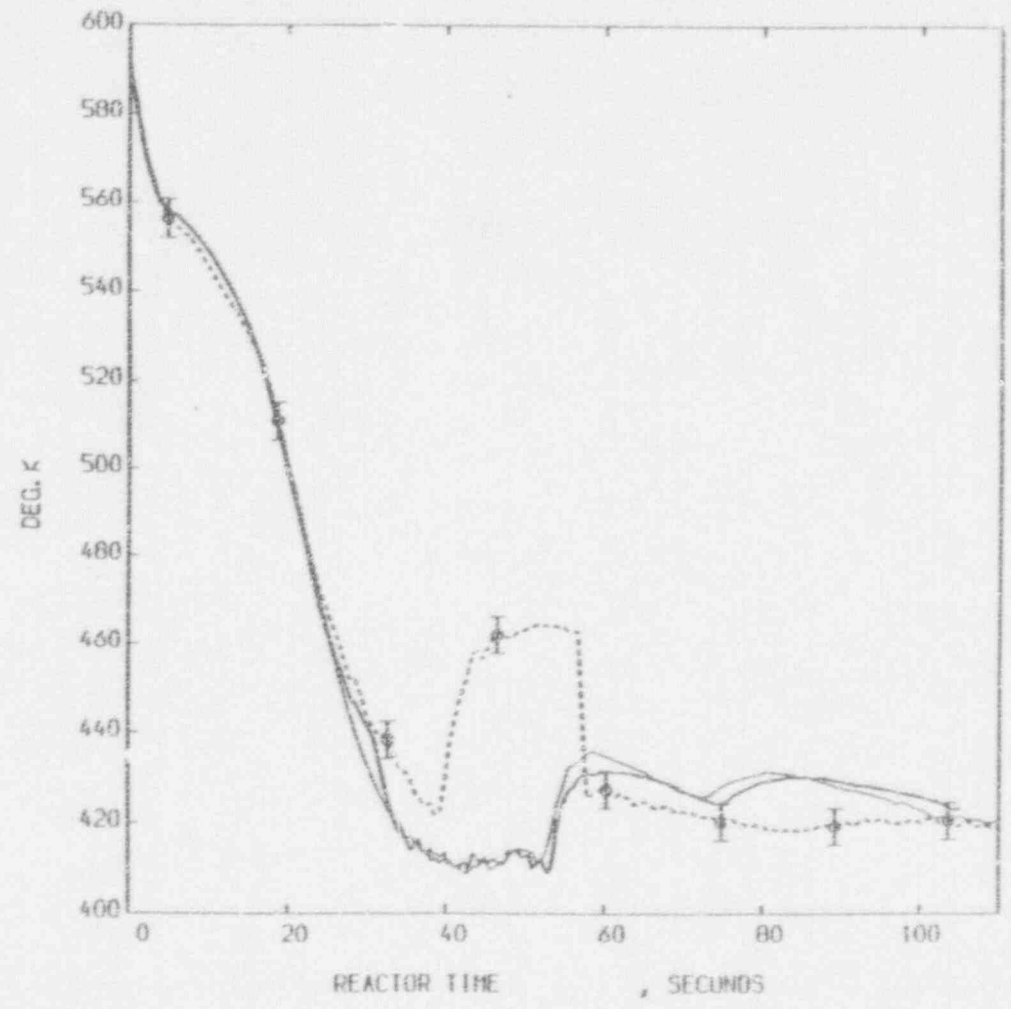
FIGURE 28   INF 1 JON'S, INF 2 ORIG, INF 3 EXP
INTACT LOOP HOT LEG - EXPERIMENTAL LOCATION PC-2

THE FOLLOWING ARE PLOTTED AGAINST REACTOR TIME

VAPOUR TEMPERATURE , TE-PC-002A , TE-PC-002B
TE-PC-002C

FIGURE 29 INF 1 JON'S, INF 2 ORIG, INF 3 EXP

INTACT LOOP HOT LEG - EXPERIMENTAL LOCATION PC-2

KEY		
SYM BOL	NAME	UNITS
—	VAPOUR TEMPERATURE , DEG.K LOC= 1/ 0/ 2 MNEM=TEMV INF=1	DEG.K
—	VAPOUR TEMPERATURE , DEG.K LOC= 1/ 0/ 2 MNEM=TEMV INF=2	DEG.K
...	TE-PC-002A , DEG.K LOC= 179/ 0/ 0 MNEM=THEL INF=3	DEG.K
— —	TE-PC-002B , DEG.K LOC= 180/ 0/ 0 MNEM=THEL INF=3	DEG.K
—	TE-PC-002C , DEG.K LOC= 181/ 0/ 0 MNEM=THEL INF=3	DEG.K

AEEW - M 2464

65

THE FOLLOWING ARE PLOTTED AGAINST REACTOR TIME

PRESSURE ,PE-PC-002

FIGURE 30 INF 1 RCN'S, INF 2 ORIG, INF 3 EXP
INTACT LOOP HOT LEG - EXPERIMENTAL LOCATION PC-2

	KEY	
SYM BOX	NAME	UNITS
	PRESSURE	,N/M**2
	LOC= 1/ 0/ 2 MHEM-PRES INF=1	
	PRESSURE	,N/M**2
	LOC= 1/ 0/ 2 MHEM-PRES INF=2	
	PE-PC-002	,MPA
	LOC= 120/ 0/ 0 MHEM-PRES INF=3	

AEEW - M 2464

Winfrith

FIGURE 31   INF 1 JON'S, INF 2 ORIG, INF 3 EXP
INTACT LOOP HOT LEG - PRESSURIZER

THE FOLLOWING ARE PLOTTED AGAINST REACTOR TIME

WATER LEVEL   ,LEPDT-P139-008,0.216

REACTOR TIME   , SECONDS

FIGURE 32 INF 1 JON'S, INF 2 ORIG, INF 3 EXP
INTACT LOOP HOT LEG - PRESSURIZER

KEY

SYM BOL	NAME	UNITS
——	WATER LEVEL ,METRES LOC= 8/ 0/ 1 MNEM-LEVE INF=1	METRES
——	WATER LEVEL ,METRES LOC= 8/ 0/ 1 MNEM-LEVE INF=2	METRES
----	LEPDT-P139-008,0.216,METRES LOC= 50/ 0/ 0 MNEM-LEVE INF=3	METRES

FIGURE 33   INF 1 JON'S, INF 2 ORIG, INF 3 EXP
EMERGENCY CORE COOLING SYSTEM

FIGURE 34 INF 1 JUN'S, INF 2 ORIG, INF 3 EXP
EMERGENCY CORE COOLING SYSTEM

AEEW - M 2464

FIGURE 35 INF 1 JON'S, INF 2 ORIG, INF 3 EXP
UPPER PLENUM PRESSURE

Winfrith

FIGURE 36 INF 1 JON'S, INF 2 ORIG, INF 3 EXP
LOWER PLENUM LIQUID AXIAL VELOCITY

Winfrith

AEEW - M 2464

73

KEY

SYM BOL	NAME	UNITS
———	LIQ AXIAL VELOCITY	,M/SEC
LOC= 50/ 9/ 1 MNEM=VL-Z INF=1		
———	LIQ AXIAL VELOCITY	,M/SEC
LOC= 50/ 9/ 1 MNEM=VL-Z INF=2		
----	FE-SUP-001	,M/SEC
LOC= 31/ 0/ 0 MNEM=FE INF=3		

M/SEC

REAC TIME , SECONDS

FIGURE 37 INF 1 JON'S, INF 2 ORIG, INF 3 EXP

UPPER PLENUM LIQUID AXIAL VELOCITY

Winfrith

KEY

SYM BOL	NAME	UNITS
——	LIQUID TEMPERATURE ,DEG. K LOC= 50/ 11/ 13 MNEM=TEML INF=1	
——	LIQUID TEMPERATURE ,DEG. K LOC= 50/ 11/ 13 MNEM=TEML INF=2	
----	TE-1ST-001 ,DEG. K LOC= 201/ 0/ 0 MNEM=THCL INF=3	

FIGURE 38   INF 1 JON'S, INF 2 ORIG, INF 3 EXP
DOWNCOMER LIQUID TEMPERATURE AT 5.0 METRES

AEEW - M 2464

75

KEY

SYM BOL	NAME	UNITS
——	LIQUID TEMPERATURE , DEG.K LOC= 50/ 10/ 13 MNEM=TEML INF=1	
——	LIQUID TEMPERATURE , DEG.K LOC= 50/ 10/ 13 MNEM=TEML INF=2	
····	TE-1ST-002 , DEG.K LOC= 202/ 0/ 0 MNEM=TMCL INF=3	

FIGURE 39   INF 1 JON'S, INF 2 ORIG, INF 3 EXP
DOWNCOMER LIQUID TEMPERATURE AT 4.2 METRES

Winfrith

AEEW - M 246A

76

KEY		
SYM BOL	NAME	UNITS
——	LIQUID TEMPERATURE , DEG.K LOC= 50/ 7/ 13 MNEM=TEML INF=1	
——	LIQUID TEMPERATURE , DEG.K LOC= 50/ 7/ 13 MNEM=TEML INF=2	
----	TE-1ST-005 , DEG.K LOC= 205/ 0/ 0 MNEM=THCL INF=3	
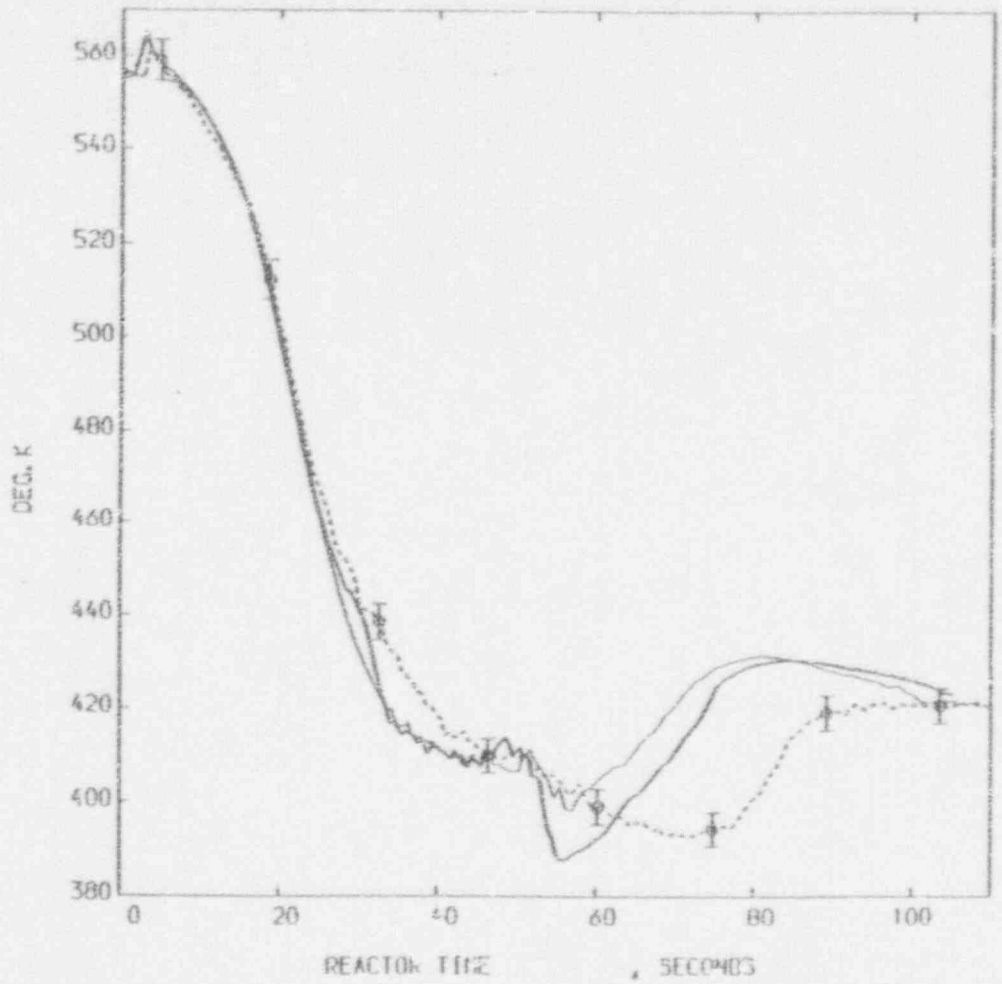
FIGURE 40   INF 1 CON'S, INF 2 ORIG, INF 3 EXP
DOWNCOMER LIQUID TEMPERATURE AT 2.4 ME

Winfrith

AEEW - M 2464

77

KEY

SYM BOL	NAME	UNITS
——	LIQUID TEMPERATURE , DEG. K	
	LOC= 50/ 1/ 13 MNEM=TEML INF=1	
——	LIQUID TEMPERATURE , DEG. K	
	LOC= 50/ 1/ 13 MNEM=TEML INF=2	
····	TE-1ST-012 , DEG. K	
	LOC= 211/ 0/ 0 MNEM=TMCL INF=3	

DEG. K

REACTOR TIME , SECONDS

FIGURE 41   INF 1 JON'S, INF 2 ORIG, INF 3 EXP
DOWNCOMER LIQUID TEMPERATURE AT 0.3 METRES

L PLENUM MOM/FLUX

Winfrith

AEEW - M 2464

78
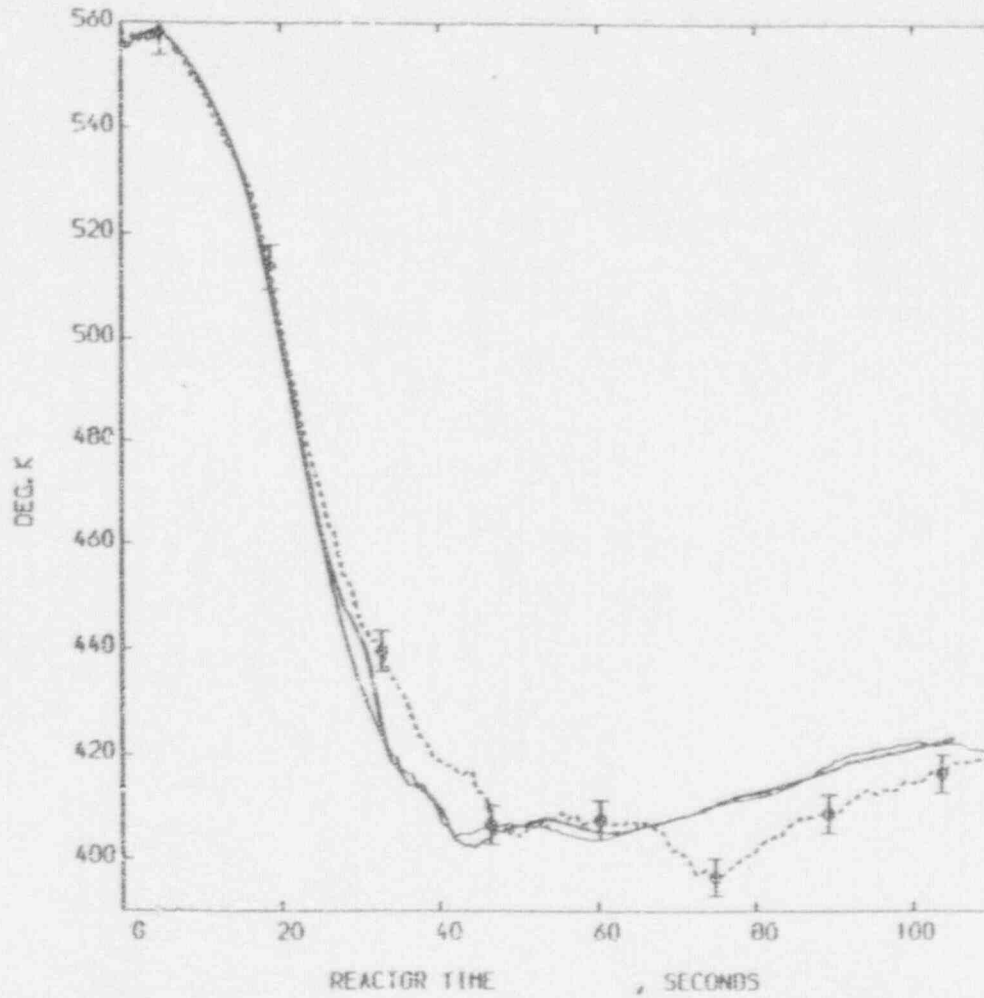
KEY		
SYM BOL	NAME	UNITS
——	L PLENUM MOM/FLUX	,KG/MS**2
——	L PLENUM MOM/FLUX	,KG/MS**2
- - -	L PLENUM MOM/FLUX	,KG/MS**2

KG/MS**2

REACTOR TIME , SECONDS
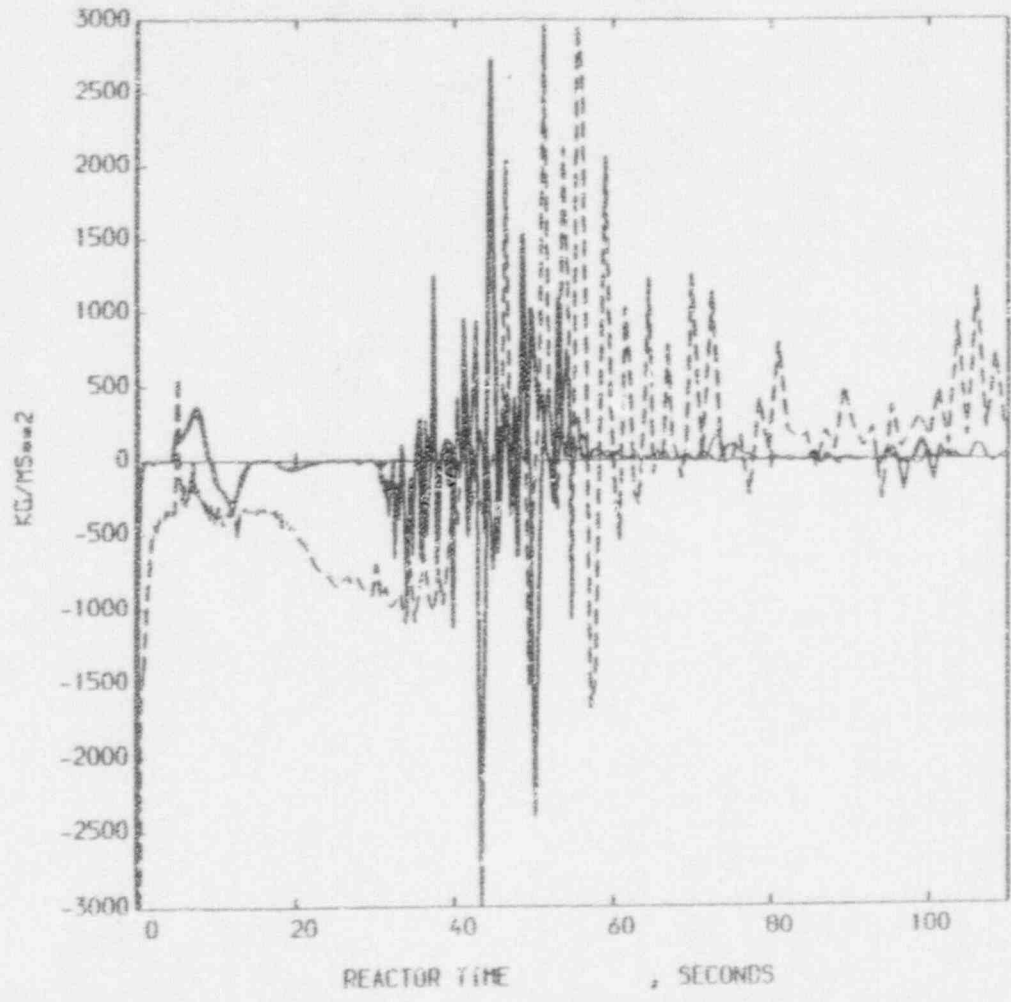
FIGURE 42 LINE 1 JON'S, LINE 2 ORIG, LINE 3 EXP
LOWER PLENUM MOMENTUM FLUX

CORE INLET MASS FLOW

A.E.E.W - M 2464

79

KEY		
SYM BOL	NAME	UNITS
——	CORE INLET MASS FLOW, KG/SEC LOC= 50/ 0/ 1 MNEM=FLCI INF=1	
——	CORE INLET MASS FLOW, KG/SEC LOC= 50/ 0/ 1 MNEM=FLCI INF=2	

KG/SEC

REACTOR TIME , SECONDS
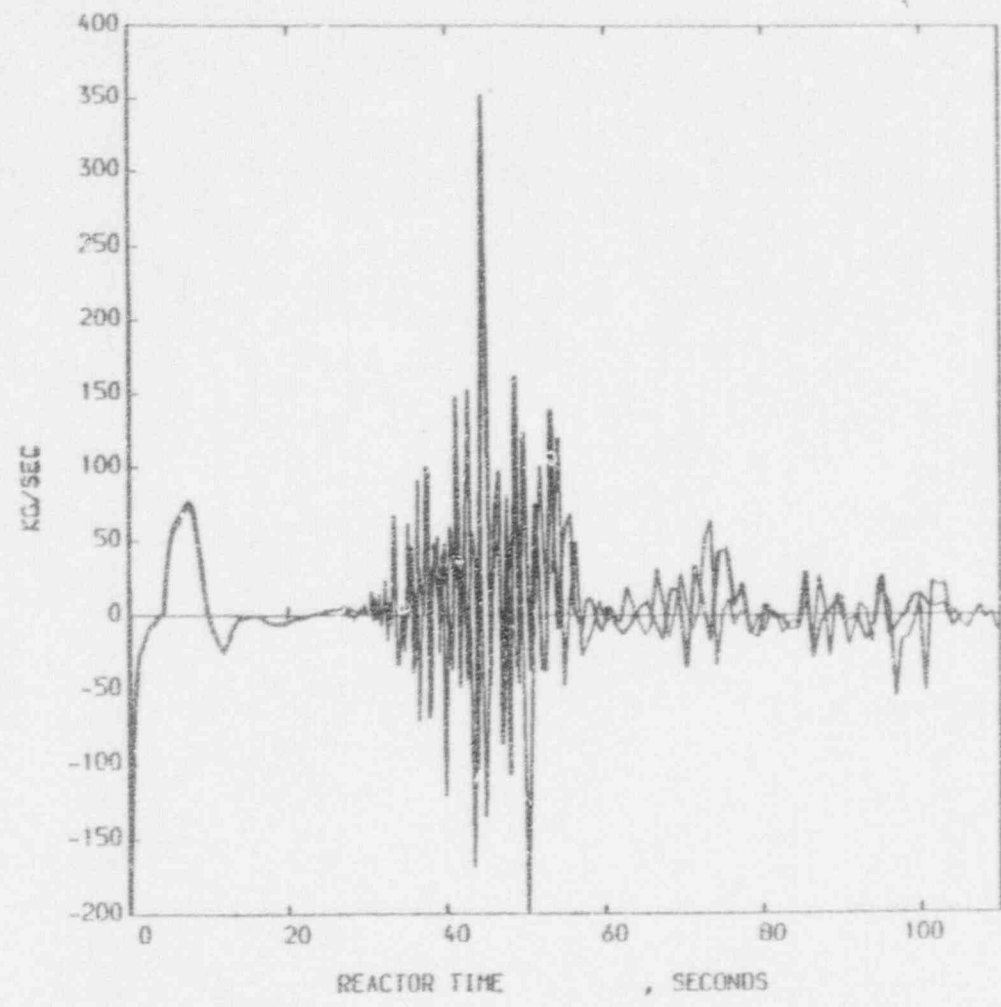
FIGURE 43 INF 1 JON'S, INF 2 ORIG
VESSEL GLOBALS

CORE OUTLET MASSFLOW

	KEY	
SYN BOL	NAME	UNITS
——	CORE OUTLET MASSFLOW, KG/SEC LOC= 50/ 0/ 1 MNEM=FLCO INF=1	
——	CORE OUTLET MASSFLOW, KG/SEC LOC= 50/ 0/ 1 MNEM=FLCO INF=2	

KG/SEC

REACTOR TIME , SECONDS
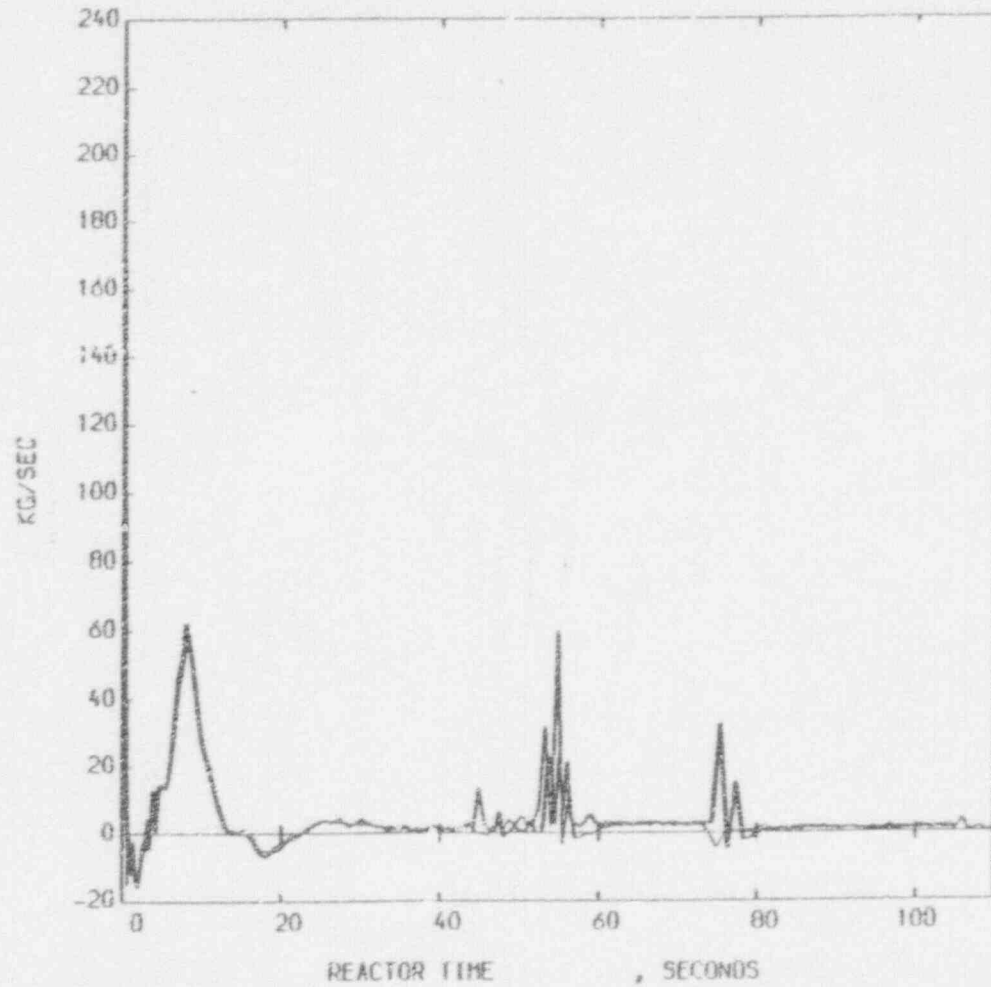
FIGURE 44   INF 1 JON'S, INF 2 ORIG
VESSEL GLOBALS

Winfrith

AEEW - M 2464

81

KEY

SYMBOL	NAME	UNITS
———	CORE LIQ VOL FRAC , LOC= 50/ 0/ 1 MNEM=LFCO INF=1	
———	CORE LIQ VOL FRAC , LOC= 50/ 0/ 1 MNEM=LFCO INF=2	

REACTOR TIME , SECONDS

FIGURE 45   INF 1 JON'S, INF 2 ORIG

VESSEL GLOBALS

THE FOLLOWING ARE PLOTTED AGAINST REACTOR TIME

L PLENM LIQ VOL FRAC

FIGURE 46 INF 1 JOIN'S, INF 2 ORIG
VESSEL GLOBALS

Winfrith

AEFW - M 2464

82

Winfrith

AEPW - M 2464

83

KEY		
SYM BOL	NAME	UNITS
——	D'COMER LIQ VOL FRAC, LOC= 50/ 0/ 1 MNEM=LFDC INF=1	
——	D'COMER LIQ VOL FRAC, LOC= 50/ 0/ 1 MNEM=LFDC INF=2	

REACTOR TIME   , SECONDS
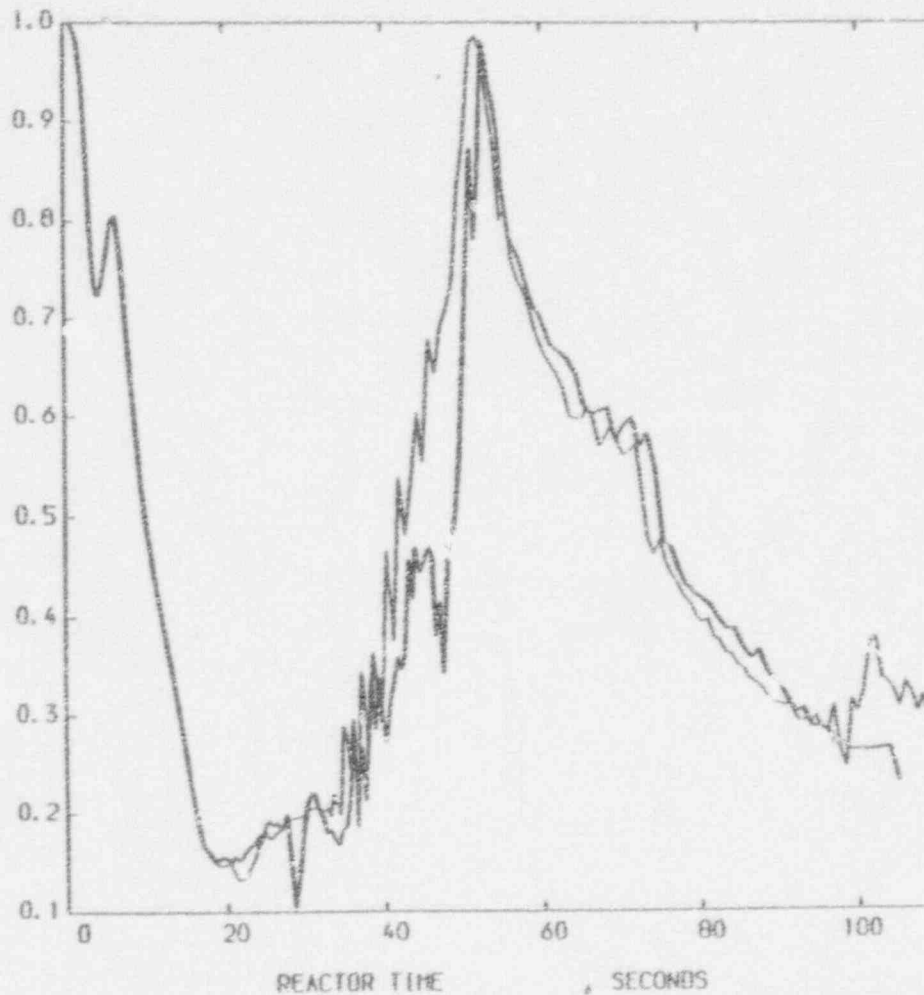
FIGURE 47   INF 1 JON'S, INF 2 ORIG
VESSEL GLOBALS
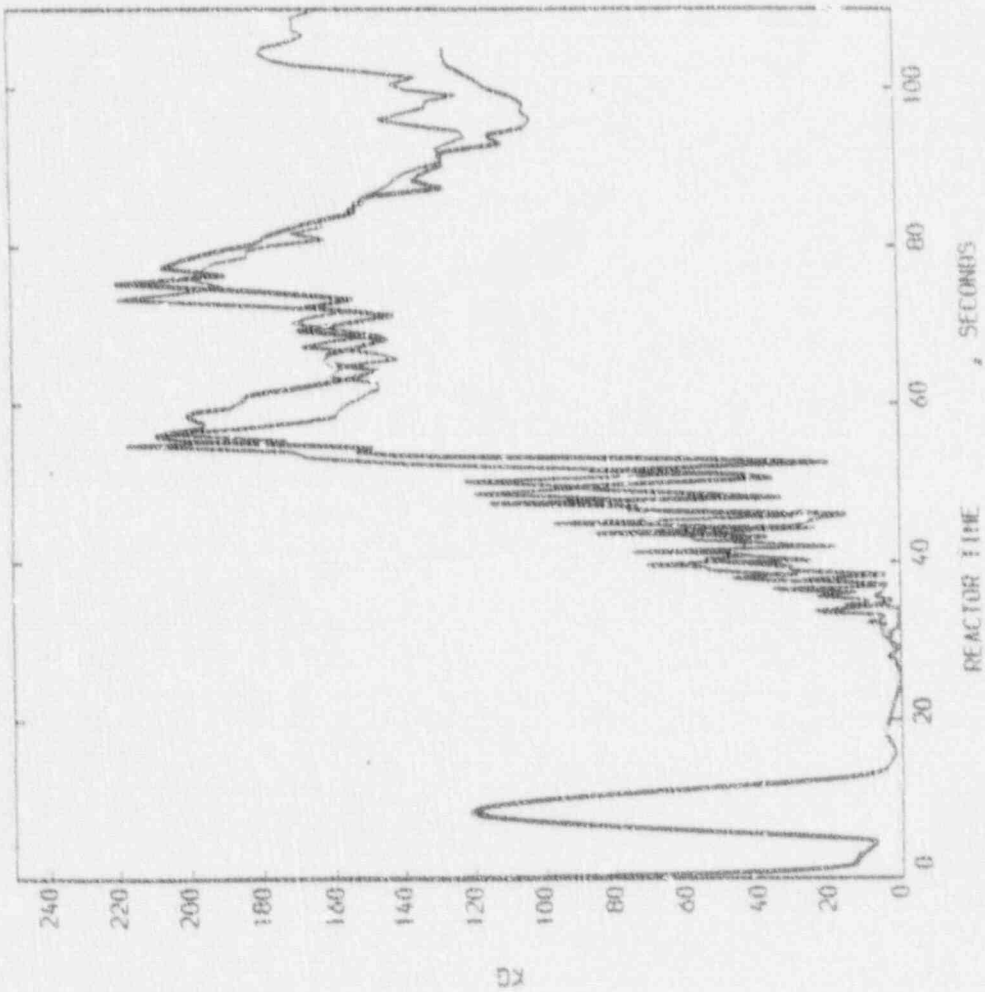
CORE LIQUID MASS

FIGURE 48 INF 1 JON'S, INF 2 ORIG.
VESSEL GLOBALS

KEY		
NAME		UNITS
	CORE LIQUID MASS	,KG
LOC= SD/ O/ $ 4PREH=3.PER INF=1		
	CORE LIQUID MASS	,KG
LOC= SD/ O/ $ MREH=MER INF=2		

KG

REACTOR TIME , SECONDS

THE FOLLOWING ARE PLOTTED AGAINST REACTOR TIME

VESSEL LIQUID MASS

FIGURE 4: INF 1 JOIN'S, INF 2 ORIG
VESSEL GLOBALS

ALEW - M 2464

FIGURE 50 INF 1 JUN'S, INF 2 ORIG
VESSEL GLOBALS

AEEW - M 2464

THE FOLLOWING ARE PLOTTED AGAINST REACTOR TIME

TOT SLAB HEAT FLUX

FIGURE 51 INF 1 JOHN'S, INF 2 ORIG
VESSEL GLOBALS

AEEW - M 2464

88

FIGURE 52   INF 1 JON'S, INF 2 ORIG
VESSEL GLOBALS

Winfrith

FIGURE 53 INF 1 JON'S, INF 2 ORIG, INF 3 EXP
CENTRAL FUEL BUNDLE CLADDING TEMPERATURES

AEEW - M 2464

90

KEY		
SYM BOL	NAME	UNITS
——	CLADDING TEMP -FINE,DEG.K LOC= 50/ 1/ 5 MNEM=THCL INF=1	
——	CLADDING TEMP -FINE,DEG.K LOC= 50/ 1/ 5 MNEM=THCL INF=2	
——	TE-SG06-011 ,DEG.K LOC= 278/ 0/ 0 MNEM=THCL INF=3	

DEG.K

REACTOR TIME , SECONDS

FIGURE 54 INF 1 JON'S, INF 2 ORIG, INF 3 EXP
CENTRAL FUEL BUNDLE CLADDING TEMPERATURES

AEEW - M 2464

91

FIGURE 55   INF 1 JON'S, INF 2 ORIG, INF 3 EXP
CENTRAL FUEL BUNDLE CLADDING TEMPERATURES

Winfrith
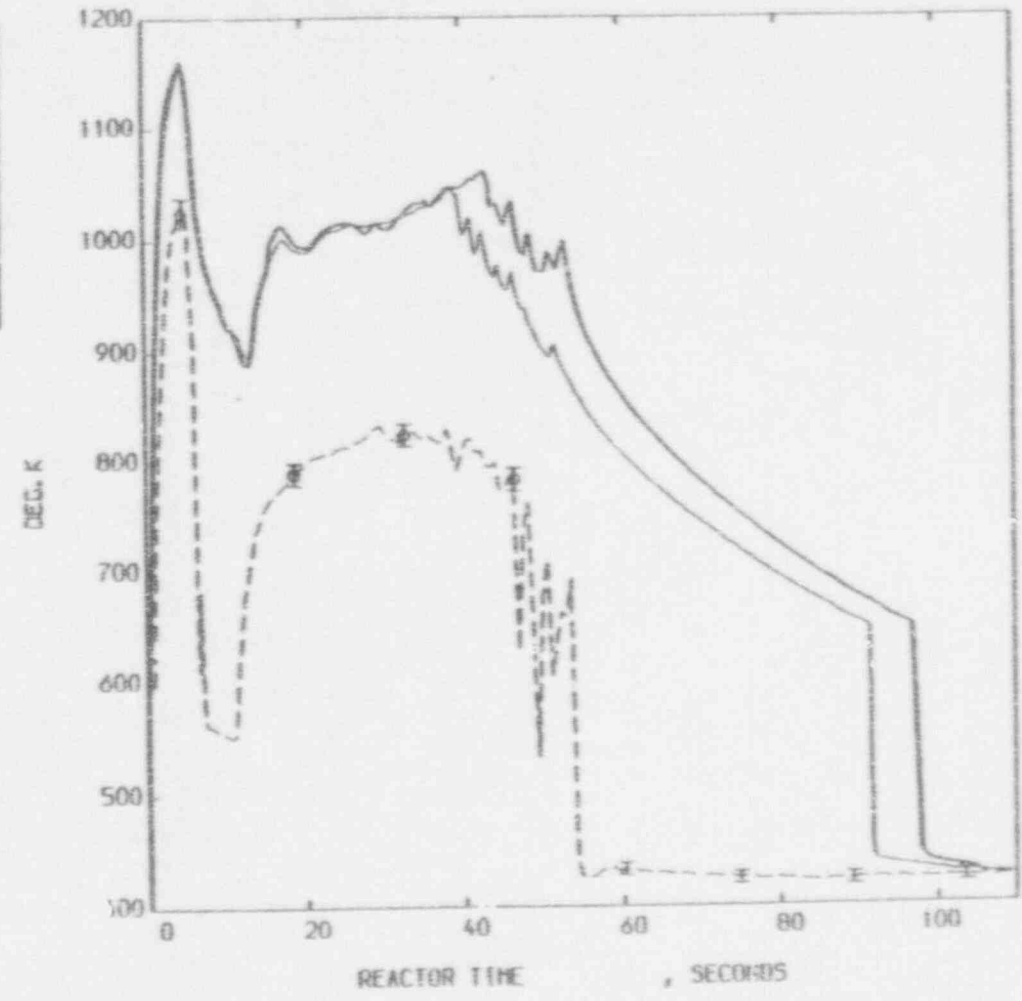
FIGURE 56   INF 1 JON'S, INF 2 ORIG, INF 3 EXP
CENTRAL FUEL BUNDLE CLADDING TEMPERATURES
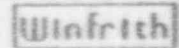
AEEW - M 2464

93

KEY		
SYM BOL	NAME	UNITS
——	CLADDING TEMP -FINE,DEG.K	
LOC= 50/ 4/ 12 MNEM=TNCL INF=1		
——	CLADDING TEMP -FINE,DEG.K	
LOC= 50/ 4/ 12 MNEM=TNCL INF=2		
--	TE-5104-027	,DEG.K
LOC= 293/ 0/ 0 MNEM=TNCL INF=3		

DEG. K

1200
1100
1000
900
800
700
600
500
400

0   20   40   60   80   100

REACTOR TIME   , SECONDS

FIGURE 57   INF 1 JON'S, INF 2 ORIG, INF 3 EXP
CENTRAL FUEL BUNDLE CLADDING TEMPERATURES

THE FOLLOWING ARE PLOTTED AGAINST REACTOR TIME

CLADDING TEMP -FINE,TE-5007-031

FIGURE 58 INF 1 JOHN'S, INF 2 ORIG, INF 3 EXP
CENTRAL FUEL BUNDLE CLADDING TEMPERATURES

KEY		
SYM BOL	NAME	UNITS
——	CLADDING TEMP -FINE,DEG.K LOC= 50/ 1/ 13 MAER=THCL INF=1	
——	CLADDING TEMP -FINE,DEG.K LOC= 50/ 1/ 13 MAER=THCL INF=2	
---	TE-5007-031 ,DEG.K LOC= 271/ 0/ 0 MAER=THCL INF=3	

AEEW = M 2464

95

KEY		
SYM BOL	NAME	UNITS
—	CLADDING TEMP -FINE,DEG.K LOC= 50/ 4/ 15 MNEM=THCL INF=1	
—	CLADDING TEMP -FINE,DEG.K LOC= 50/ 4/ 15 MNEM=THCL INF=2	
- -	TE-5106-039 ,DEG.K LOC= 297/ 0/ 0 MNEM=THCL INF=3	

DEG. K

REACTOR TIME   , SECONDS
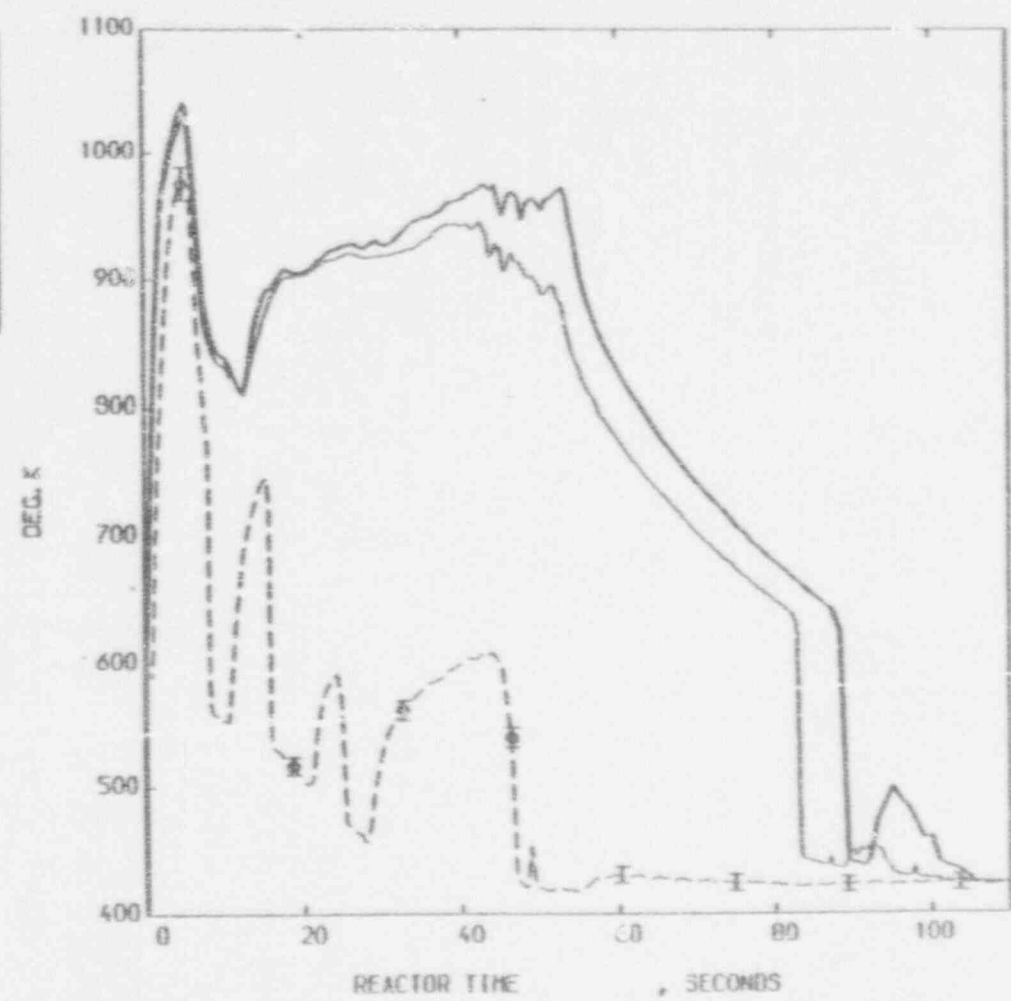
FIGURE 59   INF 1 JON'S, INF 2 ORIG, INF 3 EXP
CENTRAL FUEL BUNDLE CLADDING TEMPERATURES

Winfrith

AEEW - M 2464

96

FIGURE 60 INF 1 JON'S, INF 2 ORIG, INF 3 EXP
CENTRAL FUEL BUNDLE CLADDING TEMPERATURES

AEEW - M 2464

97

	Kc:	
SYM BOL	NAME	UNITS
——	CLADDING TEMP -FINE,DEG.K LOC= 50/ 1/ 17 MNEM=TMCL INF=1	
——	CLADDING TEMP -FINE,DEG.K LOC= 50/ 1/ 17 MNEM=TMCL INF=2	
— —	TE-5H05-049 ,DEG.K LOC= 264/ 0/ 0 MNEM=TMCL INF=3	

DEG. K

REACTOR TIME   , SECONDS

FIGURE 61   INF 1 JON'S, INF 2 ORIG, INF 3 EXP
CENTRAL FUEL BUNDLE CLADDING TEMPERATURES
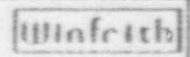
AEEW - M 2464

98

KEY		
SYM BOL	NAME	UNITS
——	CLADDING TEMP -FINE, DEG. K LOC= 50/ 1/ 20 MNEM=THCL INF=1	
——	CLADDING TEMP -FINE, DEG. K LOC= 50/ 1/ 20 MNEM=THCL INF=2	
---	TE-5G06-062 , DEG. K LOC= 281/ 0/ 0 MNEM=THCL INF=3	

FIGURE 62   INF 1 JON'S, INF 2 ORIG, INF 3 EXP
CENTRAL FUEL BUNDLE CLADDING TEMPERATURES

ROD CENTRE TEMP-FINE,TC-5007-27   ,TC-5009-27
TC-5010-27

AEEW - M 2464

99

KEY		
SYM BOL	NAME	UNITS
——	ROD CENTRE TEMP-FINE,DEG.K LOC= 50/ 1/ 12 MNEM=TMRC INF=1	
——	ROD CENTRE TEMP-FINE,DEG.K LOC= 50/ 1/ 12 MNEM=TMRC INF=2	
----	TC-5007-27 ,DEG.K LOC= 168/ 0/ 0 MNEM=TMRC INF=3	
— —	TC-5009-27 ,DEG.K LOC= 169/ 0/ 0 MNEM=TMRC INF=3	
— —	TC-5010-27 ,DEG.K LOC= 170/ 0/ 0 MNEM=TMRC INF=3	

FIGURE 63   INF 1 JON'S, INF 2 ORIG, INF 3 EXP
CENTRELINE FUEL TEMPERATURE

FIGURE 64   INF 1 JON'S, INF 2 ORIG, INF 3 EXP
FUEL ROD CLADDING TEMPERATURES - PERIPHERAL BUNDLES

101

KEY

SYM BOL	NAME	UNITS
——	CLADDING TEMP -FINE, DEG. K	
	LOC= 50/ 5/ 9 MNEM=TNCL INF=1	
——	CLADDING TEMP -FINE, DEG. K	
	LOC= 50/ 5/ 9 MNEM=TNCL INF=2	
----	TE-2H13-021 , DEG. K	
	LOC= 223/ 0/ 0 MNEM=TNCL INF=3	
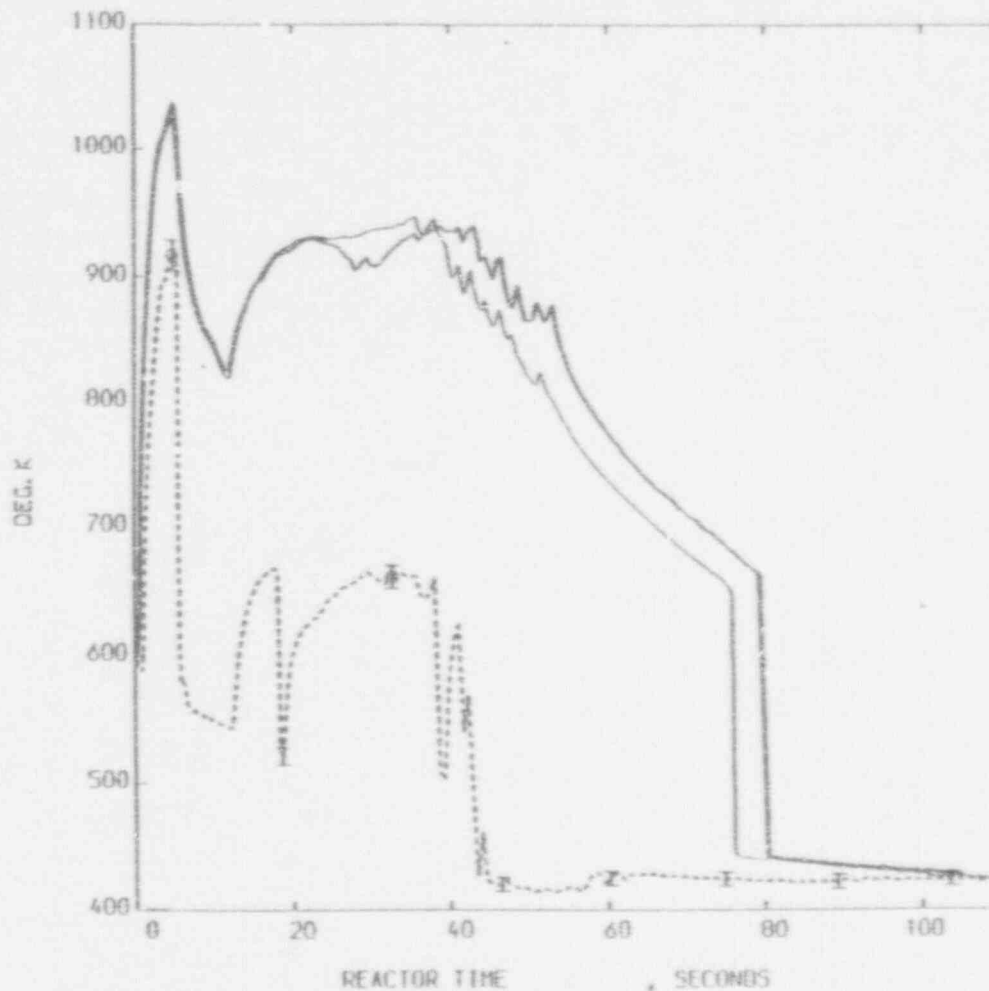
FIGURE 65   INF 1 JON'S, INF 2 ORIG, INF 3 EXP

FUEL ROD CLADDING TEMPERATURES - PERIPHERAL BUNDLES

AEEW - M 2464

102

KEY

SYM BOL	NAME	UNITS
——	CLADDING TEMP -FINE, DEG. K	
	LOC= 50/ 5/ 13 MNEM=TMCL INF=1	
——	CLADDING TEMP -FINE, DEG. K	
	LOC= 50/ 5/ 13 MNEM=TMCL INF=2	
----	TE-2G14-030 , DEG. K	
	LOC= 221/ 0/ 0 MNEM=TMCL INF=3	

DEG. K

REACTOR TIME , SECONDS

FIGURE 66   INF 1 JON'S, INF 2 ORIG, INF 3 EXP
FUEL ROD CLADDING TEMPERATURES - PERIPHERAL BUNDLES

FIGURE 67   INF 1 JON'S, INF 2 ORIG, INF 3 EXP
FUEL ROD CLADDING TEMPERATURES - PERIPHERAL BUNDLES

AEEW - M 2464

103

FIGURE 68   INF 1 JON'S, INF 2 ORIG, INF 3 EXP
FUEL ROD CLADDING TEMPERATURES - PERIPHERAL BUNDLES

AEEW - M 2464

105

KEY		
SYM BOL	NAME	UNITS
——	CLADDING TEMP -FINE,DEG.K	
	LOC= 50/ 6/ 5 MNEM=TMCL INF=1	
——	CLADDING TEMP -FINE,DEG.K	
	LOC= 50/ 6/ 5 MNEM=TMCL INF=2	
····	TE-4G14-011 ,DEG.K	
	LOC= 249/ 0/ 0 MNEM=TMCL INF=3	

DEG. K

950
900
850
800
750
700
650
600
550
500
450
400

0   20   40   60   80   100

REACTOR TIME   , SECONDS
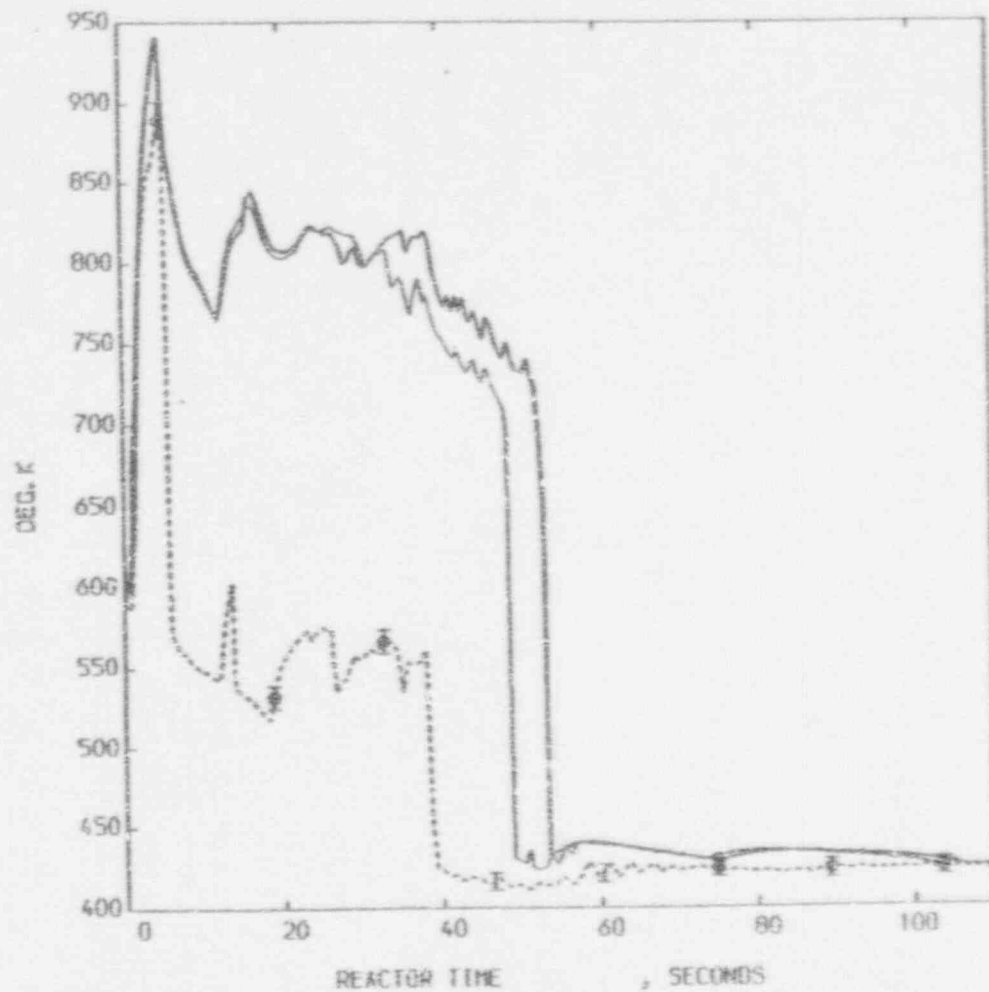
FIGURE 69 INF 1 JON'S, INF 2 ORIG, INF 3 EXP
FUEL ROD CLADDING TEMPERATURES - PERIPHERAL BUNDLES

AEEW - M 2464

106

KEY		
SYM BOL	NAME	UNITS
—1—	CLADDING TEMP -FINE, DEG.K	
	LOC= 50/ 5/ 9 MNEM=TMCL INF=1	
—2—	CLADDING TEMP -FINE, DEG.K	
	LOC= 50/ 5/ 9 MNEM=TMCL INF=2	
—3—	CLADDING TEMP -FINE, DEG.K	
	LOC= 50/ 9/ 9 MNEM=TMCL INF=1	
—+—	CLADDING TEMP -FINE, DEG.K	
	LOC= 50/ 9/ 9 MNEM=TMCL INF=2	
----	TE-4G08-021 , DEG.K	
	LOC= 248/ 0/ 0 MNEM=TMCL INF=3	

DEG. K

REACTOR TIME , SECONDS
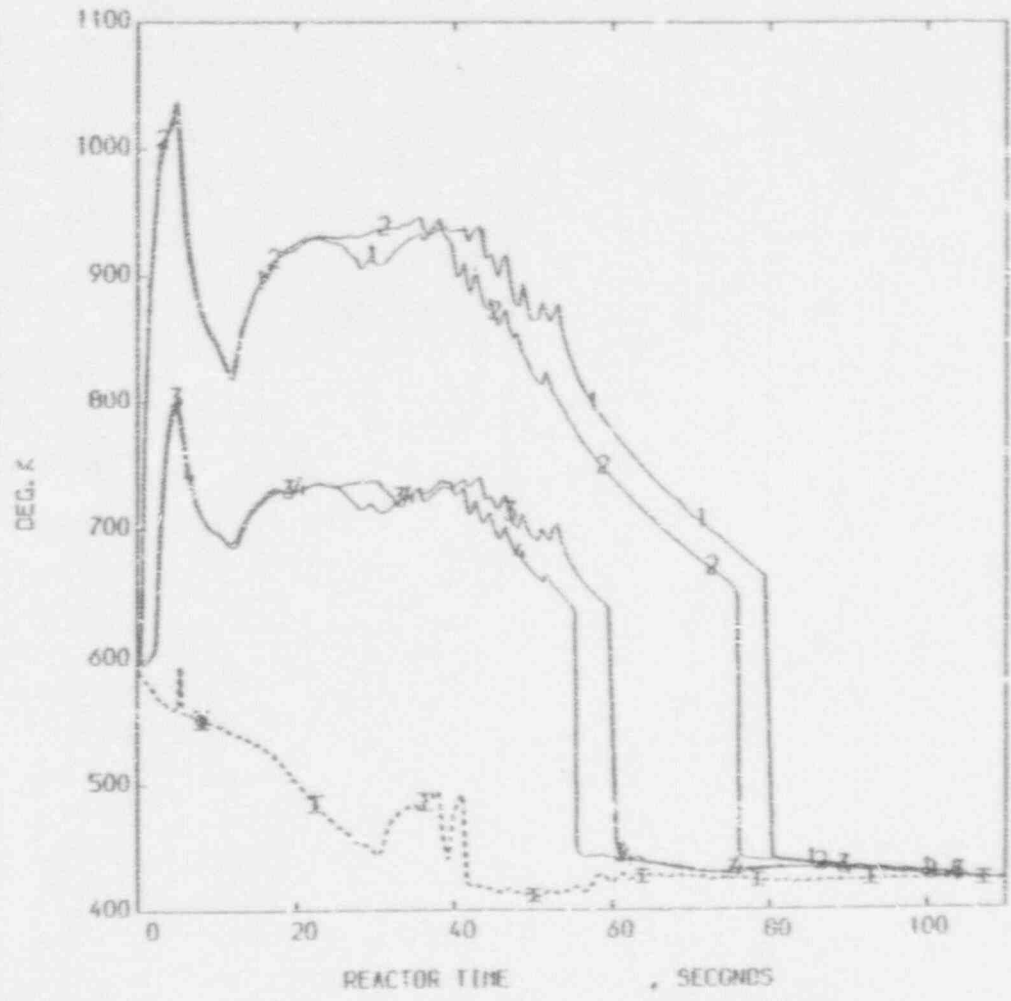
FIGURE 70   INF 1 JON'S, INF 2 ORIG, INF 3 EXP
FUEL ROD CLADDING TEMPERATURES - PERIPHERAL BUNDLES

THE FOLLOWING ARE PLOTTED AGAINST REACTOR TIME

CLADDING TEMP -FINE,TE-4H14-02B

Winfrith

KEY		
SYM BOL.	NAME	UNITS
——	CLADDING TEMP -FINE,DEG.K LOC= 50/ 6/ 12 MNEM=TMCL INF=1	
——	CLADDING TEMP -FINE,DEG.K LOC= 50/ 6/ 12 MNEM=TMCL INF=2	
----	TE-4H14-02B ,DEG.K LOC= 253/ 0/ 0 MNEM=TMCL INF=3	

DEG. K

REACTOR TIME   , SECONDS

FIGURE 71   INF 1 JON'S, INF 2 ORIG, INF 3 EXP
FUEL ROD CLADDING TEMPERATURES - PERIPHERAL BUNDLES

Winfrith

AEEW - M 2464

108

KEY

SYM BOL	NAME	UNITS
——	CLADDING TEMP -FINE,DEG.K LOC= 50/ 5/ 15 MNEM=TMCL INF=1	
——	CLADDING TEMP -FINE,DEG.K LOC= 50/ 5/ 15 MNEM=TMCL INF=2	
····	TE-4114-039 ,DEG.K LOC= 257/ 0/ 0 MNEM=TMF INF=3	

REACTOR TIME , SECONDS

FIGURE 72 INF 1 JON'S, INF 2 ORIG, INF 3 EXP
FUEL ROD CLADDING TEMPERATURES - PERIPHERAL BUNDLES

KEY

SYM BOL	NAME	UNITS
——	CLADDING TEMP -FINE,DEG.K	
	LOC= 50/ 8/ 5 MNEM=TNCL INF=1	
——	CLADDING TEMP -FINE,DEG.K	
	LOC= 50/ 8/ 5 MNEM=TNCL INF=2	
----	TE-6G14-011 ,DEG.K	
	LOC= 529/ 0/ 0 MNEM=TNCL INF=3	
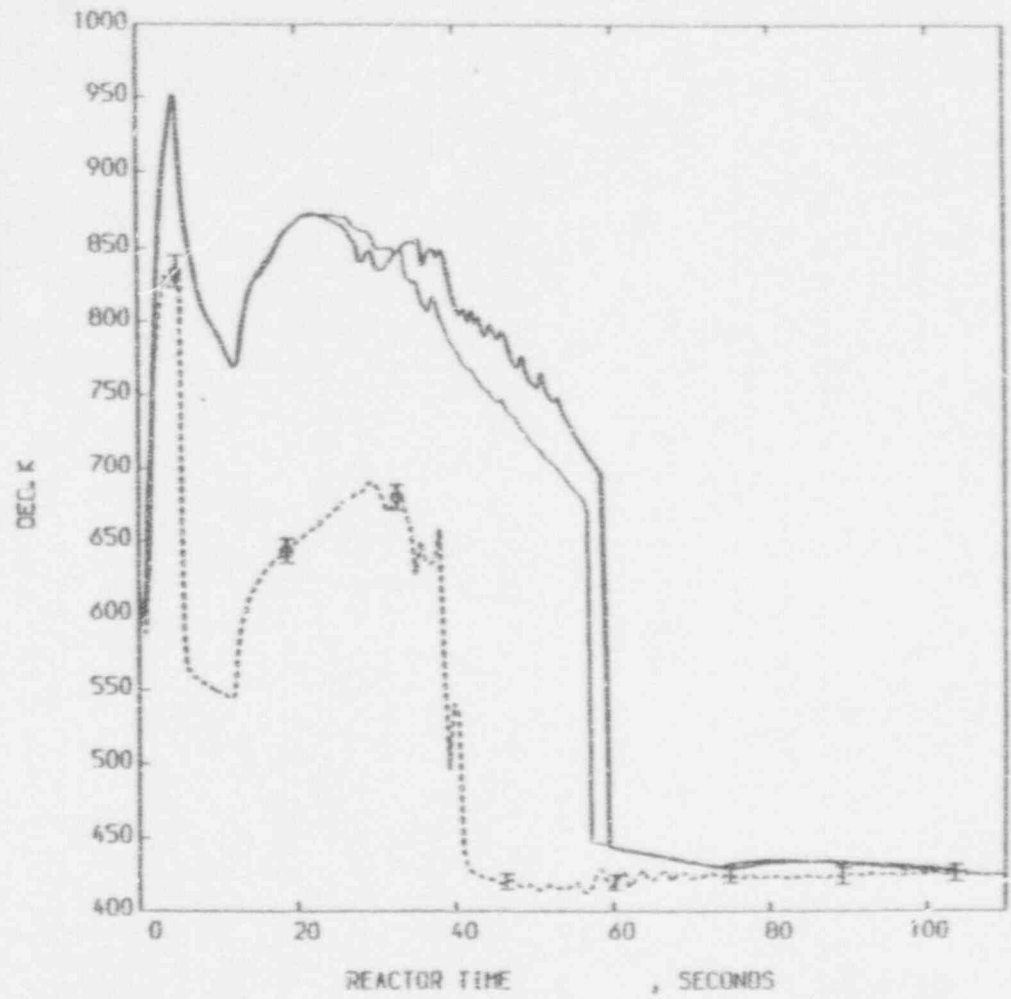
FIGURE 73 INF 1 JON'S, INF 2 ORIG, INF 3 EXP
FUEL ROD CLADDING TEMPERATURES – PERIPHERAL BUNDLES

AEEW - M 2464

110

KEY		
SYM BOL	NAME	UNITS
———	CLADDING TEMP -FINE, DEG.K LOC= 50/ 8/ 13 MNEM=THCL INF=1	
———	CLADDING TEMP -FINE, DEG.K LOC= 50/ 8/ 13 MNEM=THCL INF=2	
····	TE-6G14-030 , DEG.K LOC= 330/ 0/ 0 MNEM=THCL INF=3	

DEG. K

REACTOR TIME   , SECONDS

FIGURE 74   INF 1 JON'S, INF 2 ORIG, INF 3 EXP
FUEL ROD CLADDING TEMPERATURES - PERIPHERAL BUNDLES

Winfrith

FIGURE 75   INF 1 JON'S, INF 2 ORIG, INF 3 EXP
FUEL ROD CLADDING TEMPERATURES - PERIPHERAL BUNDLES

THE FOLLOWING ARE PLOTTED AGAINST REACTOR TIME

CLADDING TEMP -FINE,TE-6114-039
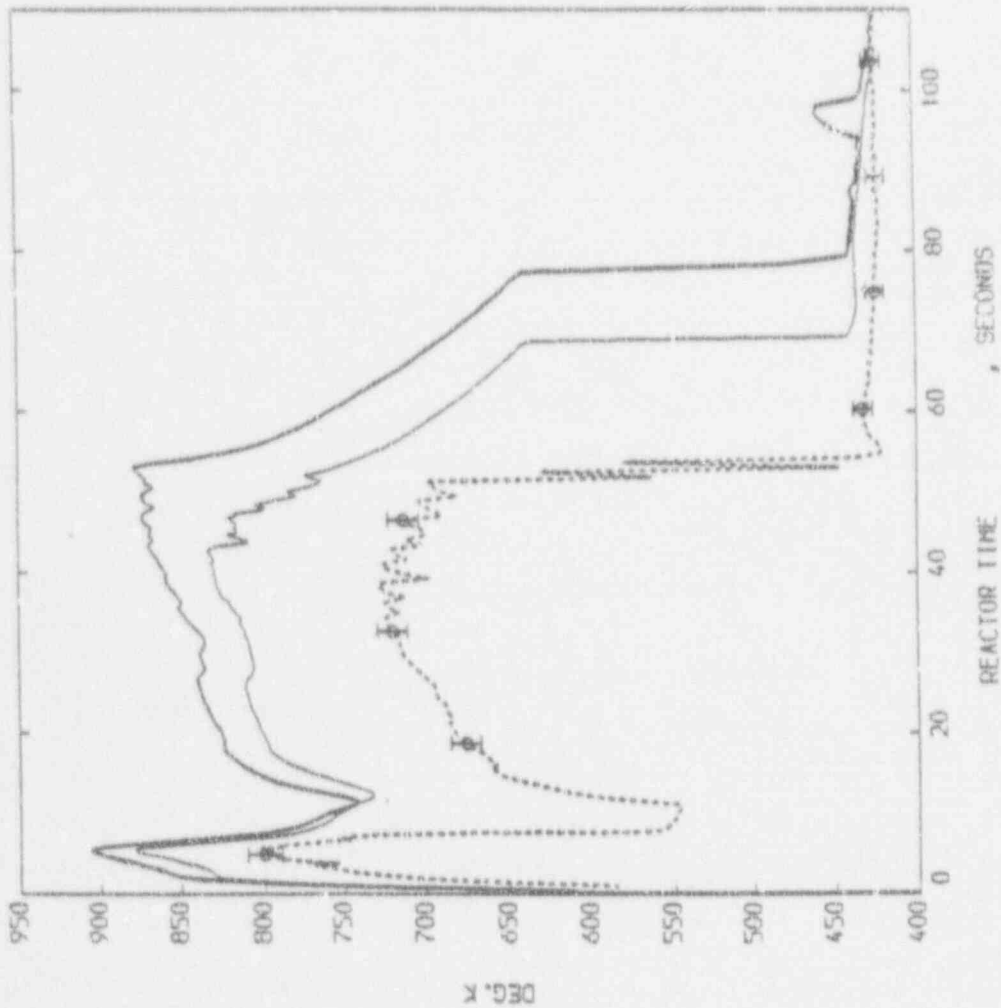
REACTOR TIME   , SECONDS

DEG. K

KEY		
SYM BOL	NAME	UNITS
——	CLADDING TEMP -FINE ,DEG. K LOC= 50/ 7/ 15 MNEM=TMCL INF=1	
——	CLADDING TEMP -FINE ,DEG. K LOC= 50/ 7/ 15 MNEM=TMCL INF=2	
----	TE-6114-039 ,DEG. K LOC= 337/ 0/ 0 MNEM=TMCL INF=3	

FIGURE 76 INF 1 JON'S, INF 2 ORIG, INF 3 EXP
FUEL ROD CLADDING TEMPERATURES – PERIPHERAL BUNDLES

AEEW – M 2464

112

AEEW - M 2464

113

FIGURE 77   INF 1 JON'S, INF 2 ORIG, INF 3 EXP
FUEL ROD CLADDING TEMPERATURES - PERIPHERAL BUNDLES

FIGURE 78   INF 1 ORIG, INF 2 ZEROGAP, INF 3 EXP
BROKEN LOOP COLD LEG - EXPERIMENTAL LOCATION BL-1

Winfrith

FIGURE 79   INF 1 ORIG, INF 2 ZEROGAP, INF 3 EXP
BROKEN LOOP COLD LEG - EXPERIMENTAL LOCATION BL-1

KEY

SYMBOL	NAME	UNITS
———	MASS FLOW RATE ,KG/SEC LOC= 41/ 0/ 3 MNEM=FLOW INF=1	
———	MASS FLOW RATE ,KG/SEC LOC= 41/ 0/ 3 MNEM=FLOW INF=2	
····	FR-BL-105 ,KG/SEC LOC= 32/ 0/ 0 MNEM=FLOW INF=3	

AEEW - M 2464

116
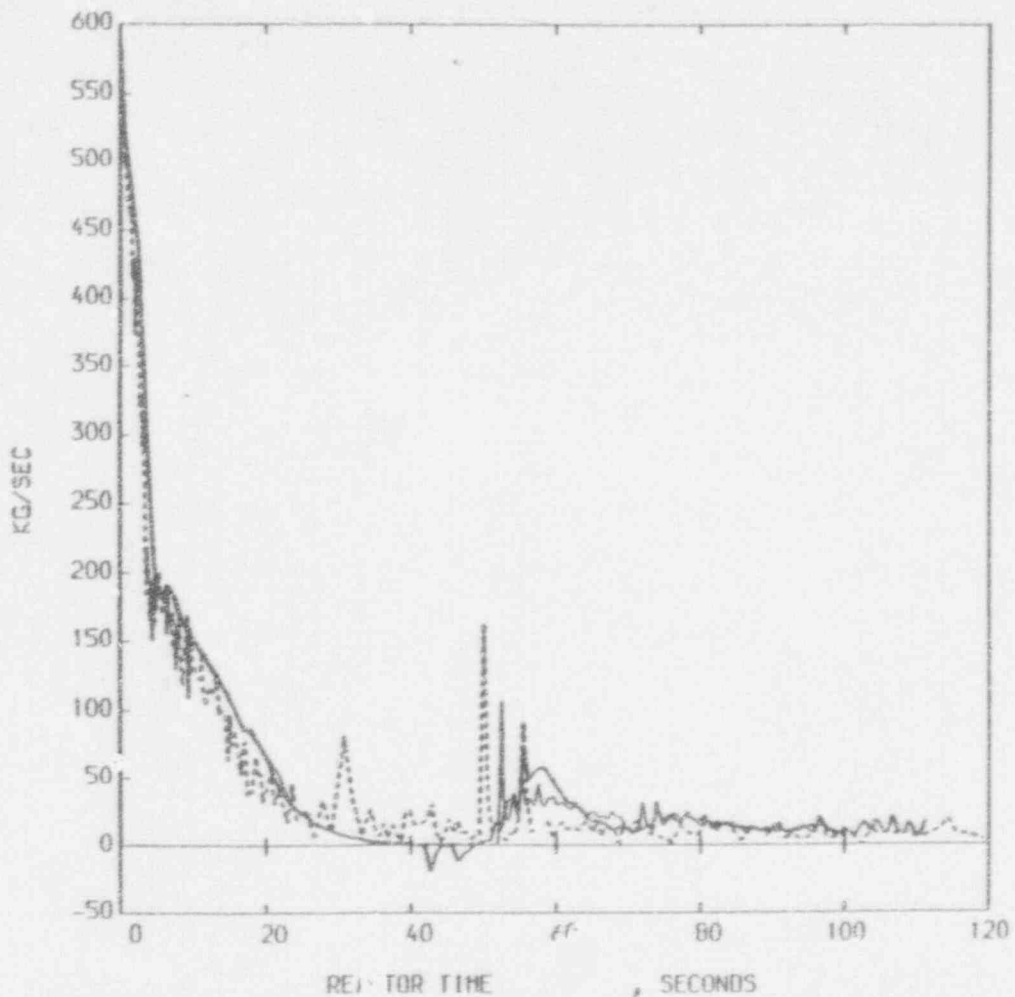
FIGURE 80   INF 1 ORIG, INF 2 ZEROGAP, INF 3 EXP
BROKEN LOOP COLD LEG – EXPERIMENTAL LOCATION BL-1

THE FOLLOWING ARE PLOTTED AGAINST REACTOR TIME

LIQUID TEMPERATURE ,TE-BL-001A

Winfrith
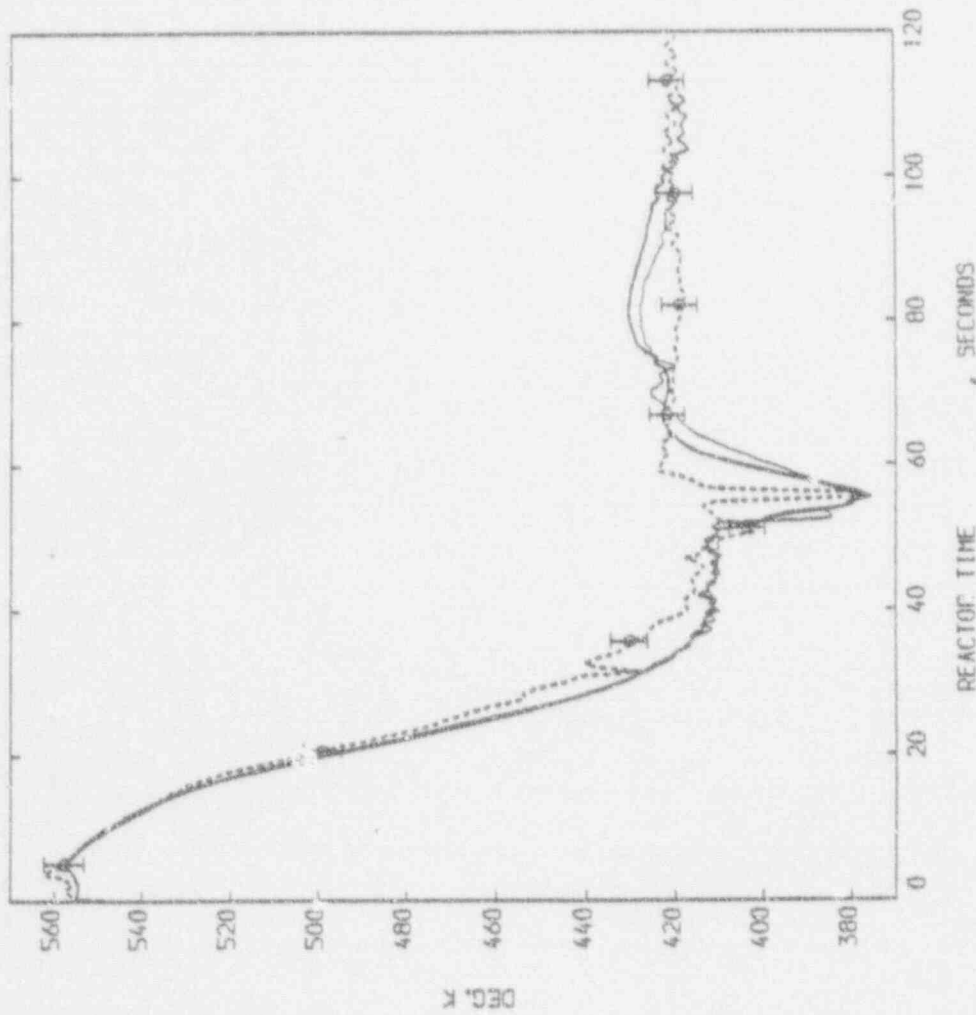
KEY	
NAME	UNITS
SYM BOL	
—— LIQUID TEMPERATURE ,DEG.K	
LOC= 41/ 0/ 3 MNEM-TEML INF=1	
—— LIQUID TEMPERATURE ,DEG.K	
LOC= 41/ 0/ 3 MNEM-TEML INF=2	
---- TE-BL-001A ,DEG.K	
LOC= 171/ 0/ 0 MNEM-TMCL INF=3	

DEG, K

REACTOR TIME , SECONDS

FIGURE 81 INF 1 ORIG, INF 2 ZEROGAP, INF 3 EXP
BROKEN LOOP COLD LEG - EXPERIMENTAL LOCATION BL-1

AEEW - M 2464

117

Winfrith

118

FIGURE 82   INF 1 ORIG, INF 2 ZEROGAP, INF 3 EXP
BROKEN LOOP COLD LEG — EXPERIMENTAL LOCATION BL-1

FIGURE 83 INF 1 ORIG, INF 2 ZEROGAP, INF 3 EXP
BROKEN LOOP COLD LEG - EXPERIMENTAL LOCATION BL-4

PRESSURE   ,PE-BL-00B

AEEW - M 2464

120

FIGURE 94   INF 1 ORIG, INF 2 ZEROGAP, INF 3 EXP
BROKEN LOOP COLD LEG - EXPERIMENTAL LOCATION BL-8

FIGURE 85 INF 1 ORIG, INF 2 ZEROGAP, INF 3 EXP
BROKEN LOOP HOT LEG - EXPERIMENTAL LOCATION BL-2
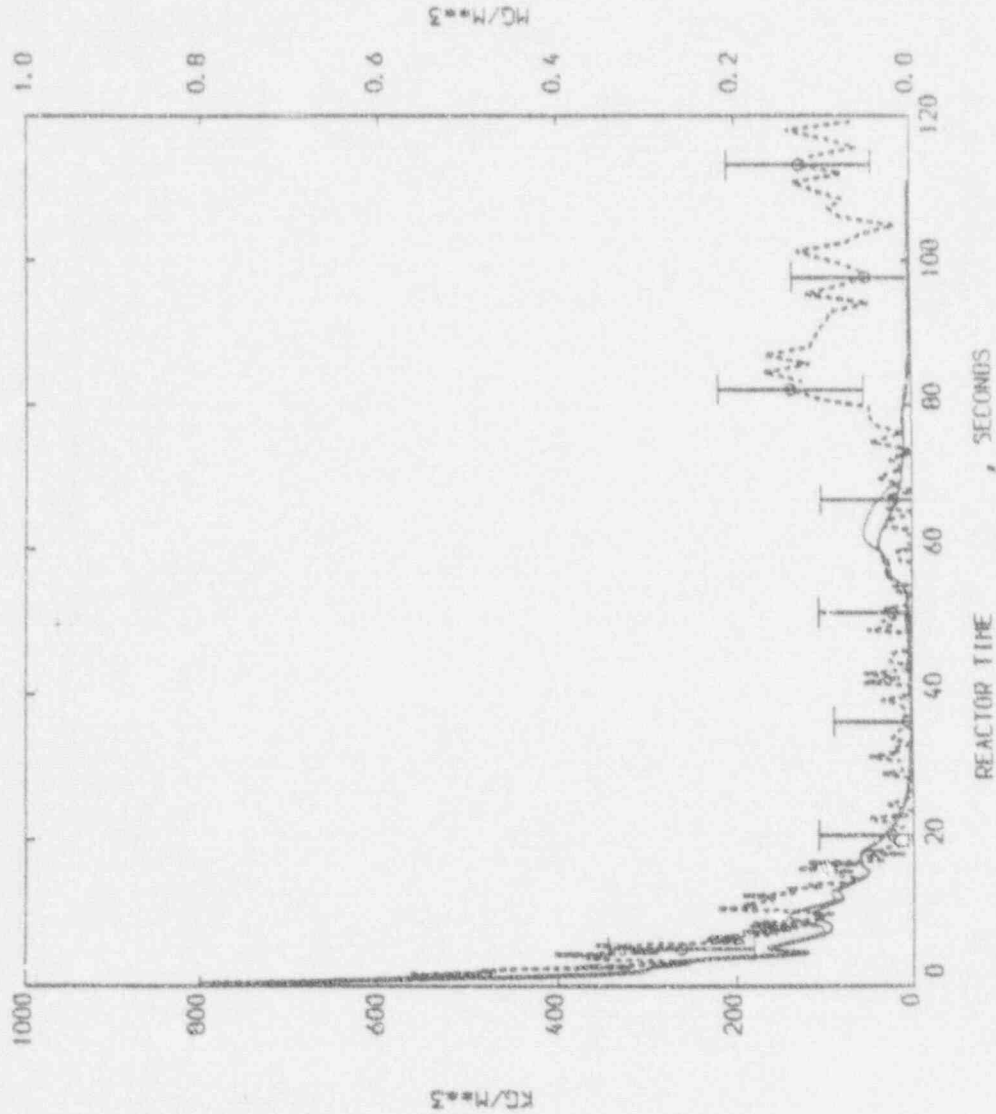
FIGURE 86 INF 1 ORIG, INF 2 ZEROGAP, INF 3 EXP
BROKEN LOOP HOT LEG - EXPERIMENTAL LOCATION BL-2

AEEW - M 2464

123

KEY		
SYM BOL	NAME	UNITS
——	MASS FLOW RATE ,KG/SEC	
	LOC= 31/ 0/ 3 MNEM=FLOW INF=1	
——	MASS FLOW RATE ,KG/SEC	
	LOC= 31/ 0/ 3 MNEM=FLOW INF=2	
----	FR-BL-205 ,KG/SEC	
	LOC= 33/ 0/ 0 MNEM=FLOW INF=3	

REACTOR TIME   , SECONDS
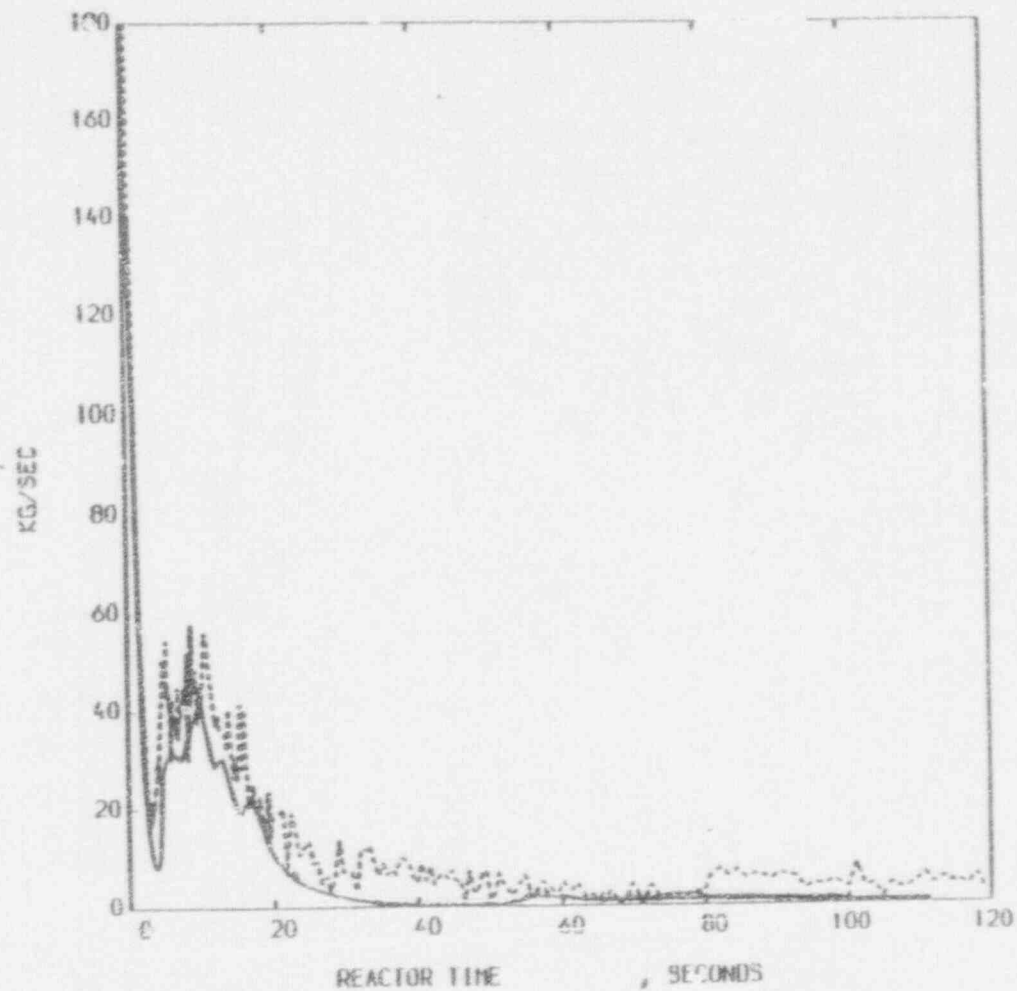
FIGURE 87   INF 1 ORIG, INF 2 ZEROGAP, INF 3 EXP
BROKEN LOOP HOT LEG - EXPERIMENTAL LOCATION BL-2

THE FOLLOWING ARE PLOTTED AGAINST REACTOR TIME

LIQUID TEMPERATURE ,TE-BL-0028

FIGURE 88 INF 1 ORIG, INF 2 ZEROGAP, INF 3 EXP
BROKEN LOOP HOT LEG - EXPERIMENTAL LOCATION BL-2

Winfrith
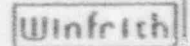
KEY		
SYM BOL	NAME	UNITS
——	VAPOR TEMPERATURE , DEG. K LOC= 31/ 0/ 3 MNEM=TEMV INF=1	
——	VAPOR TEMPERATURE , DEG. K LOC= 31/ 0/ 3 MNEM=TEMV INF=2	
----	TE-BL-002B , DEG. K LOC= 174/ 0/ 0 MNEM=TMCL INF=3	
— —	TE-BL-002C , DEG. K LOC= 175/ 0/ 0 MNEM=TMCL INF=3	

FIGURE 89   INF 1 ORIG, INF 2 ZEROGAP, INF 3 EXP
BROKEN LOOP HOT LEG - EXPERIMENTAL LOCATION BL-2

AEEW - M 2464

126

FIGURE 90   INF 1 ORIG, INF 2 ZEROGAP, INF 3 EXP
BROKEN LOOP HOT LEG - EXPERIMENTAL LOCATION BL-3

THE FOLLOWING ARE PLOTTED AGAINST REACTOR TIME
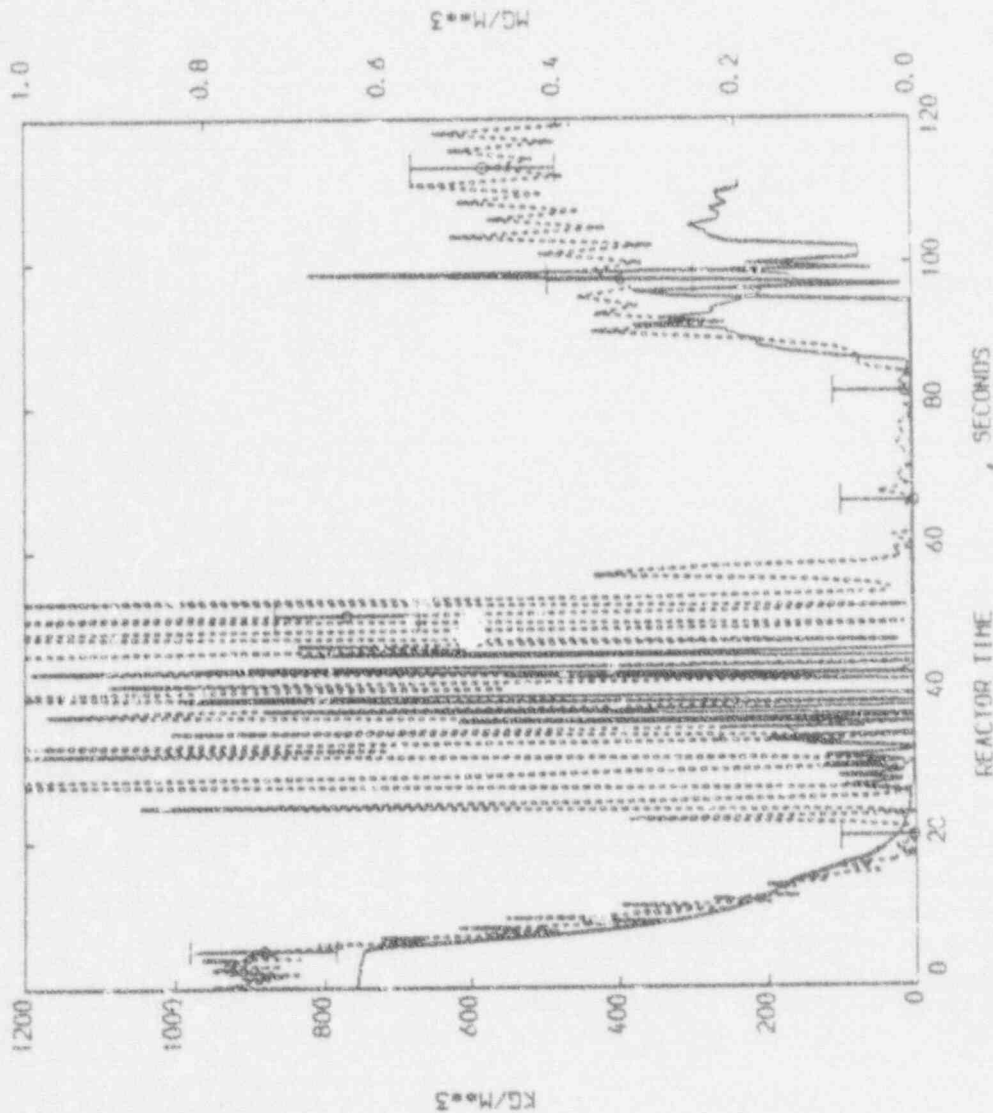
MIXTURE DENSITY ,DE-PC-001A

FIGURE 91 INF 1 ORIG, INF 2 ZEROGAP, INF 3 EXP
INTACT LOOP COLD LEG - EXPERIMENTAL LOCATION PC-1

KEY		
SYMBOL	NAME	UNITS
—	MIXTURE DENSITY LOC= 7/ 0/ 4 MXEN-DENM INF=1	,KG/M**3
—	MIXTURE DENSITY LOC= 7/ 0/ 4 MXEM-DENM INF=2	,KG/M**3
---	DE-PC-001A LOC= 13/ 0/ 0 MXEM-DENM INF=3	,MG/M**3

THE FOLLOWING ARE PLOTTED AGAINST REACTOR TIME

MASS FLOW RATE ,FR-PC-100

FIGURE 22 INF 1 ORIG, INF 2 ZEROGAP, INF 3 EXP
INTACT LOOP COLD LEG - EXPERIMENTAL LOCATION PC-1

THE FOLLOWING ARE PLOTTED AGAINST REACTOR TIME

LIQUID VELOCITY ,FE-PC-001A

FIGURE 93 INF 1 GRIG, INF 2 ZERO-P, INF 3 EXP
INTACT LOOP COLD LEG - EXPERIMENTAL LOCATION PC-1

Winfrith

AEEW - M 2464

130

KEY

SYM BOL	NAME	UNITS
——	LIQUID TEMPERATURE , DEG. K	
LOC= 7/ 0/ 4 MNEM=TEHL INF=1		
——	LIQUID TEMPERATURE , DEG. K	
LOC= 7/ 0/ 5 MNEM=TEHL INF=2		
----	TE-PC-001A , DEG. K	
LOC= 176/ 0/ 0 MNEM=THCL INF=3		
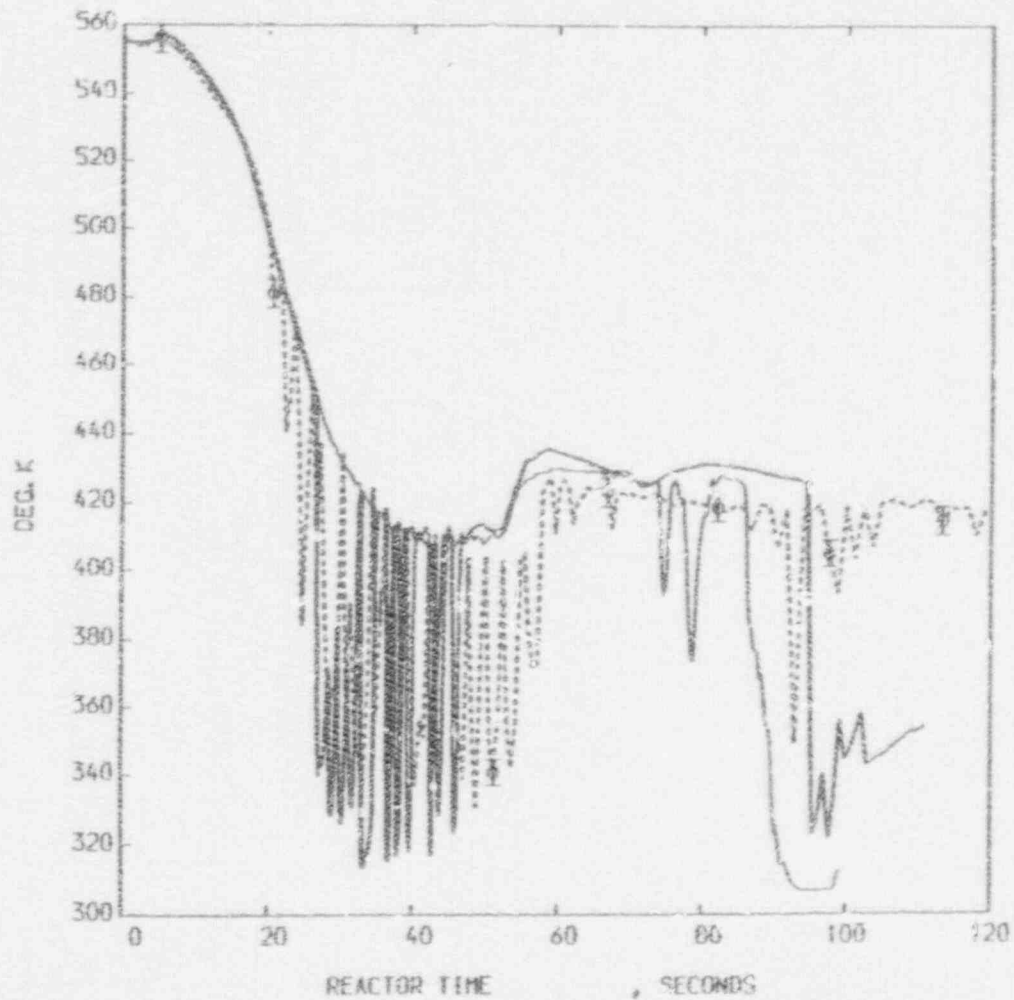
DEG. K

REACTOR TIME , SECONDS

FIGURE 94 INF 1 ORIG, INF 2 ZEROGAP, INF 3 EXP
INTACT LOOP COLD LEG — EXPERIMENTAL LOCATION PC-1

Winfrith

AEEW - M 2464

131

KEY		
SYM BOL	NAME	UNITS
——	VAPOR TEMPERATURE ,DEG.K	
	LOC= 7/ 0/ 4 MNEM=TEMV INF=1	
——	VAPOR TEMPERATURE ,DEG.K	
	LOC= 7/ 0/ 4 MNEM=TEMV INF=2	
....	TE-PC-001C ,DEG.K	
	LOC= 178/ 0/ 0 MNEM=TMEL INF=3	

DEG.K

REACTOR TIME   , SECONDS
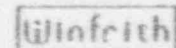
FIGURE 95 INF 1 ORIG, INF 2 ZEROGAP, INF 3 EXP

INTACT LOOP COLD LEG - EXPERIMENTAL LOCATION PC-1.

PUMP SPEED   ,FUNCTION

FIGURE 96   INF 1 ORIG, INF 2 ZEROGAP, INF 3 EXP
PUMP SPEED

AEEW - M 2464

133

FIGURE 97   INF 1 ORIG, INF 2 ZEROGAP, INF 3 EXP
INTACT LOOP HOT LEG - EXPERIMENTAL LOCATION PC-2

AEEW - M 2464

134

KEY		
SYM BOL	NAME	UNITS
——	MASS FLOW RATE	,KG/SEC
	LOC= 1/ 0/ 2 MNEM=FLOW INF=1	
——	MASS FLOW RATE	,KG/SEC
	LOC= 1/ 0/ 2 MNEM=FLOW INF=2	
----	FR-PC-201	,KG/SEC
	LOC= 37/ 0/ 0 MNEM=FLOW INF=3	
— —	FR-PC-205	,KG/SEC
	LOC= 38/ 0/ 0 MNEM=FLOW INF=3	

FIGURE 98   INF 1 ORIG, INF 2 ZEROGAP, INF 3 EXP
INTACT LOOP HOT LEG - EXPERIMENTAL LOCATION PC-2

Winfrith

AEEW - M 2464

135

KEY		
SYM BOL	NAME	UNITS
——	LIQUID TEMPERATURE , DEG. K LOC= 1/ 0/ 2 MNEM=TEML INF=1	
———	LIQUID TEMPERATURE , DEG. K LOC= 1/ 0/ 2 MNEM=TEML INF=2	
----	TE-PC-002A , DEG. K LOC= 179/ 0/ 0 MNEM=TMCL INF=3	

DEG. K

REACTOR TIME , SECONDS
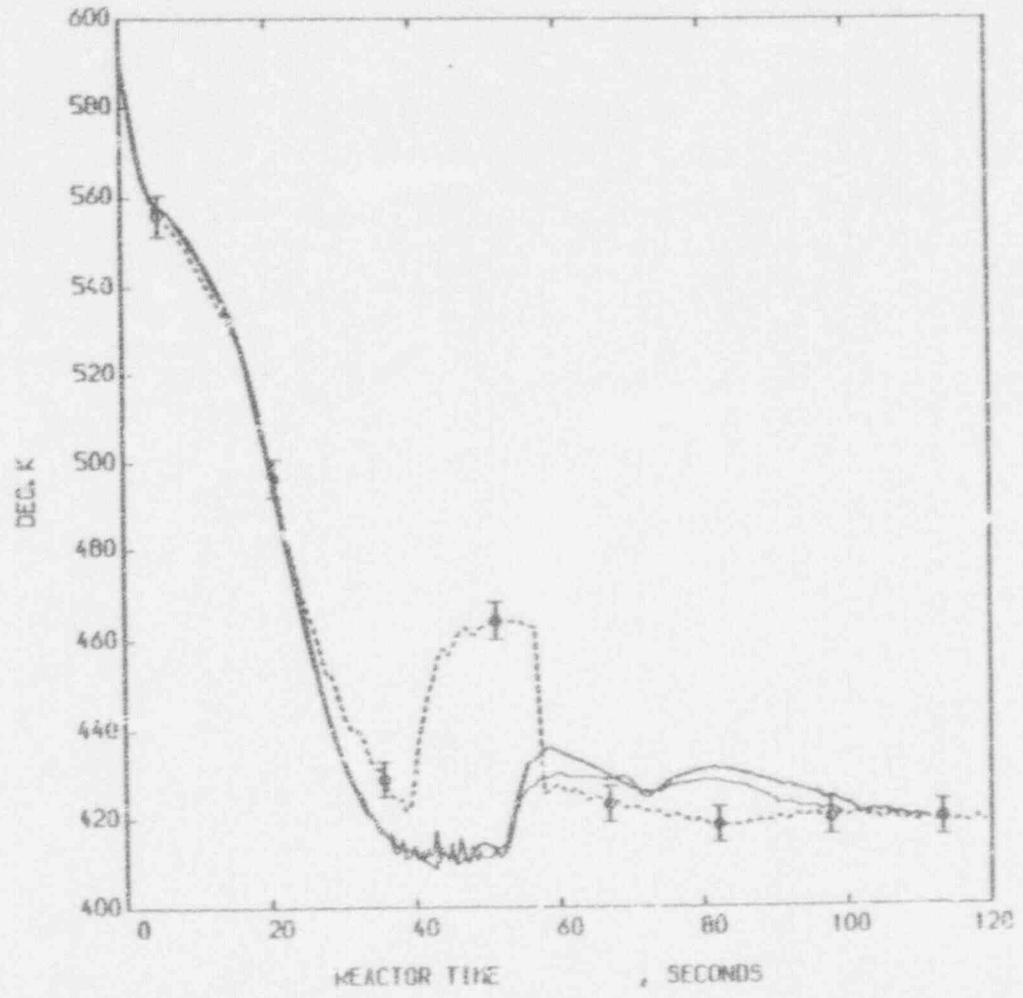
FIGURE 99   INF 1 ORIG, INF 2 ZEROGAP, INF 3 EXP

INTACT LOOP HOT LEG - EXPERIMENTAL LOCATION PC-2

THE FOLLOWING ARE PLOTTED AGAINST REACTOR TIME

VAPOR TEMPERATURE , TE-PC-002A , TE-PC-002B
TE-PC-002C

FIGURE 100 INF 1 ORIG, INF 2 ZEROGAP, INF 3 EXP
INTACT LOOP HOT LEG - EXPERIMENTAL LOCATION PC-2

AEEW - M 2464

136

KEY

SYMBOL	NAME	UNITS
————	PRESSURE LOC= 1/ 0/ 2 MNEM=PRES INF=1	,N/M**2
————	PRESSURE LOC= 1/ 0/ 2 MNEM=PRES INF=2	,N/M**2
----	PE-PC-002 LOC= 120/ 0/ 0 MNEM=PRES INF=3	,MPA

FIGURE 101   INF 1 ORIG, INF 2 ZEROGAP, INF 3 EXP
INTACT LOOP HOT LEG - EXPERIMENTAL LOCATION PC-2

FIGURE 102   INF 1 ORIG, INF 2 ZEROGAP, INF 3 EXP
INTACT LOOP HOT LEG - PRESSURIZER

1
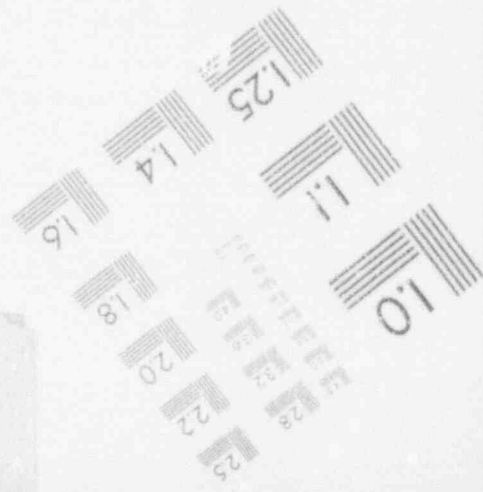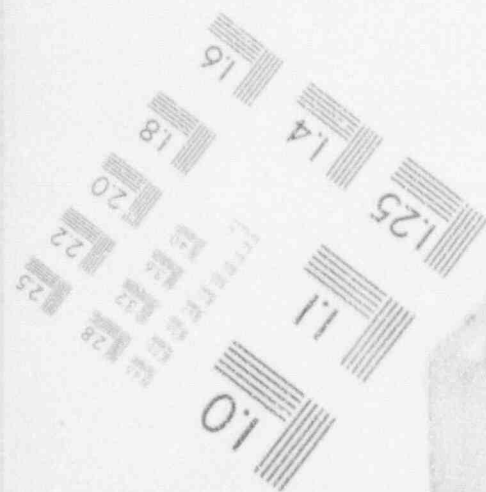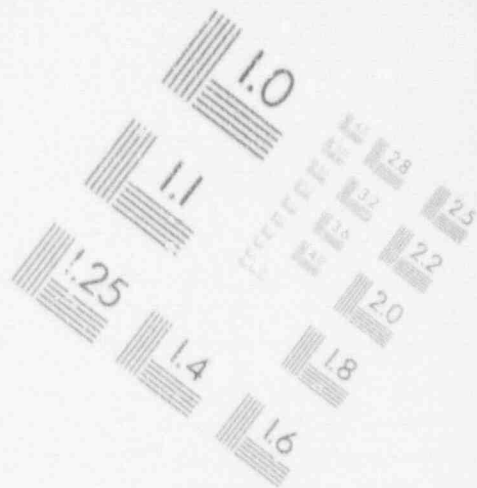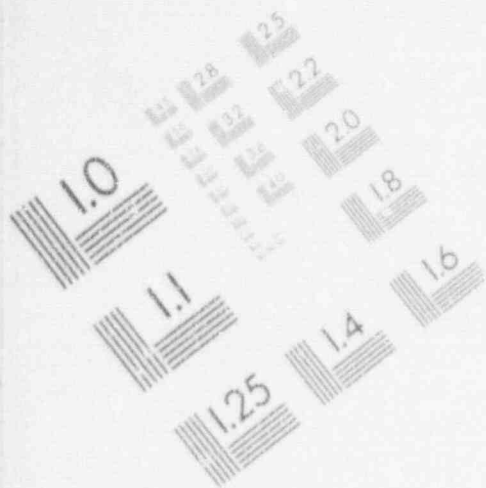
IMAGE EVALUATION
TEST TARGET (MT-3)

1

IMAGE EVALUATION
TEST TARGET (MT-3)

1.0

1.1

1.25   1.4   1.6

2.8   2.5

3.2   2.2

2.0

1.8

150mm

6"

1

IMAGE EVALUATION
TEST TARGET (MT-3)

150mm

6"

1

IMAGE EVALUATION
TEST TARGET (MT-3)

1.0

1.1

1.25   1.4   1.6

|← 150mm →|

|← 6" →|

WATER LEVEL   ,LEPOT-P139-008+0.216

Winfrith

AEEW - M 2464

139
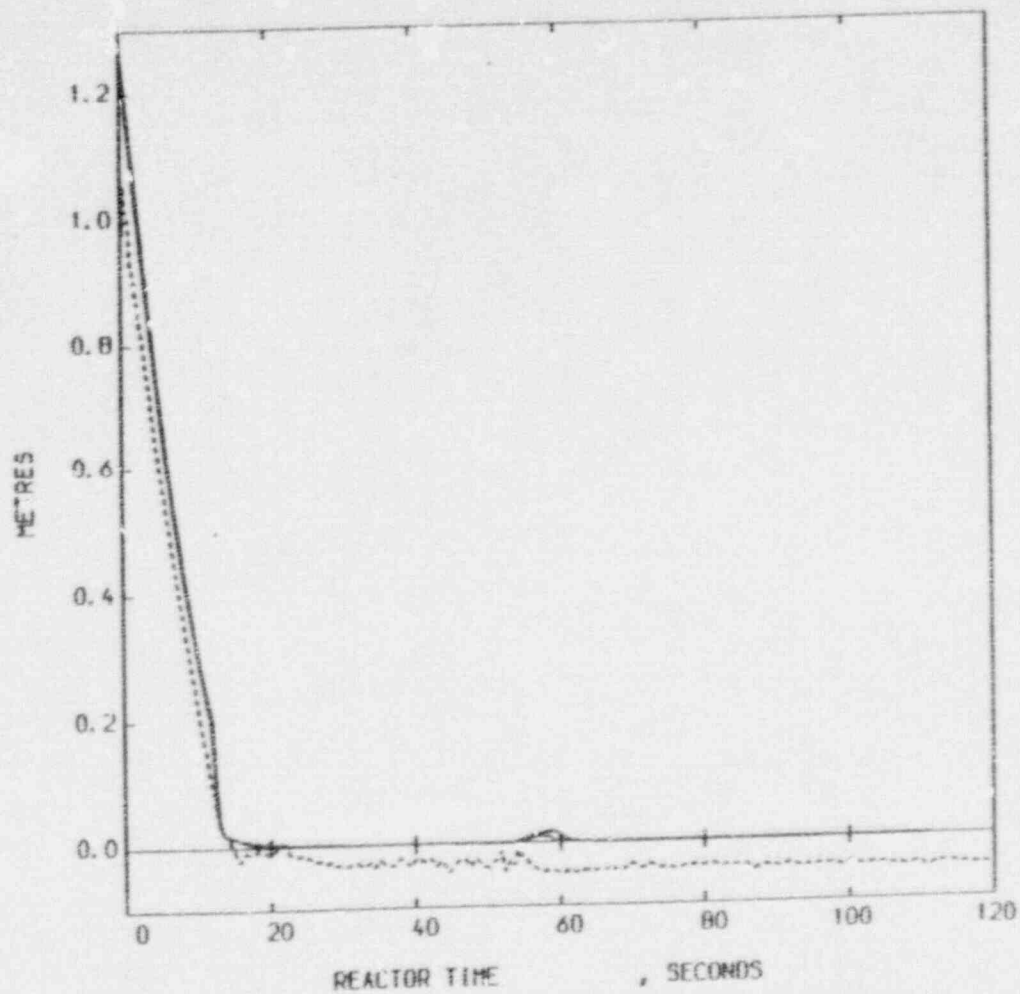
FIGURE 103   INF 1 ORIG, INF 2 ZEROGAP, INF 3 EXP
INTACT LOOP HOT LEG - PRESSURIZER

FIGURE 104 INF 1 ORIG, INF 2 ZEROGAP, INF 3 EXP
EMERGENCY CORE COOLING SYSTEM

THE FOLLOWING ARE PLOTTED AGAINST REACTOR TIME
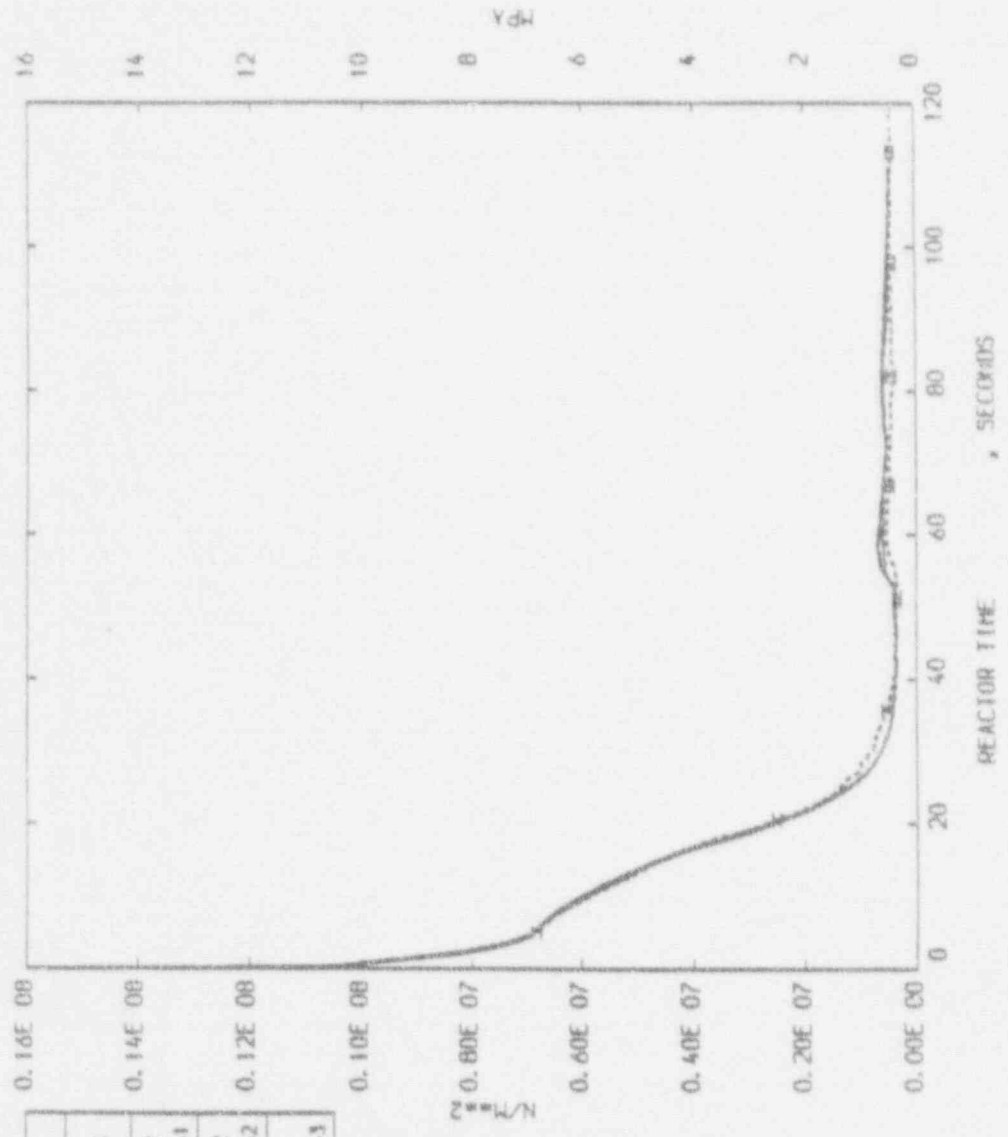
PRESSURE   ,PT-P120-043

AEEW - M 2464

141

KEY

SYM BOL	NAME	UNITS
——	PRESSURE LOC= 15/ 0/ 1 MNEM=PRES INF=1	,N/M**2
——	PRESSURE LOC= 15/ 0/ 1 MNEM=PRES INF=2	,N/M**2
----	PT-P120-043 LOC= 131/ 0/ 0 MNEM=PRES INF=3	,MPA

N/M**2

MPA

REACTOR TIME   , SECONDS

FIGURE 105   INF 1 ORIG, INF 2 ZEROGAP, INF 3 EXP
EMERGENCY CORE COOLING SYSTEM

FIGURE 106 INF 1 ORIG, INF 2 ZEROGAP, INF 3 EXP
UPPER PLENUM PRESSURE

A.E.E.W. = . 464

143

KEY

SYM BOL	NAME	UNITS
——	LIQ AXIAL VELOCITY ,M/SEC LOC= 50/ 3/ 1 MNEM=VL-Z INF=1	
——	LIQ AXIAL VELOCITY ,M/SEC LOC= 50/ 3/ 1 MNEM=VL-Z INF=2	
----	FE-SLP-001 ,M/SEC LOC= 29/ 0/ 0 MNEM=FE INF=3	

M/SEC

REACTOR TIME , SECONDS
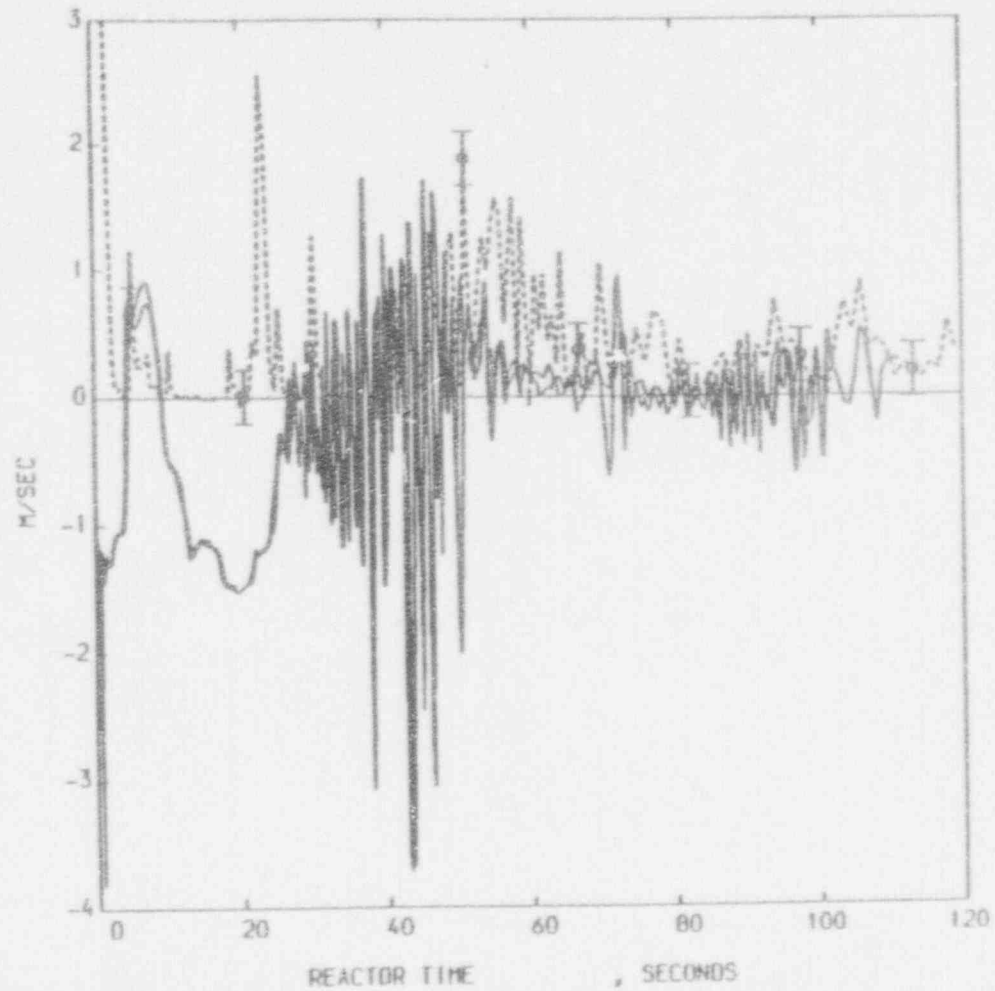
FIGURE 107 INF 1 ORIG, INF 2 ZEROGAP, INF 3 EXP
LOWER PLENUM LIQUID AXIAL VELOCITY

THE FOLLOWING ARE PLOTTED AGAINST REACTOR TIME
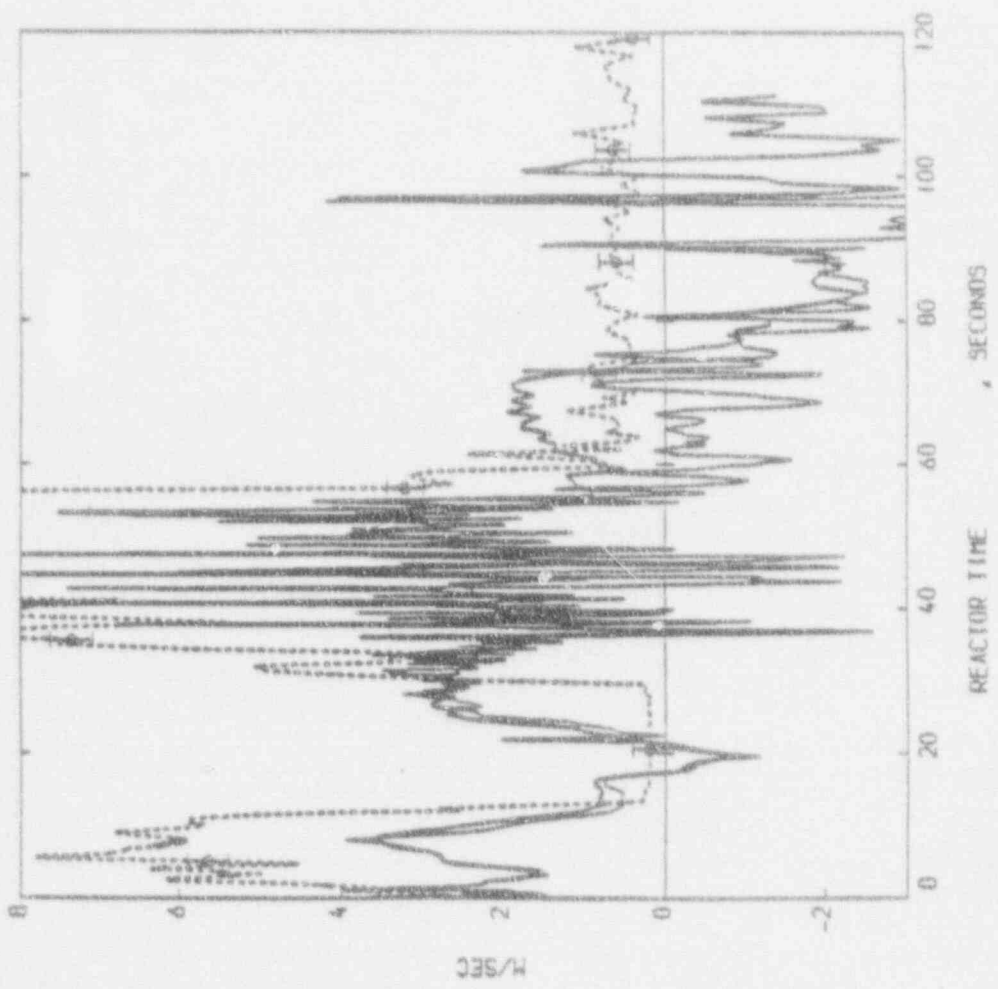
LIQ AXIAL VELOCITY ,FE-SUP-001

FIGURE 108 INF 1 ORIG, INF 2 ZEROGAP, INF 3 EXP
UPPER PLENUM LIQUID AXIAL VELOCITY
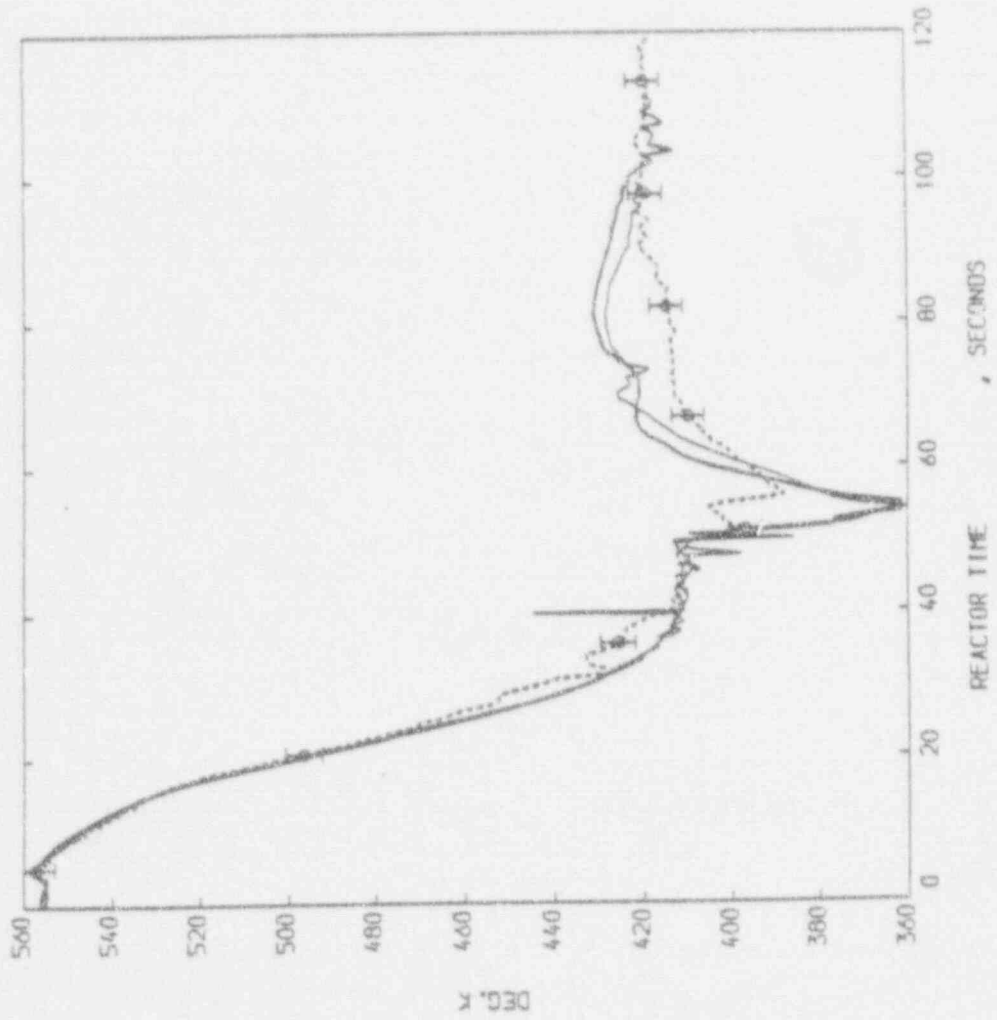
FIGURE 109 INF 1 ORIG, INF 2 ZEROGAP, INF 3 EXP
DOWNCOMER LIQUID TEMPERATURE AT 5.0 METRES

THE FOLLOWING ARE PLOTTED AGAINST REACTOR TIME

LIQUID TEMPERATURE , TE-1ST-002

Winfrith
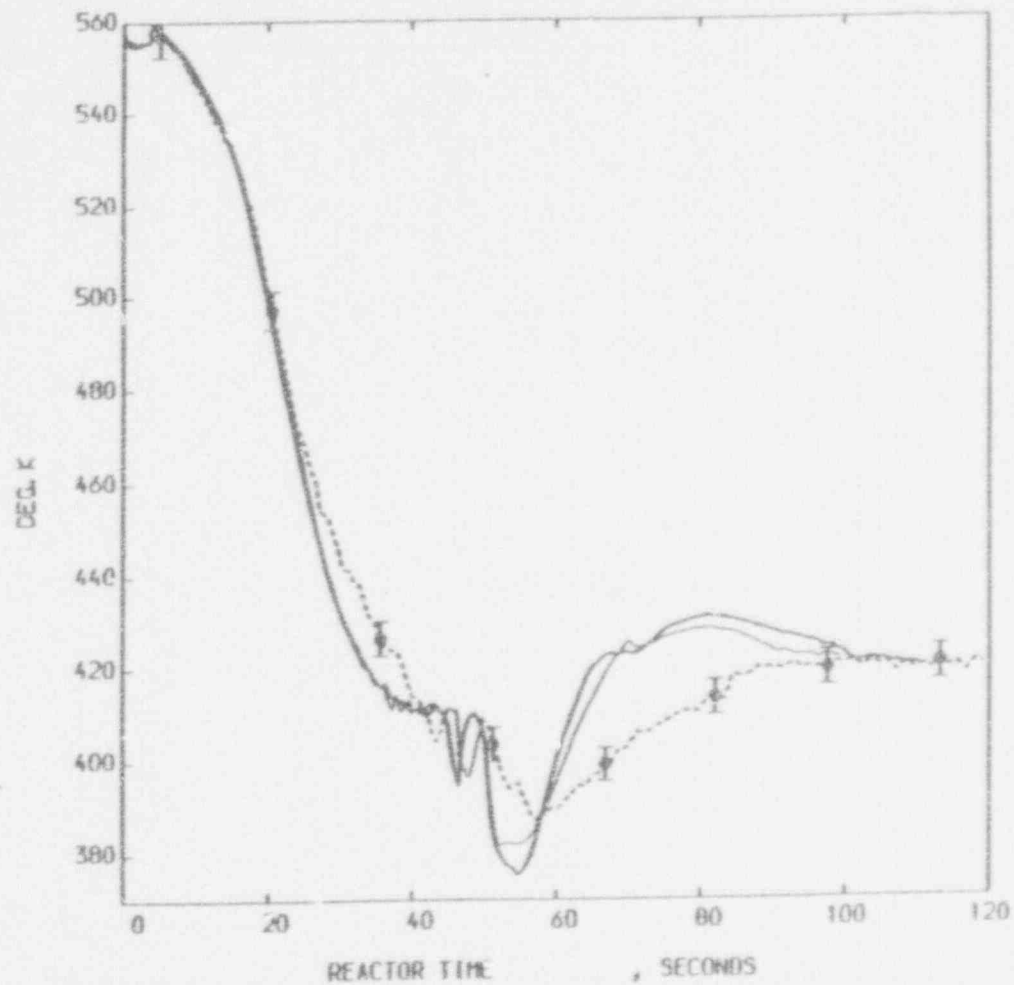
FIGURE 110   INF 1 ORIG, INF 2 ZEROGAP, INF 3 EXP
DOWNCOMER LIQUID TEMPERATURE AT 4.2 METRES

Winfrith

THE FOLLOWING ARE PLOTTED AGAINST REACTOR TIME

LIQUID TEMPERATURE , TE-151-G05
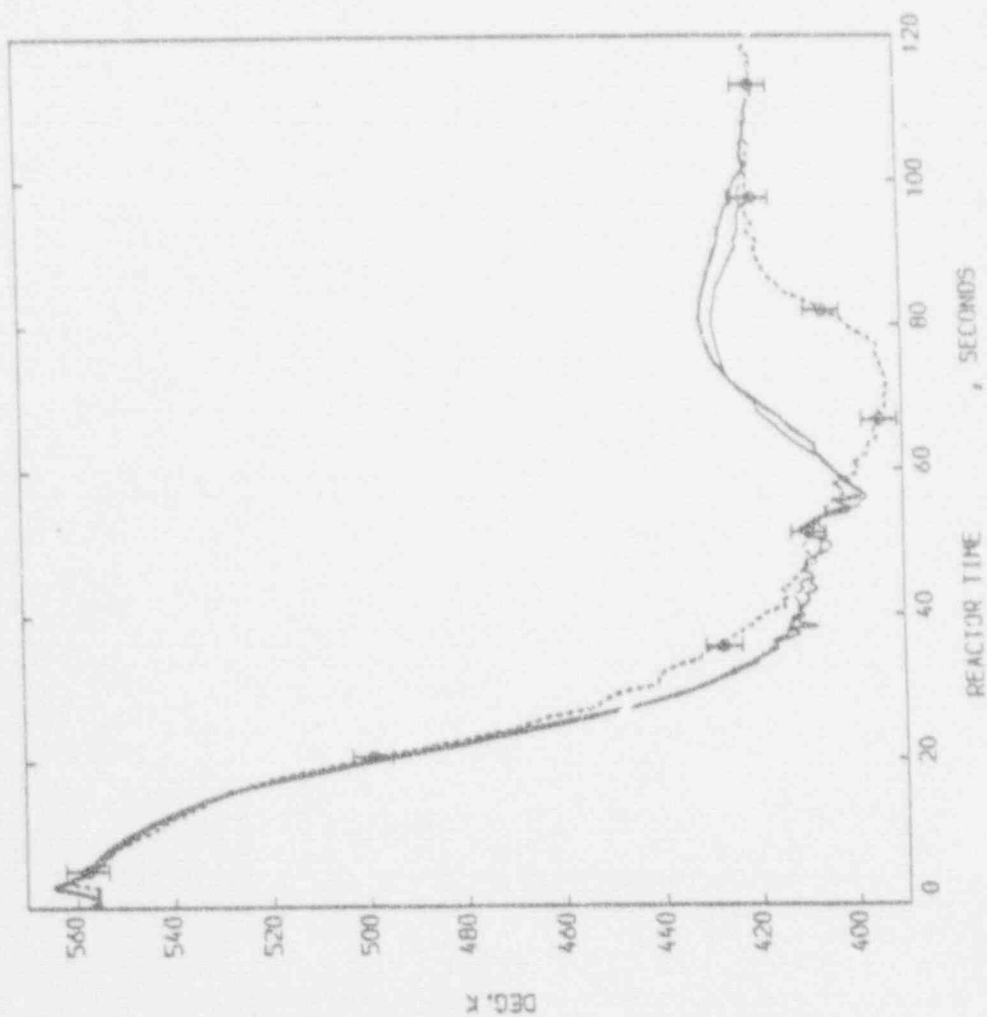
FIGURE 111 INF 1 ORIG, INF 2 ZEROGAP, INF 3 EXP
DOWNCOMER LIQUID TEMPERATURE AT 2.4 METRES

KEY		
SYM BOL	NAME	UNITS
——	LIQUID TEMPERATURE , D' 1 K LOC. 1/ 7/ 13 MNEM=TEMP INF=1	
——	LIQUID TEMPERATURE , DEG K LOC. 50/ 7/ 13 MNEM=TEMP INF=2	
----	TE-151-G05 , DEG K LOC= 205/ 0/ 0 MNEM=THCL INF=3	

FIGURE 112   INF 1 ORIG, INF 2 ZEROGAP, INF 3 EXP
DOWNCOMER LIQUID TEMPERATURE AT 0.3 METRES

FIGURE 113 LINE 1 ORIG, LINE 2 ZEROGAP, LINE 3 EXP
LOWER PLENUM MOMENTUM FLUX

FIGURE 114   INF 1 ORIG, INF 2 ZEROGAP
VESSEL GLOBALS

AEEW - M 2464

151

	KEY	
SYM BOL	NAME	UNITS
——	CORE OUTLET MASSFLOW, KG/SEC LOC= 50/ 0/ 1 MNEM=FLCO INF=1	
——	CORE OUTLET MASSFLOW, KG/SEC LOC= 50/ 0/ 1 MNEM=FLCO INF=2	

KG/SEC

REACTOR TIME   , SECONDS

FIGURE 115   INF 1 ORIG, INF 2 ZEROGAP
VESSEL GLOBALS

CORE LIQUID MASS

Winfrith

AEEW - M 2464

152

FIGURE 116   INF 1 ORIG, INF 2 ZEROGAP
VESSEL GLOBALS
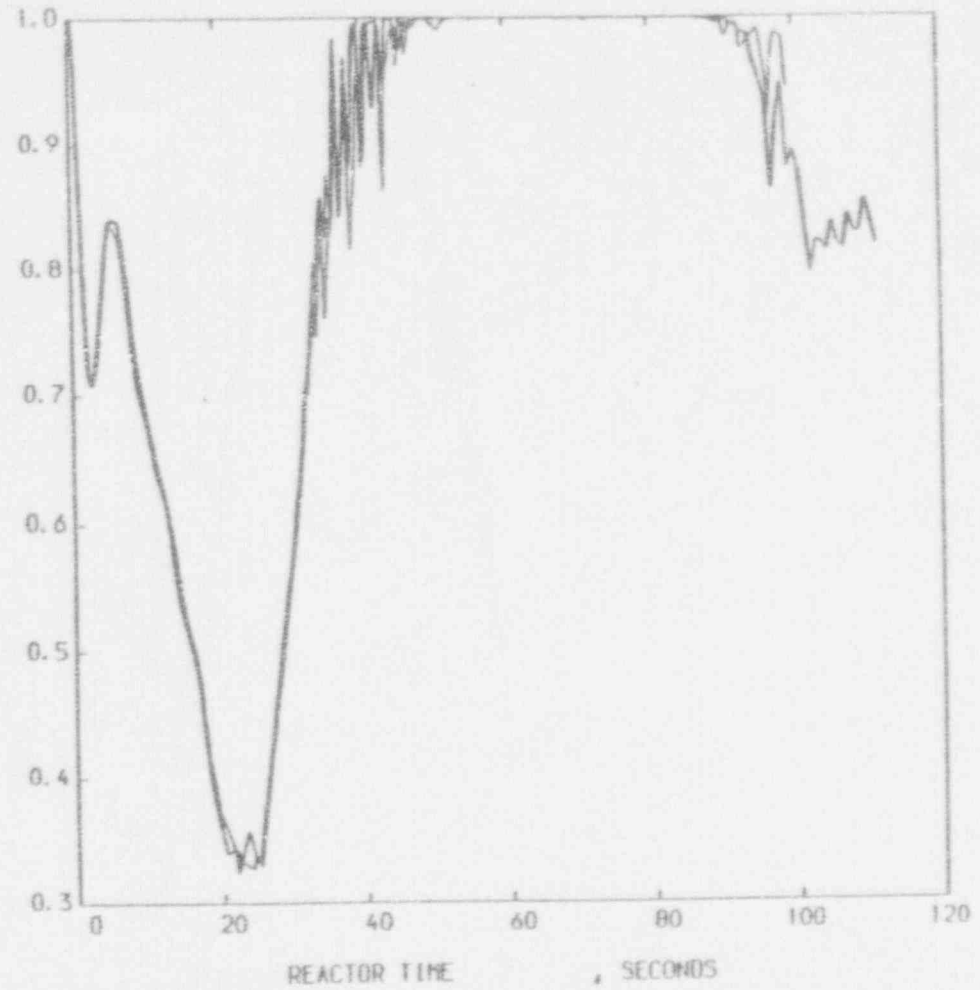
FIGURE 117   INF 1 ORIG, INF 2 ZEROGAP
VESSEL GLOBALS
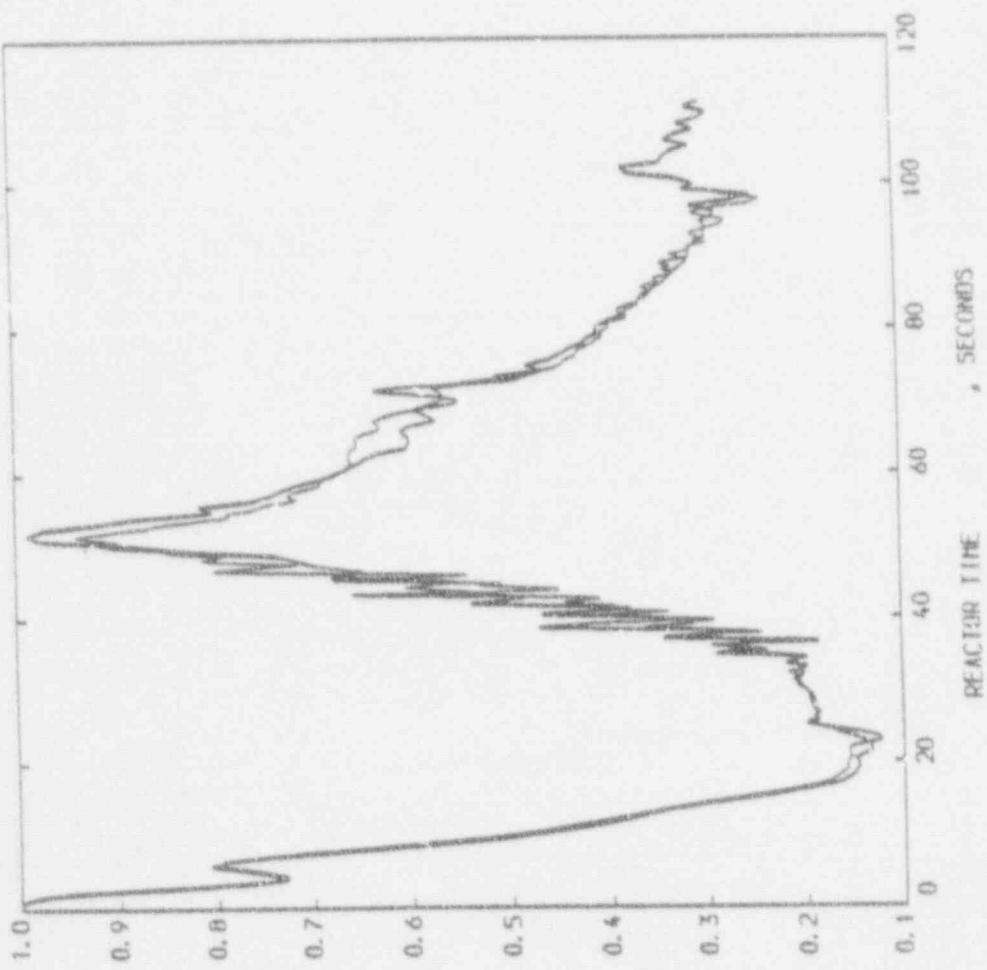
THE FOLLOWING ARE PLOTTED AGAINST REACTOR TIME

D'COMER LIQ VOL FRAC

FIGURE 118 INF 1 ORIG, INF 2 ZEROGAP
VESSEL GLOBALS

KEY		
SYMBOL	NAME	UNITS
——	D'CORNER LIQ VOL FRAC,	
	LOC= 50/ 0/ 1 NAME=LFDC INF=1	
——	D'CORNER LIQ VOL FRAC,	
	LOC= 50/ 0/ 1 NAME=LFDC INF=2	

REACTOR TIME , SECONDS

KEY		
SYM BOL	NAME	UNITS
——	CORE LIQ VOL FRAC , LOC= 50/ 0/ 1 MNEM=LFCO INF=1	
——	CORE LIQ VOL FRAC , LOC= 50/ 0/ 1 MNEM=LFCO INF=2	

REACTOR TIME   , SECONDS
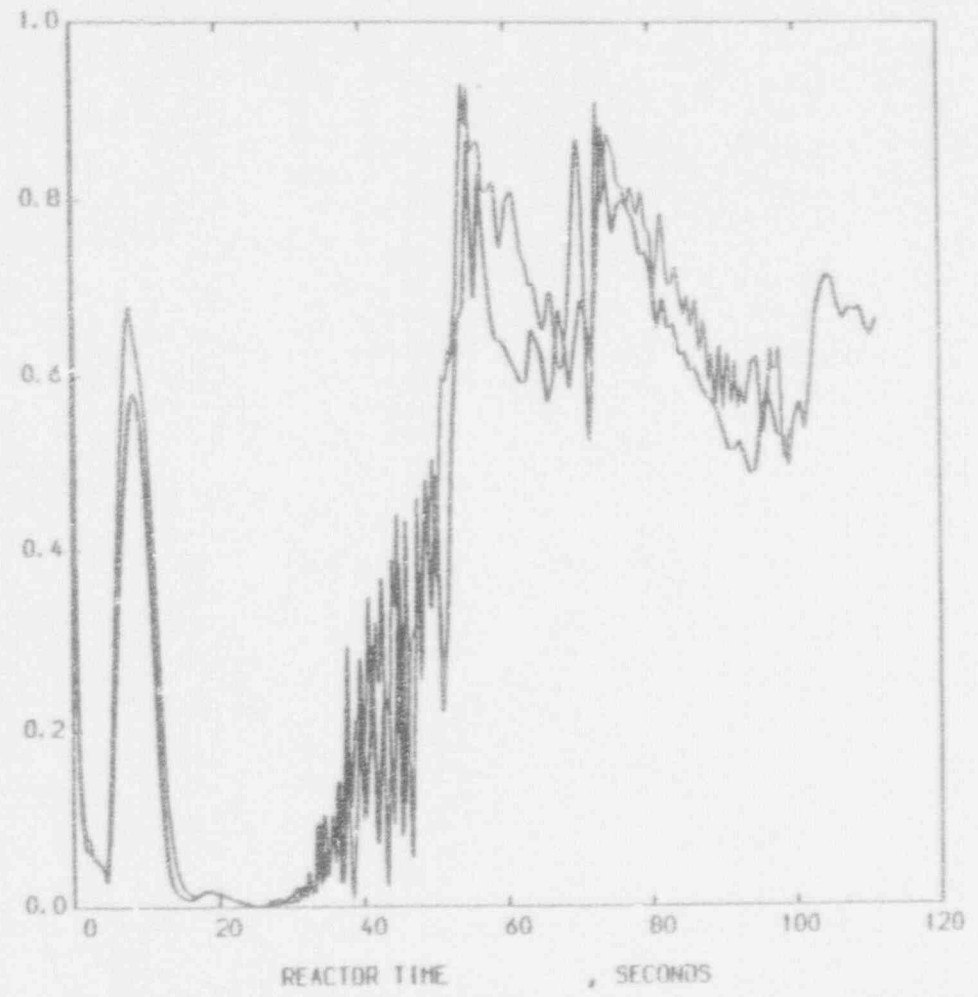
FIGURE 119   INF 1 ORIG, INF 2 ZEROGAP
VESSEL GLOBALS

THE FOLLOWING ARE PLOTTED AGAINST REACTOR TIME

VESSEL LIQUID MASS

Winfrith
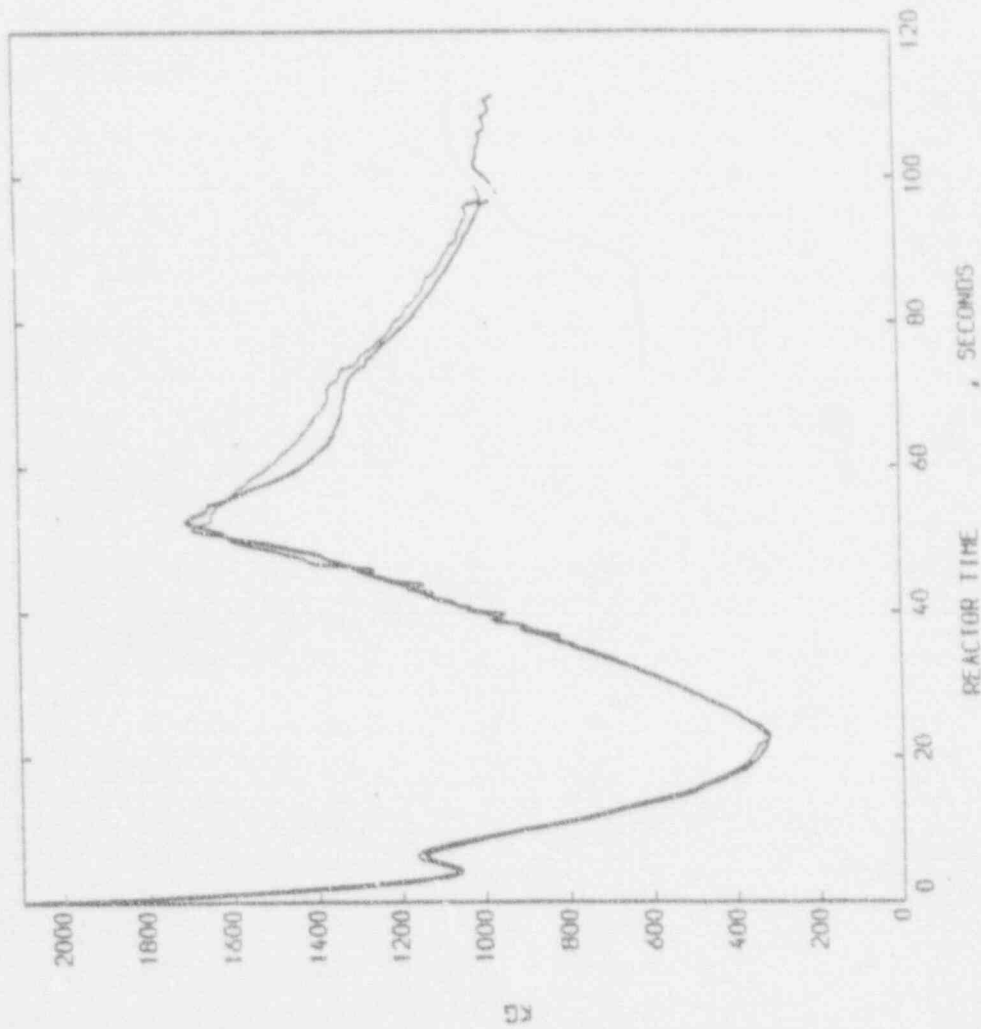
FIGURE 120 INF 1 ORIG, INF 2 ZEROGAP
VESSEL GLOBALS

AEEW - M 2464

156

AEEW - M 2464

157

KEY		
SYM BOL	NAME	UNITS
——	TOT ROD HEAT FLUX , WATTS LOC= 50/ 0/ 1 MNEM=QRDT INF=1	
——	TOT ROD HEAT FLUX , WATTS LOC= 50/ 0/ 1 MNEM=QRDT INF=2	

FIGURE 121   INF 1 ORIG, INF 2 ZEROGAP
VESSEL GLOBALS

FIGURE :22 INF 1 ORIG, INF 2 ZEROGAP
VESSEL GLOBALS

L PLENUM AVG LIQ TEM

Winfrith

AEEW - M 2464

159

KEY

SYM BOL	NAME	UNITS
——	L PLENUM AVG LIQ TEM,DEG.K LOC= 50/ 0/ 1 MNEM=TMLP INF=1	
——	L PLENUM AVG LIQ TEM,DEG.K LOC= 50/ 0/ 1 MNEM=TMLP INF=2	

DEG. K

REACTOR TIME , SECONDS
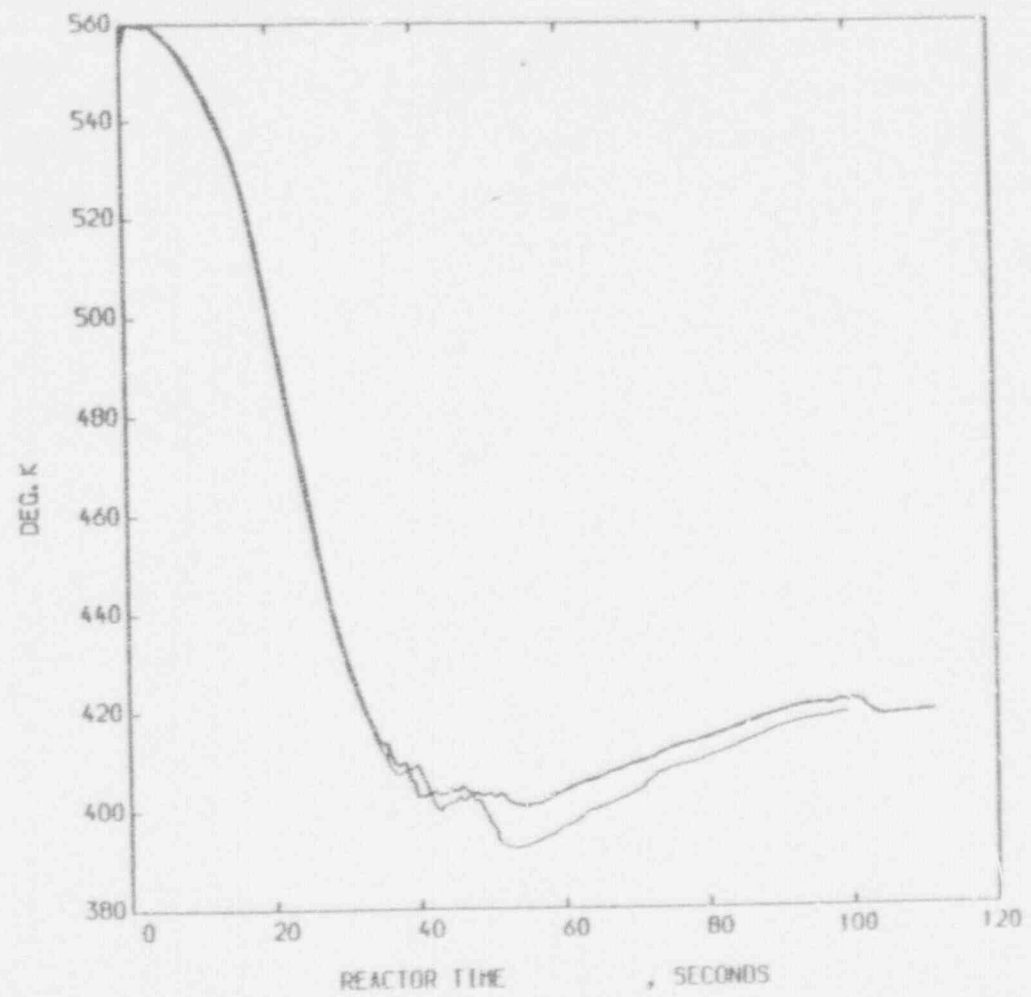
FIGURE 123 INF 1 ORIG, INF 2 ZEROGAP
VESSEL GLOBALS

THE FOLLOWING ARE PLOTTED AGAINST REACTOR TIME

CLADDING TEMP -FINE,TE-SH05-002
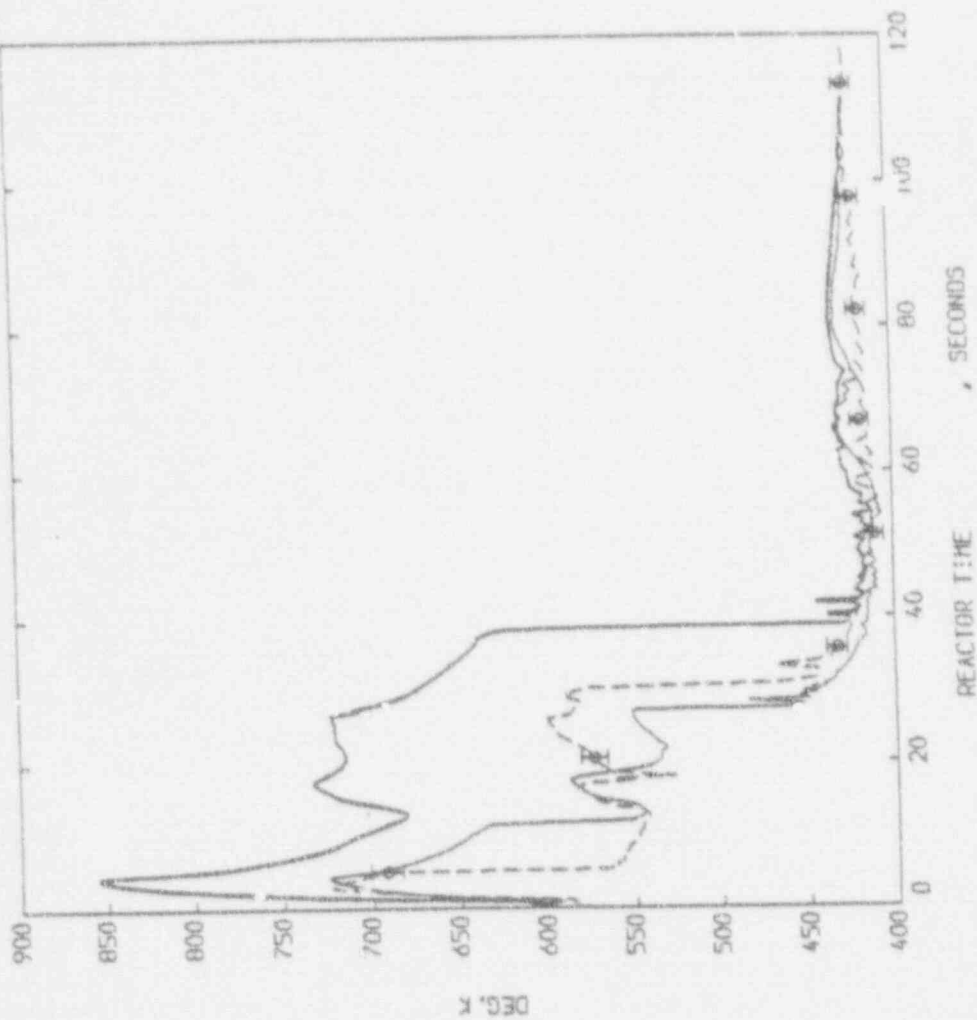
Winfrith

KEY	UNITS
SYM BOL NAME	
—— CLADDING TEMP -FINE,DEG.K LOC= 50/ 1/ 1 ANEM-TMCL INF=1	
—— CLADDING TEMP -FINE,DEG.K LOC= 50/ 1/ 1 ANEM-TMCL INF=2	
—— TE-SH05-002 ,DEG.K LOC= 282/ 0/ 0 ANEM-TMCL INF=3	

FIGURE 124 INF 1 ORIG, INF 2 ZEROGAP, INF 3 EXP
CENTRAL FUEL BUNDLE CLADDING TEMPERATURES

AEEW - M 2464

160

APEW = M 2464

161

KEY		
SYM BOL	NAME	UNITS
——	CLADDING TEMP -FINE, DEG. K LOC= 50/ 1/ 5 MNEM=TMCL INF=1	
——	CLADDING TEMP -FINE, DEG. K LOC= 50/ 1/ 5 MNEM=TMCL INF=2	
— —	TE-5G06-011 , DEG. K LOC= 278/ 0/ 0 MNEM=TMCL INF=3	
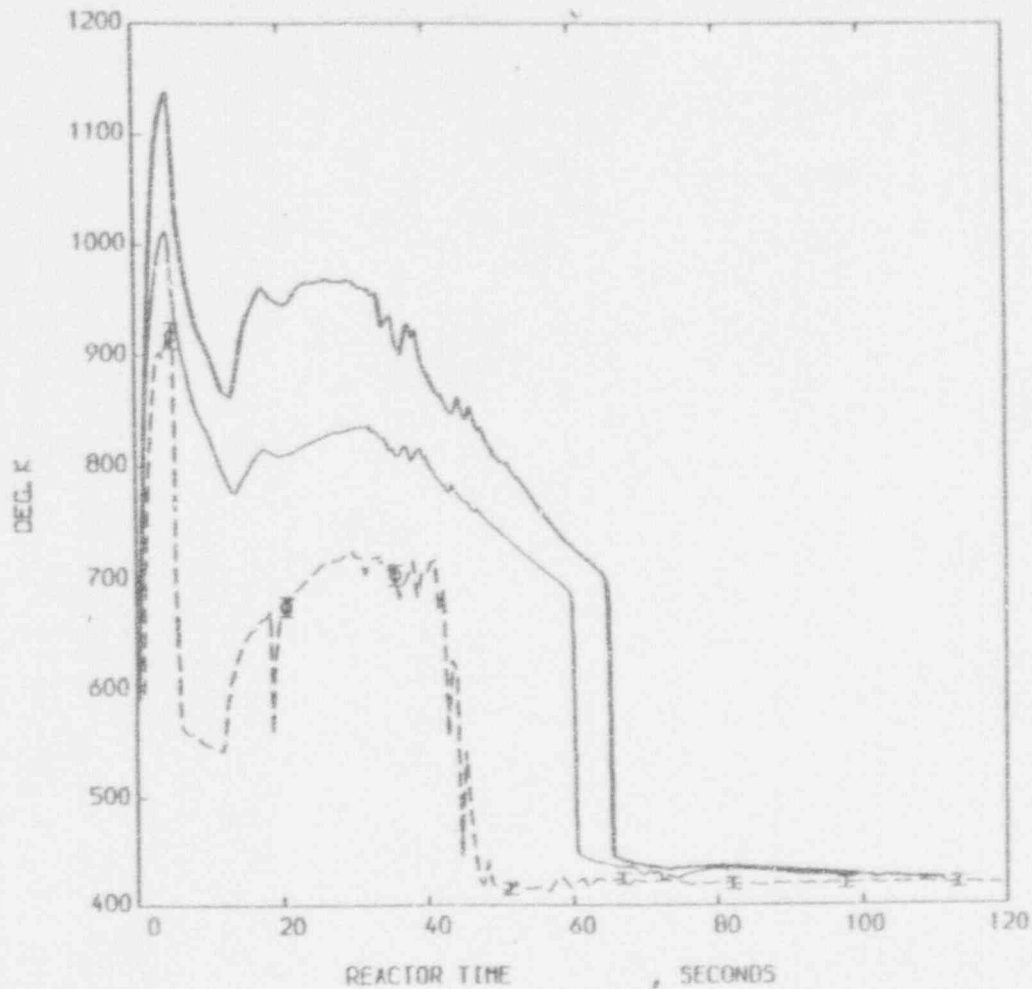
FIGURE 125   INF 1 ORIG, INF 2 ZEROGAP, INF 3 EXP
CENTRAL FUEL BUNDLE CLADDING TEMPERATURES

AEEW - M 2464

162

KEY		
SYM 90L	NAME	UNITS
——	CLADDING TEMP -FINE,DEG.K LOC= 50/ 4/ 9 MNEM=TMCL INF=1	
——	CLADDING TEMP -FINE,DEG.K LOC= 50/ 4/ 9 MNEM=TMCL INF=2	
- -	TE-5106-021 ,DEG.K LOC= 296/ 0/ 0 MNEM=TMCL INF=3	
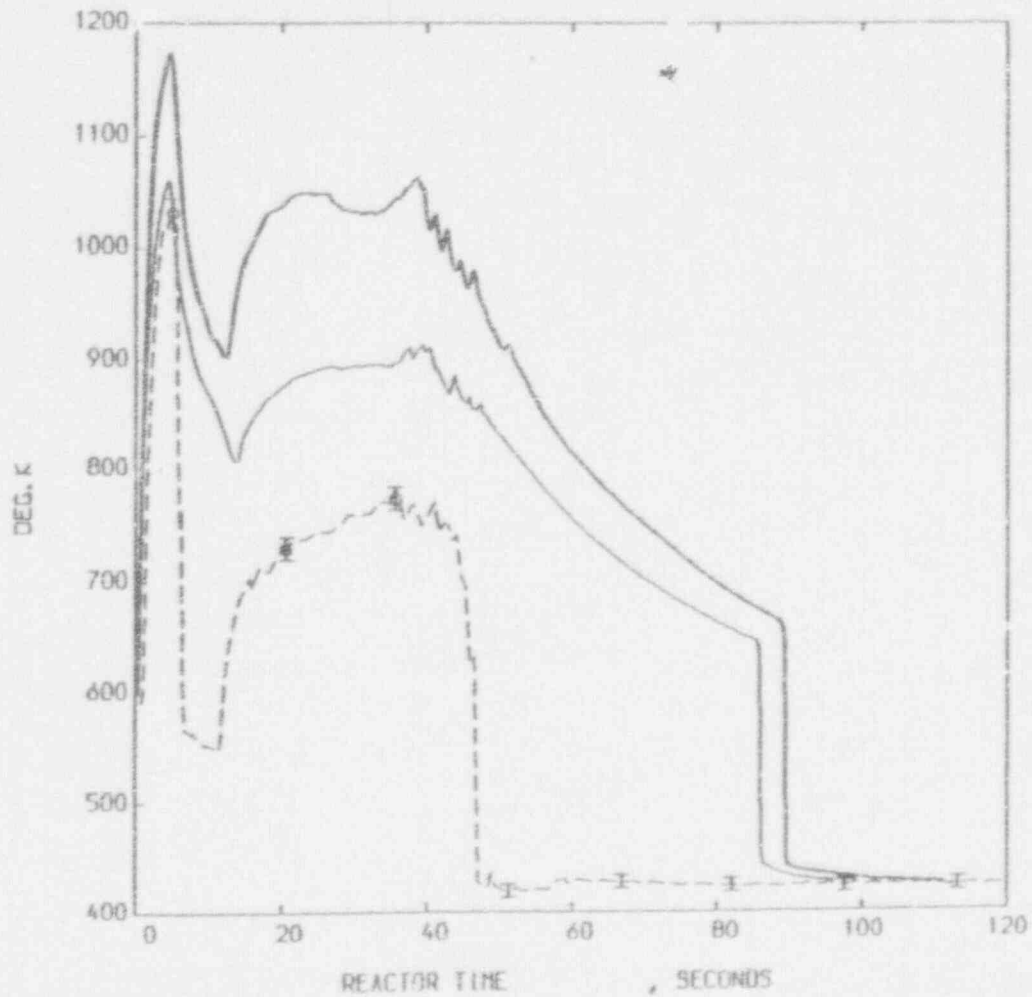
FIGURE 126   INF 1 ORIG, INF 2 ZEROGAP, INF 3 EXP
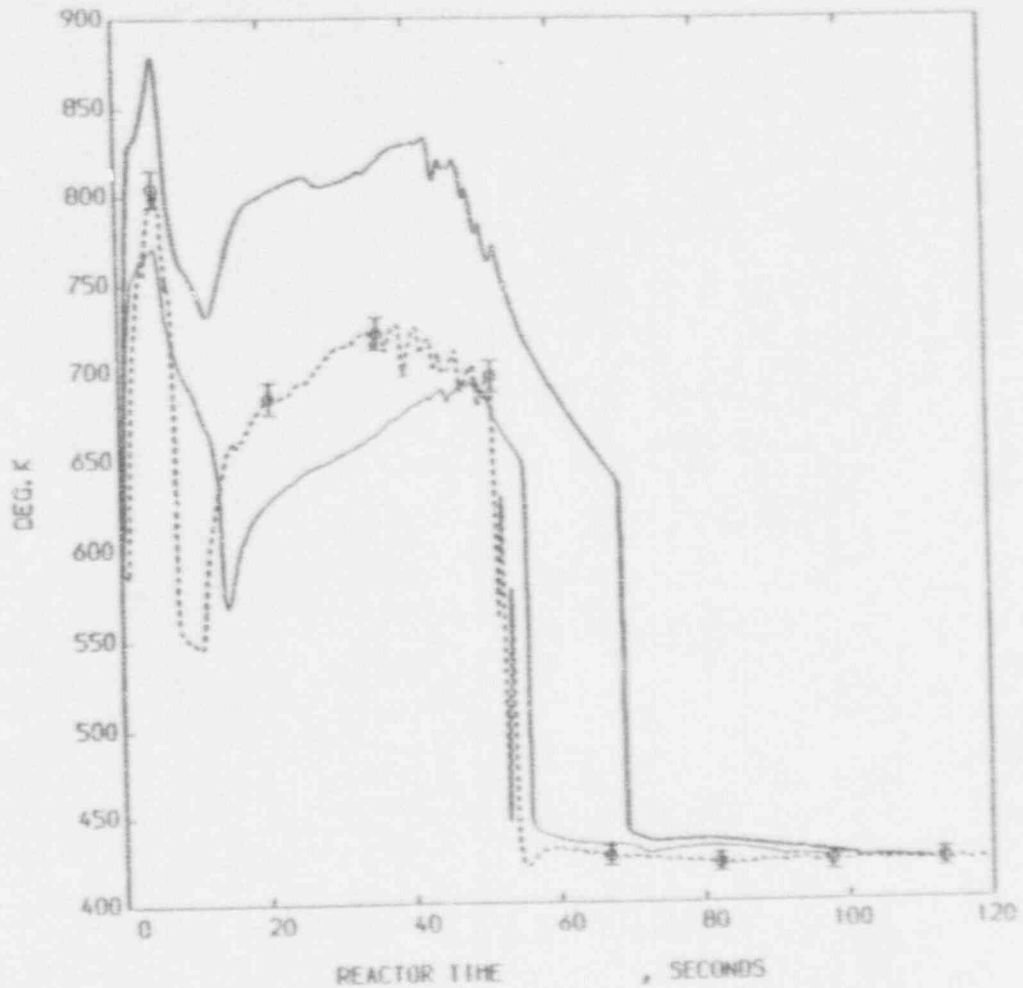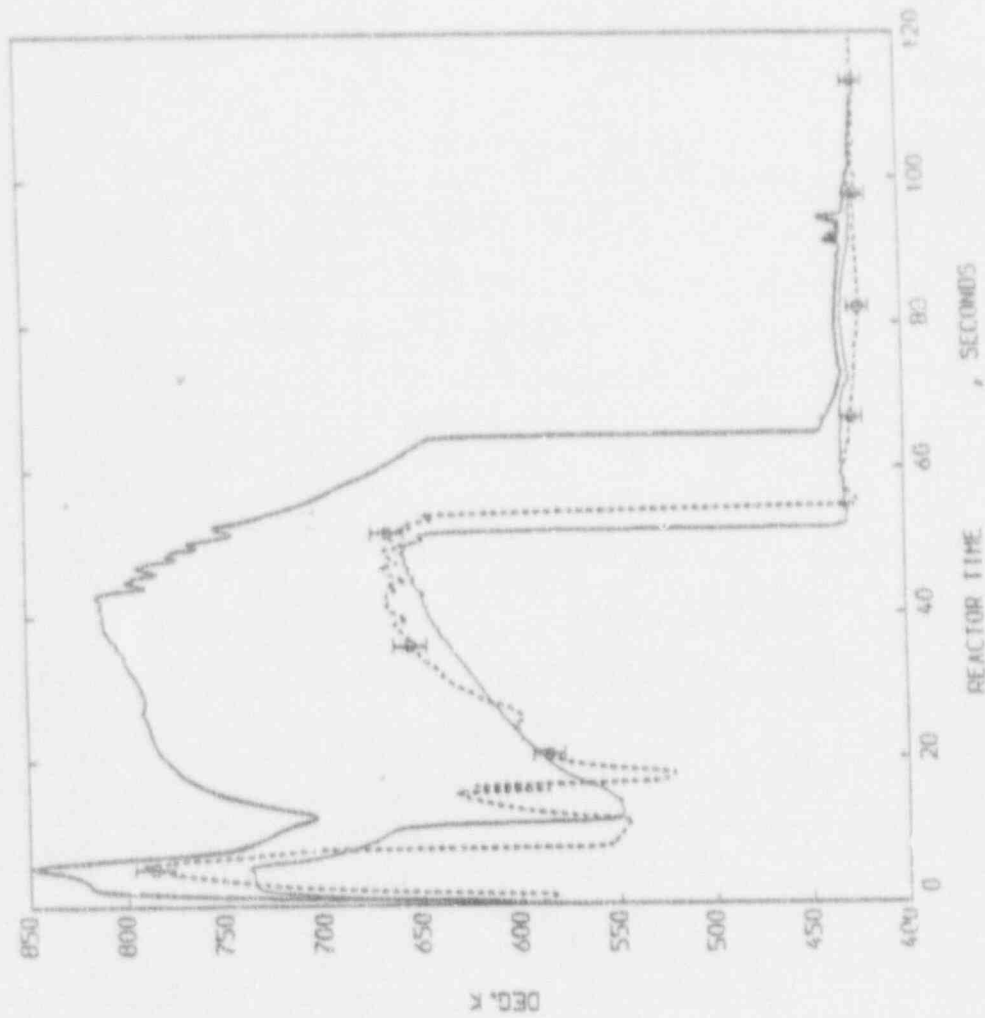CENTRAL FUEL BUNDLE CLADDING TEMPERATURES

FIGURE 127   INF 1 ORIG, INF 2 ZEROGAP, INF 3 EXP
CENTRAL FUEL BUNDLE CLADDING TEMPERATURES

THE FOLLOWING ARE PLOTTED AGAINST REACTOR TIME

CLADDING TEMP -FINE,TE-5I04-027

AEEW - M 2464

164

KEY		
SYM BOL	NAME	UNITS
——	CLADDING TEMP -FINE,DEG.K LOC= 50/ 4/ 12 MNEM=TMCL INF=1	
——	CLADDING TEMP -FINE,DEG.K LOC= 50/ 4/ 12 MNEM=TMCL INF=2	
— —	TE-5I04-027 ,DEG.K LOC= 293/ 0/ 0 MNEM=TMCL INF=3	

DEG. K

REACTOR TIME , SECONDS

FIGURE 128   INF 1 ORIG, INF 2 ZEROGAP, INF 3 EXP
CENTRAL FUEL BUNDLE CLADDING TEMPERATURES

FIGURE 129   INF 1 ORIG, INF 2 ZEROGAP, INF 3 EXP
CENTRAL FUEL BUNDLE CLADDING TEMPERATURES

FIGURE 130 INF 1 ORIG, INF 2 ZEROGAP, INF 3 EXP
CENTRAL FUEL BUNDLE CLADDING TEMPERATURES

FIGURE 131 INF 1 ORIG, INF 2 ZEROGAP, INF 3 EXP
CENTRAL FUEL BUNDLE CLADDING TEMPERATURES

THE FOLLOWING ARE PLOTTED AGAINST REACTOR TIME
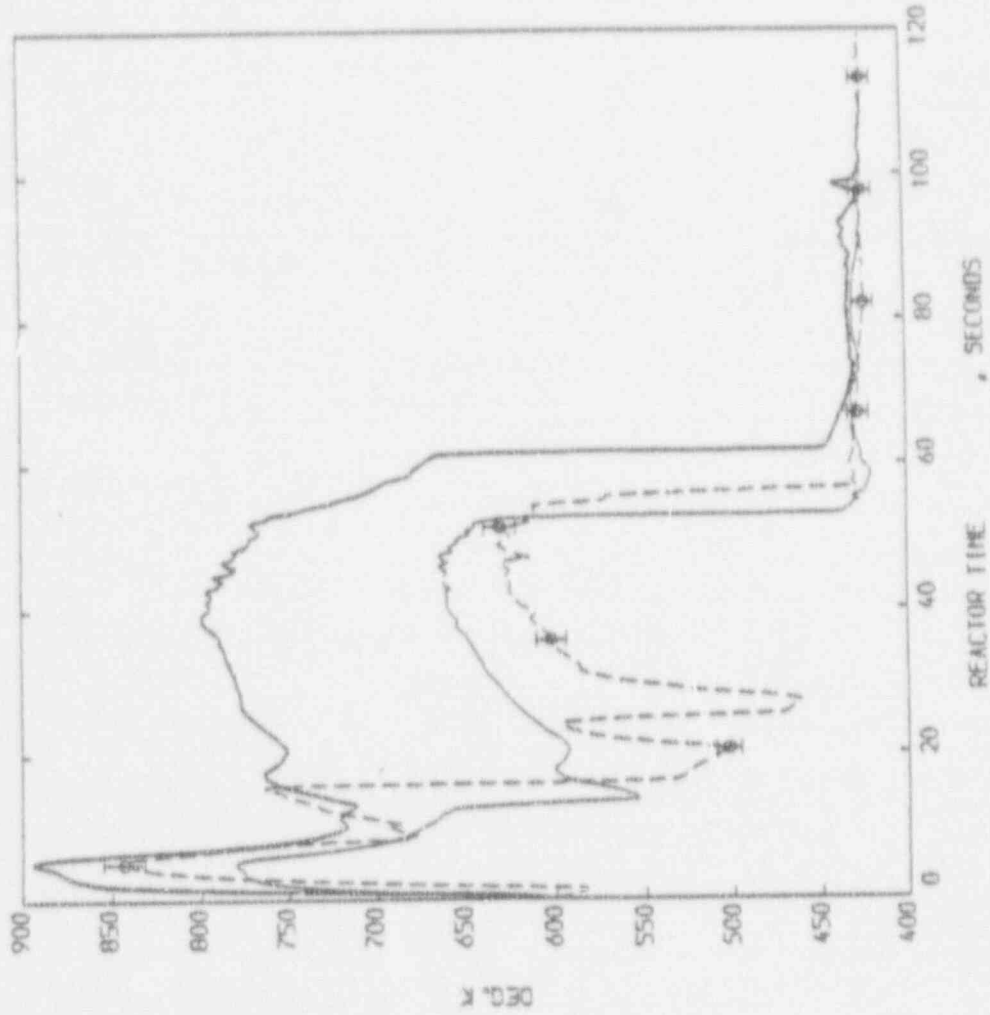
CLADDING TEMP -FINE, TE-5M05-049

FIGURE 132 INF 1 ORIG, INF 2 ZEROGAP, INF 3 EXP
CENTRAL FUEL BUNDLE CLADDING TEMPERATURES

Winfrith

THE FOLLOWING ARE PLOTTED AGAINST REACTOR TIME

CLADDING TEMP -FINE, TE-SG06-062
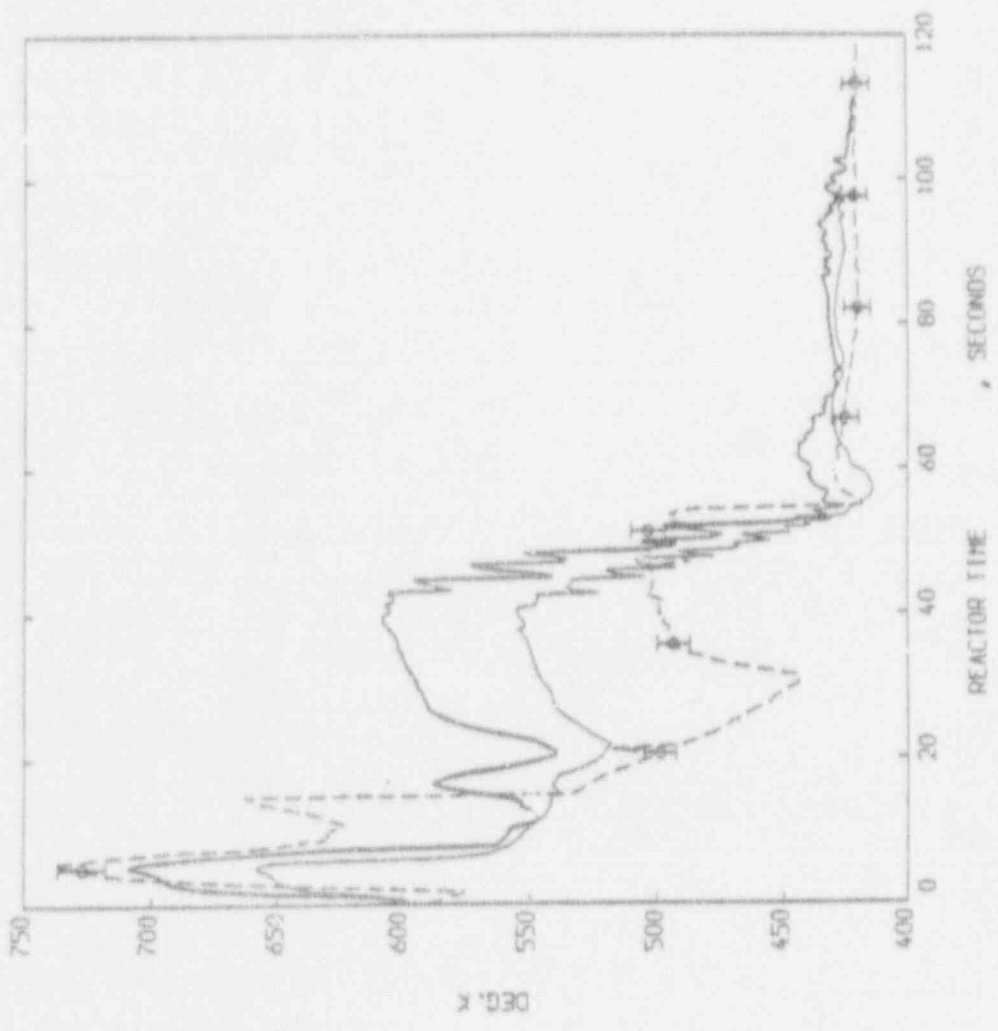
FIGURE 133 INF 1 ORIG, INF 2 ZEROGAP, INF 3 EXP
CENTRAL FUEL BUNDLE CLADDING TEMPERATURES

KEY .!		
SYM BRK	NAME	UNITS
	CLADDING TEMP -FINE, DEG.K	
	LOC= SG/ 1/ 20 AMREM-TMCL INF=1	
	CLADDING TEMP -FINE, DEG.K	
	LOC= SG/ 1/ 20 AMREM-TMCL INF=2	
	TE-SG06-062	,DEG.K
	LOC= 281/ 0/ 0 AMREM-TMCL INF=3	

FIGURE 134 INF 1 ORIG, INF 2 ZEROGAP, INF 3 EXP
CENTRELINE FUEL TEMPERATURE

THE FOLLOWING ARE PLOTTED AGAINST REACTOR TIME

CLADDING TEMP -FINE,TF 2614-011

KEY		
SYM BOL	NAME	UNITS
——	CLADDING TEMP -FINE,DEG.K LOC= 50/ 5/ 5 MMER-TMEL INF=1	
——	CLADDING TEMP -FINE,DEG.K LOC= 50/ 5/ 5 MMER-TMEL INF=2	
----	TF-2614-011 ,DEG.K LOC= 220/ 0/ 0 MMER-TMEL INF=3	

DEG. K

REACTOR TIME , SECONDS
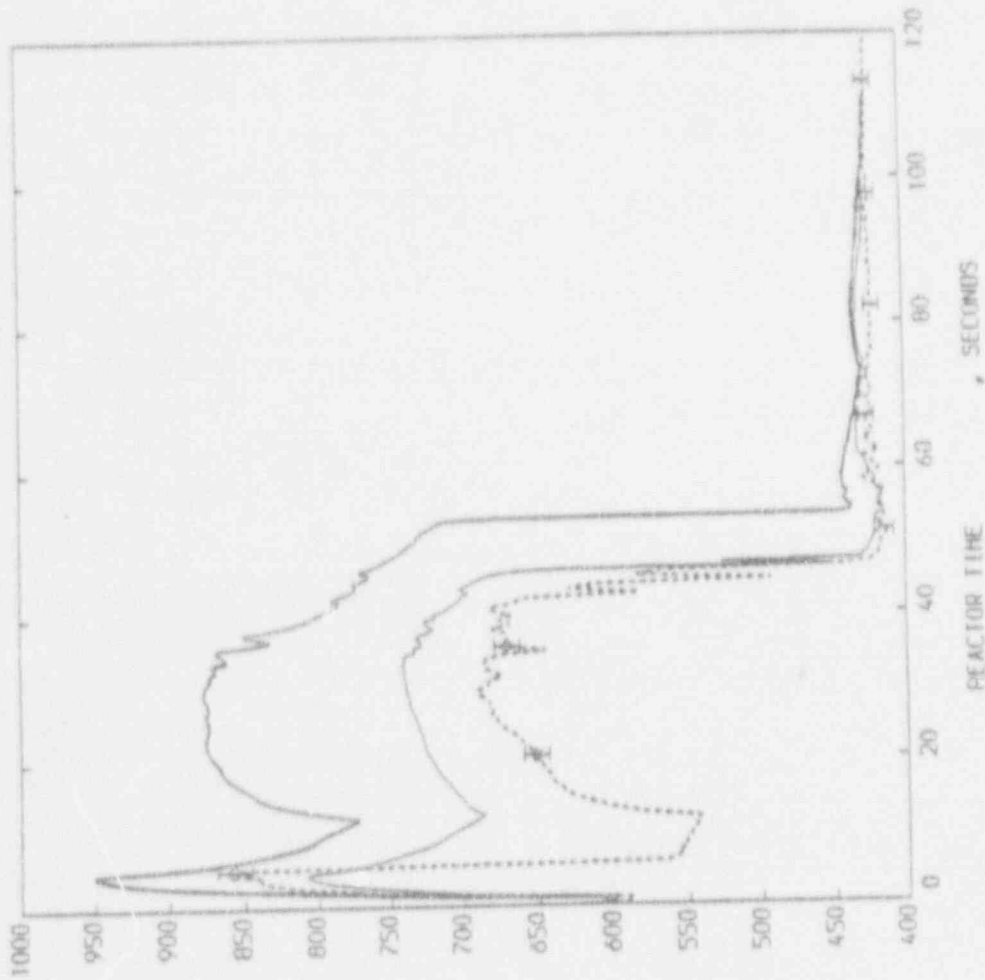
FIGURE 135 INF 1 ORIG, INF 2 ZEROGAP, INF 3 EXP
FUEL ROD CLADDING TEMPERATURES - PERIPHERAL BUNDLES

AEEW - M 2464

171

FIGURE 136   INF 1 ORIG, INF 2 ZEROGAP, INF 3 EXP
FUEL ROD CLADDING TEMPERATURES - PERIPHERAL BUNDLES

THE FOLLOWING ARE PLOTTED AGAINST REACTOR TIME

CLADDING TEMP -FINE, TE-2G14-030

FIGURE 137   INF 1 ORIG, INF 2 ZEROGAP, INF 3 EXP
FUEL ROD CLADDING TEMPERATURES - PERIPHERAL BUNDLES

KEY		
SYM BOL	NAME	UNITS
——	CLADDING TEMP -FINE, DEG.K	
	LOC= 50/ 5/ 13 MMEM-THCL INF=1	
——	CLADDING TEMP -FINE, DEG.K	
	LOC= 50/ 5/ 13 MMEM-THCL INF=2	
.....	TE-2G14-030 , DEG.K	
	LOC= 221/ 0/ 0 MMEM-THCL INF=3	

THE FOLLOWING ARE PLOTTED AGAINST REACTOR TIME
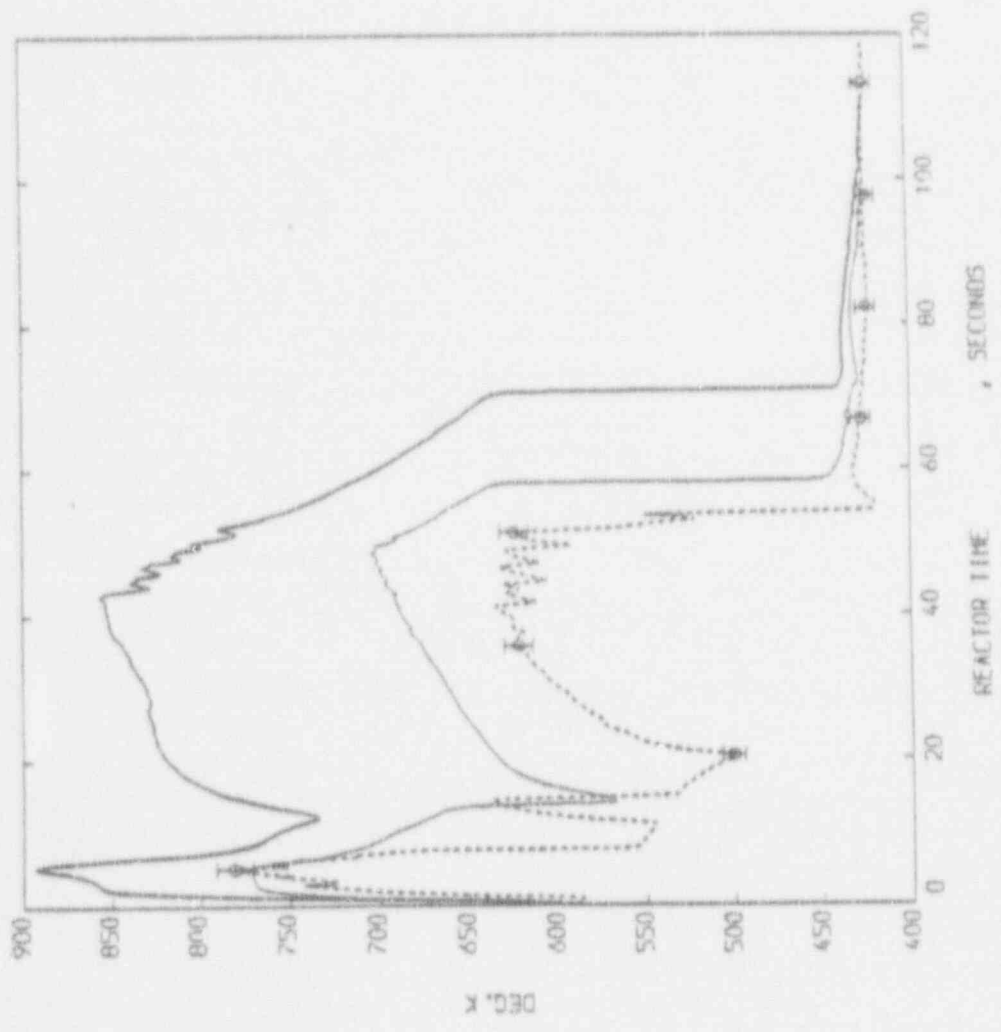
CLADDING TEMP -FINE,TE-2114-039

FIGURE 138 INF 1 ORIG, INF 2 ZEROGAP, INF 3 EXP
FUEL ROD CLADDING TEMPERATURES - PERIPHERAL BUNDLES

KEY		
SYM BOL	NAME	UNITS
	CLADDING TEMP -FINE,DEG.K	
	LOC= 50/ 8/ 15 MAERA-THCL INF=1	
	CLADDING TEMP -FINE,DEG.K	
	LOC= 50/ 8/ 15 MAERA-THCL INF=2	
	TE-2114-039 ,DEG.K	
	LOC= 229/ 0/ 0 MAERA-THCL INF=3	

THE FOLLOWING ARE PLOTTED AGAINST REACTOR TIME

CLADDING TEMP -FINE,TE-2H13-049

FIGURE 139 INF 1 ORIG, INF 2 ZEROGAP, INF 3 EXP
FUEL ROD CLADDING TEMPERATURES - PERIPHERAL BUNDLES
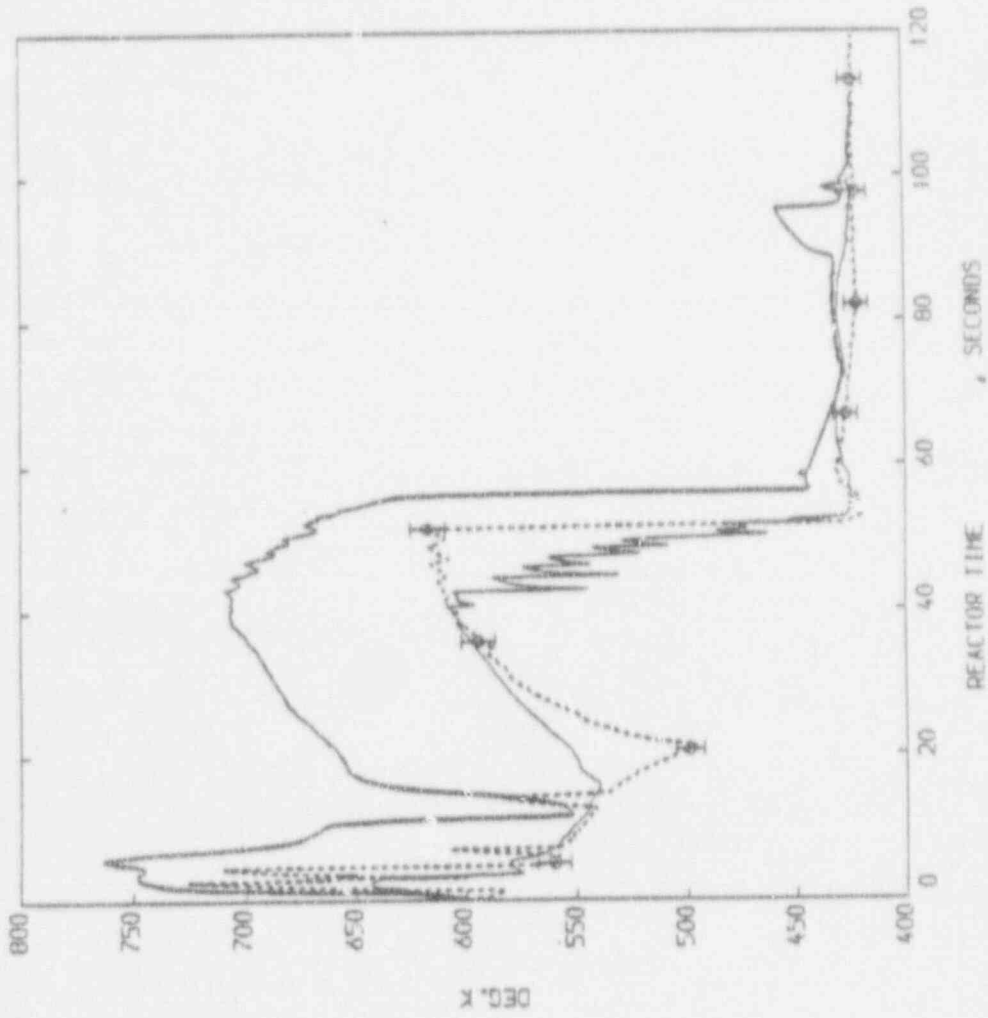
KEY		
SYM BOL	NAME	UNITS
	CLADDING TEMP -FINE,,DEG.K	
	LOC= 50/ 5/ 17 MMETH=TMCL INF=1	
	CLADDING TEMP -FINE,,DEG.K	
	LOC= 50/ 5/ 17 MMETH=TMCL INF=2	
	TE-2H13-049 ,DEG.K	
	LOC= 224/ 0/ 0 MMETH=TMCL INF=3	

FIGURE 140   INF 1 ORIG, INF 2 ZEROGAP, INF 3 EXP
FUEL ROD CLADDING TEMPERATURES - PERIPHERAL BUNDLES

Winfrith

AEEW · M 2464

177

FIGURE 141   INF 1 ORIG, INF 2 ZEROGAP, INF 3 EXP
FUEL ROD CLADDING TEMPERATURES - PERIPHERAL BUNDLES

KEY

SYMBOL	NAME	UNITS
——	CLADDING TEMP -FINE,DEG.K LOC= 50/ 6/ 12 MNEM=TMCL INF=1	
——	CLADDING TEMP -FINE,DEG.K LOC= 50/ 6/ 12 MNEM=TMCL INF=2	
····	TE-4H14-02B ,DEG.K LOC= 253/ 0/ 0 MNEM=TMCL INF=3	

DEG. K

REACTOR TIME   , SECONDS

AEEW - M 2464

178

FIGURE 142   INF 1 ORIG, INF 2 ZEROGAP, INF 3 EXP
FUEL ROD CLADDING TEMPERATURES - PERIPHERAL BUNDLES

FIGURE 143   INF 1 ORIG, INF 2 ZEROGAP, INF 3 EXP
FUEL ROD CLADDING TEMPERATURES - PERIPHERAL BUNDLES

FIGURE 144 INF 1 ORIG, INF 2 ZEROGAP, INF 3 EXP
FUEL ROD CLADDING TEMPERATURES - PERIPHERAL BUNDLES

FIGURE 145 INF 1 ORIG, INF 2 ZEROGAP, INF 3 EXP
FUEL ROD CLADDING TEMPERATURES - PERIPHERAL BUNDLES

THE FOLLOWING ARE PLOTTED AGAINST REACTOR TIME

CLADDING TEMP -FINE, TE-0H15-026
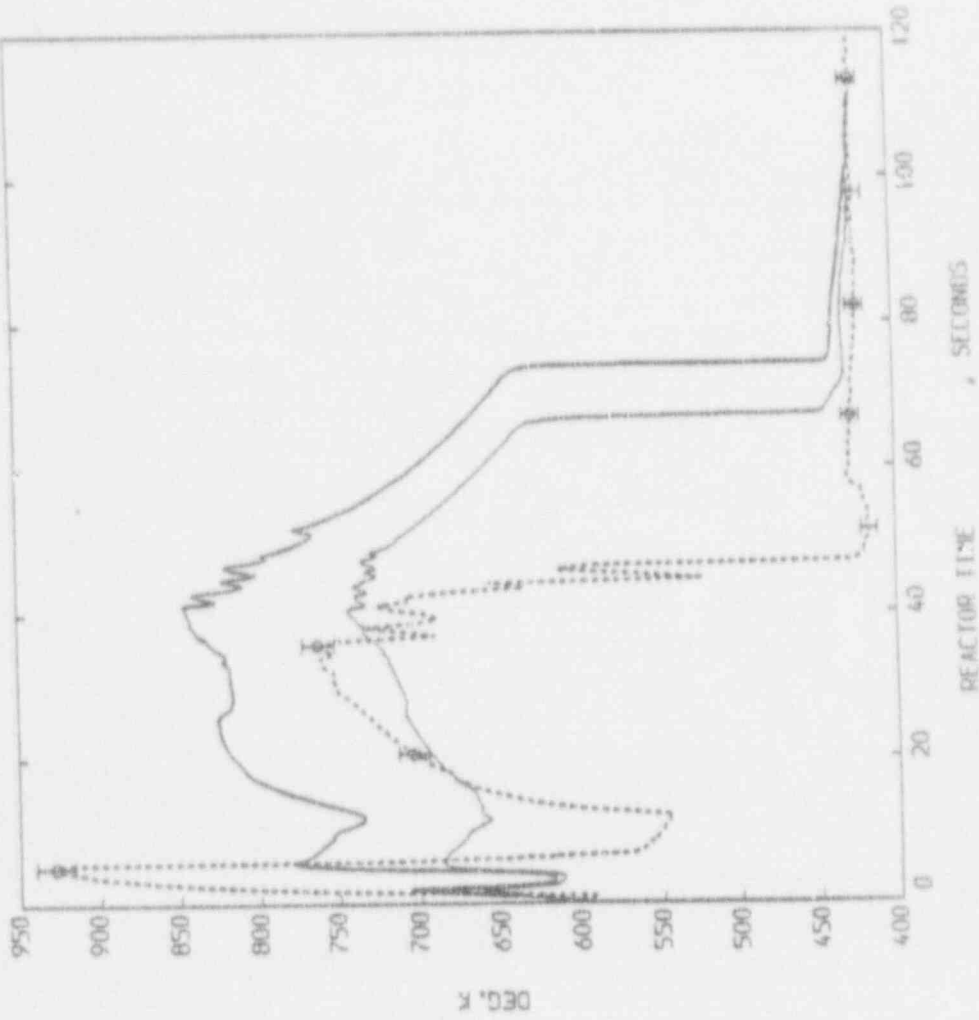
FIGURE 146 INF 1 ORIG, INF 2 ZEROGAP, INF 3 EXP
FUEL ROD CLADDING TEMPERATURES - PERIPHERAL BUNDLES

SYM BOL	NAME	UNITS
——	CLADDING TEMP -FINE, DEG.K	
	LOC= 50/ 7/ 11 INNER-INCL INF=1	
——	CLADDING TEMP -FINE, DEG.K	
	LOC= 50/ 7/ 11 INNER-INCL INF=2	
·····	TE-0H15-026 , DEG.K	
	LOC= 335/ 0/ 0 INNER-INCL INF=3	

Winfrith

AEEW - M 2464

183

FIGURE 147 INF 1 ORIG, INF 2 ZEROGAP, INF 3 EXP
FUEL ROD CLADDING TEMPERATURES - PERIPHERAL BUNDLES

THE FOLLOWING ARE PLOTTED AGAINST REACTOR TIME

CLADDING TEMP -FINE, TE-6G14-045

FIGURE 148 INF 1 ORIG, INF 2 ZEROGAP, INF 3 EXP
FUEL ROD CLADDING TEMPERATURES - PERIPHERAL BUNDLES

KEY		UNITS
SYM BOL	NAME	
——	CLADDING TEMP -FINE ,DEG.K	
	LOC= 50/ 8/ 16 MAEH-TMCL INF=1	
——	CLADDING TEMP -FINE ,DEG.K	
	LOC= 50/ 8/ 16 MAEH-TMCL INF=2	
.....	TE-6G14-045 ,DEG.K	
	LOC= 331/ 0/ 0 MAEH-TMCL INF=3	

THE FOLLOWING ARE PLOTTED AGAINST REACTOR TIME

PRESSURE   ,PE-BL-001
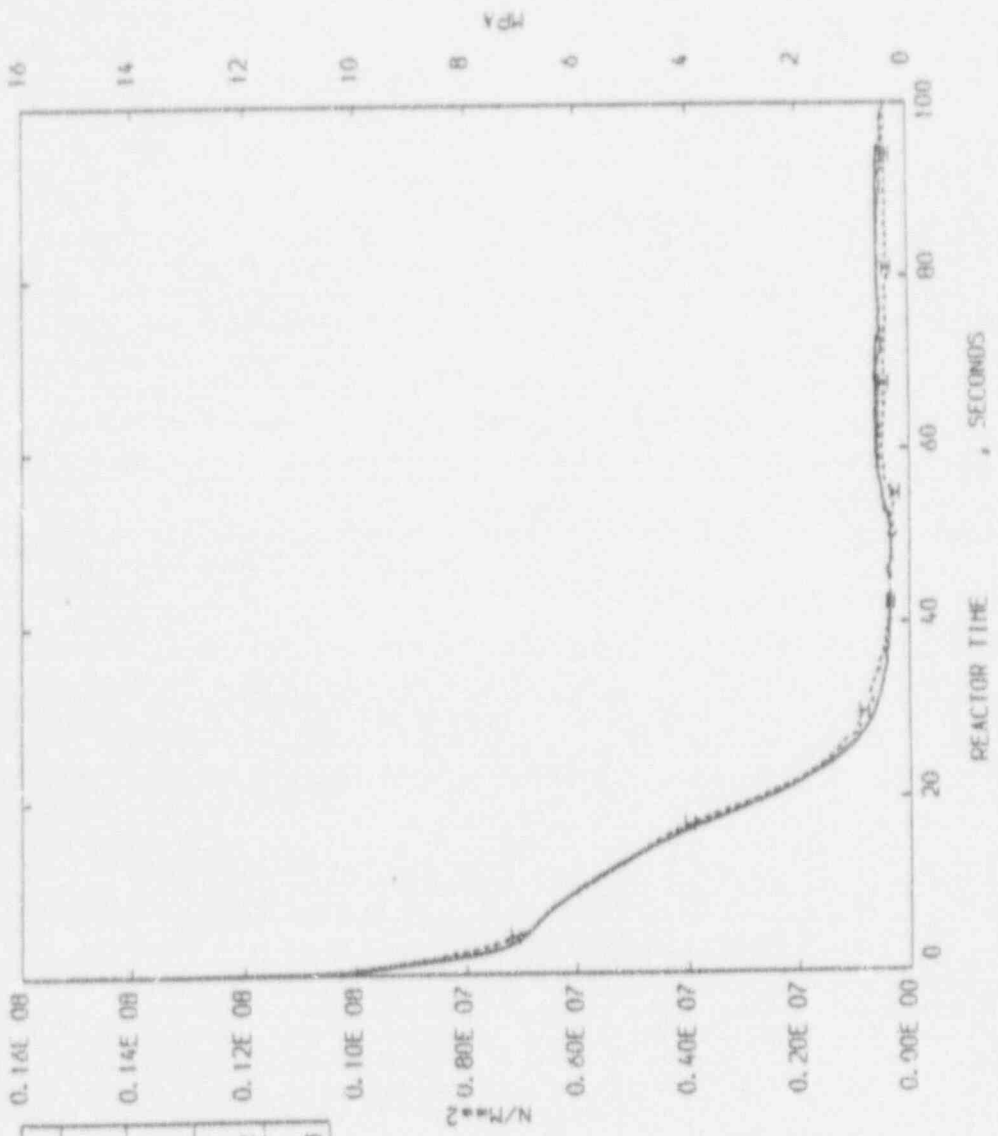
FIGURE 149   INF 1 ISHARP, INF 2 ZEROGAP, INF 3 EXP
BROKEN LOOP COLD LEG - EXPERIMENTAL LOCATION BL-2

	KEY	
SYM BOL	NAME	UNITS
	PRESSURE	,N/M**2
	LOC= 41/ 0/ 3 MNEM=PRES INF=1	
	PRESSURE	,N/M**2
	LOC= 41/ 0/ 3 MNEM=PRES INF=2	
	PE-BL-001	,MPA
	LOC= 113/ 0/ 0 MNEM=PRES INF=3	

THE FOLLOWING ARE PLOTTED AGAINST REACTOR TIME
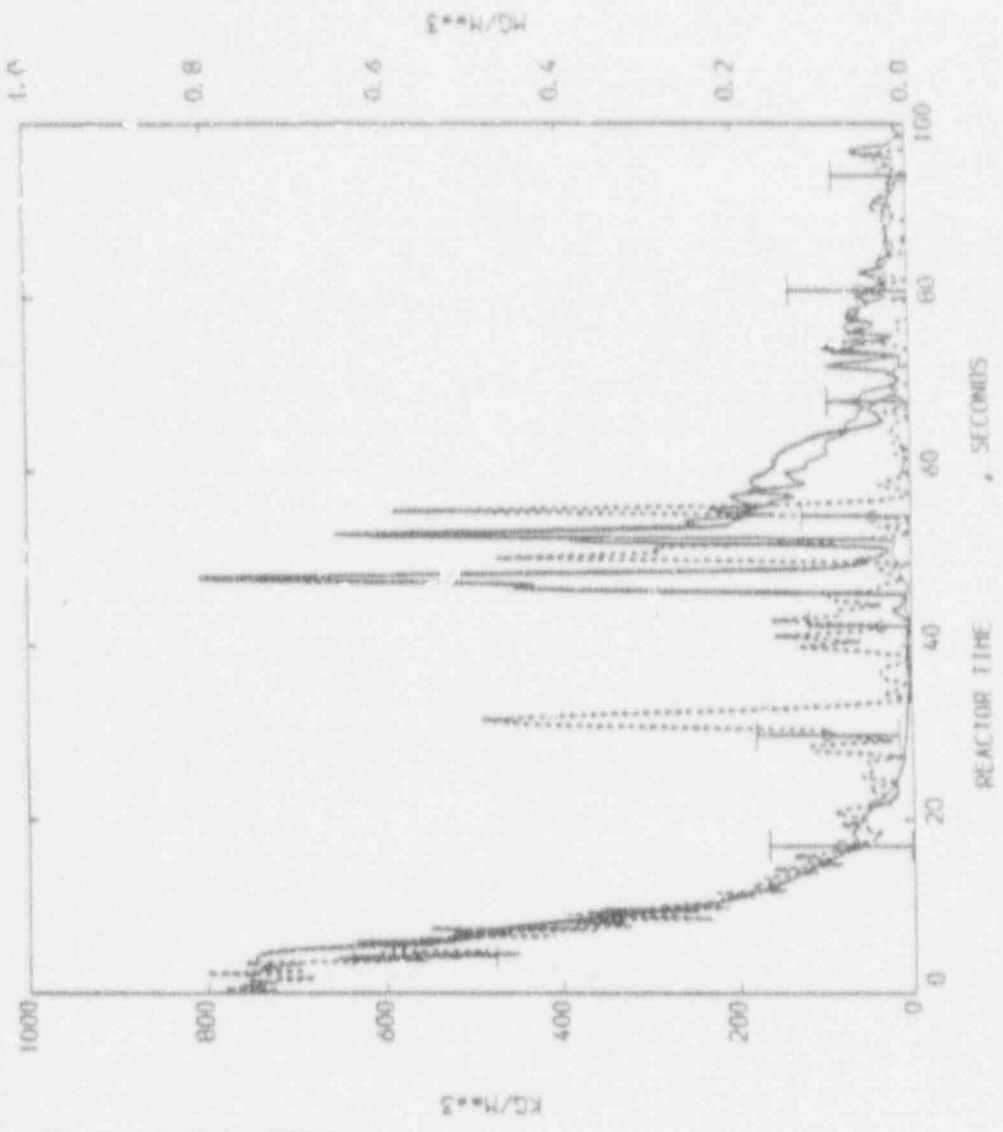
MIXTURE DENSITY ,DE-BL-001A

FIGURE 150 INF 1 ISHARP, INF 2 ZEROGAP, INF 3 EXP
BROKEN LOOP COLD 'EG - EXPERIMENTAL LOCATION cL-1

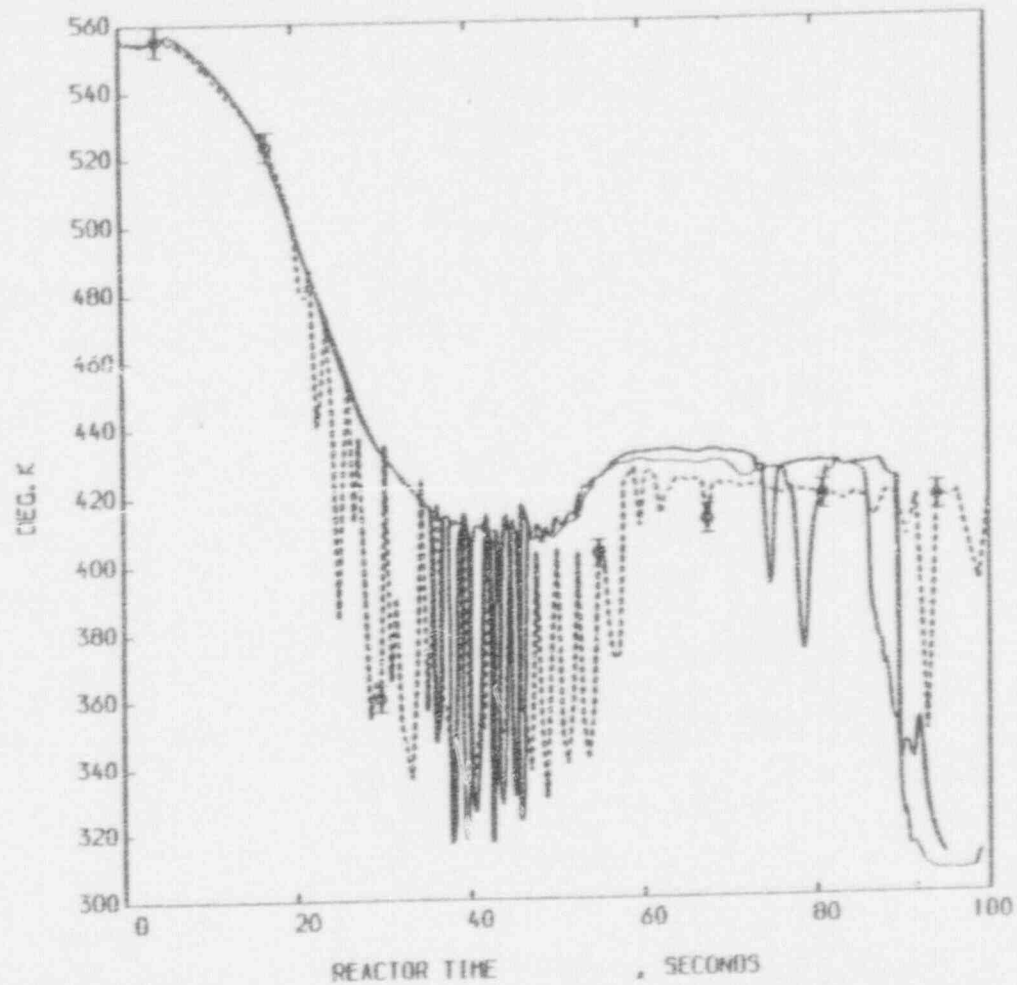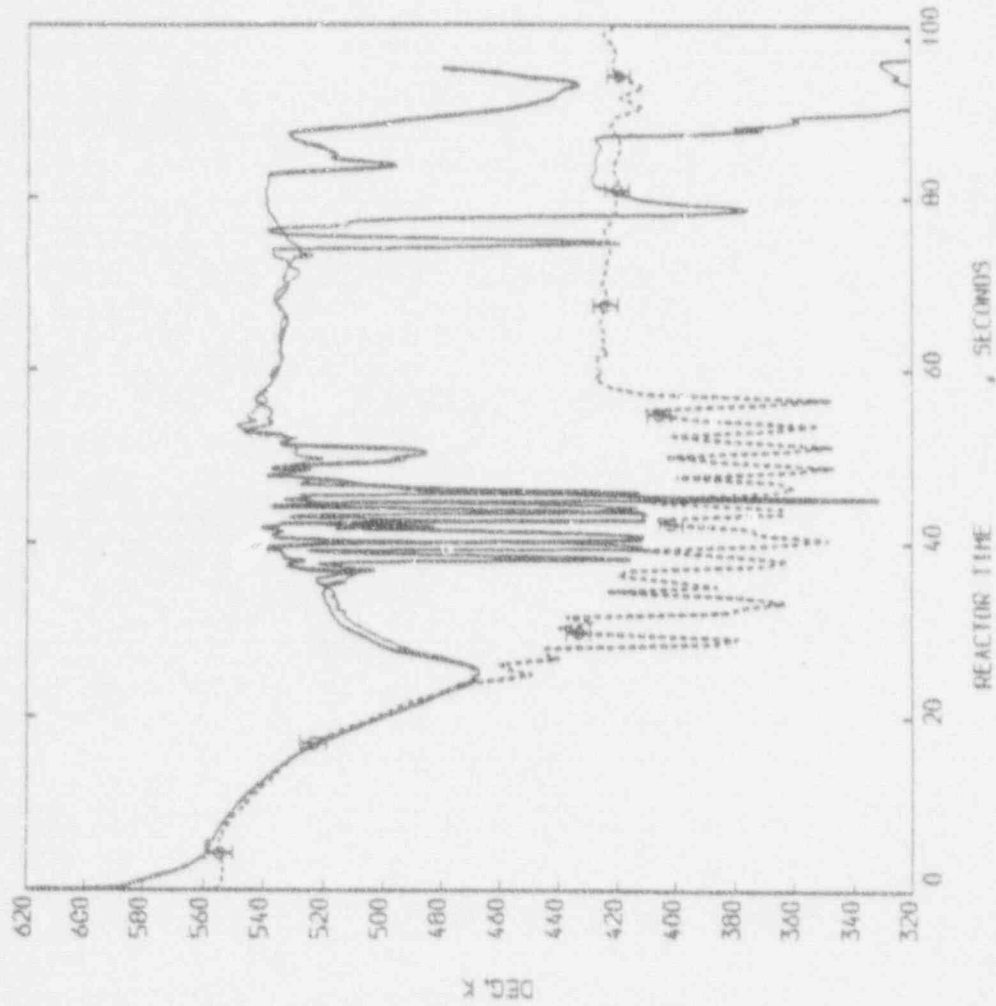| KEY		
SYM BOL	NAME	UNITS
——	MIXTURE DENSITY ,KG/M**3 LOC= 41/ 0/ 3 ISHARP-DENM INF=1	,KG/M**3
— —	MIXTURE DENSITY ,KG/M**3 LOC= 41/ 0/ 3 MAEH-DENM INF=2	,KG/M**3
····	DE-BL-001A LOC= 7/ 9/ 0 MAEH-DENM INF=3	,MG/M**3

MG/M**3

KG/M**3

REACTOR TIME , SECONDS

FIGURE 151   INF 1 ISHARP, INF 2 ZEROGAP, INF 3 EXP
BROKEN LOOP COLD LEG - EXPERIMENTAL LOCATION BL-I

THE FOLLOWING ARE PLOTTED AGAINST REACTOR TIME

LIQUID TEMPERATURE ,TE-BL-001A

FIGURE 152 INF 1 ISHARP, INF 2 ZEROGAP, INF 3 EXP
BROKEN LOOP COLD LEG - EXPERIMENTAL LOCATION BL-1

FIGURE 153 INF 1 ISHARP, INF 2 ZEROGAP, INF 3 EXP
BROKEN LOOP COLD LEG - EXPERIMENTAL LOCATION BL-1

PRESSURE ,PE-BL-004

Winfrith

FIGURE 154   INF 1 ISHARP, INF 2 ZEROGAP, INF 3 EXP
BROKEN LOOP COLD LEG – EXPERIMENTAL LOCATION BL-4

THE FOLLOWING ARE PLOTTED AGAINST REACTOR TIME
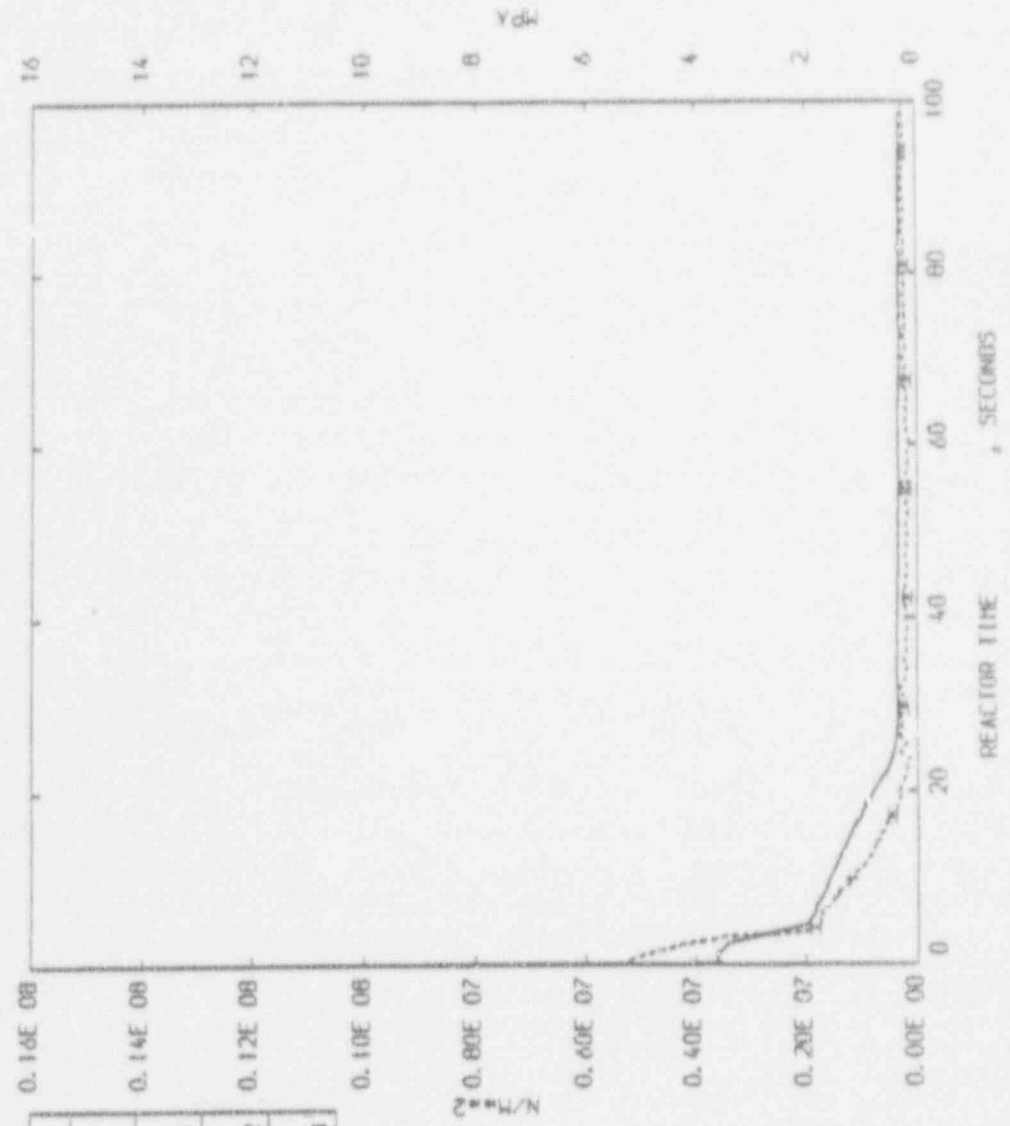
PRESSURE ,PE-BL-00B

KEY

SYM BOL	NAME	UNITS
——	PRESSURE LOC. 41/ 0/ 5 PREM-PRES INF-1	,N/M**2
———	PRESSURE LOC. 41/ 0/ 5 PREM-PRES INF-2	,N/M**2
-------	PE-BL-00B LOC-11B/ 0/ 0 PREM-PRES INF-3	,MPA

FIGURE 155 INF 1 ESHARP, INF 2 ZEROGAP, INF 3 EXP
BROKEN LOOP COLD LEG - EXPERIMENTAL LOCATION BL-8

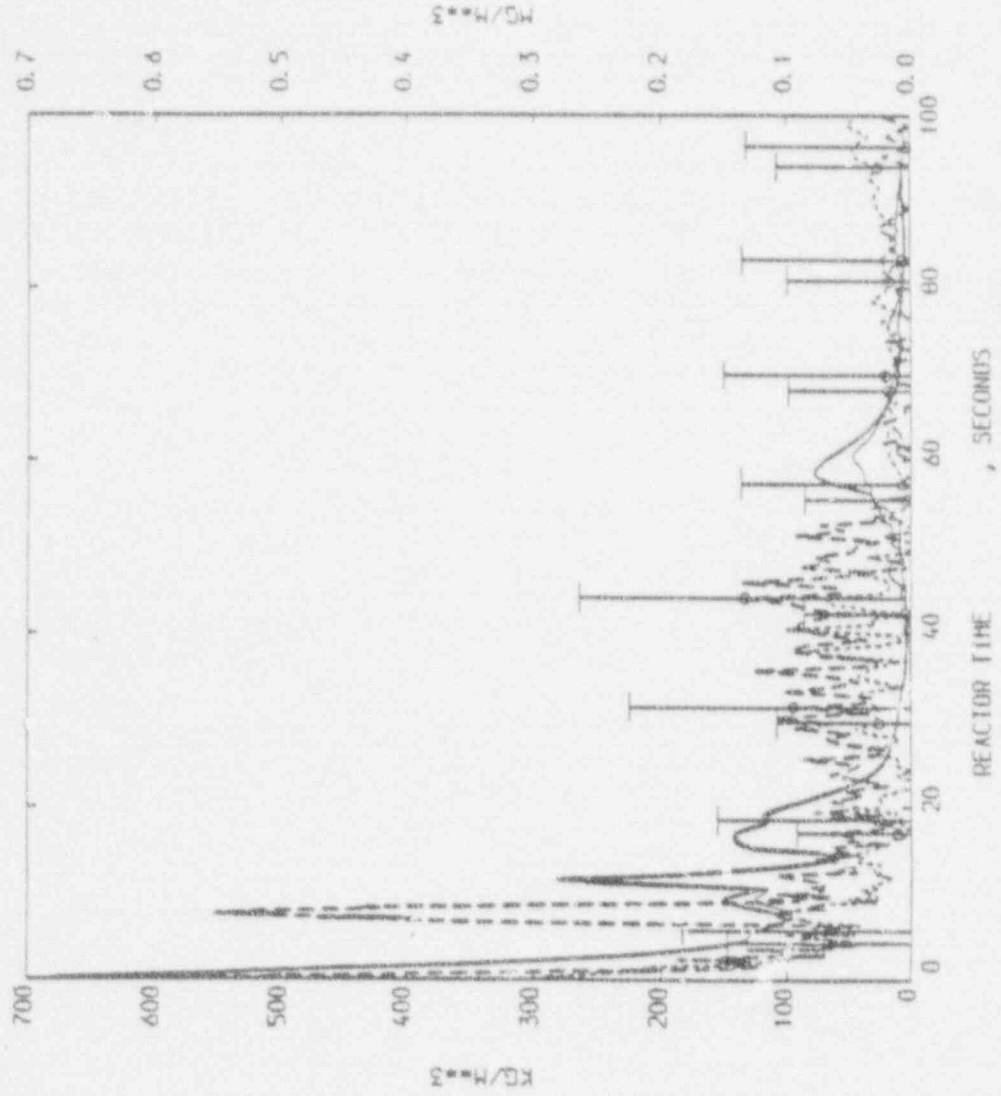THE FOLLOWING ARE PLOTTED AGAINST REACTOR TIME

PRESSURE   , PE-BL-002

AEEW - M 2464

192

FIGURE 156   INF : ISHARP, INF 2 ZEROGAP, INF 3 EXP
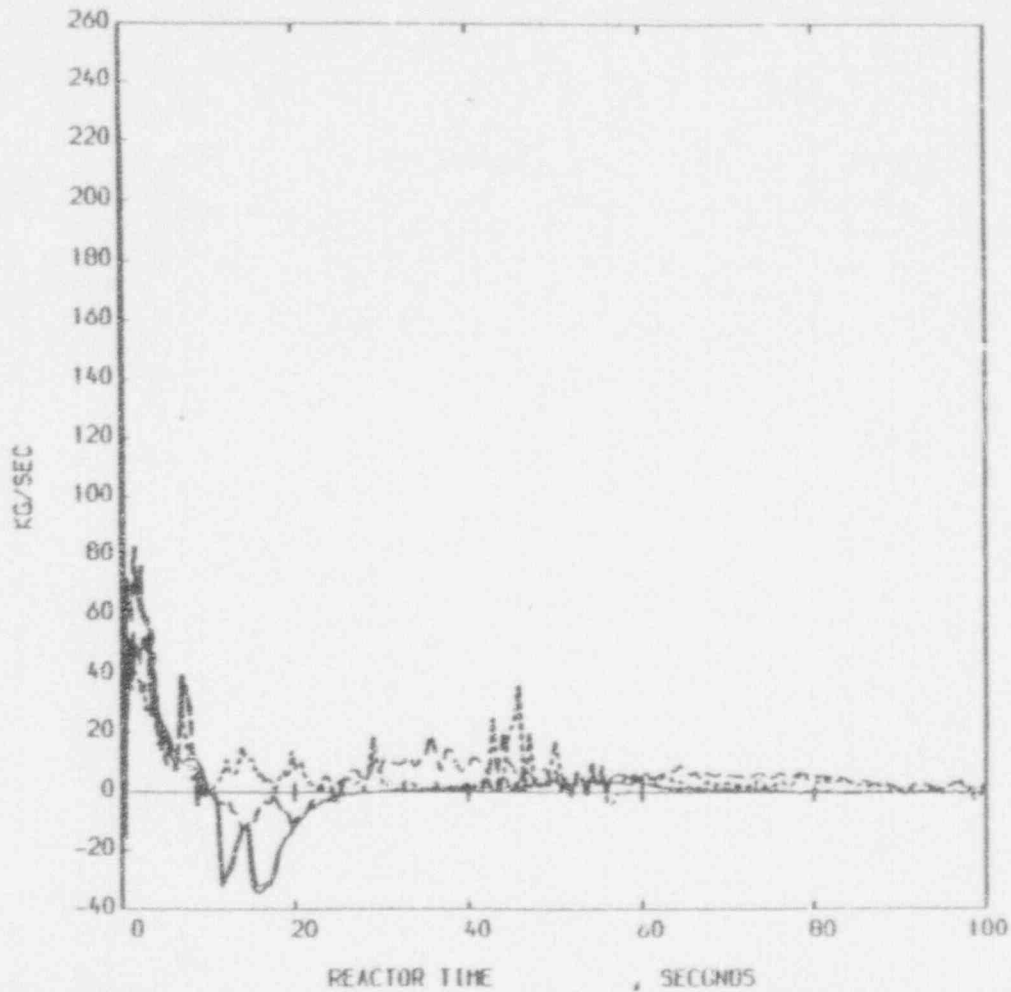BROKEN LOOP HOT LEG - EXPERIMENTAL LOCATION BL-2

FIGURE 157   INF 1 ISHARP, INF 2 ZEROGAP, INF 3 EXP
BROKEN LOOP HOT LEG - EXPERIMENTAL LOCATION BL-2

THE FOLLOWING ARE PLOTTED AGAINST REACTOR TIME

MASS FLOW RATE   ,FR-BL-205

FIGURE 158 INF 1 ISHARP, INF 2 ZEROGAP, INF 3 EXP
BROKEN LOOP HOT LEG - EXPERIMENTAL LOCATION BL-2

	KEY	
SYM BOL	NAME	UNITS
——	MASS FLOW RATE	,KG/SEC
	LOC= 31/ 0/ 3 MMEM-FLOW INF=1	
- - -	MASS FLOW RATE	,KG/SEC
	LOC= 31/ 0/ 7 MMEM-FLOW INF=2	
......	FR-BL-205	,KG/SEC
	LOC= 33/ 0/ 0 MMEM-FLOW INF=3	

194

KEY

SYM BOL	NAME	UNITS
——	LIQUID TEMPERATURE , DEG.K LOC= 31/ 0/ 3 MNEM=TENL INF=1	
——	LIQUID TEMPERATURE , DEG.K LOC= 31/ 0/ 3 MNEM=TENL INF=2	
····	TE-BL-002B , DEG.K LOC= 174/ 0/ 0 MNEM=TNCL INF=3	

FIGURE 159   INF 1 ISHARP, INF 2 ZEROGAP, INF 3 EXP
BROKEN LOOP HOT LEG – EXPERIMENTAL LOCATION BL-2

THE FOLLOWING ARE PLOTTED AGAINST REACTOR TIME
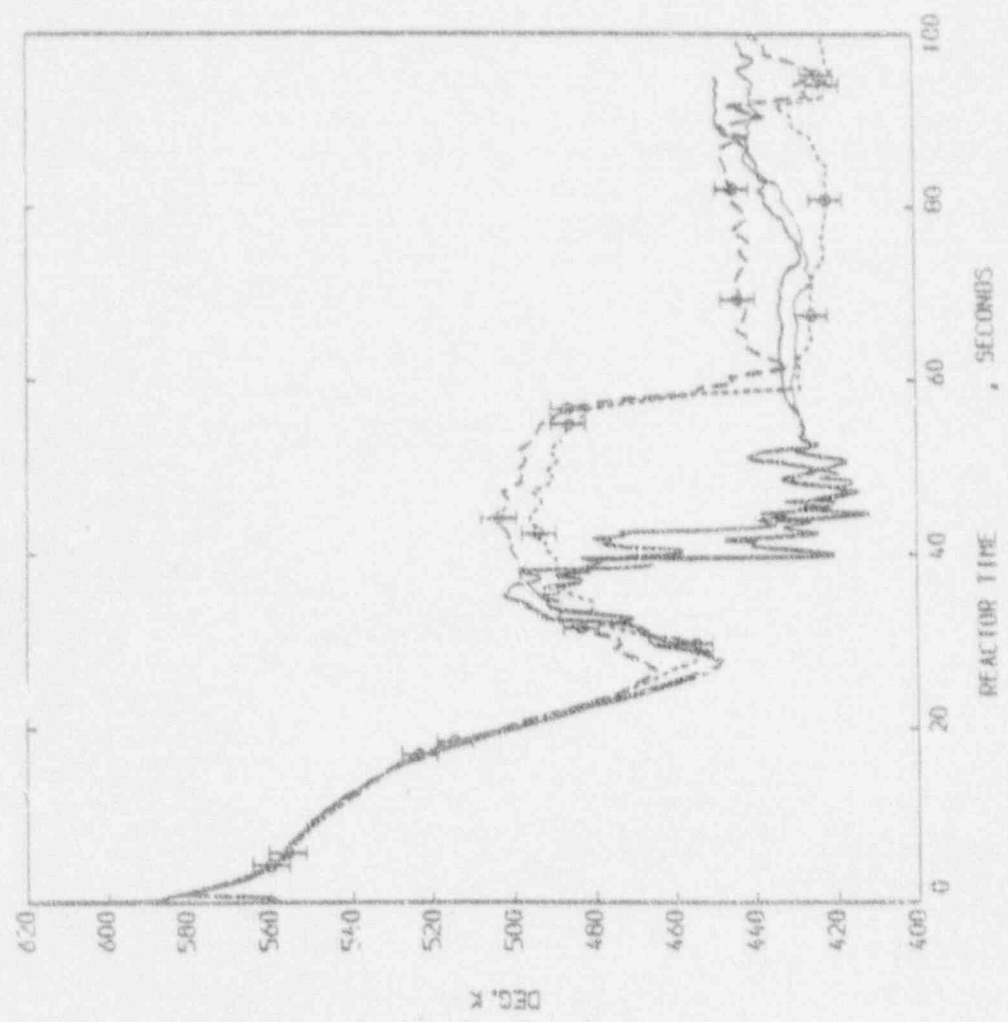
VAPOUR TEMPERATURE ,TE-BL-0028 ,TE-BL-002C
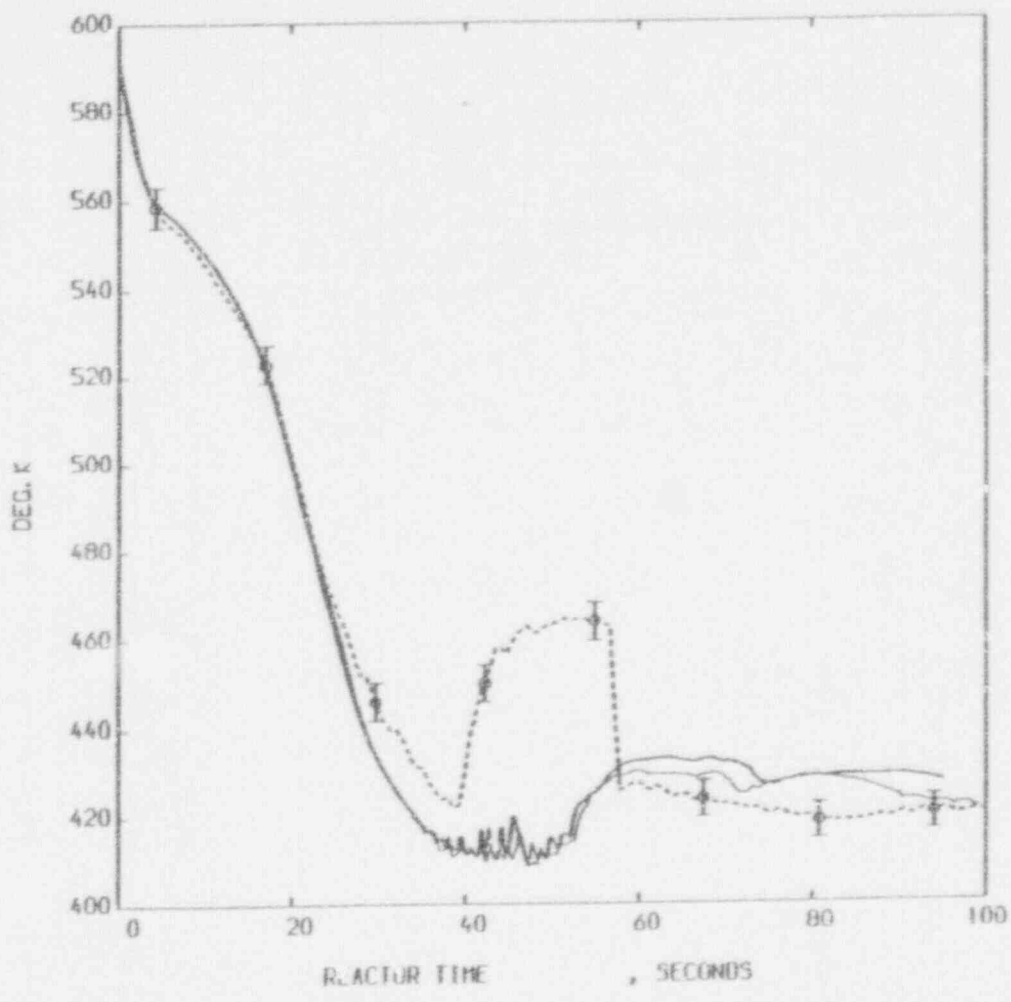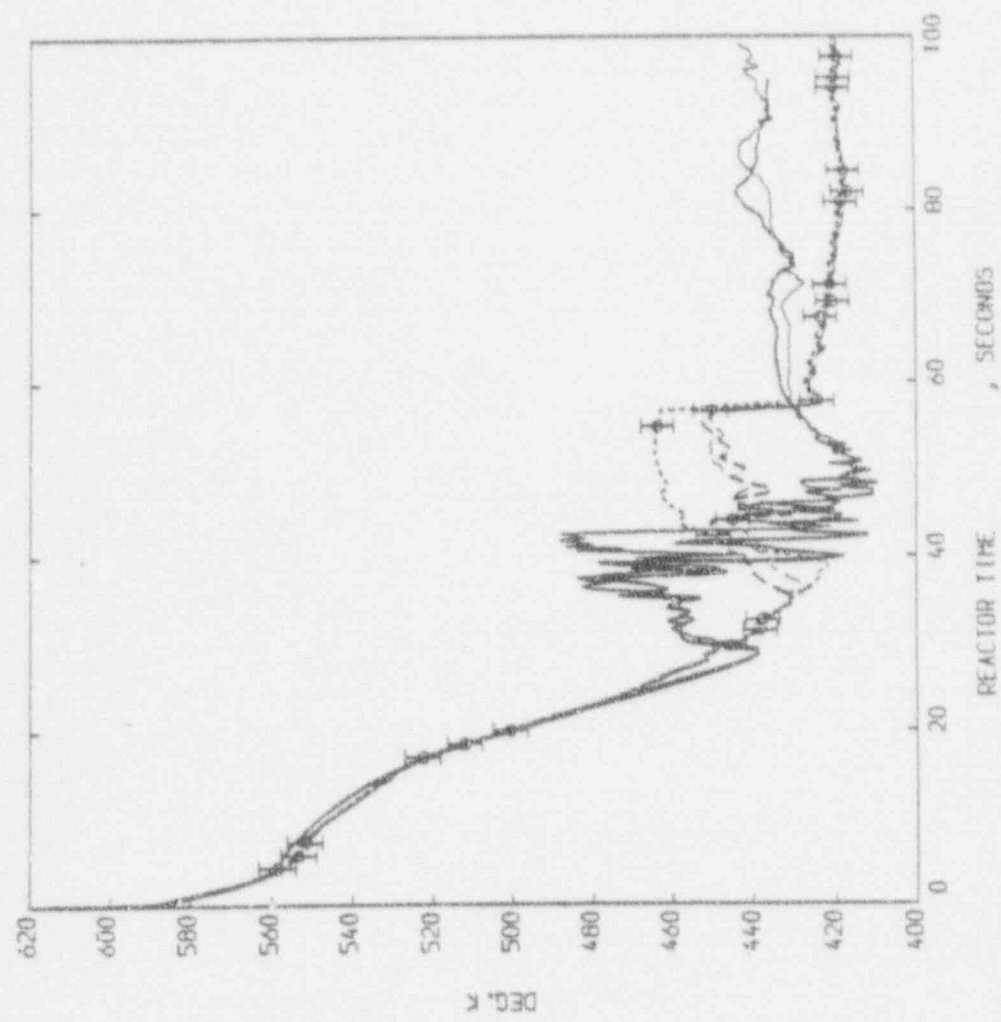

FIGURE 160   INF 1 ISHARP, INF 2 ZEROGAP, INF 3 EXP
BROKEN LOOP HOT LEG - EXPERIMENTAL LOCATION BL-2

A92W - M 2464

THE FOLLOWING ARE PLOTTED AGAINST REACTOR TIME
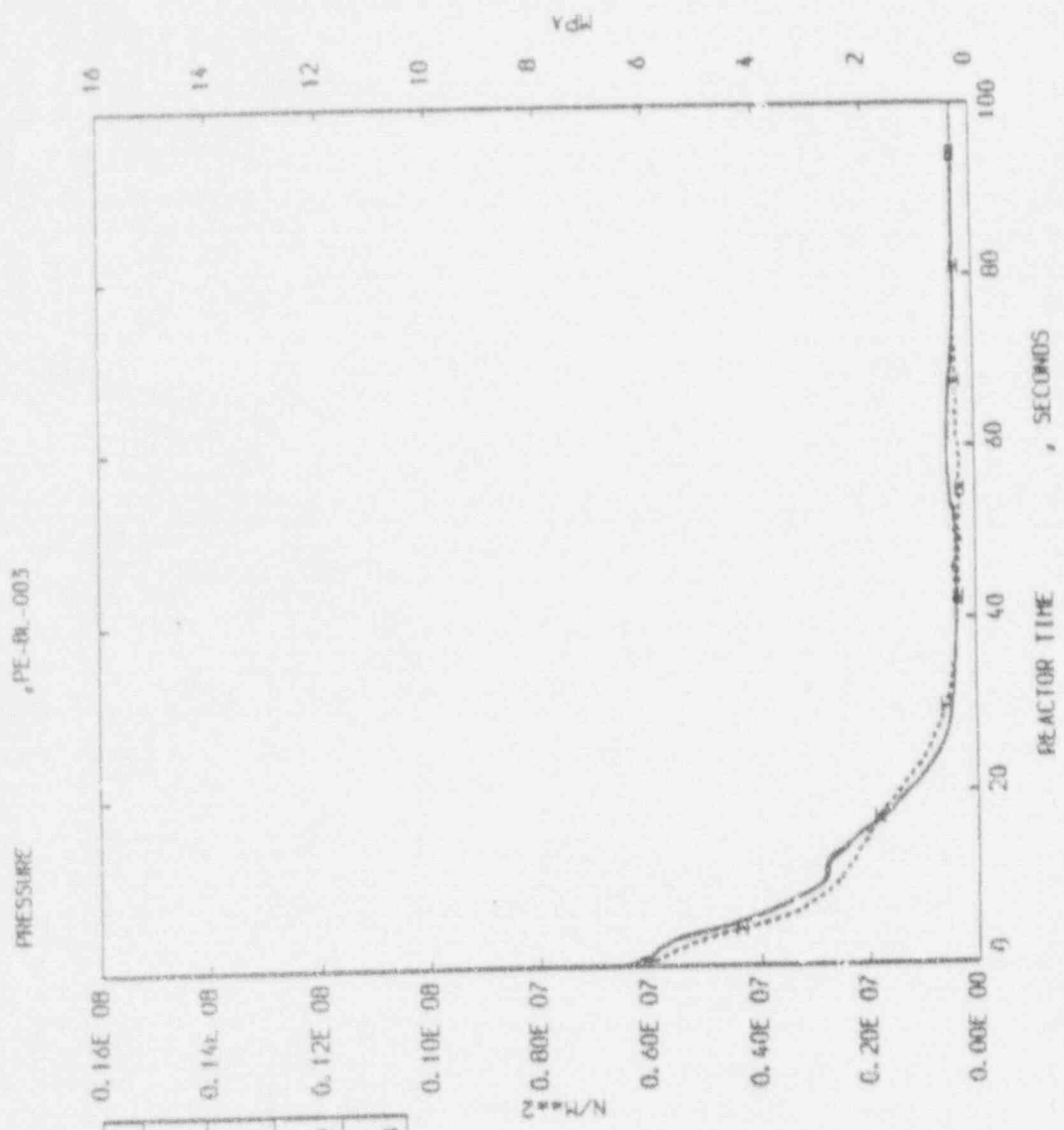
PRESSURE   „PE-BL-003

FIGURE 161 INF 1 ISHARP, INF 2 ZEROGAP, INF 2 EXP
BROKEN LOOP HOT LEG - EXPERIMENTAL LOCATION BL-3

	KEY	
SYM BOL	NAME	UNITS
——	PRESSURE LOC. 31/ 0/ 17 MREM-PRES INF=1	„N/M**2
——	PRESSURE LOC. 31/ 0/ 17 MREM-PRES INF=2	„N/M**2
----	PE-BL-003 LOC. 115/ 0/ 0 MREM-PRES INF=3	„MPA

THE FOLLOWING ARE PLOTTED AGAINST REACTOR TIME

MIXTURE DENSITY   ,DE-PC-001A

FIGURE 162 INF 1 ISHARP, INF 2 ZEROGAP, INF 3 EXP
INTACT LOOP COLD LEG - EXPERIMENTAL LOCATION PC-1

AEEW - M 2464

199

KEY

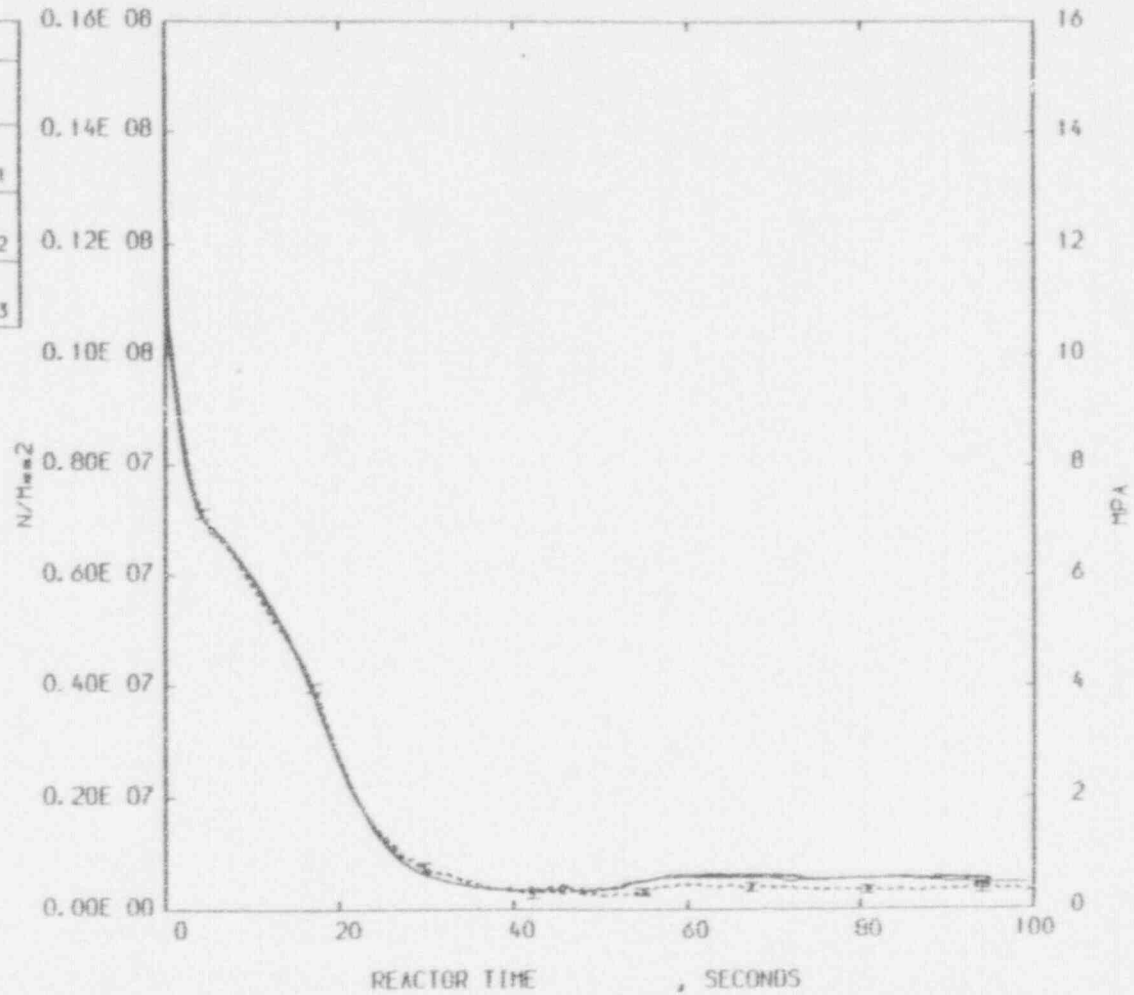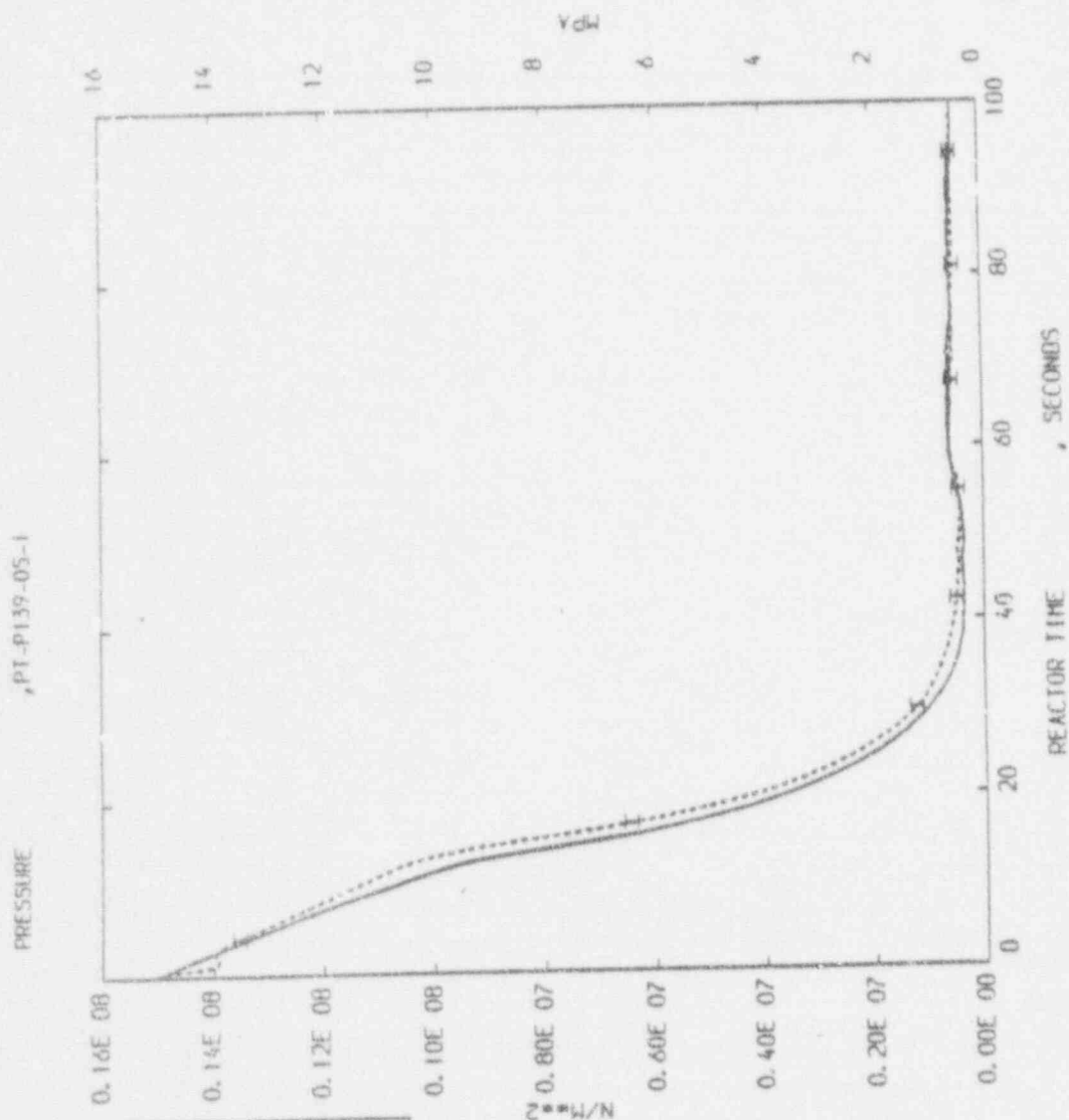| SYM BOL	NAME	UNITS
——	MASS FLOW RATE	,KG/SEC
	LOC= 7/ 0/ 4 MNEM=FLOV INF=1	
——	MASS FLOW RATE	,KG/SEC
	LOC= 7/ 0/ 4 MNEM=FLOV INF=2	
----	FR-PC-100	,KG/SEC
	LOC= 34/ 0/ 0 MNEM=FLOV INF=3	
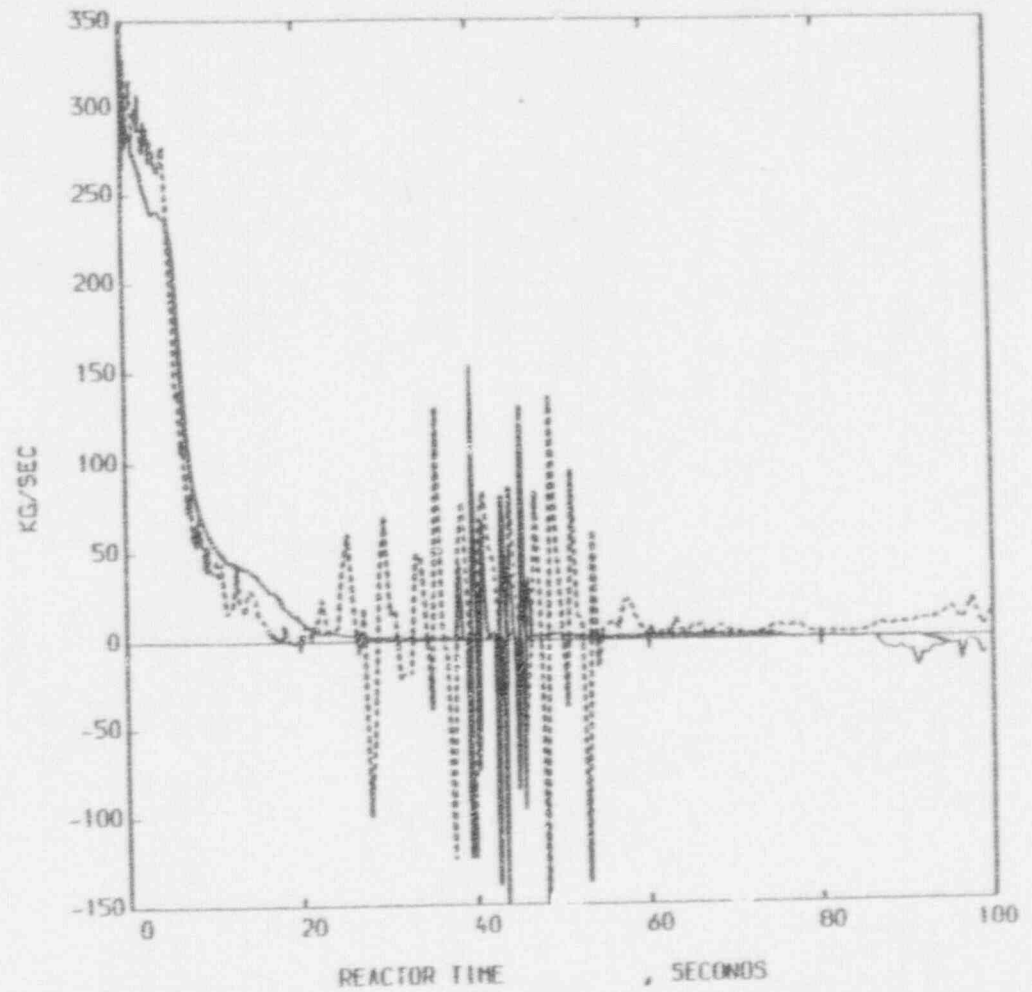
FIGURE 163   INF 1 ISHARP, INF 2 ZEROGAP, INF 3 EXP
INTACT LOOP COLD LEG - EXPERIMENTAL LOCATION PC-1

THE FOLLOWING ARE PLOTTED AGAINST REACTOR TIME

LIQUID VELOCITY ,FE-PC-001A

FIGURE 164 INF 1 ISHARP, INF 2 ZEROGAP, INF 3 EXP
INTACT LOOP COLD LEG - EXPERIMENTAL LOCATION PC-1

KEY
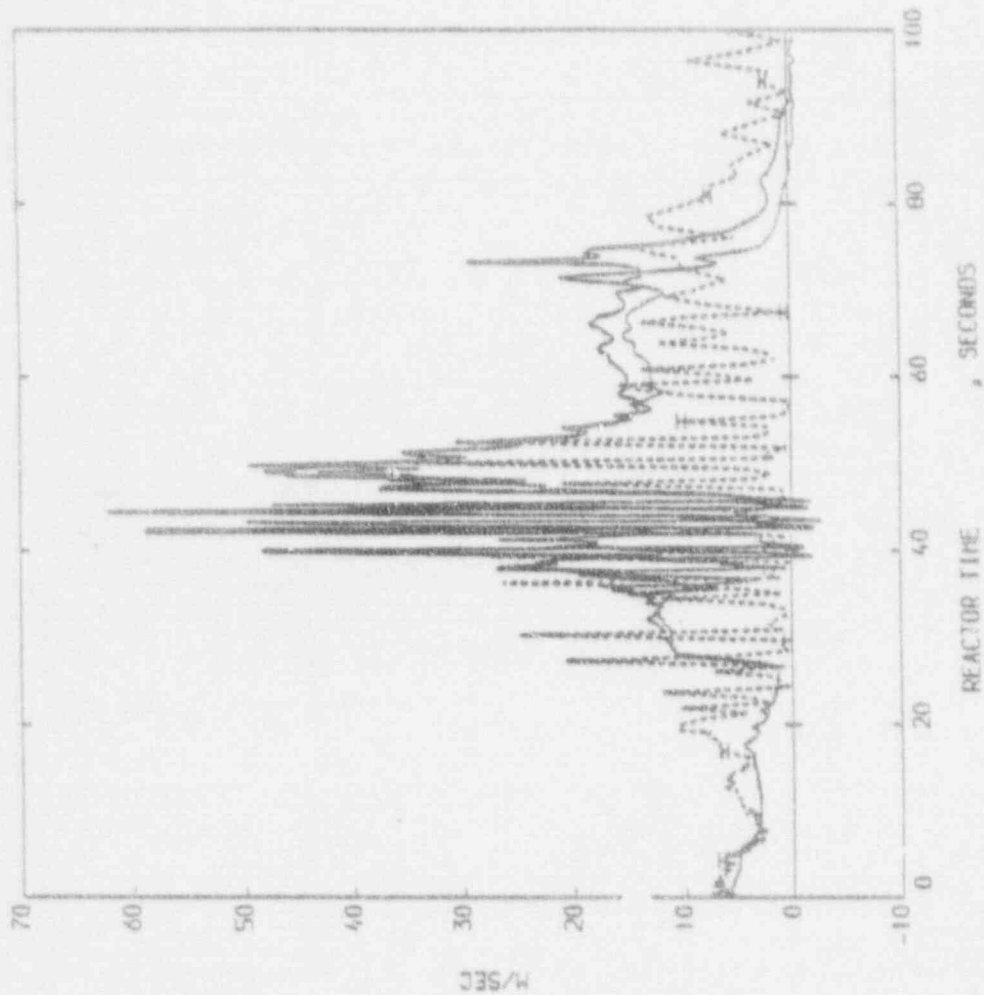
SYM BOL	NAME	UNITS
	LIQUID VELOCITY ,M/SEC	
	LOC= 7/ 0/ 4 MMEM-VLIO INF-1	
	LIQUID VELOCITY ,M/SEC	
	LOC= 7/ 0/ 4 MMEM-VLIO INF-2	
	FE-PC-001A ,M/SEC	
	LOC= 20/ 0/ 0 MMEM-FE INF-3	

THE FOLLOWING ARE PLOTTED AGAINST REACTOR TIME

LIQUID TEMPERATURE , TE-PC-001A

Winfrith

AEEW - M 2464

201

FIGURE 165   INF 1 ISHARP, INF 2 ZEROGAP, INF 3 EXP

INTACT LOOP COLD LEG - EXPERIMENTAL LOCATION PC-1

THE FOLLOWING ARE PLOTTED AGAINST REACTOR TIME

VAPOR TEMPERATURE , TE-PC-001C

FIGURE 166 INF 1 1SHARP, INF 2 ZEROGAP, INF 3 EXP
INTACT LOOP COLD LEG - EXPERIMENTAL LOCATION PC-1

SYM BOL	NAME	UNITS
	VAPOR TEMPERATURE , DEG.K LOC= 7/ 0/ 4 MMESH-TEMV INF =1	
	VAPOR TEMPERATURE , DEG.K LOC= 7/ 0/ 4 MMESH-TEMV INF =2	
	TE-PC-001C , DEG.K LOC= 179/ 0/ 0 MMESH-TMCL INF =3	

KEY

FIGURE 167 INF 1 1SHARP, INF 2 ZEROGAP, INF 3 EXP
PUMP SPEED

FIGURE 168   INF 1 ISHARP, INF 2 ZEROGAP, INF 3 EXP
INTACT LOOP HOT LEG - EXPERIMENTAL LOCATION PC-2

AEEW - M 2464

KEY		
SYM BOL	NAME	UNITS
——	MASS FLOW RATE	,KG/SEC
LOC= 1/ 0/ 2 MNEM=FLOW INF=1		
——	MASS FLOW RATE	,KG/SEC
LOC= 1/ 0/ 2 MNEM=FLOW INF=2		
----	FR-PC-201	,KG/SEC
LOC= 37/ 0/ 0 MNEM=FLOW INF=3		
— —	FR-PC-205	,KG/SEC
LOC= 38/ 0/ 0 MNEM=FLOW INF=3		

FIGURE 169   INF 1 ISHARP, INF 2 ZEROGAP, INF 3 EXP

INTACT LOOP HOT LEG - EXPERIMENTAL LOCATION PC-2

FIGURE 170   INF 1 ISHARP, INF 2 ZEROGAP, INF 3 EXP
INTACT LOOP HOT LEG - EXPERIMENTAL LOCATION PC-2

FIGURE 171 INF 1 ISHARP, INF 2 ZEROGAP, INF 3 EXP
INTACT LOOP HOT LEG - EXPERIMENTAL LOCATION PC-2

AEEW : M 2464

208

KEY

SYM BOL	NAME	UNITS
——	PRESSURE	,N/M**2
	LOC= 1/ 0/ 2 MNEM=PRES INF=1	
——	PRESSURE	,N/M**2
	LOC= 1/ 0/ 2 MNEM=PRES INF=2	
----	PE-PC-002	,MPA
	LOC= 120/ 0/ 0 MNEM=PRES INF=3	

FIGURE 172   INF 1 ISHARP, INF 2 ZEROGAP, INF 3 EXP
INTACT LOOP HOT LEG - EXPERIMENTAL LOCATION PC-2

FIGURE 173 INF 1 ISHARP, INF 2 ZEROGAP, INF 3 EXP
INTACT LOOP HOT LEG - PRESSURIZER

THE FOLLOWING ARE PLOTTED AGAINST REACTOR TIME

WATER LEVEL   ,LEPDI-P139-DOB+0.216

FIGURE 174 INF 1 ISHARP, INF 2 ZEROGAP, INF 3 EXP
INTACT LOOP HOT LEG - PRESSURIZER
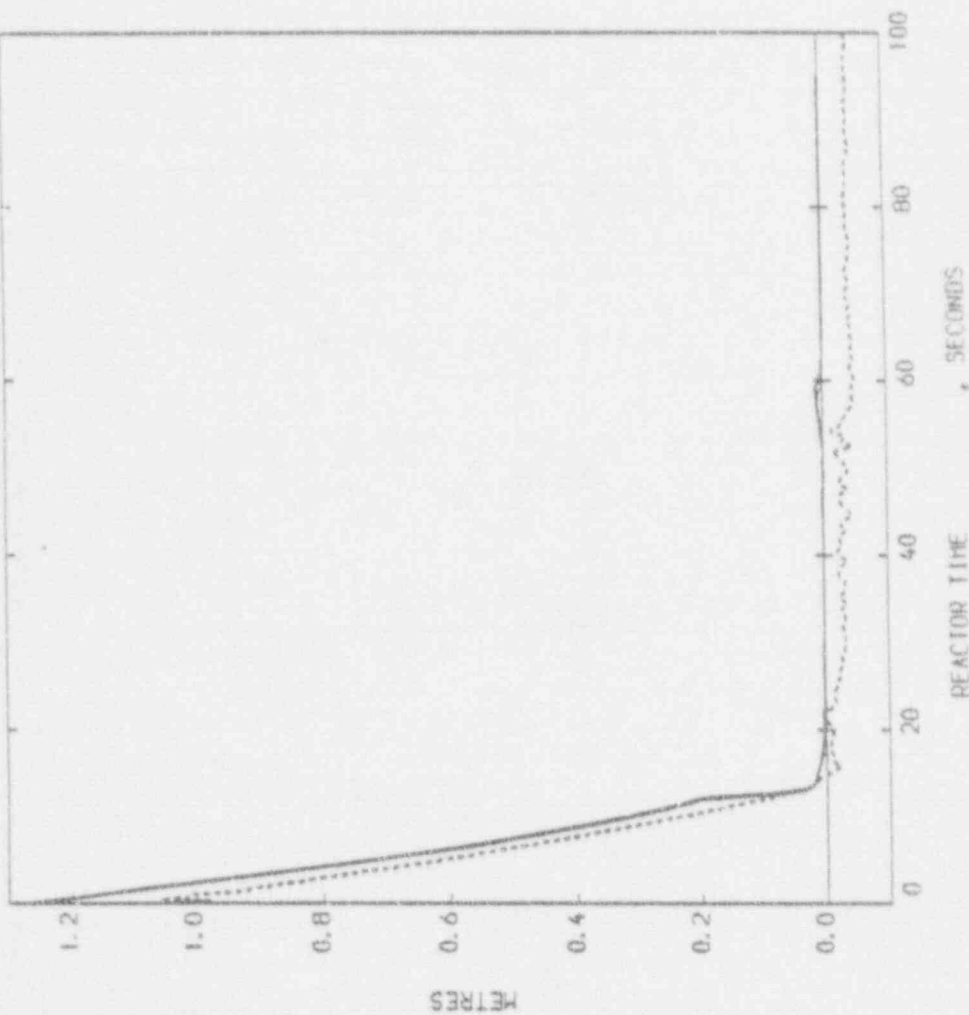
KEY		
SYM BOL	NAME	UNITS
	WATER LEVEL ,METRES	
	LOC= 8/ 0/ 1 MNETH-LEVE INF=1	
	WATER LEVEL ,METRES	
	LOC= 8/ 0/ 1 MNETH-LEVE INF=2	
	LEPDI-P139-DOB+0.216,METRES	
	LOC= 50/ 0/ 0 MNETH-LEVE INF=3	

Winfrith

KEY		
SYM BOL	NAME	UNITS
——	WATER LEVEL LOC= 15/ 0/ 1 MNEM=LEVE INF=1	,METRES
——	WATER LEVEL LOC= 15/ 0/ 1 MNEM=LEVE INF=2	,METRES
----	LE-ECC-01A LOC= 51/ 0/ 0 MNEM=LEVE INF=3	,METRES

FIGURE 175   INF 1 ISHARP, INF 2 ZEROGAP, INF 3 EXP
EMERGENCY CORE COOLING SYSTEM

FIGURE 176 INF 1 ISHARP, INF 2 ZEROGAP, INF 3 EXP
INTACT LOOP HOT LEG - PRESSURIZER

Winfrith

AEEW = M 2464

213

FIGURE 177   INF 1 ISHARP, INF 2 ZEROGAP, INF 3 EXP
UPPER PLENUM PRESSURE

Winfrith

A.E.E.W - M 2464

214

KEY		
SYM BOL	NAME	UNITS
——	LIQ AXIAL VELOCITY ,M/SEC LOC= 50/ 3/ 1 MNEM=VL-Z INF=1	
——	LIQ AXIAL VELOCITY ,M/SEC LOC= 50/ 3/ 1 MNEM=VL-Z INF=2	
----	FE-SLP-001 ,M/SEC LOC= 29/ 0/ 0 MNEM=FE INF=3	

M/SEC

REACTOR TIME   , SECONDS

FIGURE 178 INF 1 ISHARP, INF 2 ZEROGAP, INF 3 EXP
LOWER PLENUM LIQUID AXIAL VELOCITY

Winfrith

KEY		
SYM BOL	NAME	UNITS
——	LIQ AXIAL VELOCITY ,M/SEC LOC= 50/ 9/ 1 MNEM=VL-Z INF=1	
——	LIQ AXIAL VELOCITY ,M/SEC LOC= 50/ 9/ 1 MNEM=VL-Z INF=2	
----	FE-SUP-001 ,M/SEC LOC= 31/ 0/ 0 MNEM=FE INF=3	

FIGURE 179   INF 1 ISHARP, INF 2 ZEROGAP, INF 3 EXP
UPPER PLENUM LIQUID AXIAL VELOCITY

FIGURE 180   INF 1 ISHARP, INF 2 ZEROGAP, INF 3 EXP
DOWNCOMER LIQUID TEMPERATURE AT 5.0 METRES

KEY		
SYM BOL	NAME	UNITS
——	LIQUID TEMPERATURE	,DEG.K
LOC= 50/ 10/ 13 MNEM=TEML INF=1		
——	LIQUID TEMPERATURE	,DEG.K
LOC= 50/ 10/ 13 MNEM=TEML INF=2		
----	TE-1ST-002	,DEG.K
LOC= 202/ 0/ 0 MNEM=TMEL INF=3		

DEG. K

REACTOR TIME , SECONDS

FIGURE 181   INF 1 ISHARP, INF 2 ZEROGAP, INF 3 EXP
DOWNCOMER LIQUID TEMPERATURE AT 4.2 METRES

Winfrith

THE FOLLOWING ARE PLOTTED AGAINST REACTOR TIME

LIQUID TEMPERATURE , TE-1ST-005

FIGURE 182 INF 1 ISHARP, INF 2 ZEROGAP, INF 3 EXP
DOWNCOMER LIQUID TEMPERATURE AT 2.4 METRES

KEY:		
SYM BOL	NAME	UNITS
——	LIQUID TEMPERATURE , DEG.K	
	LOC= 50/ 7/ 13 MNEM=TEML INF=1	
— —	LIQUID TEMPERATURE , DEG.K	
	LOC= 50/ 7/ 13 MNEM=TEML INF=2	
----	TE-1ST-005 , DEG.K	
	LOC= 205/ 0/ 0 MNEM=TMCL INF=3	

REACTOR TIME , SECONDS

DEG. K

Winfrith

219

KEY
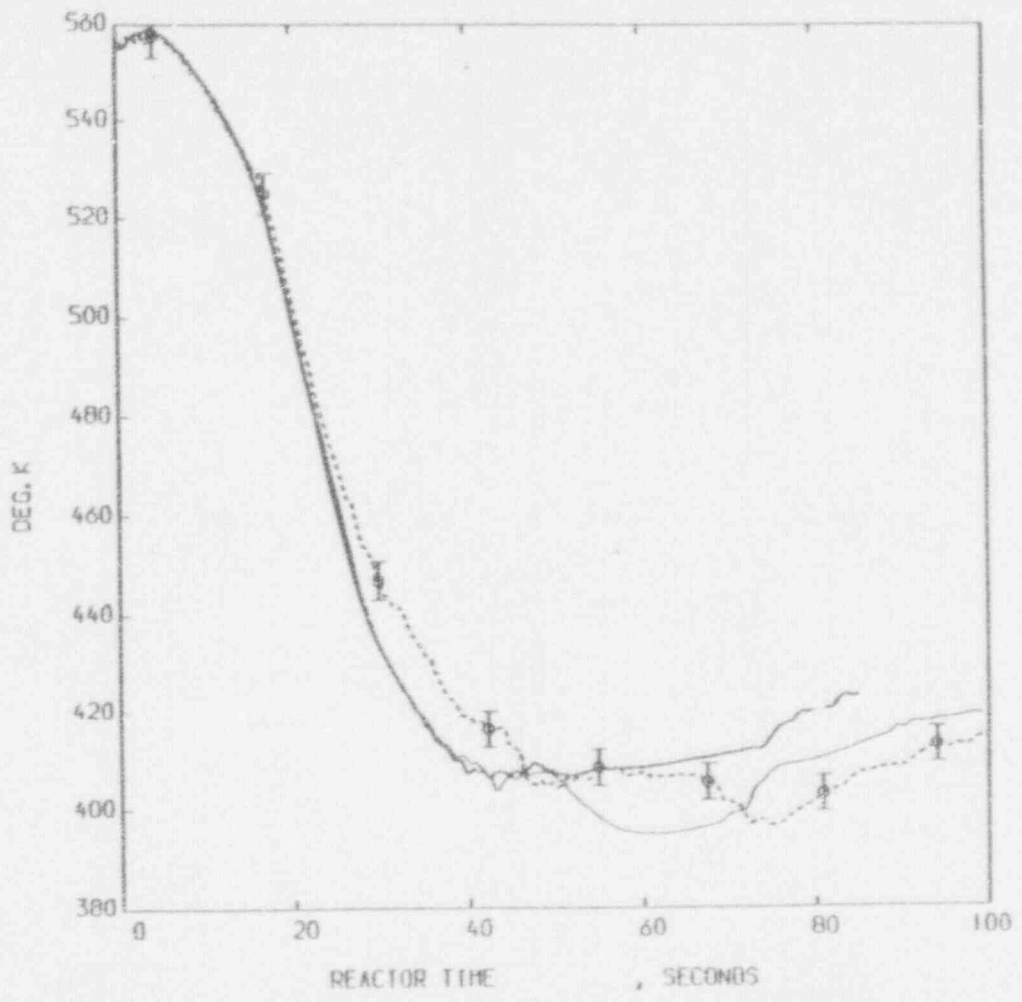
SYM BOL	NAME	UNITS
———	LIQUID TEMPERATURE ,DEG.K LOC= 50/ 1/ 13 MNEM=TEML INF=1	
———	LIQUID TEMPERATURE ,DEG.K LOC= 50/ 1/ 13 MNEM=TEML INF=2	
-----	TE-1ST-012 ,DEG.K LOC= 211/ 0/ 0 MNEM=TMCL INF=3	

FIGURE 183   INF 1 ISHARP, INF 2 ZEROGAP, INF 3 EXP
DOWNCOMER LIQUID TEMPERATURE AT 0.3 METRES

FIGURE 184 LINE 1 ISHARP, LINE 2 ZEROGAP, LINE 3 EXP
LOWER PLENUM MOMENTUM FLUX

THE FOLLOWING ARE PLOTTED AGAINST REACTOR TIME

CORE INLET MASS FLOW

FIGURE 185 INF 1 1SHARP, INF 2 ZEROGAP
VESSEL GLOBALS
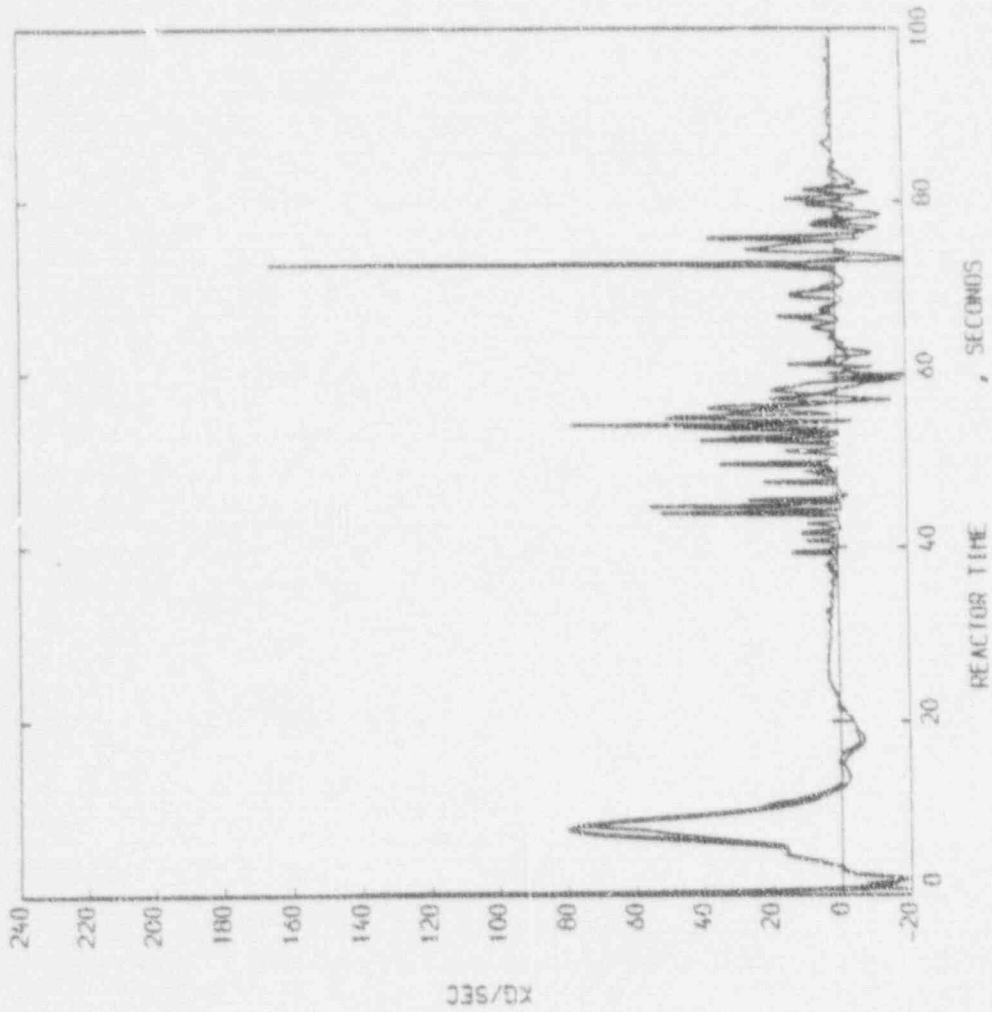
KEY	
NAME	UNITS
SYMBOL	
CORE INLET MASS FLOW,KG/SEC	
LOC = SO/ 0/ 1 MREM=FLC1 INF=1	
CORE INLET MASS FLOW,KG/SEC	
LOC = SO/ 0/ 1 MREM=FLC1 INF=2	

FIGURE 186 INF 1 1SHARP, INF 2 ZEROGAP
VESSEL GLOBALS

THE FOLLOWING ARE PLOTTED AGAINST REACTOR TIME

CORE LIQUID MASS

FIGURE 187 INF 1 ISHARP, INF 2 ZEROGAP
VESSEL GLOBALS

	KEY	
SYM BOL	NAME	UNITS
	CORE LIQUID MASS	KG
	LOC = 50/ 0/ 1 MREH-LMER INF=1	
	CORE LIQUID MASS	KG
	LOC = 50/ 0/ 1 MREH-LMER INF=2	

THE FOLLOWING ARE PLOTTED AGAINST REACTOR TIME

L PLENM LIQ VOL FRAC

FIGURE 188 INF 1 ISHARP, INF 2 ZEROGAP
VESSEL GLOBALS

SYM BOL	NAME	UNITS
	L PLENM LIQ VOL FRAC, LOC= 50/ 0/ 1 MBEM-LFLP INF=1	
	L PLENM LIQ VOL FRAC, LOC= 50/ 0/ 1 MBEM-LFLP INF=2	

KEY
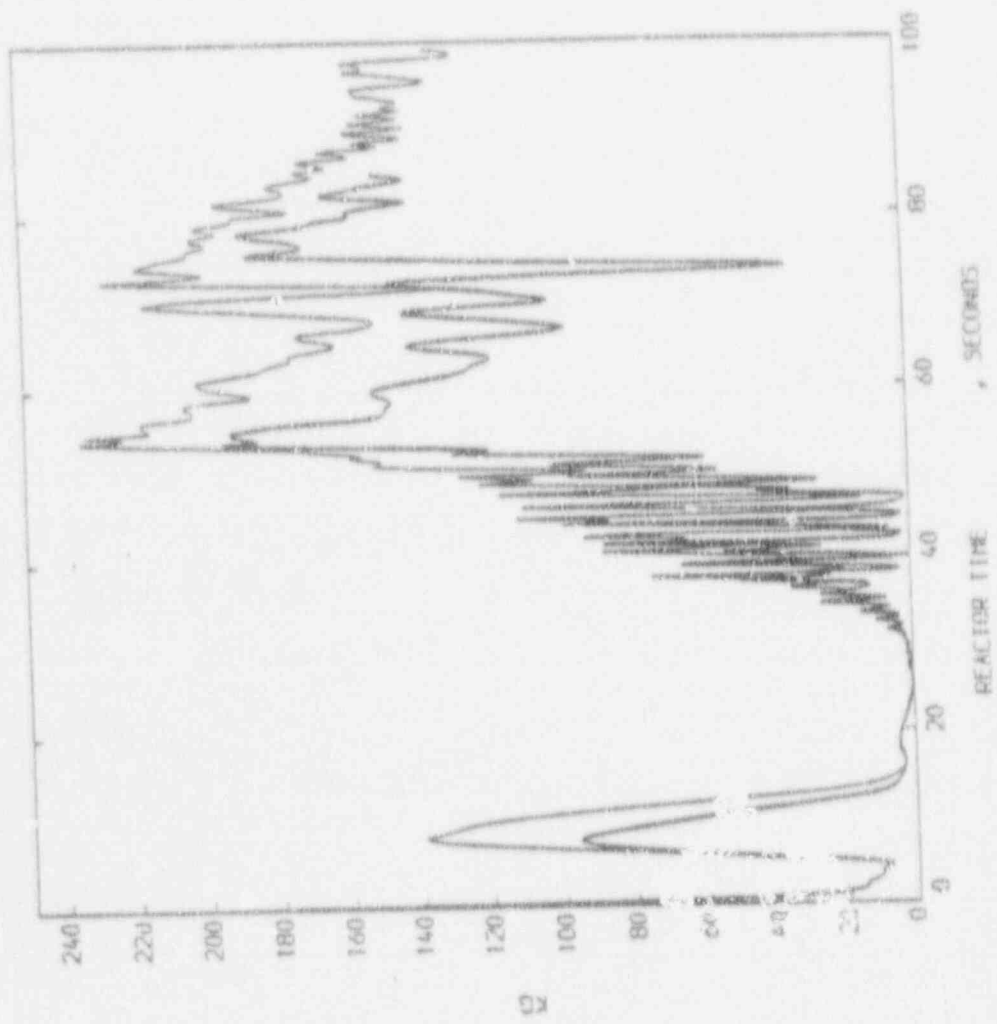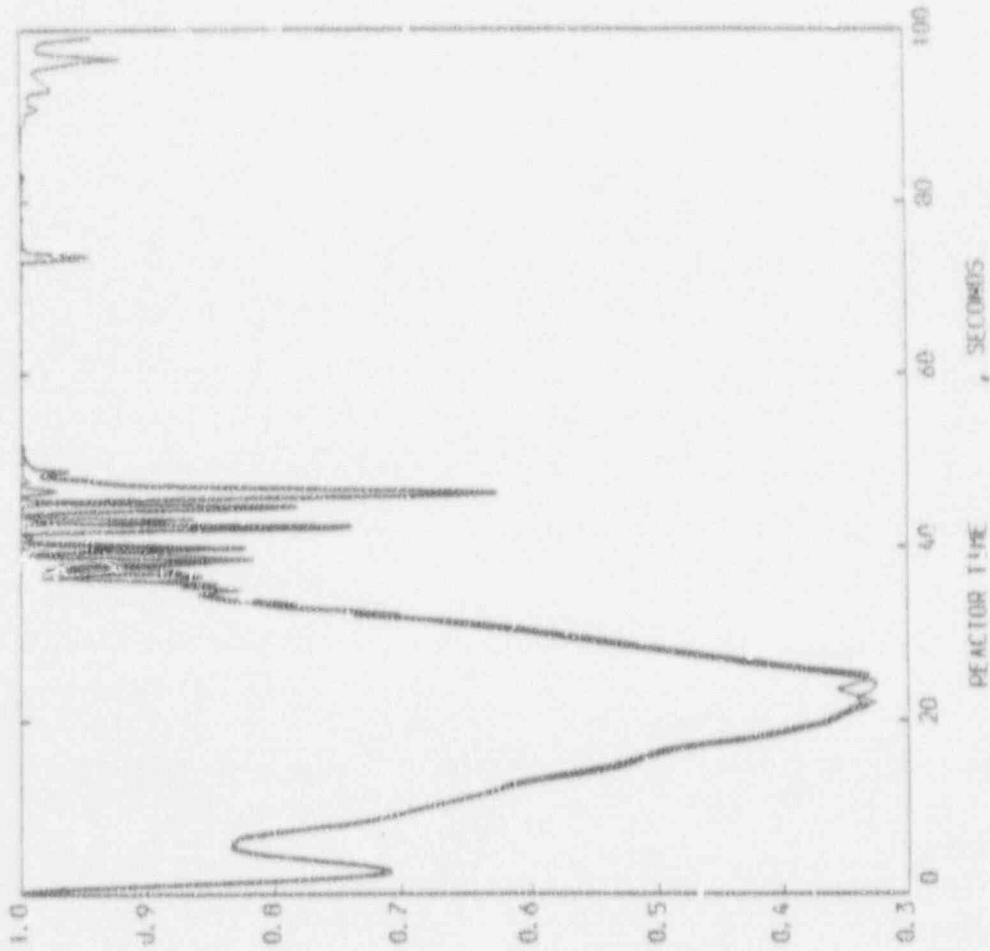
THE FOLLOWING ARE PLOTTED AGAINST REACTOR TIME

D'CORNER LIQ VOL FRAC
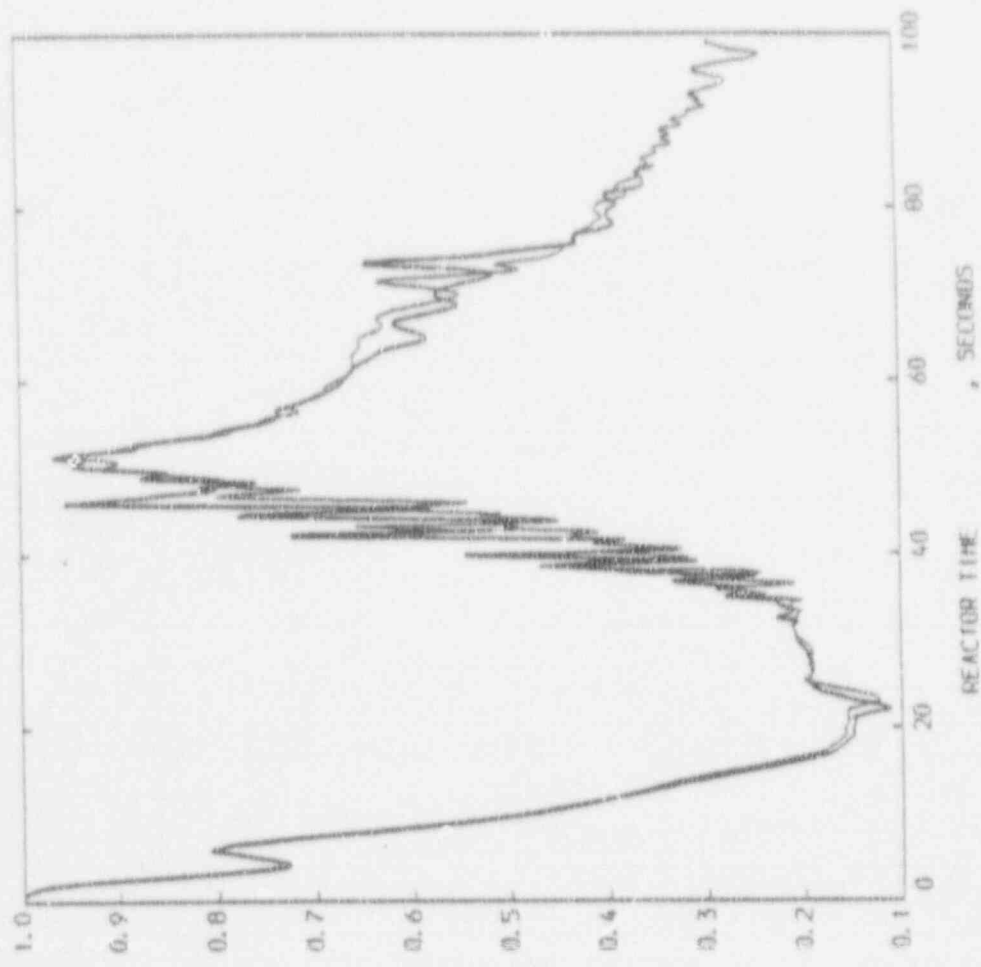
FIGURE 189 INF 1 ISHARP, INF 2 ZEROGAP
VESSEL GLOBALS

KEY

SYMBOL	NAME	UNITS
	D'CORNER LIQ VOL FRAC, LOC= 50/ 0/ 1 MAEM=LFRC INF=1	
	D'CORNER LIQ VOL FRAC, LOC= 50/ 0/ 1 MAEM=LFRC INF=2	

REACTOR TIME   , SECONDS

CORE LIQ VOL FRAC

Winfrith

AEEW - M 2464

226

KEY		
SYM BOL	NAME	UNITS
——	CORE LIQ VOL FRAC	,
LOC= 50/ 0/ 1 MNEM=LFCO INF=1		
——	CORE LIQ VOL FRAC	,
LOC= 50/ 0/ 1 MNEM=LFCO INF=2		

REACTOR TIME , SECONDS
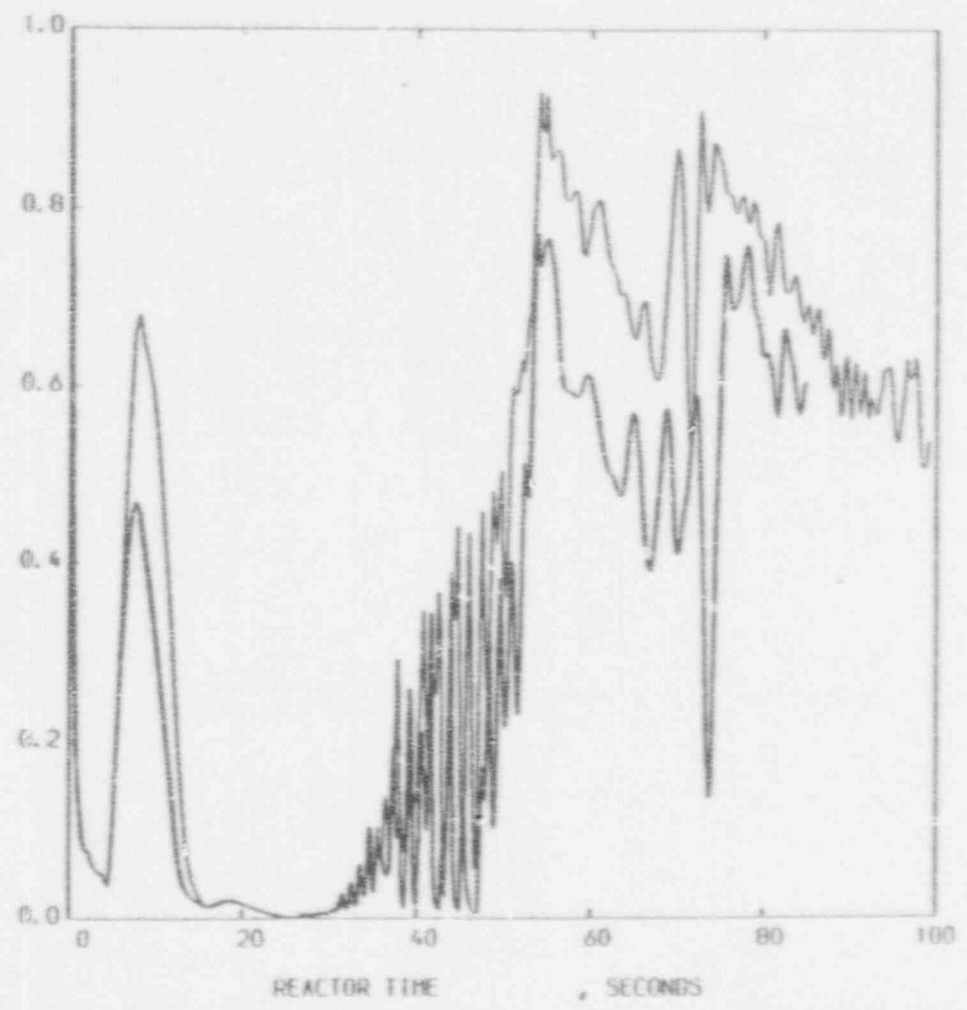
FIGURE 190   INF 1 ISHARP, INF 2 ZEROGAP
VESSEL GLOBALS

VESSEL LIQUID MASS

AEEW - M 2464

227

KEY		
SYM BOL	NAME	UNITS
——	VESSEL LIQUID MASS ,KG	
	LOC= 50/ 0/ 1 MNEM=LMVS INF=1	
——	VESSEL LIQUID MASS ,KG	
	LOC= 50/ 0/ 1 MNEM=LMVS INF=2	

REACTOR TIME , SECONDS

FIGURE 191   INF 1 ISHARP, INF 2 ZEROGAP
VESSEL GLOBALS

FIGURE 192 INF 1 ISHARP, INF 2 ZEROGAP
VESSEL GLOBALS

THE FOLLOWING ARE PLOTTED AGAINST REACTOR TIME

TOT SLAB HEAT FLUX

KEY

SYM COL	NAME	UNITS
—	TOT SLAB HEAT FLUX , WATTS	WATTS
	1.0E= 50/ 0/ 1 ISHARP-0SLT INF=1	
---	TOT SLAB HEAT FLUX , WATTS	WATTS
	1.0E= 50/ 0/ 1 ZEROGAP-0SLT INF=2	

FIGURE 193 INF 1 ISHARP, INF 2 ZEROGAP
VESSEL GLOBALS

FIGURE 174 INF 1 ISHARP, INF 2 ZEROGAP
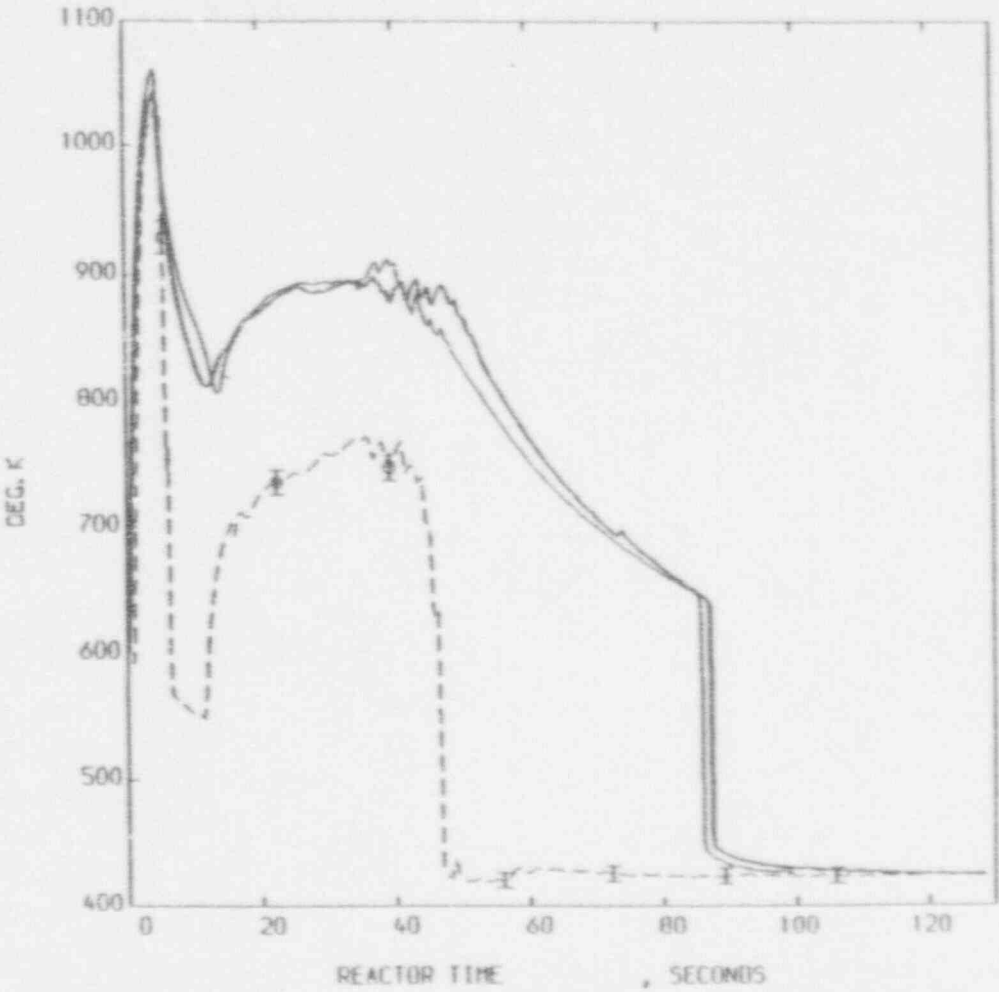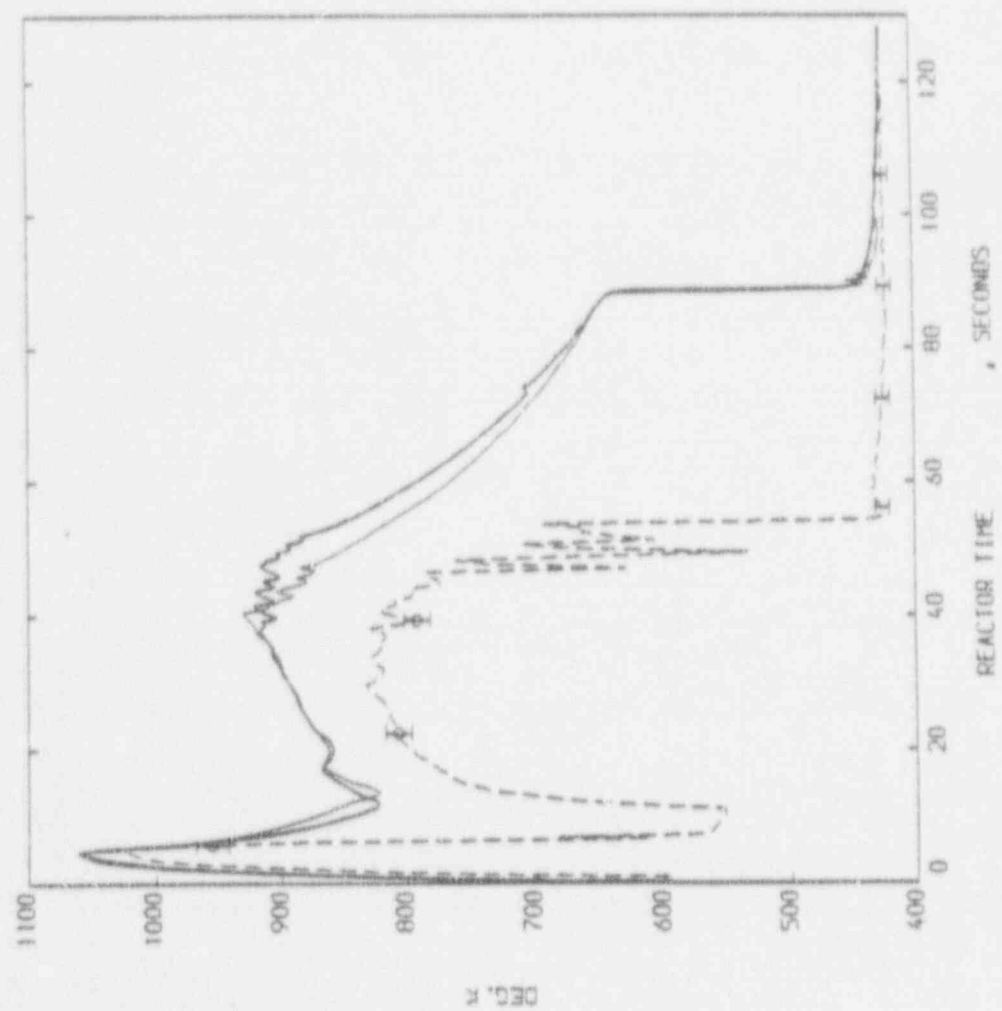
VESSEL GLOBALS

FIGURE 195   INF 1 ISHARP, INF 2 ZEROGAP, INF 3 EXP
CENTRAL FUEL BUNDLE CLADDING TEMPERATURES

THE FOLLOWING ARE PLOTTED AGAINST REACTOR TIME

CLADDING TEMP -FINE,TE-SG06-011

DEC, K

1050
1000
950
900
850
800
750
700
650
600
550
500
450
400

REACTOR TIME , SECONDS

0   20   40   60   80   100   120

KEY	
SYM BOL	NAME	UNITS
——	CLADDING TEMP -FINE,DEG,K LOC= 56/ 1/ 5 MAEM-THEL INF=1	
——	CLADDING TEMP -FINE,DEG,K LOC= 56/ 1/ 5 MAEM-THEL INF=2	
---	TE-SG06-011 ,DEG,K LOC= 278/ 0/ 0 MAEM-THEL INF=3	

FIGURE 196 INF 1 ISHARP, INF 2 ZEROGAP, INF 3 EXP
CENTRAL FUEL BUNDLE CLADDING TEMPERATURES

AEEW - M 2464
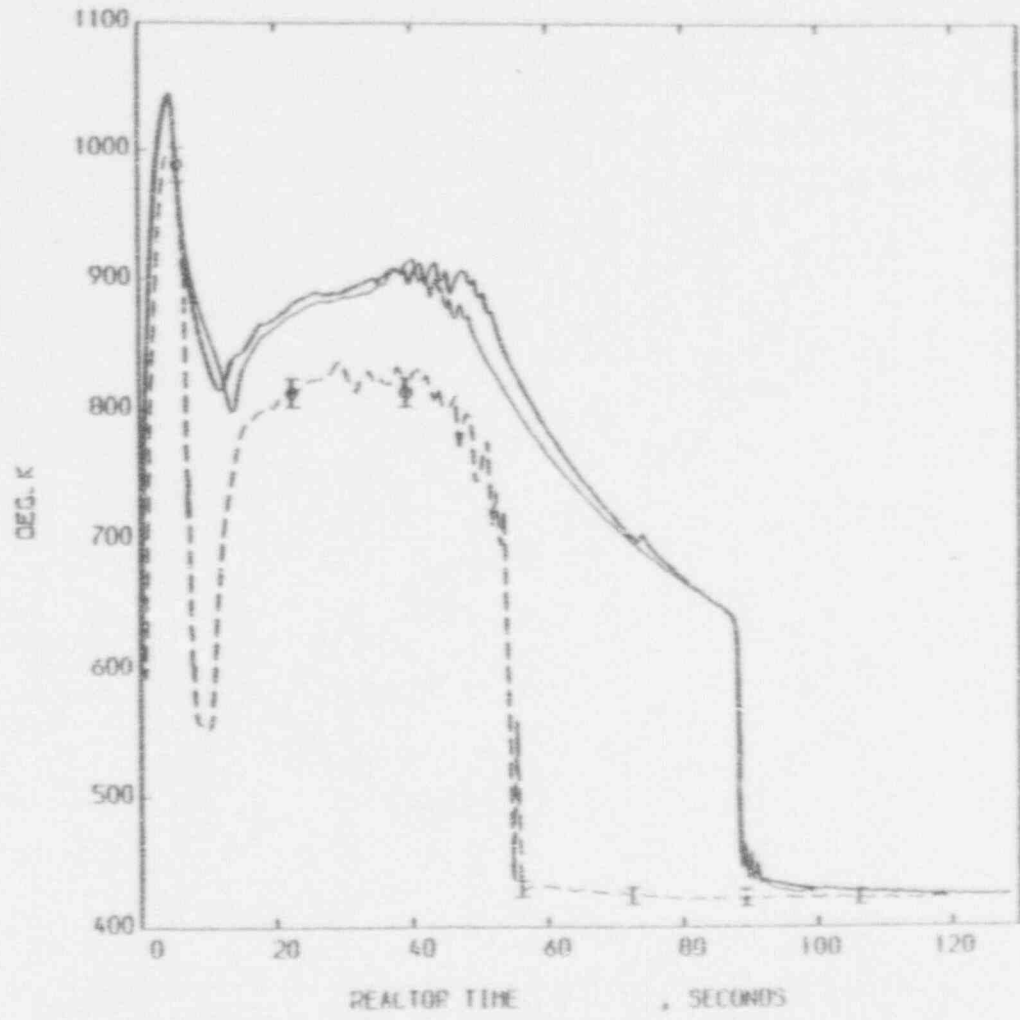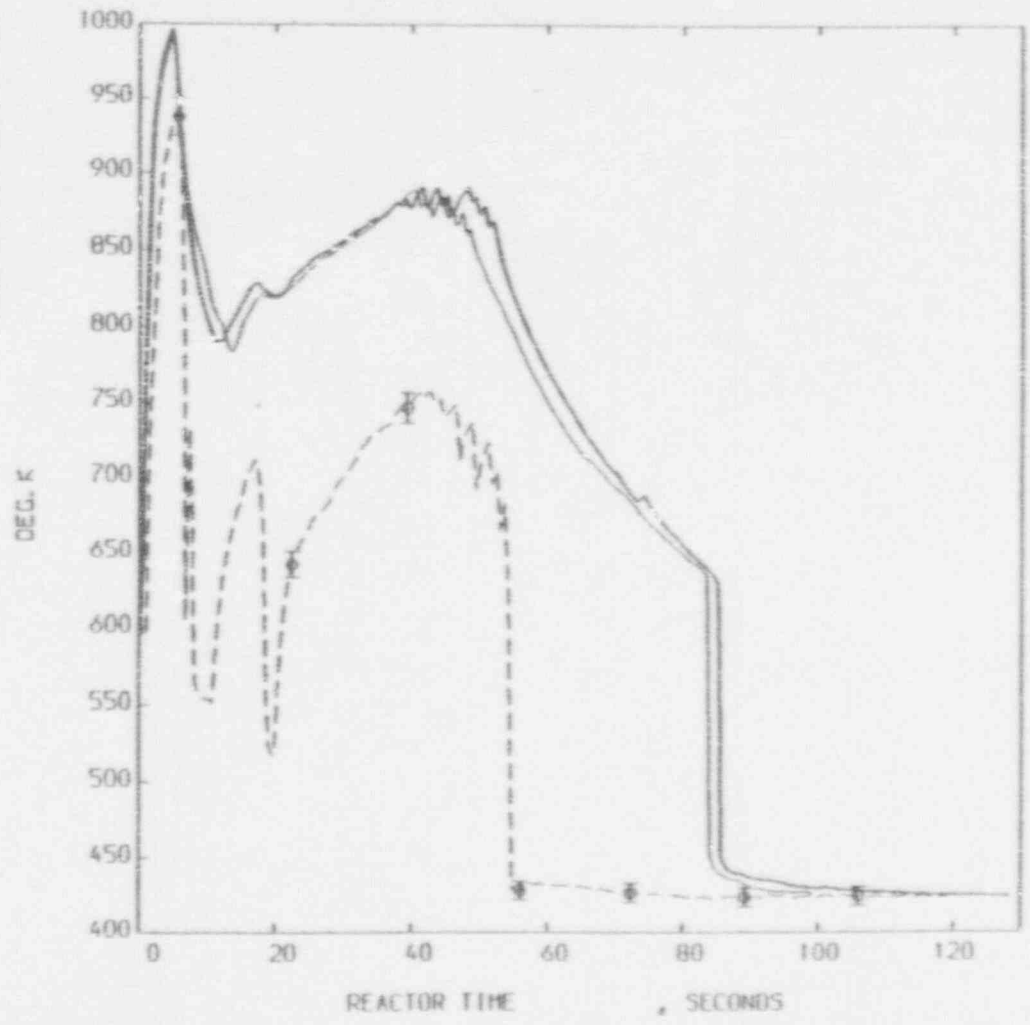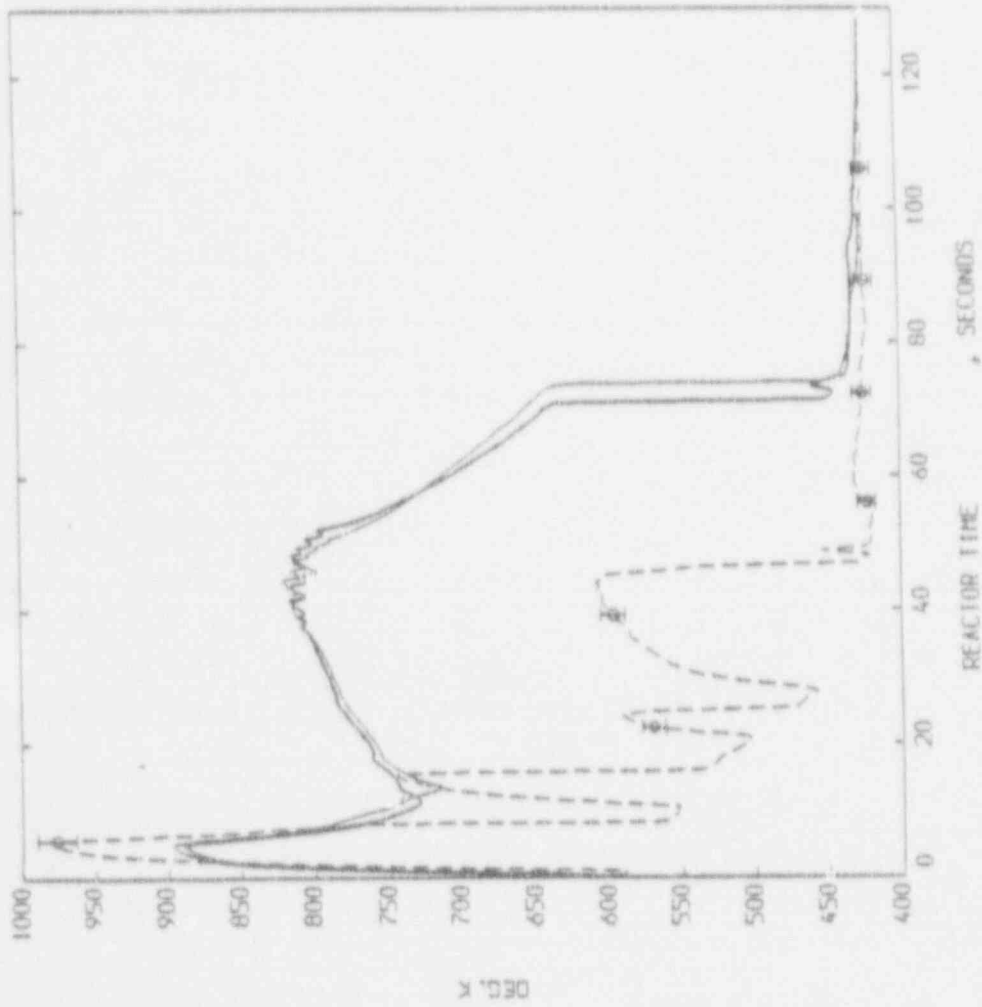
232

AEEW - M 2464

233

FIGURE 197 INF 1 ISHARP, INF 2 ZEROGAP, INF 3 EXP
CENTRAL FUEL BUNDLE CLADDING TEMPERATURES

THE FOLLOWING ARE PLOTTED AGAINST REACTOR TIME

CLADDING TEMP -FINE,TE-5W06-024

FIGURE 198 INF 1 ISHARP, INF 2 ZEROGAP, INF 3 EXP
CENTRAL FUEL BUNDLE CLADDING TEMPERATURES

KEY		UNITS
SYMBOL	NAME	
	CLADDING TEMP -FINE,DEG.K	
	LOC= 50/ 1/ 10 MIMEN-TMCL INF=1	
	CLADDING TEMP -FINE,DEG.K	
	LOC= 50/ 1/ 10 MIMEN-TMCL INF=2	
	TE-5W06-024 ,DEG.K	
	LOC= 205/ 0/ 0 MIMEN-TMCL INF=3	

REACTOR TIME , SECONDS

DEG.K

Winfrith

KEY

SYM BOL	NAME	UNITS
——	CLADDING TEMP -FINE, DEG. K LOC= 50/ 4/ 12 MNEM=THCL INF=1	
——	CLADDING TEMP -FINE, DEG. K LOC= 50/ 4/ 12 MNEM=THCL INF=2	
——	TE-5104-027 ,DEG. K LOC= 293/ 0/ 0 MNEM=THCL INF=3	

FIGURE 199 INF 1 ISHARP, INF 2 ZEROGAP, INF 3 EXP
CENTRAL FUEL BUNDLE CLADDING TEMPERATURES

FIGURE 200   INF 1 ISHARP, INF 2 ZEROGAP, INF 3 EXP
CENTRAL FUEL BUNDLE CLADDING TEMPERATURES

THE FOLLOWING ARE PLOTTED AGAINST REACTOR TIME

CLADDING TEMP -FINE, TE-5106-039

FIGURE 201 INF 1 ISHARP, INF 2 ZEROGAP, INF 3 EXP
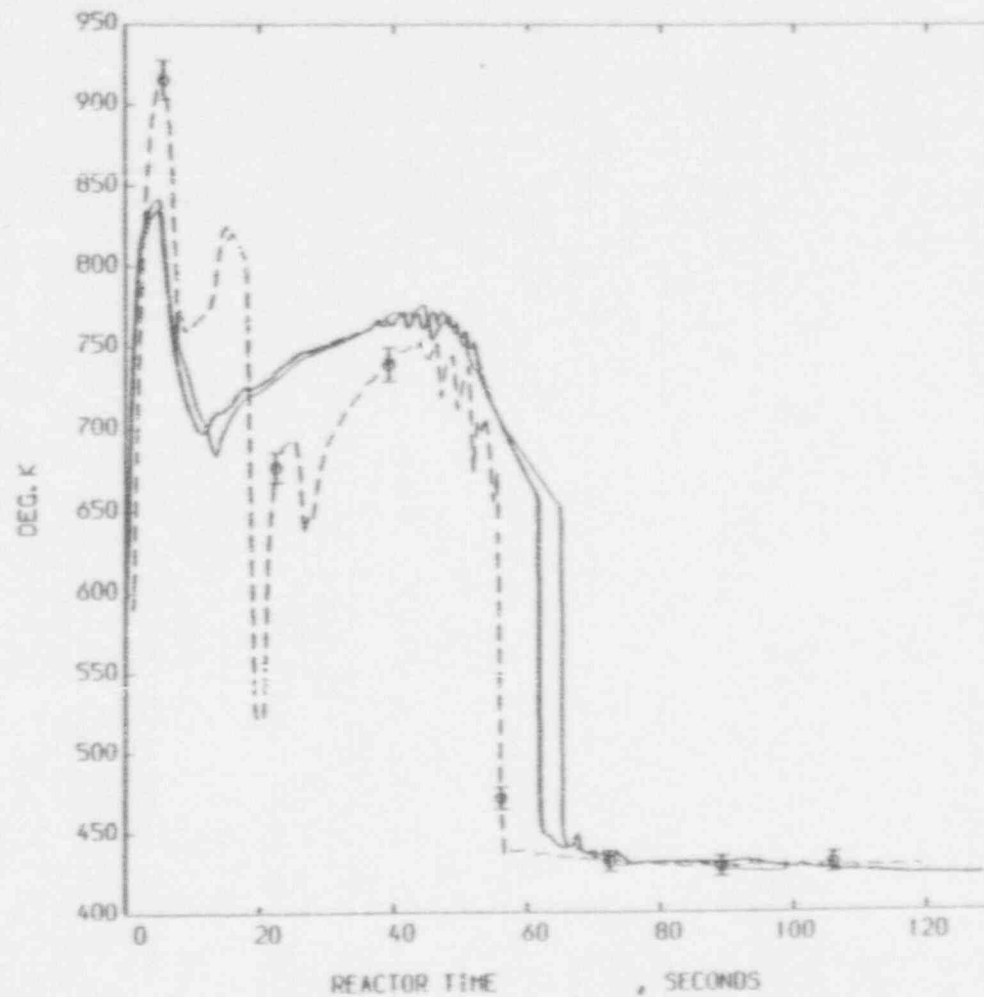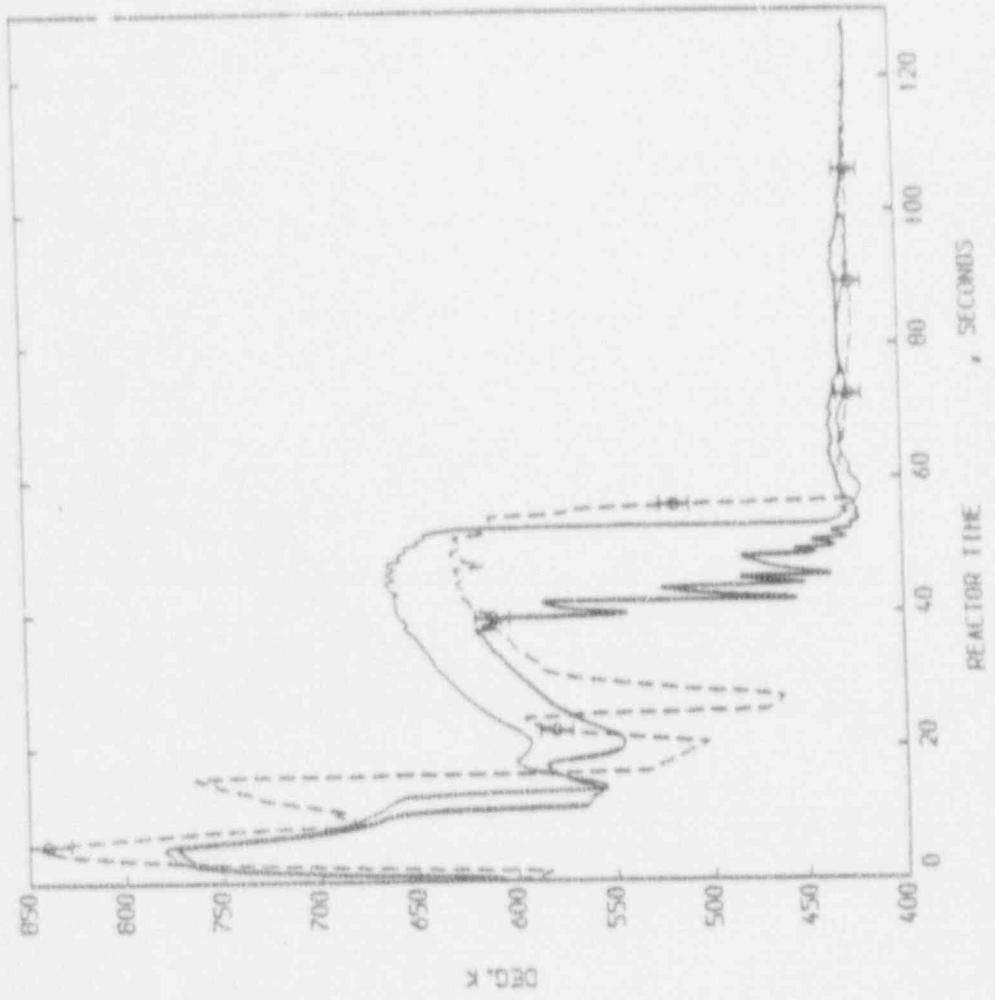CENTRAL FUEL BUNDLE CLADDING TEMPERATURES

Winfrith

FIGURE 202   INF 1 ISHARP, INF 2 ZEROGAP, INF 3 EXP
CENTRAL FUEL BUNDLE CLADDING TEMPERATURES
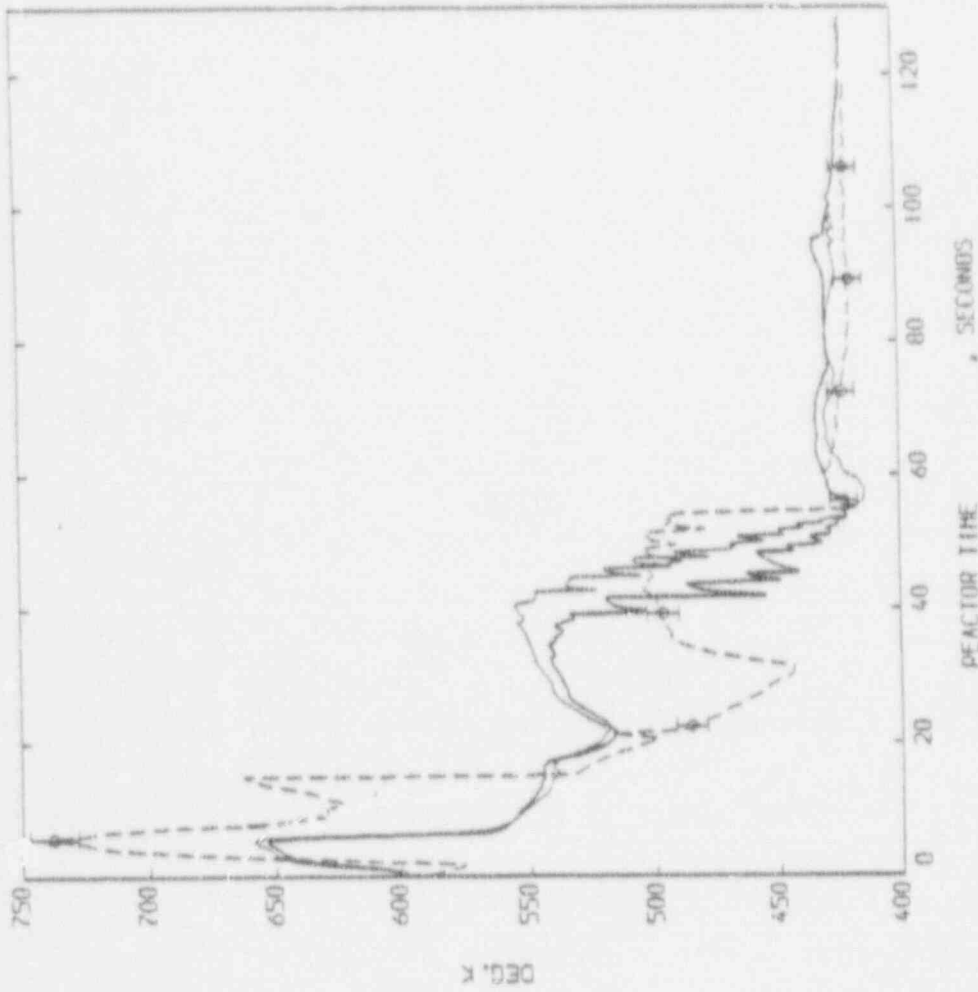
THE FOLLOWING ARE PLOTTED AGAINST REACTOR TIME

CLADDING TEMP -FINE, TE-SH05-049

FIGURE 203 INF 1 ISHARP, INF 2 ZEROGAP, INF 3 EXP
CENTRAL FUEL BUNDLE CLADDING TEMPERATURES

FIGURE 204 INF 1 ISHARP, INF 2 ZEROGAP, INF 3 EXP
CENTRAL FUEL BUNDLE CLADDING TEMPERATURES

ROD CENTRE TEMP-FINE, TC-5007-27   , TC-5009-27
TC-5010-27

Winfrith

AEEW - M 2464

261

KEY		
SYM BOL	NAME	UNITS
――	ROD CENTRE TEMP-FINE, DEG. K LOC= 50/ 1/ 12 MNEM=TMRC INF=1	
――	ROD CENTRE TEMP-FINE, DEG. K LOC= 50/ 1/ 12 MNEM=TMRC INF=2	
----	TC-5007-27 , DEG. K LOC= 168/ 0/ 0 MNEM=TMRC INF=3	
― ―	TC-5009-27 , DEG. K LOC= 169/ 0/ 0 MNEM=TMRC INF=3	
― ―	TC-5010-27 , DEG. K LOC= 170/ 0/ 0 MNEM=TMRC INF=3	

FIGURE 205   INF 1 ISHARP, INF 2 ZEROGAP, INF 3 EXP
CENTRELINE FUEL TEMPERATURE

Winfrith

FIGURE 206   INF 1 ISHARP, INF 2 ZEROGAP, INF _ EXP
FUEL ROD CLADDING TEMPERATURES - PERIPHERAL BUNDLES

THE FOLLOWING ARE PLOTTED AGAINST REACTOR TIME

CLADDING TEMP -FINE, TE-2H13-021

FIGURE 207 INF 1 ISHARP, INF 2 ZER.GAP, INF 3 EXP
FUEL ROD CLADDING TEMPERATURES - PERIPHERAL BUNDLES

THE FOLLOWING ARE PLOTTED AGAINST REACTOR TIME

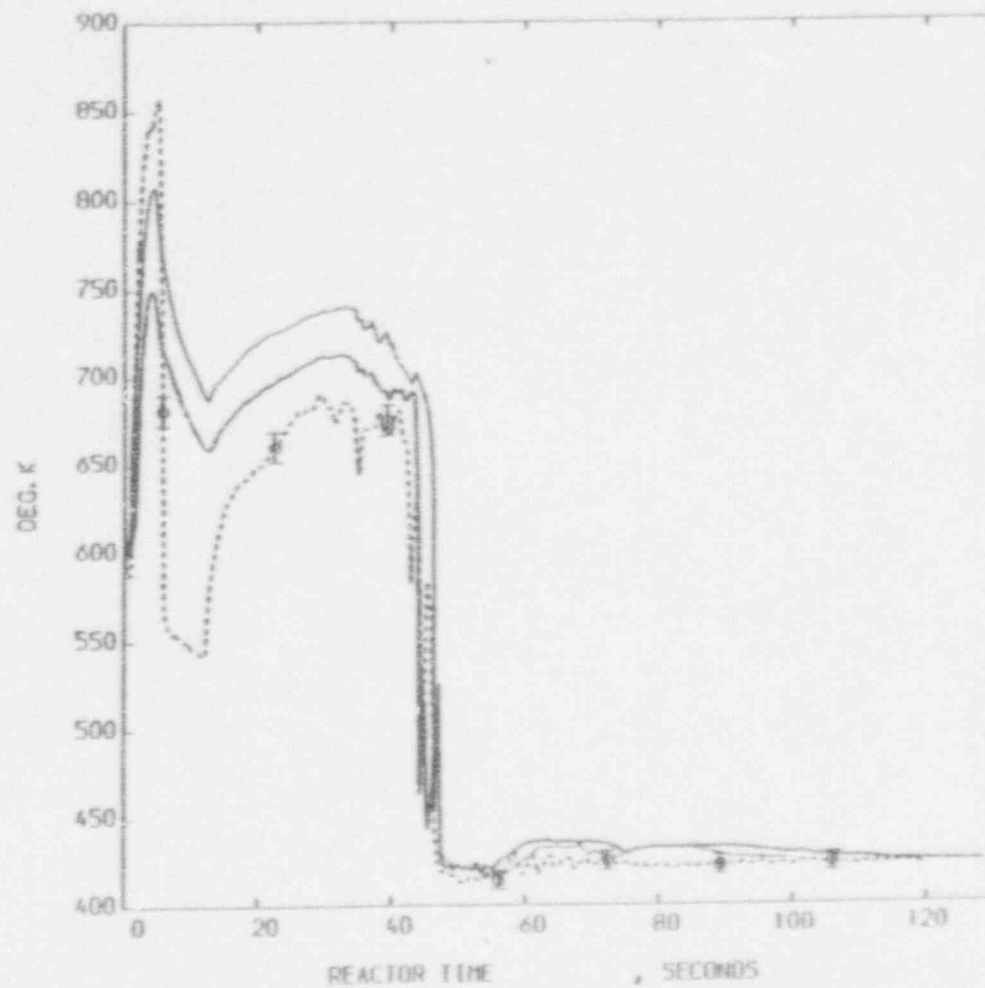CLADDING TEMP -FINE,TE-2G14-030

FIGURE 208 INF 1 : SHARP, INF 2 ZEROGAP, INF 3 EXP
FUEL ROD CLADDING TEMPERATURES - PERIPHERAL BUNDLES

THE FOLLOWING ARE PLOTTED AGAINST REACTOR TIME

CLADDING TEMP -FINE,TE-2114-039

FIGURE 209 INF 1 ISHARP, INF 2 ZEROGAP, INF 3 EXP
FUEL ROD CLADDING TEMPERATURES - PERIPHERAL BUNDLES

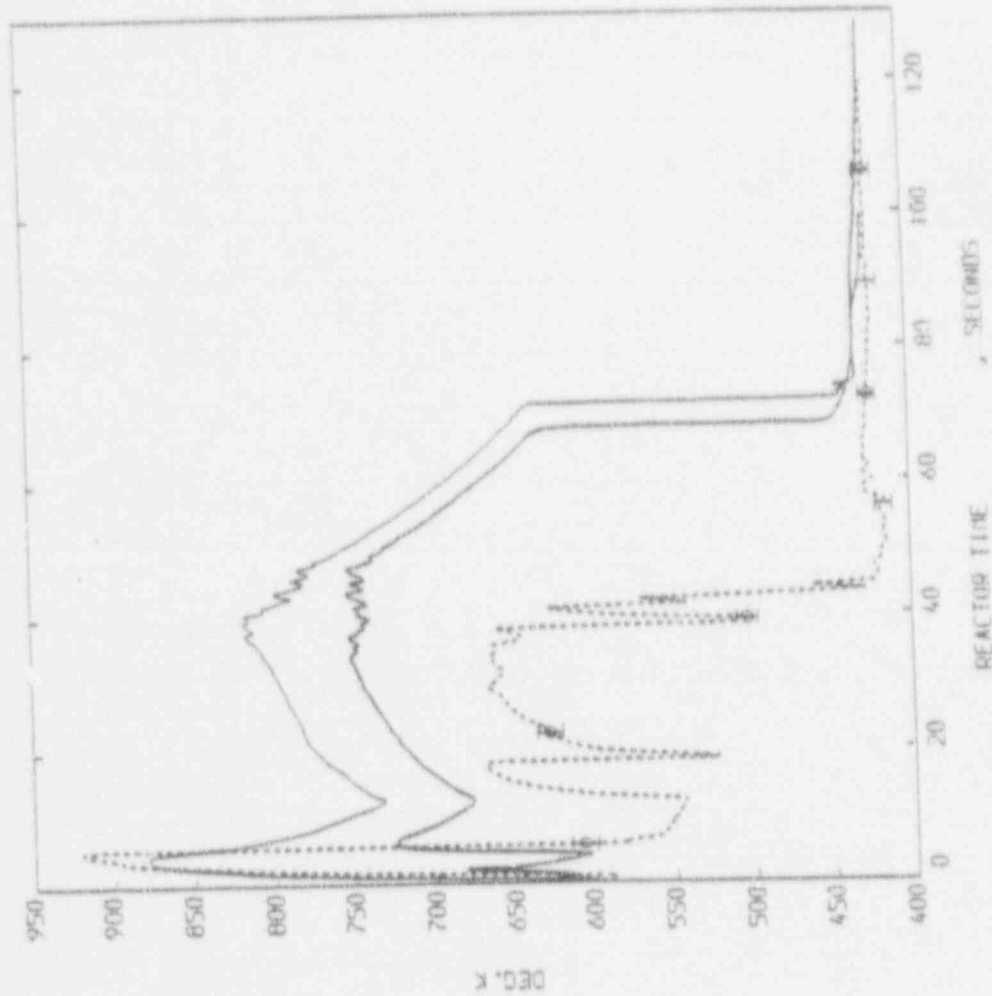| KEY	
SYMBOL	**NAME** **UNITS**
———	CLADDING TEMP -FINE,DEG.K
	LOC= 50/ 8/ 15 MMEM-TACL INF=1
———	CLADDING TEMP -FINE,DEG.K
	LOC= 50/ 8/ 15 MMEM-TACL INF=2
------	TE-2114-039 ,DEG.K
	LOC= 229/ 0/ 0 MMEM-TACL INF=3

Winfrith

FIGURE 210   INF 1 ISHARP, INF 2 ZEROGAP, INF 3 EXP
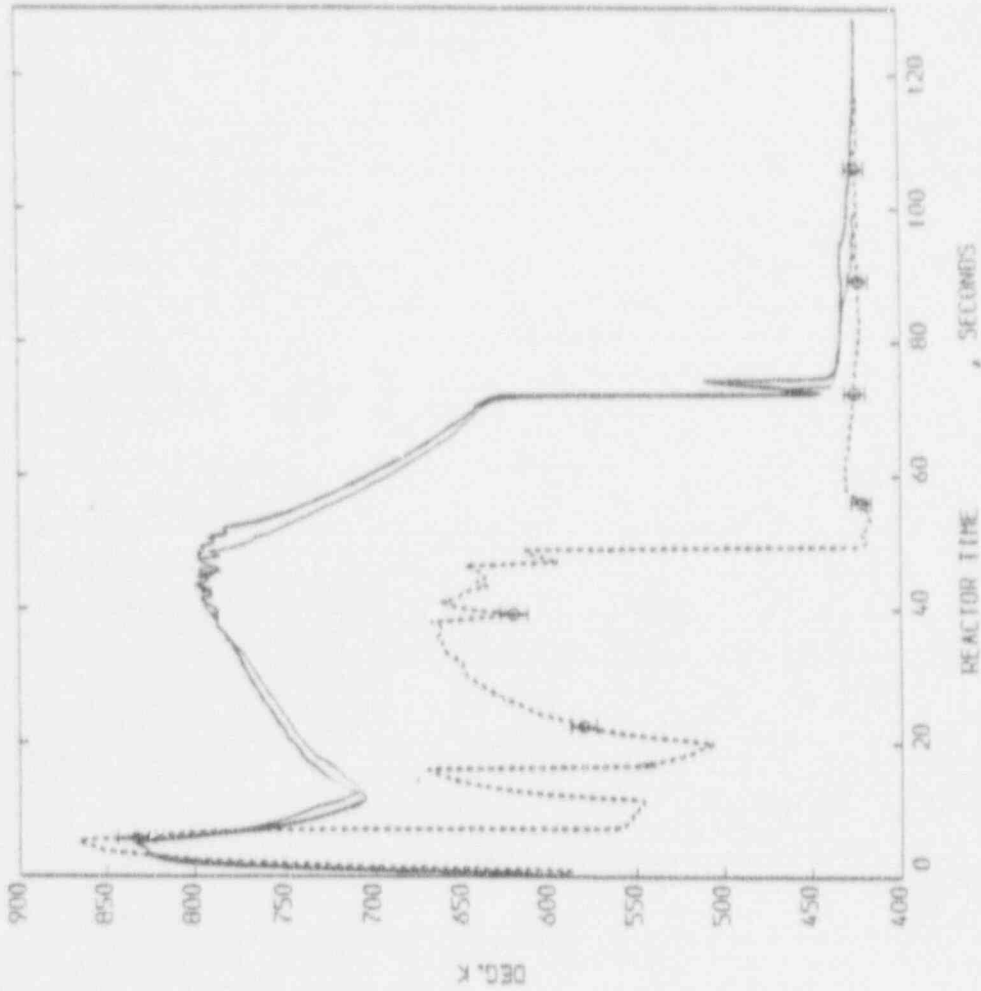FUEL ROD CLADDING TEMPERATURES - PERIPHERAL BUNDLES

THE FOLLOWING ARE PLOTTED AGAINST REACTOR TIME

CLADDING TEMP -FINE, TE-4G14-D11

DEG. K

900
800
750
700
650
600
550
500
450
400

REACTOR TIME , SECONDS

0   20   40   60   80   100   120

KEY

SYM BOL	NAME	UNITS
——	CLADDING TEMP -FINE, DEG.K LOC= 50/ 6/ 5 MNEM=TMCL INF=1	
——	CLADDING TEMP -FINE, DEG.K LOC= 50/ 6/ 5 MNEM=TMCL INF=2	
····	TE-4G14-D11 , DEG.K LOC= 24/ 0/ 0 MNEM=TMCL INF=3	

FIGURE 211 INF 1 ISHARP, INF 2 ZEROGAP, INF 3 EXP
FUEL ROD CLADDING TEMPERATURES - PERIPHERAL BUNDLES

FIGURE 212 INF 1 ISHARP, INF 2 ZEROGAP, INF 3 EXP
FUEL ROD CLADDING TEMPERATURES - PERIPHERAL BUNDLES

THE FOLLOWING ARE PLOTTED AGAINST REACTOR TIME

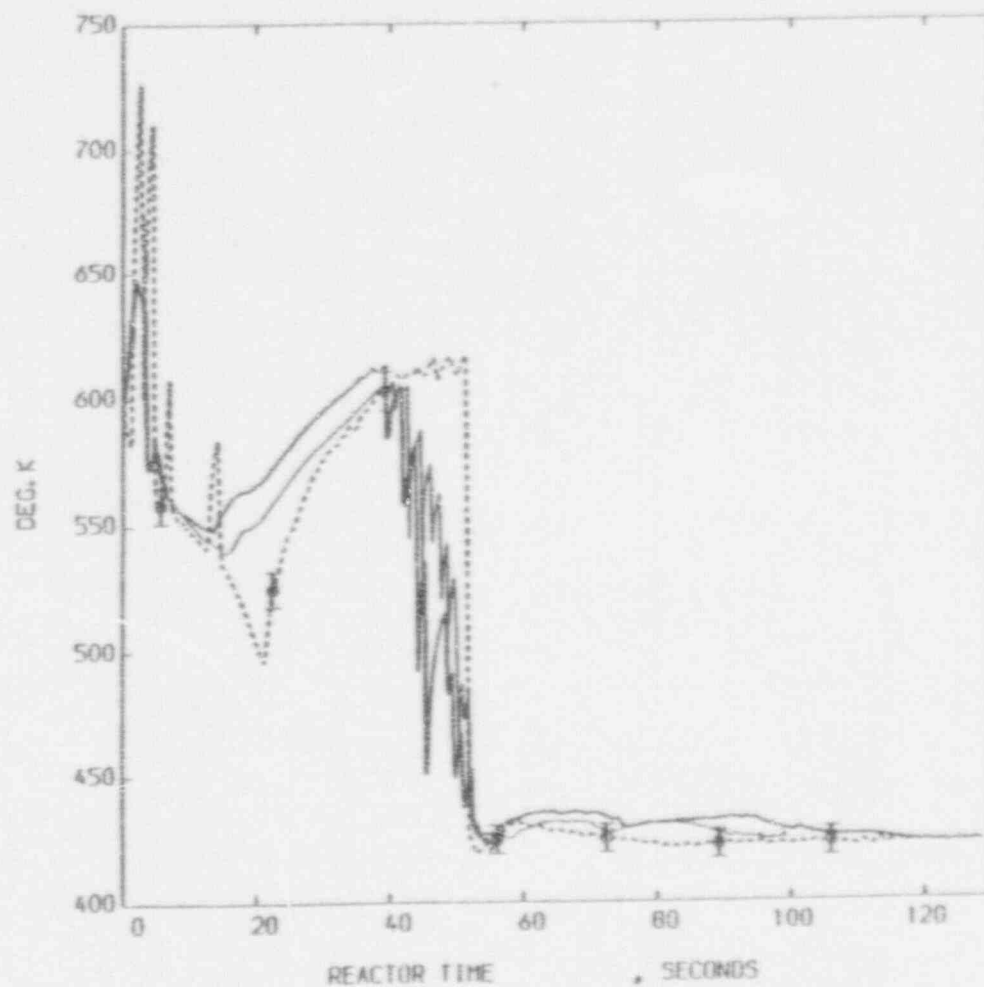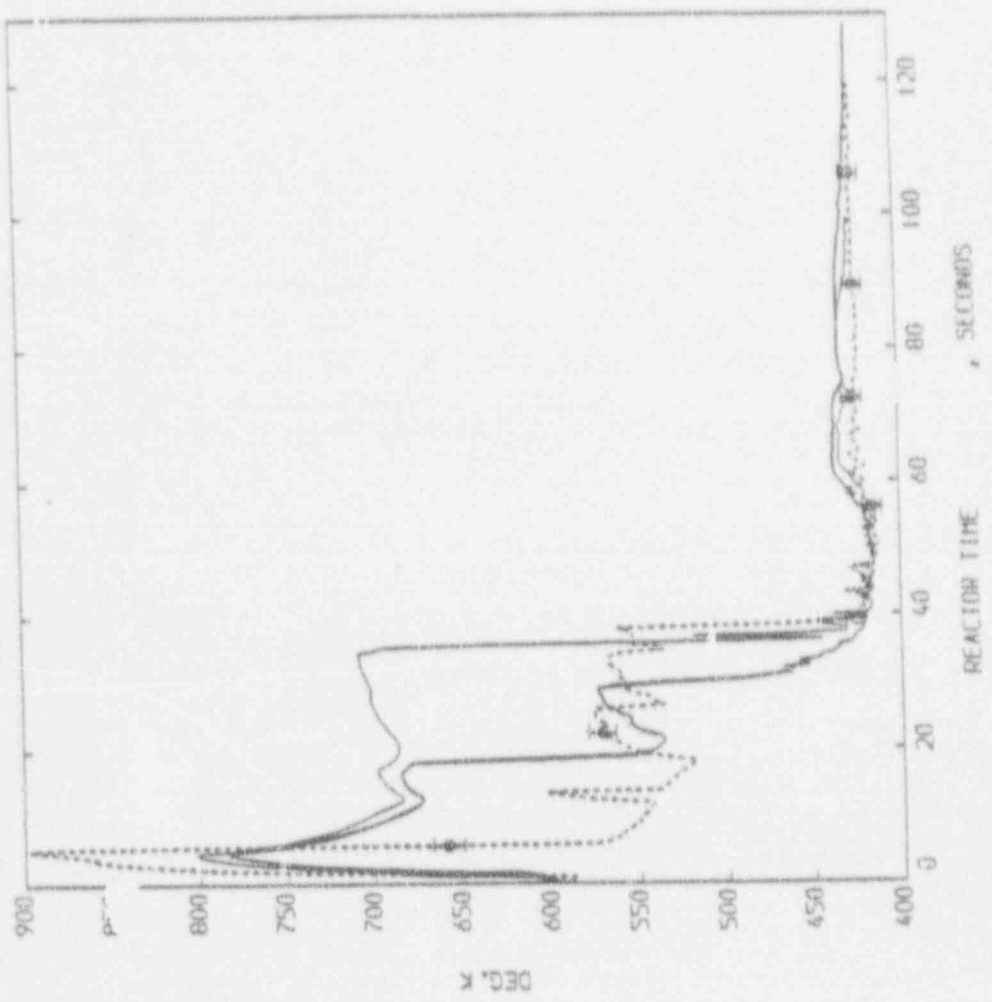CLADDING TEMP -FINE,TE-4H14-02B

FIGURE 213   INF 1 ISHARP, INF 2 ZEROGAP, INF 3 EXP
FUEL ROD CLADDING TEMPERATURES - PERIPHERAL BUNDLES

THE FOLLOWING ARE PLOTTED AGAINST REACTOR TIME

CLADDING TEMP -FINE, TE-4114-039

FIGURE 214 INF 1 FSHARP, INF 2 ZEROGAP, INF 3 EXP
FUEL ROD CLADDING TEMPERATURES - PERIPHERAL BUNDLES

SYM BOL	KEY NAME	UNITS
	CLADDING TEMP -FINE, DEG.K LOC= 50/ 5/ 15 PANEM-TACL INF-1	DEG.K
	CLADDING TEMP -FINE, DEG.K LOC= 50/ 5/ 15 PANEM-TACL INF-2	DEG.K
	TE-4114-039 LOC= 2577 0/ 0 PANEM-TACL INF-3	DEG.K

250

THE FOLLOWING ARE PLOTTED AGAINST REACTOR TIME

CLADDING TEMP -FINE, TE-6G14-011
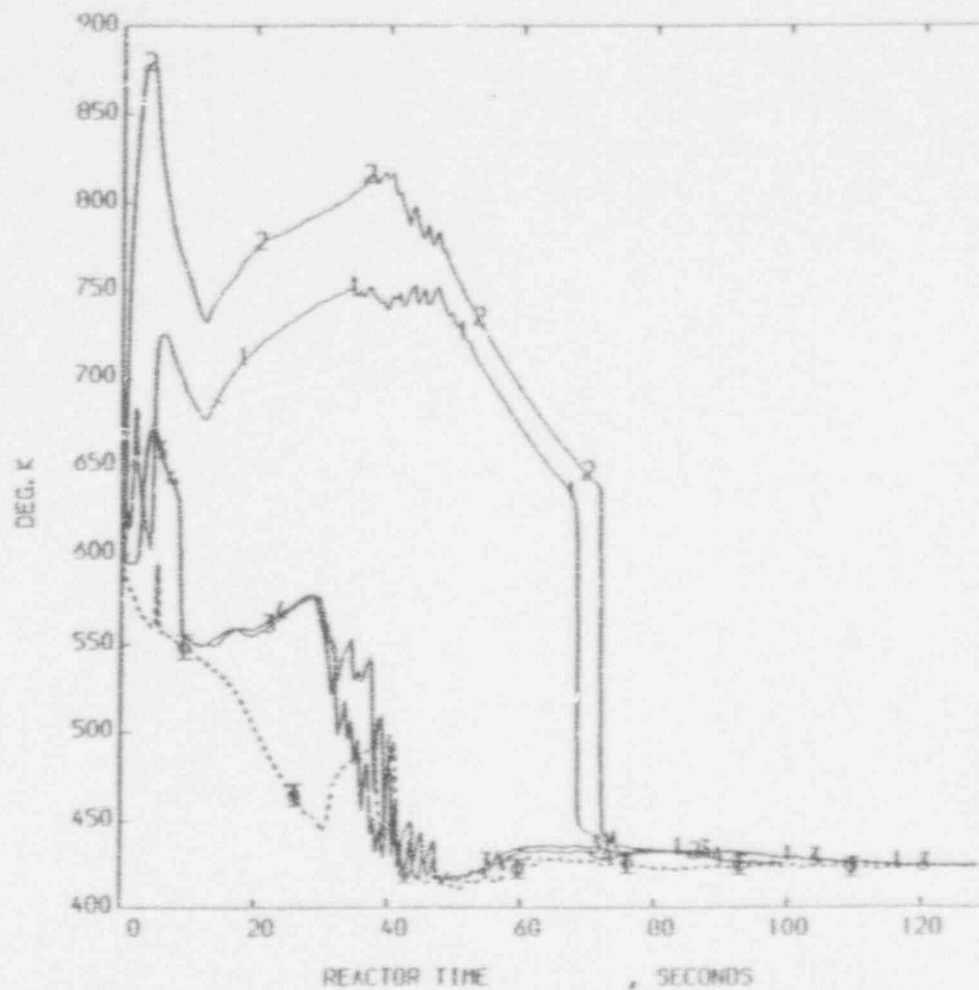
FIGURE 215 INF 1 ISHARP, INF 2 ZEROGAP, INF 3 EXP
FUEL ROD CLADDING TEMPERATURES - PERIPHERAL BUNDLES

Winfrith

TE 2 SHAFP : PLOTTED AGAINST REACTOR TIME

CLADDING TEMP -FINE,TE.6614-030
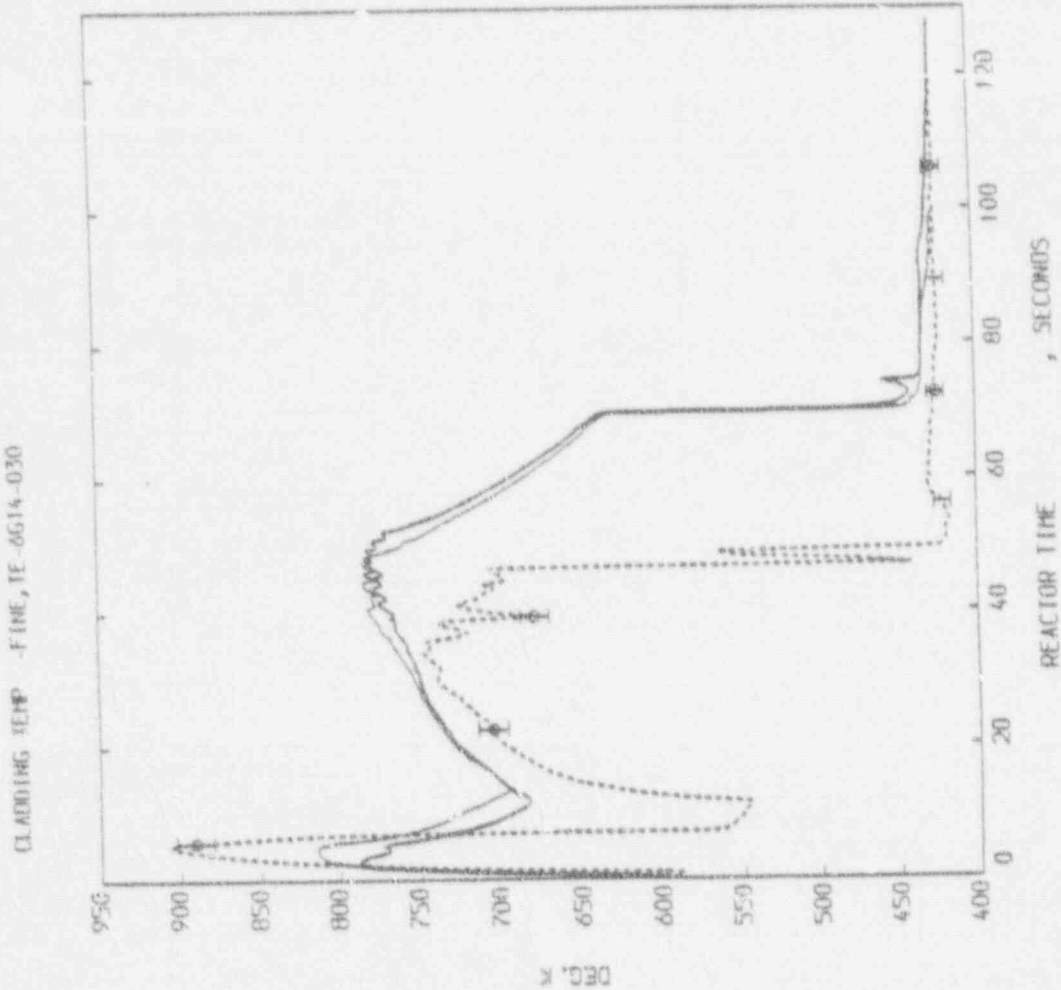
DEG, K

REACTOR TIME , SECONDS

KEY

SYM BOL	NAME	UNITS
	CLADDING TEMP -FINE,DEG.K	
	LOC. 50/ 0/ 13 MM-M-THCL INF=1	
	CLADDING TEMP -FINE,DEG.K	
	LOC. 50/ 0/ 13 MM-M-THCL INF=2	
	TE.6614-030 , DEG.K	
	LOC. 350/ 0/ 0 MM-M-MCL INF=3	

FIGURE 216 INF 1 ISHARP, INF 2 ZEROGAP, INF 3 EXP
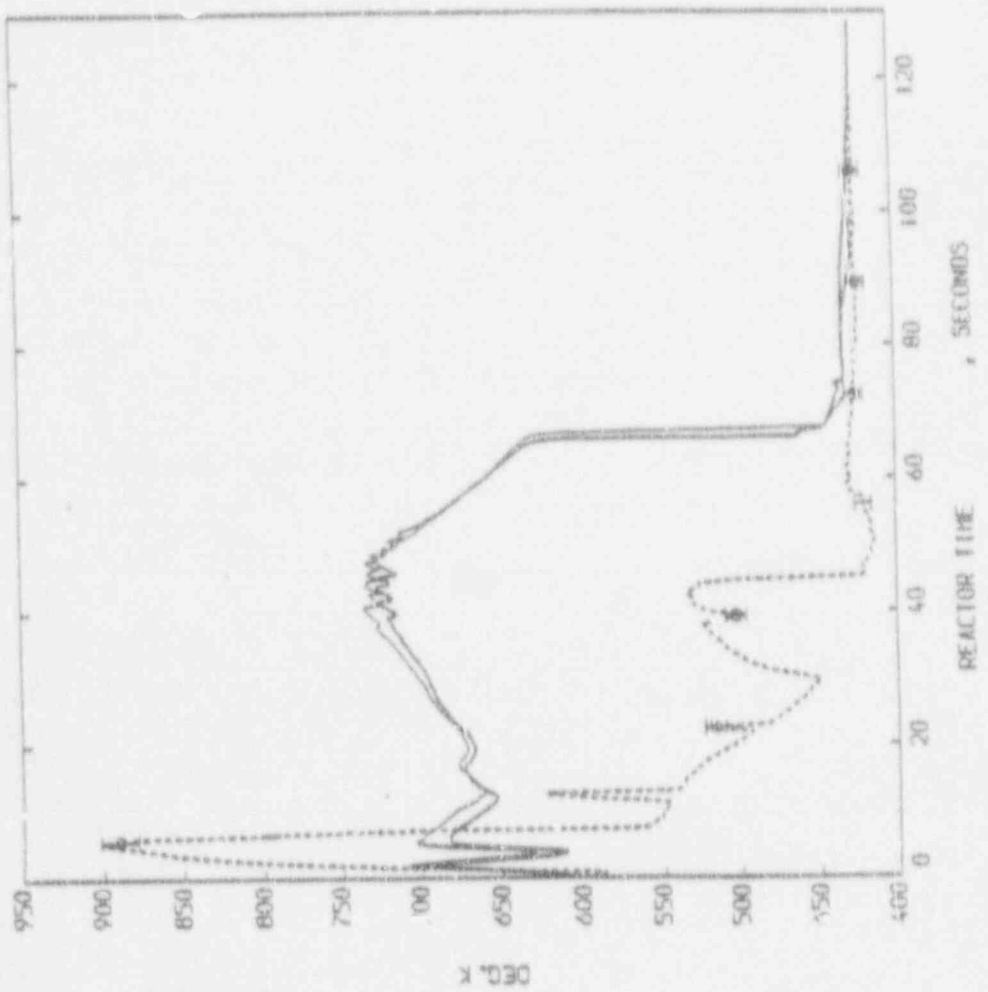FUEL ROD CLADDING TEMPERATURES - PERIPHERAL BUNDLES

FIGURE 217 INF 1 ISHARP, INF 2 ZEROGAP, INF 3 EXP
FUEL ROD CLADDING TEMPERATURES - PERIPHERAL BUNDLES

Winfrith

FIGURE 218   INF 1 ISHARP, INF 2 ZEROGAP, INF 3 EXP
FUEL ROD CLADDING TEMPERATURES - PERIPHERAL BUNDLES

FIGURE 219   INF 1 ISHARP, INF 2 ZEROGAP, INF 3 EXP
FUEL ROD CLADDING TEMPERATURES - PERIPHERAL BUNDLES

DISTRIBUTION

PWR HEAT TRANSFER AND HYDRAULICS WORKING GROUP

Mr M W F Coney	CEGB	CERL Kelvin Avenue, Leatherhead, Surrey
Dr M J Bird	AEEW	338/B41
Dr A J Wickett	AEEW	214/A32
Mr I Brittain	AEEW	201/A32
Mr K G Pearson	AEEW	333/B41
Dr D B Utton	NNC	c/o Reports Section, Library, Booths Hall, Chelford Road, Knutsford, Cheshire WA16 9QZ
Mr K Routledge	NNC	c/o Reports Section, Library, Booths Hall, Chelford Road, Knutsford, Cheshire
Mr D Coucill	BNF	Springfields Works, Salwick, Preston, Lancs
Mr P C Hall	CEGB	Barnett Way, Barnwood, Gloucestershire
Dr P R Farmer	CEGB	HSD, Courtenay House, 18 Warwick Lane, London EC4P 3EB
Dr L C Daniels	UKAEA	Bldg 392, AERE Harwell
Dr T J Haste	UKAEA	Springfields NPDL, Salwick, Preston, Lancs
Mr D W McLaughlin	UKAEA	CLF 125, SRD Culcheth, Warrington
Mr B Chojnowski	CEGB	Marchwood Engineering Labs, Marchwood, Southampton
Dr M El-Shanawany	CEGB	HSD, Nuclear Safety Branch, Courtenay House, 18 Warwick Lane, London EC4P 3EB

ADDITIONAL

AEE WINFRITH, DORCHESTER, DORSET, DT2 8DH

Mr M H Butterfield	309/B41	(Summary Only)
Dr I H Gibson	236/A32	
Dr G R Kimber	221/A32	(Summary Only)
Dr P Coddington	270/A32	(5 copies)
Mr R Potter	209/A32	
Mr A Neill	267/A32	(Summary Only)
Miss E Allen	266/A32	(Summary Only)
Dr C Richards	260/A32	
Dr D A Williams	210/A32	(Summary Only)
Dr A L Nichols	102/A50	(Summary Only)
Dr S R Kinnersly	203/A32	
Dr J N Lillington	217/A32	(Summary Only)
Mr C R Gill	229/A32	(3 copies)

UKAEA, SAFETY AND RELIABILITY DIRECTORATE, WIGSHAW LANE, CULCHETH, WARRINGTON

Mr R N H McMillan   CLF 112   (Summary Only)
Dr A A Debenham   CLC 002   (Summary Only)
Mr P Clough   (Summary Only)

UKAEA, RISLEY NPDE, WARRINGTON, WA3 6AT

Reports Library
Mr A Parry   E417   (Summary Only)

UKAEA, AERE HARWELL, DIDCOT, OXON, OX11 ORA

Dr D Hicks   G35, Bldg 77
Mr M R Everett   Bldg 329   (Summary Only)
Dr G F Hewitt   TH 392.7

UKAEA, RISLEY, NPDL, WARRINGTON, WA3 6AT

Dr W E Gardner   3/103
Dr N Davies   CH481   (Summary Only)

UKAEA SPRINGFIELDS NPDL, SALWICK, PRESTON, PR3 ORR

Mr R D Stacey   Bldg 321   (Summary Only)
Mr A J Manley   (Summary Only)

UKAEA, WINDSCALE NL., SELLAFIELD, SEASCALE, CUMBRIA

Mr A Garlick   (Summary Only)

BNFL, SPRINGFIELDS WORKS, SALWICK, PRESTON, PR3 OXJ

Mr D A Howl   Bldg 382   (Summary Only)
Mr J P Cooth   Bldg 382   (Summary Only)

NNC, BOOTH'S HALL, CHELFORD ROAD, KNUTSFORD, CHESHIRE

Dr K R Barry   (Summary Only)
Mr R J Tinsley   (Summary Only)

NNC Risley, Warrington Road, Risley, Warrington

Dr D Briney   (Summary Only)

CEGB, COMPUTING BUREAU, 85 PARK STREET, LONDON SE1

Mr L Wilson   (Summary Only)

CEGB, HEALTH AND SAFETY DEPARTMENT, NUCLEAR SAFETY BRANCH, 18 WARWICK LANE
LONDON, EC4 4EB

Mr J R Harrison   (Summary Only)

LOFT PROGRAMME REVIEW GROUP

TECHNICAL RESEARCH CENTER OF FINLAND (VTT), NUCLEAR ENGINEERING LABORATORY, POE 169, SF-00181 HELSINKI 18, FINLAND

Mr Heikke Holmstrom

EIDGENÖSSISCHES INSTITUT FÜR REAKTORFORSCHUNG, CH-8303 WÜRENLINGEN, SWITZERLAND

Mr O M Mercier

ÖSTERREICHISCHES FORSCHUNGSZENTRUM, SEIBERSDORF GESELLSCHAFT MBH, C/O EG&G IDAHO INC, PO BOX 1625, IDAHO FALLS, ID 83415, USA

Dipl Phys S Michael Modro

UNIDAD ELECTRICA SA, C/ FRANCISCO GERVAS 3, E-28020 MADRID, SPAIN

Mr Jose Puga

OFFICE OF NUCLEAR REACTOR REGULATION, US NUCLEAR REGULATORY COMMISSION, WASHINGTON DC 20555, USA

Dr Brian Sheron

JAPAN ATOMIC ENERGY RESEARCH INSTITUTE, TOKAI-MURA, NAKA-GUN, IBARAKI-KEN 219-11, JAPAN

Dr Kanji Tasaka

US DEPARTMENT OF ENERGY, OFFICE OF NUCLEAR POWER SYSTEMS, MS B-107, WASHINGTON DC 20555, USA

Mr D F Giessing

EPRI, PO BOX 10412, PALO ALTO, CA 94304, USA

Mr M Merilo

ENTE NAZIONALE ENERGIE ALTERNATIVE, CRE CASACCIA, SP ANGUILLARESE KM 1 + 300, CP NR 2400, I-00100 ROME, ITALY

Dr Giorgio Palazzi

CEGB, PROJECT MANAGEMENT TEAM, BOOTHS HALL, CHELFORD ROAD, KNUTSFORD, CHESHIRE

Mr N Buttery
Mr M E Durham   (Summary Only)
Dr M M Chestnutt   (Summary Only)
Mr P George   (Summary Only)
Dr R Garnsey   (Summary Only)

CEGB, CERL, KELVIN AVENUE, LEATHERHEAD, SURREY

Dr G C Gardner   (Summary Only)
Mr N Newman   (Summary Only)

CEGB, BERKELEY NUCLEAR LABORATORIES, BERKELEY, GLOUCESTERSHIRE, GL13 9PB

Dr D Witherington   (Summary Only)
Dr S J Board   (Summary Only)
Ms J P Longworth   (Summary Only)

CEGB, GDCD BARNWOOD, BARNETT WAY GLOUCESTER, GLOUCESTERSHIRE, GL4 7RS

Mr C Harwood   (Summary Only)
Mr I Pugh   (Summary Only)
Mr P D Jenkins   (Summary Only)
Mr K H Ardron
Mr J R D Jones   (Summary Only)

CEGB, MARCHWOOD ENGINEERING LABORATORIES, SOUTHAMPTON, HAMPSHIRE, SO4 4ZB

Dr B Chojnowski   (Summary Only)

SOUTH OF SCOTLAND ELECTRICITY BOARD, CATHCART HOUSE, SPEAN STREET, GLASGOW, SCOTLAND

Mr D R Reeks   (Summary Only)

NUCLEAR INSTALLATIONS INSPECTORATE, HEALTH AND SAFETY EXECUTIVE, ST PETERS HOUSE, STANLEY PRECINCT, BALLIOL ROAD, BOOTLE, L20 3LZ

Mr C Potter
Mr J F Campbell
Dr S A Harbison

STUDSVIK ENERGITEKNIK AB, S-61182 NYKOPING, SWEDEN

Mr O Sandervaag

US NUCLEAR REGULATORY COMMISSION, WASHINGTON DC 20555, USA

Dr Robert Van Houten

EG&G, IDAHO INC, PO BOX 1625, IDAHO FALLS, ID 83415, USA

Dr D Croucher

OECD NUCLEAR ENERGY AGENCY, 38 BOULEVARD SUCHET, F-75016 PARIS, FRANCE

Mr Ralph Caruso

1 MELSTOCK AVENUE, DORCHESTER, DORSET

Mr J Fell

INTERNATIONAL CODE ASSESSMENT AND APPLICATIONS PROGRAMME

USNRC, SILVER SPING, WASHINGTON DC 20555, USA

Mr D Bessette
Mr L Shotkin

LOS ALAMOS NATIONAL LABORATORY, ~ BOX 1663, LOS ALAMOS, NEW MEXICO 87545, USA

Dr R Jenks
Mr D Liles

EG&G (IDAHO) INC, INEL, PO BOX 1625, IDAHO FALLS, IDAHO 83415, USA

Mr G Wilson

LIBRARIES

Dounreay	-2
Harwell	-2
Risley	-4
Springfields	-2
Windscale	-2
Winfrith	-4

TRAC-PF1/MOD1 Calculations of LOFT Experiment LP-02-6

5 AUTHOR(S)

P. Coddington, C. Gill

8 PERFORMING ORGANIZATION — NAME AND ADDRESS (If NRC provide Division, Office or Region, U.S. Nuclear Regulatory Commission and mailing address, if contractor provide name and mailing address.)

Winfrith Technology Centre
United Kingdom Atomic Energy Authority
Winfrith, Dorchester
Dorset, England DT 28 DH

10 SUPPLEMENTARY NOTES

11 ABSTRACT (200 words or less)

Experiment LP-02-6 was the First Large Break (200% Double Ended Cold Leg) Loss-of-
Coolant Accident (LOCA) Experiment carried out in the Loss-Of Fluid Test (LOFT)
Facility under the auspices of the Organization For Economic Cooperation and
Development (OECD).

This report contains a comparison of the results of experiment LP-02-6 with those
of TRAC-PF1/MOD1 calculation.

12 KEY WORDS/DESCRIPTORS (List words or phrases that will assist researchers in locating the report.)

ICAP Program, TRAC-PF1, LP-02-6, LOCA, Large Break

13 AVAILABILITY STATEMENT

Unlimited

14 SECURITY CLASSIFICATION

(This Page)

Unclassified

(This Report)

Unclassified

15 NUMBER OF PAGES

16 PRICE